ON THE DYNAMICS OF DRAW TEXTURING

by

David Stuart Brookstein

B.T.E., Georgia Institute of Technology
(1971)

S.M., Massachusetts Institute of Technology
(1973)

SUBMITTED IN PARTIAL FULFILLMENT
OF THE REQUIREMENTS FOR THE
DEGREE OF DOCTOR OF SCIENCE IN
MECHANICAL ENGINEERING
AT THE
MASSACHUSETTS INSTITUTE OF TECHNOLOGY
February, 1976

Signature of Author .....
Department of Mechanical Engineering, August 28, 1975

Certified by .....
Thesis Supervisor

Accepted by .....
Chairman, Department Committee on Graduate
Students

ON THE DYNAMICS OF DRAW TEXTURING

by

DAVID STUART BROOKSTEIN

Submitted to the Department of Mechanical Engineering on August 11, 1975 in partial fulfillment of the requirements for the Degree of Doctor of Science.

ABSTRACT

This study is concerned with the mechanics and dynamics of a process for increasing bulk, softness, cover and stretch of thermoplastic continuous filament yarns. In particular this investigation focuses on the interactions between the feed yarn and the texturing machine in the draw texturing process. It treats the cases of both steady state and transient operation. The degree of filament drawing, the cold, hot, cooling and post spindle twist distributions, the threadline tension, and the threadline torque are shown to possess a non-linear relationship dictated by machine-material parameters. This study presents a tractable model for determining analytically threadline torque, tension, and twist distributions,- given information on machine settings and on material properties. Considerable attention is devoted to the determination of twist distribution in the threadline during transient operation.

The results of numerous observations of threadline response were compared with the data generated from the analysis of threadline operation. In general, the agreement between theory and experiment is good.

Thesis Supervisor: Stanley Backer
Title: Professor of Mechanical Engineering

ACKNOWLEDGMENTS

I would like to thank E.I. du Pont de Nemours and Company, Burlington Industries, and Westvaco for their financial support during my stay at M.I.T. Extra thanks go to Du Pont for supplying the yarns used for this study.

I am gratefully indebted to Professor J.J. Thwaites of the University of Cambridge for his fruitful suggestions and critical appraisal of this work during his stays at the Fibers and Polymers Laboratories at M.I.T.

I would also like to convey my appreciation to Dr. Subhash K. Batra, Mr. Steven C. Smith, and Dr. Raymond Z. Naar for their helpful conversations with regard to this study.

Without Ms. Guddi Wassermann-Ladda the completion of this work might have taken a longer time to materialize than it did. Her superior laboratory skills were used to the fullest advantage in accumulating the data needed for this study. To her goes my sincerest gratitude.

I would like to thank Ms. Laurel Silverman for performing the Herculean task of typing this manuscript.

Over the years my stay at M.I.T. was made that much more pleasant by my acquaintance with Miss Dorothy Eastman. Her assurance helped me through many trying days.

Finally, I would like to thank my supervisor Professor Stanley Backer. However, I am unable to adequately express my appreciation in words for his guidance, appraisal, and above all his patience. His support of my work over the last four years will always be remembered. The only fitting expression I have is thank you.

to Sue and Kara

TABLE OF CONTENTS

ON THE DYNAMICS OF DRAW TEXTURING

Chapter 1

INTRODUCTION

Texturing is a process whereby yarn stretch, bulk, absorbency, and improved hand are provided through the introduction of "permanent" crimp into otherwise straight continuous filaments. Fabrics made from textured yarns have captured a large share of the textile apparel market. The popularity of garments made from textured yarns results from improved wear performance, freedom from wrinkling, and high bulk or cover power.

Yarn texturing can be accomplished by any one of at least a dozen techniques; however, most texturing is accomplished by the false twist process. This single process sequentially twists, heat sets, and untwists a thermoplastic filament bundle in a continuous operation. A schematic diagram showing the yarn path through a typical pin-spindle false twist machine is pictured in Figure 1.1.

Yarn is removed from the supply package, fed at a controlled rate over the heater, through the false twist pin-spindle, and then onto a takeup package. Twisted yarn moving between the feed rollers and spindle is heat set before passing through the rotating spindle.

The elements of false twisting can be presented rather simply. If a stationary multifilament yarn is held at both

Figure 1.1

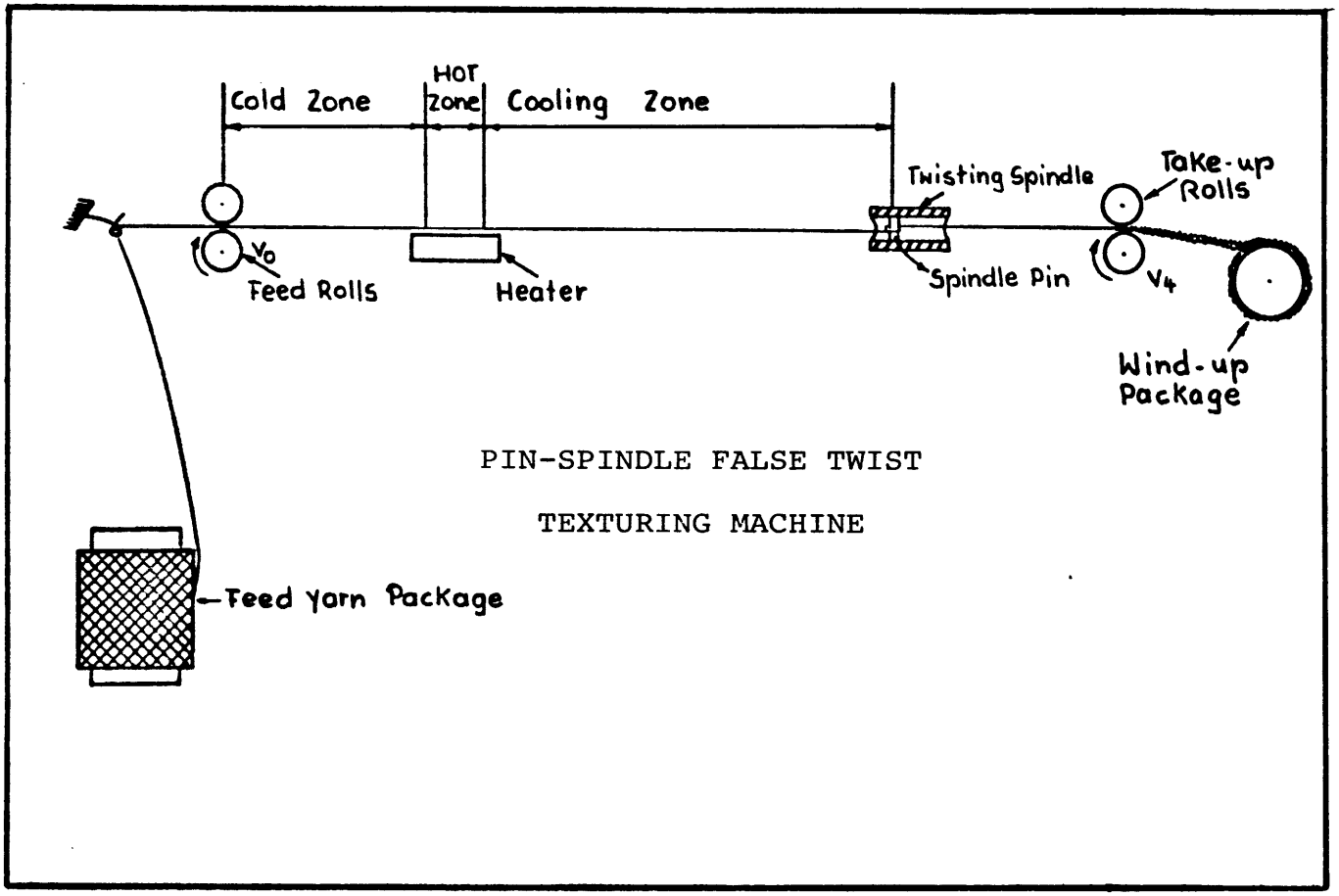
Cold Zone
Hot zone
Cooling Zone
Twisting Spindle
Take-up Rolls
V_0
Feed Rolls
Heater
Spindle Pin
V_4
Wind-up Package
PIN-SPINDLE FALSE TWIST
TEXTURING MACHINE
Feed Yarn Package

ends and twisted by a spindle at its center, equal amounts of twist with opposite directions of spirality will be imparted to each side, as seen in Figure 1.2.

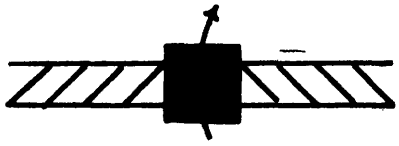

Figure 1.2

If each half of the yarn is considered separately, it is observed that the twist is real; however, the algebraic sum of twist throughout the yarn is zero. Now with the twisting element rotating continuously and yarn moving through it, the twist on the downstream side of the spindle is carried away through the take-up rollers and twist from the upstream side of the twister moves across the spindle to the downstream side. Once a yarn segment has moved through the twisting element, the twisting direction relative to that yarn segment is reversed and the segment is untwisted. At the same time, more twist is inserted at the feed rollers so that at steady state operation, a stationary zone of twisted yarn appears upstream of the spindle and twist free yarn occupies the downstream zone. This condition is illustrated in Figure 1.3.

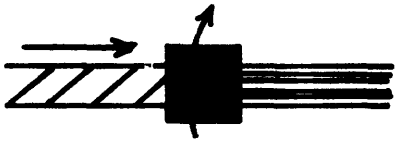

Figure 1.3

Twisting can be performed either by a pin-spindle or by a friction bushing. The yarn paths on each such spindle are

shown in Figure 1.4. For the pin-spindle system operating at steady state the segment of yarn which is about to enter the spindle generally rotates once for each spindle rotation. In the bush system the yarn will rotate $R_{bushing}/R_{yarn}$ times for each bush rotation, provided that no rotational slippage occurs. However, in virtually all friction twisting, rotational slippage does occur at the spindle. The ratio of bushing to yarn rotation varies from machine to machine and from time to time on a given machine. This thesis deals with the pin-spindle twisting system which dominates in the U.S. textile industry at present.

In the pin-spindle system, a heater is placed in the upstream zone, between the feed rollers and the spindle, with enough space left for the yarn to cool before being untwisted at the spindle. This upstream zone is termed the texturing zone, in which continuous twisting, heat setting and cooling are carried out, followed by untwisting downstream of the spindle. The presence of the heater causes two levels of twist to occur in the threadline in the texturing zone for reasons to be discussed later. However, threadline tension and torque along the texturing zone are uniform. A schematic diagram of the threadline characteristics during steady state operation is shown in Figure 1.5.

Until recently, most feed yarns for texturing were manufactured by fiber producers, via extrusion and drawing.

Figure 1.4

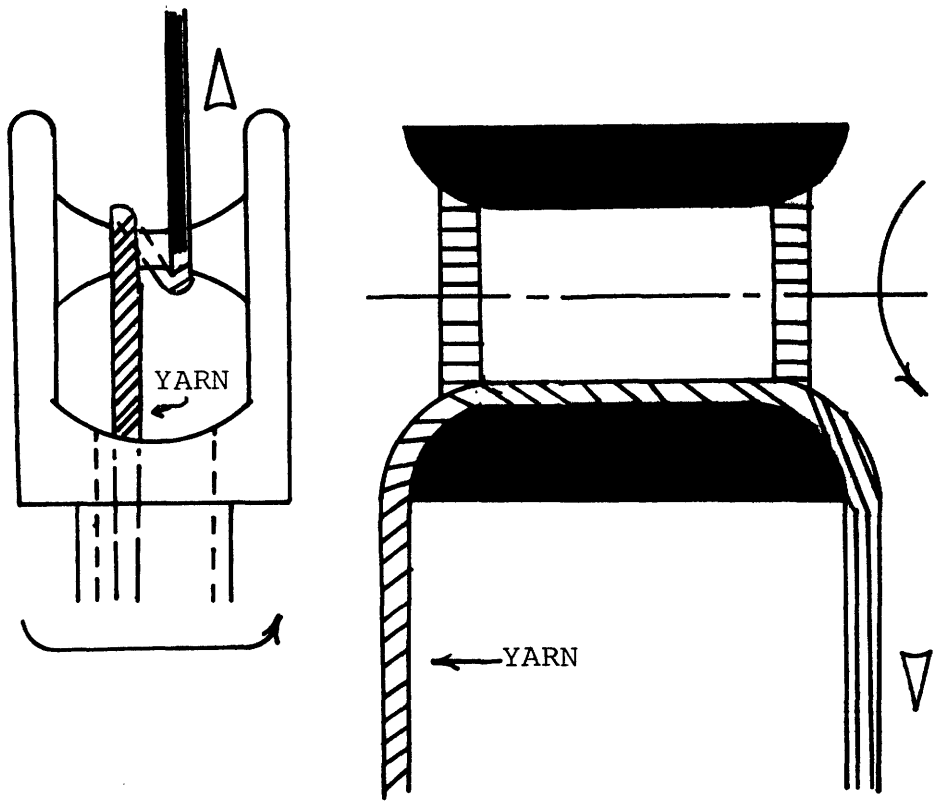

PIN-SPINDLE

FRICTION BUSHING

Figure 1.5

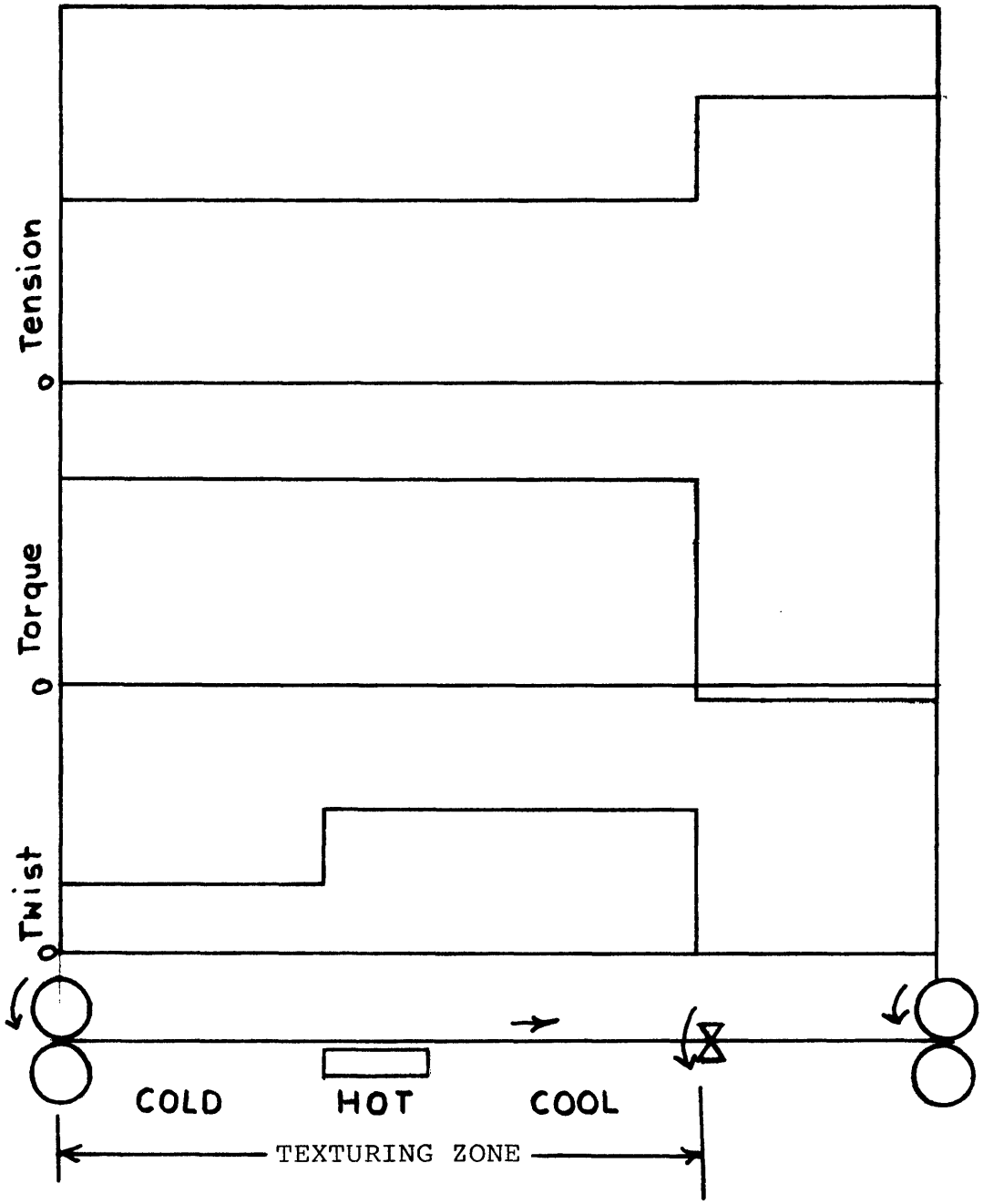

Typical Threadline Characteristics

Texturing of this fully drawn yarn was then undertaken by the textile manufacturer. In 1966 Mey[1] reported on studies of the combination of drawing and texturing processes. By 1972 selected American and European fiber producers began to integrate drawing processes with false twist texturing. This innovation is called false twist draw-texturing or simply, draw texturing.

There are two basically different methods of draw texturing: the sequential process and the simultaneous process. In the sequential process, the drawing operation, which preceeds false twisting, is carried out in a separate zone on the machine. Since the local processes of drawing and texturing are thus isolated in the sequential process, the resulting yarns are essentially the same as those produced from previously drawn yarn by the conventional texturing process. In the simultaneous process, the yarn moves into the cold portion of the texturing zone where it receives some cold twist. At or near the entrance to the heater further twisting occurs and at this point the yarn draws, both actions taking place simultaneously.

Yarns produced in this way show several distinct differences from conventional false twist textured yarns and from those draw textured yarns produced by the sequential process, the most important difference being that fabrics made from simultaneously draw textured yarns have a more uniform dyed

appearance than those made from conventional false twist textured yarns.[2] Thwaites shows that this superiority is associated with the modified light reflectance of the simultaneously drawn yarns[2].

This thesis will deal primarily with that simultaneous draw texturing process which employs pin-spindle twisting.

One problem encountered with the simultaneous draw texturing process is that when essentially unoriented amorphous polyester is used as the feed yarn, the filament bundle loses strength and/or the separate filaments fuse together as soon as the yarn is heated above its glass transition temperature for several seconds [3]. As a result, "stringup" of the texturing machine becomes very difficult. A solution to this problem is to use a relatively amorphous, yet somewhat preoriented, polyester feed yarn, which does not soften and lose its strength as rapidly upon heating. This preoriented polyester yarn (POY PET) can be produced simply by high speed winding of the freshly extruded filament bundle, without the provision of a separate drawing operation. Thus, there is a major economic advantage in the production of partially oriented yarn (rather than conventionally drawn yarn) and in its usage as feed stock for simultaneous draw texturing processes. For the latter methods employ yarns which have been extruded and partially drawn in a single process while conventional texturing requires yarns which are drawn to their final

draw ratio in a process separate from the extrusion process.

A successful draw texturing operation depends on the quality of its feed yarn as well as on the control of its process to produce consistently uniform quality yarn on an hour to hour and day to day basis. Once a draw-texturing machine is adjusted for a given operation, the textile manufacturer expects it to produce large quantities of yarn possessing uniform crimp with no residual twist. In mechanical terms this implies threadline torque and tensions which are constant in time from spindle position to position in a given machine and from machine to machine. Any variation experienced in generalized threadline forces (tension or torque) may cause variation in crimp level or in subsequent dyeing behavior of the output yarn or it may introduce real twist in the post spindle region as a consequence of periodic twist slippage past the rotating spindle. The textured yarn producer must make certain decisions as to the setting of machine and/or material parameters, on the basis of resulting product quality. As of this time, such decisions are made on the basis of preliminary experimental trials or in accordance with past production experience. This thesis seeks to provide a quantitative basis for anticipating the effect of variations in feed material properties and of machine parameters on the draw texturing process during both steady and non-steady operation.

Chapter 2

STEADY STATE OPERATION

2.1 INTRODUCTION

False twist draw texturing is a textile process which manifests strong interactions between feed material and machine. Once the texturing machine is set for given feed and take-up roller velocities, spindle speed, and texturing zone heater temperature, the yarn being processed reacts to the given machine conditions by twisting, drawing, uptwisting, heat setting and untwisting. The degree of filament drawing, the cold, hot and cooling twist levels, the threadline tension, and the threadline torque are determined by a complex non-linear relationship of machine-material parameters. A block diagram of the process is shown in Figure 2.1. A full understanding of this diagram must await the detailed analysis of texturing mechanics to be presented later, but it suffices at present to emphasize certain essential features of its construction. Note first that all mass flow moves from left to right, i.e. from feed roller to take up roller. Second, the twist originates at the spindle and moves to its left, upstream, or to its right, downstream. Finally, generalized threadline forces operating at each station of the texturing zone interact directly.

This section provides a tractable model for analytically

SCHEMATIC DIAGRAM OF FALSE TWIST TEXTURING

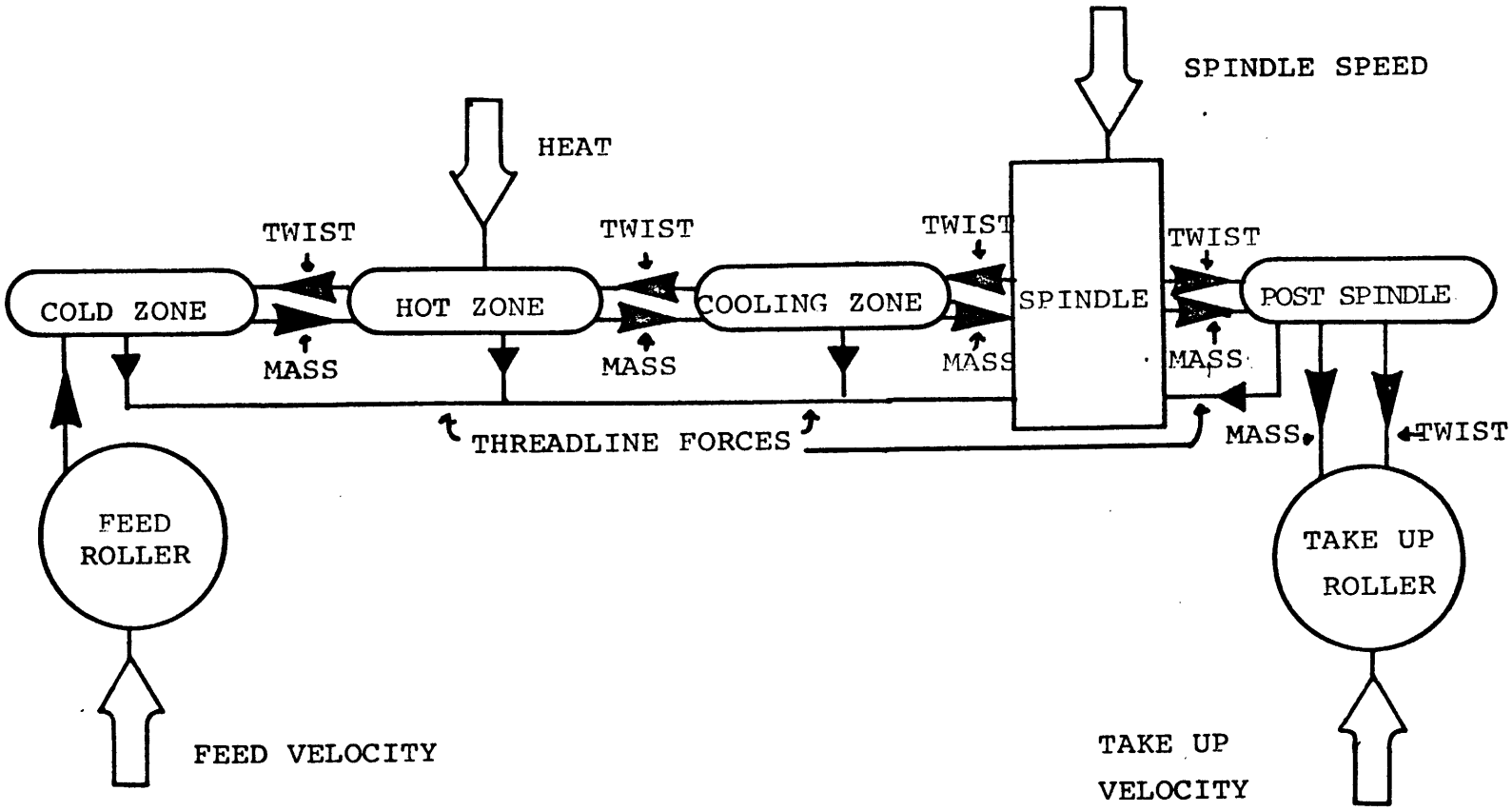

Figure 2.1

determining threadline torque, tension, and twist distribution, given information on machine settings and on material properties. Later, these analytical solutions will be compared with experimental data to test the validity of the model. In addition, a parametric survey will be presented to show the effect of different feed yarn properties on threadline behavior.

2.2 METHOD OF SOLUTION

The false twist draw texturing process can be divided into zones as shown in Figure 2.2.

Figure 2.2

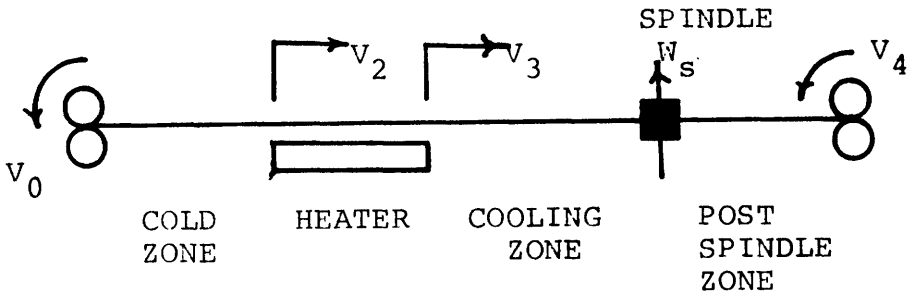

V_0 = Feed roller linear velocity

V_2 = Linear velocity of cold twisted yarn

V_3 = Linear velocity of hot twisted yarn

V_4 = Take up roller linear velocity

W_s = Angular velocity of false twist spindle

In this device, yarn enters the cold zone, twists, tra-

verses to the heater, simultaneously draws and uptwists, cools, progresses to the spindle, crosses the spindle and untwists. Between the feed rollers and the spindle, threadline torque and tension are considered uniform since for our particular system, negligible friction occurs between the yarn and the heater plate. Because of the extremely small yarn masses involved inertial effects are considered negligible for the rotating threadline. Justification of this assumption is given in the Appendix 1. Since the threadline torque and tension are uniform along the texturing zone, we can chose any yarn cross section in this zone for the purpose of analyzing tension and torque. For this analysis we must determine the local material-system constitutive relations, the local yarn geometry, and the system compatibility at each cross section.

As a first approach, the pin-spindle texturing machine can be thought of as a device that deforms yarn at both cold and hot temperatures. The feed rollers, the take up rollers, and the rotating false twist spindle are the deforming devices; the heater is the temperature treatment device. Generalized threadline forces, i.e. torque and tension, are consequences of the deformation and temperature treatment. During steady state operation, the condition of 100% pin-spindle efficiency is defined as the condition when the cooling yarn segment about to enter the spindle, rotates once for every turn of

that spindle. It is assumed that the hot yarn segment upstream of the cooling zone rotates at this same velocity since experimental observations of twist distribution in the threadline show relatively little difference between hot and cooling zone twist levels [4]. The system can also be thought of as running at steady state if there is continual rotational slippage of the cooling yarn relative to the spindle. For example, in the case of 80% efficiency, the cooling yarn segment will rotate 0.8 times for every turn of the spindle. This analysis will consider the case for 100% efficiency; however, if the efficiency were given, that case could be easily handled with the present analysis.

During steady state operation, the yarn in the cooling zone progresses downstream one twist pitch for each spindle rotation. As this yarn moves through the spindle, the spindle untwists one turn of twist and the given pitch length is untwisted completely. In the case of non-steady operation this condition of one twist pitch of linear motion per spindle revolution need not prevail. Treatment of the non-steady state condition follows in Chapter 3.

As the untwisted filaments enter the cold zone, they are strained and twisted, the net result being that the filament bundle contracts longitudinally. This contraction results in a reduction of yarn linear velocity according to continuity requirements. The mechanics of cold zone twist

contraction is examined in Section 2.3.2.

The physical motivation for the yarn to twist upon entry into the cold zone is the existence of a threadline torque field. In Section 2.3.4 we show that cold zone tension is a function of cold zone twist and cold filament strain. We can express cold zone yarn tension as a function of certain unknowns of the system:

$$T_{\text{cold zone}} = F_1 \ (e_{\text{cold}}, P_c) \qquad (2\text{-}1)$$

where e_{cold} = cold filament strain

P_c = cold zone twist (radians/unit twisted length)

Cold zone yarn torque has one component due to filament tension and one due to filament bending and filament twisting. Since the filaments in the twisted yarn are constrained to lie approximately in right cylindrical helices, they are bent and twisted about their individual axes. The filament bending and torsional moments resulting form this deformation can be resolved along the yarn axis so as to determine their contribution to total threadline torque. Platt el al.[5] has analytically determined this relation, showing that yarn torque due to fiber torsion and bending is a function of the torsional rigidity of the fiber, its bending rigidity, and its geometrical path in the yarn structure. Accordingly, we can express cold zone yarn torque due to fiber bending and torsion as

$$M_{t \text{ cold zone (bending, torsion)}} = F_2 (EI, GI_p, P_c) \quad (2\text{-}2)$$

where EI = fiber bending rigidity

GI_p = fiber torsional rigidity

P_c = cold zone twist

Filament tension can be readily determined from filament strain and can then be radially resolved and multiplied by the appropriate radius (corresponding to the filament position in the yarn structure) to determine the individual tensile component of yarn torque. This tensile component can be expressed as:

$$M_{t \text{ cold zone (tension)}} = F_3 (e_{cold}, P_c) \quad (2\text{-}3)$$

Combining (2-2) and (2-3) we can express the total torque in a yarn section from the cold zone as

$$M_{tc} = F_4 (P_c, e_{cold}, EI, GI_p) \quad (2\text{-}4)$$

EI and GI_p are known properties of the filaments. P_c and e_{cold} are unknown and must be determined. Therefore there are two equations with four unknowns relating to the threadline in the cold zone, i.e.:

$$M_{tc};\ T_c;\ e_c;\ P_c$$

In order to generate more independent simultaneous equations it is necessary to choose another threadline cross section with different geometry, different material-system con-

stitutive relations, and different system compatibility. Towards this end, a cross section of the hot drawn yarn at the base of the threadline drawing "neck" is analyzed. In section 2.3.6 we demonstrate that hot zone filament tension is a function of both hot and cold zone yarn twist, cold and hot yarn linear velocity, and the hot draw material-system constitutive relation. On the assumption that the material constitutive relation, $\overline{MCR}$, for the hot drawing yarn can be determined, hot yarn tension can be expressed as:

$$T_{\text{hot zone}} = F_5(V_2, V_3, P_c, P_h, \overline{MCR}) \qquad (2\text{-}5)$$

where V_2 = linear velocity of the cold yarn

V_3 = linear velocity of the hot yarn

P_c = cold zone twist (radians/unit twisted length)

P_h = hot zone twist (radians/unit twisted length)

Taking the component of filament hot tension perpendicular to the yarn axis we can determine the contribution of tension to yarn torque in the hot zone:

$$M_{t\ (\text{tension})} = F_6(V_2, V_3, P_c, P_h) \qquad (2\text{-}6)$$

This derivation is presented in Section 2.3.7.

The objective of the false twist texturing process is to temporarily deform thermoplastic filaments into a twisted configuration and then to stress relax them before untwisting by passing the twisted yarn over a heater whose temper-

ature is above the crystal melting temperature of the feed yarn. If this process is to be effective, components of yarn torque due to fiber bending and fiber torsion should be relaxed out over the heater. If this relaxation occurs, as Naar[6] points out, the torque in the yarn over the heater should be due primarily to individual fiber tension. This assumption is to some extent justified when one looks at the twist distribution of the yarn over the heater. Once the torque due to cold fiber torsion and cold fiber bending is relaxed, one observes a dramatic twist crankup at the heater entrance which is necessary to keep the torque constant. Total torque in the hot zone is primarily the torque due to fiber tension and accordingly can be expressed as:

$$M_{t \text{ hot zone}} = M_{t \text{ hot zone (tension)}} \tag{2-7}$$

By equating (2-1) and (2-5) and equations (2-4) and (2-7), which corresponds to equalizing tension and torque through the threadline, we can reduce our system of equations to two equations with five unknowns. EI and GI_p are assumed given. These are shown for

Equal Tension in Cold and Hot Zones

$$0 = F_1(e_{cold}, P_c) - F_5(V_2, V_3, P_c, P_h) \tag{2-8}$$

Equal Torque in Cold and Hot Zones

$$0 = F_4(e_{cold}, P_c, EI, GI_p) - F_7(V_2, V_3, P_c, P_h) \qquad (2\text{-}9)$$

In Section 2.3.3 we show how cold filament strain is analytically related to cold yarn contraction and to the ratio of feed roller velocity and translational velocity of the cold twisted yarn. Cold strain can be expressed as:

$$e_{cold} = F_8(V_2, V_0, P_c) \qquad (2\text{-}10)$$

where V_2 = Linear velocity in the cold zone

V_0 = Linear velocity of the feed roller

P_c = Cold twist (radians/twisted length)

As indicated, for steady state operation, the hot twisted yarn segment progresses downstream one pitch length during the time it takes for the spindle to rotate one revolution. Therefore the linear velocity of the twisted cooling yarn segment, V_b, as it enters the spindle is :

$$V_b = \frac{1}{2\pi P_s} \Big/ \frac{1}{2\pi\omega_s} = \frac{\omega_s}{P_s} \qquad (2\text{-}11)$$

where ω_s = Spindle speed, (radians per second)

It has been observed that the difference between local twist in the cooling (therefore setting) zone, P_s, and the local twist at the exit of the heater, P_h is negligible. Likewise the difference between the linear velocity of the

threadline as it leaves the heater and as it enters the spindle is considered to be negligible. This permits a re-writing of equation (2-11) in the form

$$P_h = \omega_s / V_3 \tag{2-12}$$

The spindle speed is a given quantity, therefore we need to determine the threadline velocity at the heater exit V_3. It is shown in Section 2.3.9 that the given value of take up roll velocity can be used to determine V_3.

With the appropriate mathematical substitutions the system of equations outlined in this section can be reduced to three nonlinear simultaneous equations with three unknowns:

$$0 = u(V_2, e_c, P_c) - v(V_2, P_c) \tag{2-13}$$

$$0 = x(V_2, e_c, P_c) - y(V_2, P_c) \tag{2-14}$$

$$0 = z(V_2, e_c, P_c) \tag{2-15}$$

where e_c is e_{cold}

Equations (2-13), (2-14), and (2-15) are solved by the computer subroutine "YARN " which is listed in Appendix 5. The three equations are reduced to a single equation with the unknown, P_c, and the value of P_c satisfying the single equation is determined. Given the value of P_c for a given set of machine parameters, the corresponding values of V_2 and e_c are then determined. When the solution for P_c,e_c, and

V_2 is found, they are substituted back into equations (2-1), (2-5), (2-4) and (2-7) to determine the threadline tension and threadline torque.

In summary, this method of solution makes possible the determination of the threadline tension, threadline torque, and threadline twist distribution given the feed roller and take up roller velocities, spindle speed, and the material properties of the feed yarn. It remains to provide specific relationships for cold and hot tension, cold and hot torque, hot twist, hot twist contraction, and cold twist contraction. This is done in Section 2.3.

2.3 STEADY STATE THREADLINE MECHANICS

2.3.1 Continuous Twisting of Filament Yarns

As untwisted feed yarn is delivered by the feed rollers into the texturing zone and is exposed to the threadline torque, the yarn uptwists until its torque reaches that of threadline. As the yarn uptwists, its filaments are extended, partially because of the threadline tension and partially because of the tortuous path lengths the filaments are forced to follow in conforming to the geometry of twists. Filaments lying on relatively high helix angles in the outer radial layers of the yarn, are prone to extend to a greater extent then filaments located closer to the yarn center. The presence of such differential strain was first recognized by Morton[7] who suggested that the magnitude of the differential strains would be reduced with the occurrence of interchange between outer and inner filaments. A continuing interchange of this nature tends to equalize filament tensions throughout the yarn during steady state twisting. This cyclical interchange of fiber position is known as radial migration. Backer & Yang[4] demonstrated that radial migration does occur at the entrance to the texturing zone at the feed rollers. On the basis of these observations Naar[6] assumed that the filaments in the cold yarn segment of the texturing zone are under equal tension. We adopt this assumption as part of our model system.

2.3.2 Cold Zone Twist Contraction

When yarn is twisted under a given tension it will contract because of the longer path lengths that the outer filaments must follow. The resulting contraction is quantitized by a "contraction factor" defined as:

$$C_r = \frac{\text{Length of Zero Twist Yarn}}{\text{Length of Twisted yarn}} \qquad (2\text{-}16)$$

The length of a projected segment of a filament lying in a twisted yarn is compared with the same length of filament in an untwisted yarn in Figure 2.3. The contraction factor of the filament yarn segment of Figure 2.3 is obviously sec θ.

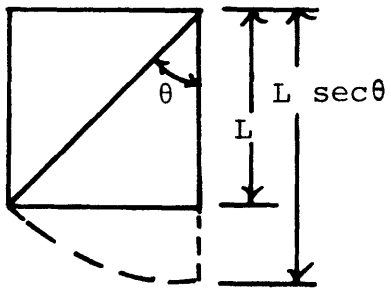

Figure 2.3

Hearle's Model of Twist Contraction

Consider a twisted yarn of length h as shown in Figure 2.4.

Figure 2.4

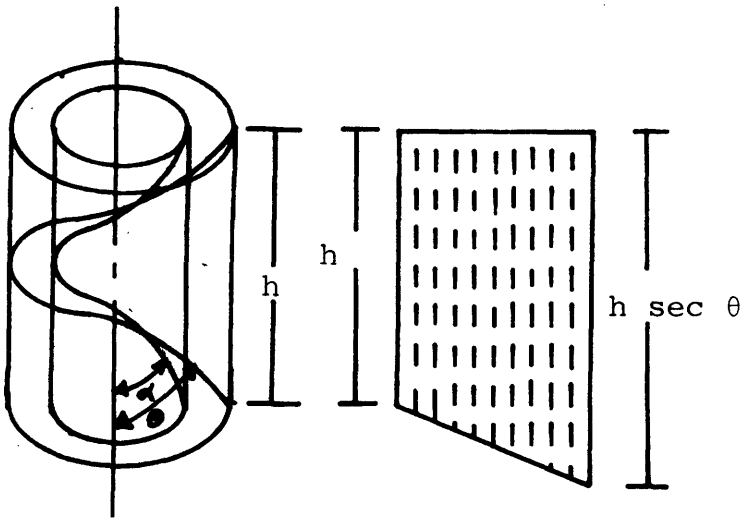

Hearle [8] assumes that because of radial migration the difference in the path length of twisted filaments in a given segment of yarn vs. the length of the twisted yarn is spread uniformly over all the filaments in a relatively long segment of yarn. He shows that the distribution of lengths in a short segment is linear and therefore the contraction factor equals the arithmetic average of the minimum filament length (equal to yarn length) and maximum filament length (for outside layer). The contraction factor for this yarn model is

$$C_r = \frac{(1+\sec\theta)}{2} \qquad (2\text{-}17)$$

where θ is the surface helix angle of the yarn.

Alternative Model of Twist Contraction

Hearle's model of twist contraction essentially averages the length of the filaments in a yarn segment over its cross sectional area. Alternatively we can average the filament lengths over the yarn radius. This method will disproportionately weigh the average towards a lower value than that obtained from Hearle's model since there are fewer fibers in central yarn radial positions compared to the number of fibers in outer radial positions. The alternative model for twist contraction is formulated as

$$C_r = \frac{\int_0^R \sec\theta\, dR}{\int_0^R dR}$$

or
$$C_r = 1/2\left[\frac{\ln(\tan\theta+\sec\theta)}{\tan\theta} + \sec\theta\right] \qquad (2\text{-}18)$$

The predicted value of contraction factor using either model must be compared with the measured values. Experimental values of twist contraction in the cold zone are compared to the predicted values using both models below for five different cold segments derived using different machine twists.

COLD YARN TWIST CONTRACTION

Machine Twist	Measured*	Hearles' Model	Alternative Model
50	1.053	1.091	1.063
60	1.139	1.190	1.136
65	1.158	1.207	1.148
70	1.165	1.213	1.153
80	1.191	1.247	1.178

Comparison of the measured values to both models indicates that the alternative model for twist contraction in the cold zone predicts closer values to the measured ones. Nonetheless, both models will be included separately in the steady state prediction of threadline behavior (i.e., threadline tension, threadline torque, cold threadline twist, and hot threadline twist.)

*By untwisting in a twist tester, yarn segments which had been twisted in the texturing apparatus. The tension of untwisting equalled the texturing tension.

2.3.3 Flow Continuity in Cold Zone

During steady state operation of the texturing process, the product of the linear density of the yarn and the local translational yarn velocity (mass flow rate) must be constant at any station in the texturing threadline, i.e.

$$D\ V|_X = \text{constant} \qquad (2\text{-}19)$$

where D = Yarn denier (linear density)

V = Linear velocity of yarn

X = Linear location on threadline, i.e. its station

The linear density of a textile yarn is usually expressed in terms of its denier, defined as the weight in grams of 9000 yarn meters.

The machine configuration between the feed rollers and the cold zone is illustrated in Figure 2.5

Figure 2.5

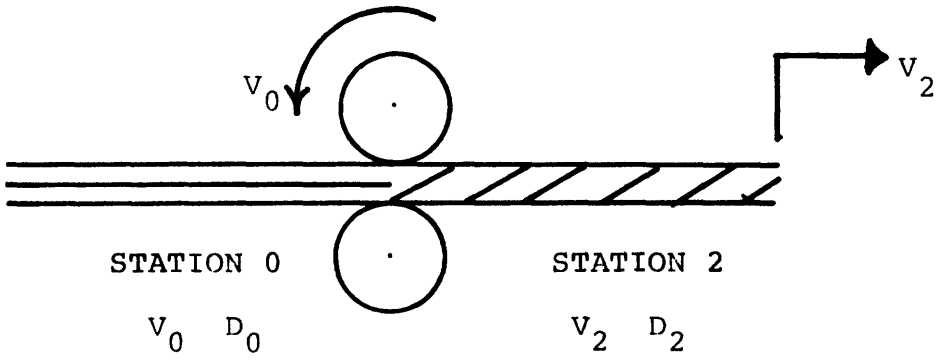

At each of these two stations, the mass flow rate is constant, i.e.

$$V_0 D_0 = V_2 D_2 \qquad (2\text{-}20)$$

where V_0 = Linear velocity of feed roller and of the feed yarn passing through

V_2 = Linear velocity of twisted yarn under threadline tension

D_0 = Denier of feed yarn under no tension

D_2 = Denier of twisted yarn under threadline tension

The contraction factor is defined as:

$$C_r = \frac{\text{untwisted yarn length}}{\text{twisted yarn length}}\Bigg|_{\substack{\text{constant filament} \\ \text{strain}}} \qquad (2\text{-}21)$$

The denier ratio for constant filament strain as specified for station 2 is:

$$\frac{D_2}{\frac{D_0}{1+e_{cold}}} = \frac{\text{grams/twisted yarn length}}{\text{grams/untwisted yarn length}}\Bigg|_{\substack{\text{constant} \\ \text{filament} \\ \text{strain}}} \qquad (2\text{-}22)$$

where e_{cold} is the filament strain in the cold zone at station 2.

Substituting (2-20) into (2-22) we obtain

$$e_{cold} = \frac{V_2}{V_0} C_r - 1 \qquad (2\text{-}23)$$

2.3.4 Cold Zone Tension

Given the tensile strain level of the filaments in the cold zone, we use the measured constitutive relationship to determine filament tension. The corresponding yarn tension in the cold zone entrance at station #2 is then determined by resolving the filament tensions in the direction of the yarn axis by multiplying filament tension by the cosines of local helix angles. Thus the cold yarn tension, T_c, is simply expressed as:

$$T_c = E_c e_c A_{f_i} \Sigma N_i \cos\theta_i \qquad (2\text{-}24)$$

where E_c = Cold filament extensional modulus

e_c = Cold Filament strain (assumed uniform for all filaments)

A_f = Cross sectional area of filament

N_i = Number of filaments in i^{th} radial layer

i = i^{th} radial layer helix angle

Equation (2-24) is fully developed in Chapter 3.

2.3.5 Cold Zone Torque

Naar[6] proposes that yarn torque at the entrance to the cold zone in the false twist texturing threadline is simply due to components of individual filament bending moments, filament torsional moments, and filament tension. Thus he neglects transverse interfiber stresses and interfiber fric-

tion. We assume that interfiber transverse stresses or interfiber friction do not play a significant role in developing yarn torque at the cold zone entrance. However, as is discussed later, transverse interfiber stresses and friction do contribute to the high values of incremental torsional rigidity observed in the yarn segment downstream of the cold zone entrance and in the cooling yarn segment downstream of the heater. If the filaments do not exceed their elastic limit during their traverse of the cold zone, they should not stress relax significantly before reaching the heater and the cold yarn twist level should remain uniform.

Actually, there is some stress relaxation of the cold filaments, which results in the yarn slowly gaining twist as it moves downstream towards the heater. For simplicity of analysis, this slight uptwist will be neglected.

For the case of elastic fiber, Platt et al.[5] have shown that the components of yarn torque due to fiber bending and fiber torsion are:

$$M_{t \text{ cold zone (bending)}} = \frac{EI \sin^3\theta}{R} \qquad (2\text{-}25)$$

$$M_{t \text{ cold zone (torsion)}} = GI_p P_c \cos^3\theta \qquad (2\text{-}26)$$

where EI = Filament bending modulus

GI_p = Filament torsional modulus

θ = Helix angle of filament in yarn

R = Radial position of filament in yarn

P_c = Cold twist (radians/twisted length)

The yarn torque due to filament bending and filament torsion is simply the summation of the individual components of torque from each filament. The components of individual filament tension that are perpendicular to the yarn axis are multiplied by their local radial position in the yarn to determine the tensile contribution of the filaments to the yarn torque. This can be expressed as:

$$M_{t \text{ cold zone (tension)}} = E_c e_c A_{f_i} \Sigma N_i R_i \sin\theta_i \qquad (2\text{-}27)$$

The <u>total torque</u> in the cold zone is then:

$$M_{t \text{ cold zone}} = EI \sum_i \frac{N_i \sin^3\theta}{R_i} + GI_p P_{c_i} \Sigma N_i \cos^3\theta + E_c e_c A_{f_i} \Sigma N_i R_i \sin\theta_i \qquad (2\text{-}28)$$

Equation (2-28) is fully developed in Chapter 3.

2.3.6 <u>Hot Zone Tension</u>

The threadline tension at the hot zone entrance is due to the components of filament drawing forces resolved in the direction of the yarn axis. These drawing forces are determined by the filament draw ratio and the material-system constitutive behavior. The draw ratio of each filament is dependent on its radial position, on the amount of uptwist taking place at the heater entrance and on the ratio of yarn velocity before and after the drawing neck. Brookstein[9]

has shown, in studies of sequential cross sections through the necking zone, that there is little opportunity for additional radial migration at this point in the threadline. However, the radial migration pattern developed at the cold zone entrance persists. Therefore the filament whose position, upon entering the hot zone, is on the outside yarn layer, stays on the outside while it is drawn. From this we deduce that filaments on the outside of the neck have a greater path length to follow and therefore draw more than filaments centrally located in the hot yarn.

On the other hand, because of the radial migration which took place at the cold zone entrance, interchange of radial position will occur for each filament along its length as it enters the hot zone. This interchange assures that each filament will be subjected to different draw ratios along its length. However, the average draw ratio in a long yarn segment is equal for all filaments. Figure 2.6 shows an example of how draw ratio may vary along a yarn length for two different filaments.

Figure 2.6

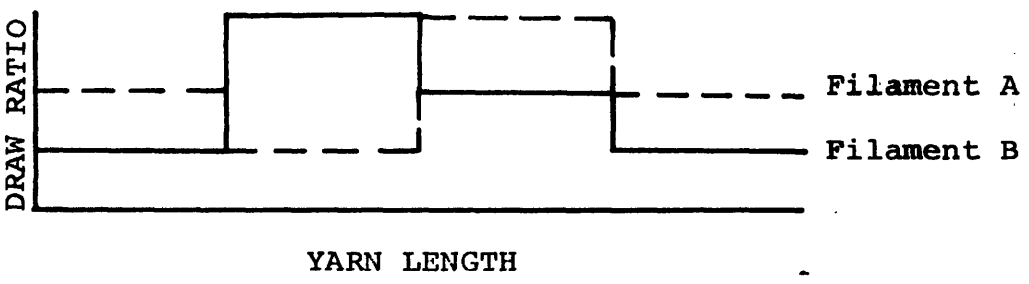

The filament drawing extension in the hot zone can be determined from its path length as is shown in Figure 2.7.

Figure 2.7

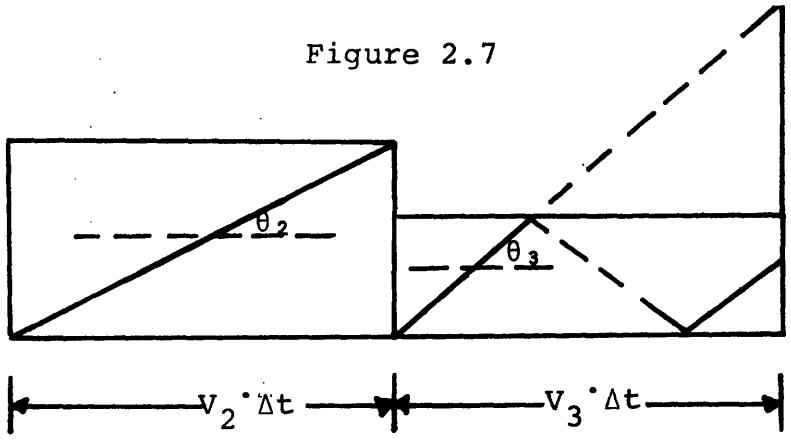

Let $V_2 \Delta t$ = Length of yarn entering the neck in time Δt

$V_3 \Delta t$ = Length of yarn leaving the neck in time Δt

Each $(V_2 \cdot \Delta t)$ yarn length contains $(V_2 \sec\theta_2 \cdot \Delta t)$ filament length. As this length moves through the hot yarn neck during Δt it is drawn to the new length $(V_3 \sec\theta_3 \cdot \Delta t)$. Thus the filament drawing extension in the neck is simply:

$$\text{Extension} = \frac{V_3 \sec\theta_3 \Delta t - V_2 \sec\theta_2 \Delta t}{V_2 \sec\theta_2 \Delta t} \qquad (2\text{-}29)$$

$$= \frac{V_3 \sec\theta_3}{V_2 \sec\theta_2} - 1 \qquad (2\text{-}30)$$

It should be pointed out that filament drawing extension expressed in eq. (2-29) does not include the cold zone strain referred to in (2-23). For it can be shown that the cold modulus of the filament far exceeds its "drawing modulus" and thus the levels of filament extension present in the cold

zone are about two orders of magnitude lower than the drawing extensions. Therefore neglect of cold strain is justified when determining filament drawing extension.

Having determined filament drawing extension by means of eq. (2-30), we must now develop information on its constitutive relationship. And from the latter we will be able to calculate filament drawing tensions.

Since the constitutive behavior of fibrous polymers incorporates the influence of temperature and strain rate, it was deemed advisable to measure the local extension behavior under the same machine conditions as in actual texturing. The MITEX False Twisting Apparatus was accordingly used as a continuous extensometer by simply bypassing the pin spindle and measuring the threadline tension for different draw ratios and temperatures. The load-extension data were fit to polynomial expressions through regression analysis and the expression shown below forms the material-system constitutive relationships used in determining filament tensions in the hot draw-uptwist zone:

$$\text{Filament Tension} = A\,(\text{Draw Ratio})^2 + B(\text{Draw Ratio})^3 \qquad (2\text{-}31)$$

The data on which (2-31) is based, are presented in Appendix 3. Finally the threadline tension at the hot zone entrance can be determined from knowledge of hot zone geometry,

filament extensions, and material-system constitutive relations. Hot zone tension is expressed simply, as:

$$T_{\text{hot zone}} = \sum_i \text{Tension}_i N_i \cos\theta_i \qquad (2\text{-}32)$$

Substituting (2-31) into (2-32) we obtain

$$T_{\text{hot zone}} = \sum_i \left\{ A(\text{Draw Ration}_i)^2 + B(\text{Draw Ratio}_i)^3 \right\} N_i \cos_i\theta \qquad (2\text{-}33)$$

where N_i = Number of filaments in i^{th} radial layer

θ_i = Helix angle of the i^{th} radial layer

Draw Ratio_i = Draw Ratio of filaments in the i^{th} radial yarn layer

A,B are experimentally determined material-system properties.

2.3.7 Hot Zone Torque

The heater is provided in the texturing zone to effect heat setting of the thermoplastic feed yarn. In mechanical terms, this takes place as a result of hot relaxation of cold zone fiber stresses. As indicated, the filament stresses in the cold zone included bending, torsional and tensile stresses. But as the above mentioned components of threadline torque are heat relaxed, the line torque cannot be kept constant unless the yarn uptwists, which according to all observations it does. This uptwisting incurs some additional filament

bending and torsion strains but the resulting stresses are negligible due to the extremely low hot moduli. For the case of the added tensile strains, due to drawing the filament tensions increase significantly to provide the requisite threadline tension. Accordingly, the assumption in our model is that threadline torque at the heater entrance is based solely on filament tensile forces. Thus hot yarn torque can be expressed as:

$$M_{t\ \text{hot zone}} = \sum_i \text{Load}_i N_i R_i \sin\theta_i \qquad (2\text{-}34)$$

or substituting (2-31) into (2-34)

$$M_{t\ \text{hot zone}} = \sum_i (A\ \text{Draw Ratio}_i^2 + B\ \text{Draw Ratio}_i^3)\ N_i R_i \sin\theta_i \qquad (2\text{-}35)$$

2.3.8 Calculation of Twist

As indicated previously, there are essentially two levels of twist in the texturing threadline: the cold zone twist (which is a fraction of the hot zone twist) and the hot zone twist. We assume that the hot zone twist and the cooling zone twist are equal.

If the hot zone rotational velocity is W_h and the cold zone rotational velocity W_c then the relative rotational velocities before and after the hot zone entrance is $W_h - W_c$ and this quantity determines the rate of uptwist at this

station according to

$$P_{h(\text{incremental})} = \frac{W_h - W_c}{V_3} \qquad (2\text{-}36)$$

where W_h = Angular velocity of hot twisted yarn segment (radians/second)

W_c = Angular velocity of cold twisted yarn segment (radians/second)

V_3 = Linear velocity of hot twisted yarn

$P_{h\ (\text{incremental})}$ = hot uptwist/hot twisted length (radians/twisted length)

The hot incremental twist is added to the twist that already exists in the cold zone due to the angular velocity of the cold zone

$$P_c = W_c/V_2 \qquad (2\text{-}37)$$

where P_c = Cold twist (radians/cold twisted length)

V_2 = Linear velocity of cold twisted yarn segment

The cold twist per unit cold twisted length is reduced as the cold yarn segment is extended by the ratio V_2/V_3 so that the cold twist per unit hot twisted length, $P_{c/h}$, is

$$P_{c/h} = P_c\ V_2/V_3 = \frac{W_c V_2}{V_2 V_3} = W_c/V_3 \qquad (2\text{-}38)$$

The <u>total</u> hot twist per unit hot twisted length is obtained by adding (2-36) and (2-38)

$$P_h = W_c/V_3 + \frac{W_h - W_c}{V_3} = W_h/V_3 \qquad (2\text{-}39)$$

where P_h = Hot twist per unit hot twisted length

2.3.9 Calculation of Hot Twisted Yarn Velocity

Experimental observation of the twist distribution on the spindle surface indicates that the twisted yarn in the texturing zone generally untwists at the last quadrant of the spindle surface[4]. From this fact it can be assumed that the tension in the yarn during untwisting is approximately equal to the post spindle threadline tension. The approximate twist distribution at the spindle is illustrated below.

Figure 2.8

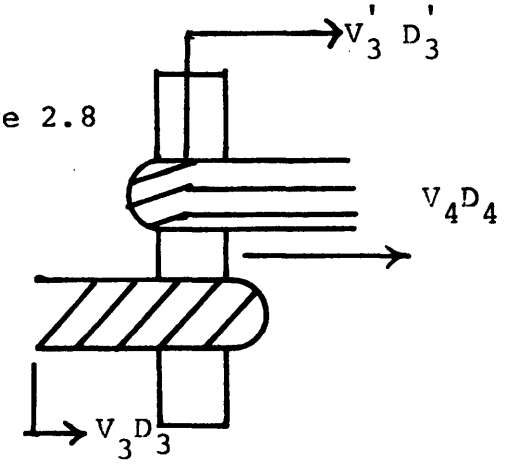

The mass continuity requirement is expressed as:

$$V_3 D_3 = V_3' D_3' = V_4 D_4 \qquad (2\text{-}40)$$

where V_3 = Linear velocity of twisted yarn, before spindle

V_3' = Linear velocity of twisted yarn, at post

spindle tension

V_4 = Linear velocity of untwisted yarn, at post spindle tension

D_3 = Denier of twisted yarn, before spindle

D'_3 = Denier of twisted yarn, at post spindle tension

D_4 = Denier of untwisted yarn, at post spindle tension

The friction between the yarn and spindle causes the tension in the yarn to rise as the yarn progresses downstream around the spindle surface. This tension differential and hence yarn strain differential causes the yarn denier in the last quadrant of the spindle to decrease slightly. Therefore

$$D_3' \ (1 + \varepsilon_{yarn}) = D_3 \qquad (2\text{-}41)$$

where ε_{yarn} = yarn strain differential across the pin

Now $$V_3 D_3 = V'_3 D'_3 \qquad (2\text{-}40)$$

Then $$\frac{V'_3}{V_3} = (1 + \varepsilon_{yarn}) \qquad (2\text{-}42)$$

From (2-40) and (2-42)

$$V'_3 D'_3 = V_4 D_4 \qquad (2\text{-}40)$$

and $$V_3(1 + \varepsilon_{yarn})D'_3 = V_4 D_4 \qquad (2\text{-}43)$$

The cooling twist contraction factor for the cooling yarn, $\underline{Cr}_{cool}$, can be expressed as

$$\underline{Cr}_{cool} = \frac{V_4}{V'_3} = \frac{D'_3}{D_4} \qquad (2\text{-}44)$$

Substituting (2-44) into (2-43) we obtain

$$V_3(1 + \varepsilon_{yarn}) = \frac{V_4}{\underline{Cr}_{cool}} \qquad (2\text{-}45)$$

Again we must make the decision as to which model for cooling yarn twist contraction factor we should use in the analysis. Experimental evidence given below indicates that Hearle's Model for cooling yarn twist contraction fits the experimental data closer than does the Alternative Model.

Cooling Yarn Twist Contraction

1.60 Draw Ratio 210°C Heater Temperature

Machine Twist	Measured	Hearle's Model	Alternative Model
50	1.263	1.305	1.220
60	1.396	1.438	1.330
65	1.592	1.601	1.468
80	1.795	1.926	1.745

Experimental evidence presented in Appendix 2 shows that for a range of steady state operating condition, the tensile gradient of the threadline across the spindle will result in incremental yarn strains, e_y, of less than 1%. And since the

filament strains in the draw region of the texturing zone are of the order of 60% to 80%, it follows that for the common range of draw texturing conditions, neglect of the strain gradient across the spindle will not significantly affect the calculated value of hot threadline velocity, V_3.

2.3.10 Calculation of Yarn Radii

Most draw texturing feed yarn filaments have circular cross sections. When twisted in a yarn structure the filaments generally take the spatial geometry shown in Figure 2.9. For 34 or 30 filament feed yarns (common apparel yarn structures) there is one central core filament surrounded by three radial layers of filaments. It is common practice to model the structure with 6 filaments in the first layer followed by 12 filaments in the second layer and either 15 or 11 filaments in the outer radial layer depending on the total number of filaments in the structure. The cold yarn radius is then seven times the cold filament radius. Table 2.1 compares the actual cold yarn radii with calculated values. The agreement is good.

When a filament is drawn in the draw texturing process, the ratio of drawn filament radius to the undrawn filament radius is

$$\frac{r_{drawn}}{r_{undrawn}} = \sqrt{\frac{\rho_{undrawn}}{\rho_{drawn}} \frac{1}{\text{draw ratio}}} \qquad (2\text{-}46)$$

where ρ = filament density

Figure 2.9

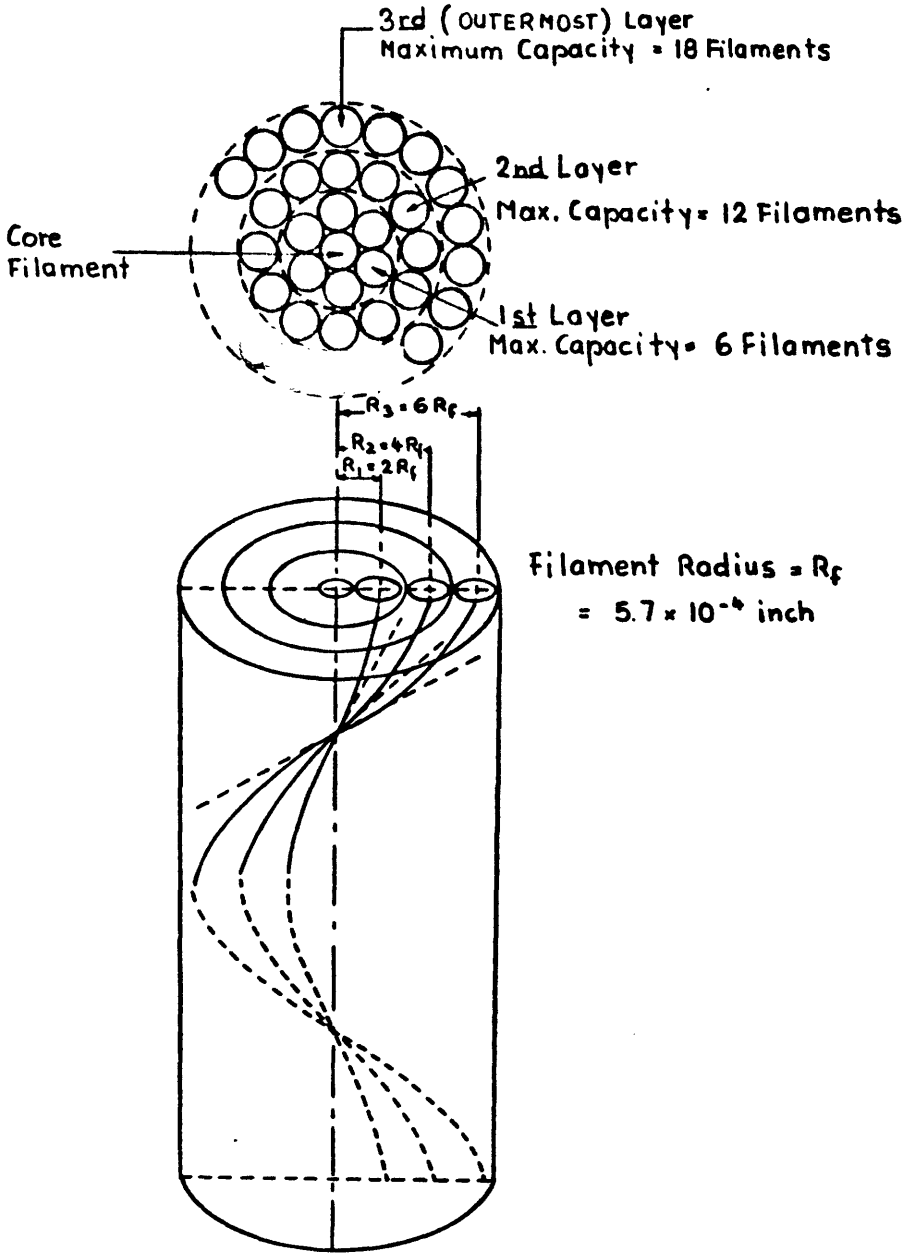

YARN STRUCTURE FOR POY POLYESTER

245/30 DENIER

Table 2.1 YARN DIMENSIONS FOR POY POLYESTER 245/30 DENIER

					1.60 DRAW RATIO	
Machine Twist	Draw Ratio	Heater Temperature	Measured Cold Radius (10^{-4})in	Calculated Cold Radius (10^{-4})in	Measured Hot Radius (10^{-4})in	Calculated Hot Radius (10^{-4})in
50	1.6	210°C	39.1	39.9	28.1	31.1
60	1.6	210°C	40.9	39.9	30.2	31.1
65	1.6	210°C	39.9	39.9	29.2	31.1
70	1.6	210°C	40.6	39.9	30.4	31.1
80	1.6	210°C	40.0	39.9	32.8	31.1
50	1.6	190°C	38.5	39.9	27.0	31.1
60	1.6	190°C	38.0	39.9	28.1	31.1
65	1.6	190°C	39.3	39.9	29.1	31.1
70	1.6	190°C	38.8	39.9	30.1	31.1
65	1.6	230°C	38.5	39.9	28.3	31.1
65	1.57	210°C	39.9	39.9	29.0	31.4
65	1.64	210°C	38.9	39.9	27.9	30.7

Shealy and Kitson[10] show that the ratio of densities for partially drawn polyester to drawn polyester is 0.972. Thus the ratio of filament radii for POY PET according to (2-46) is

$$\frac{r_{drawn}}{r_{undrawn}} = .986 \sqrt{\frac{1}{\text{draw ratio}}}$$

Thus we conclude that a good approximation of the hot yarn radius is:

$$\frac{r_{hot\ yarn}}{r_{cold}} = .986 \frac{1}{\sqrt{\text{machine draw ratio}}} \qquad (2\text{-}47)$$

Using (2-47) for various threadlines we obtain the values of hot yarn radii given in Table 2.1. These predicted values are compared to measured values and manifest good agreement.

For the purpose of computation the radial distance from each filament centroid in a given layer to the yarn center is used as the radius of that yarn layer. For example, the radius of the third radial layer is 6 filament radii, rather than 6 1/2. The latter quantity represents the outer radius of that layer.

2.3.11 Summary

An analysis of steady state threadline mechanics has been presented in this section, with a view towards determining steady state levels of threadline torque and threadline tension, as well as twist distribution over the entire texturing zone. To undertake calculations based on this analysis,

one requires information concerning texturing machine settings (i.e. spindles speed, feed roller velocity, take up roller velocity, and heater temperature) and feed stock material properties. No additional information or measurements are necessary. The treatment of the threadline mechanics incorcorporates several simplifications and assumptions in accord with numerous experimental observations:

1. All filaments are strained equally in the twisted yarn of the cold zone.
2. The effect of interfiber friction and transverse stresses on threadline torque is considered negligible at the cold zone and hot zone entrances.
3. The friction between yarn and spindle does not significantly affect linear velocities of the threadline in draw texturing.
4. Hot zone threadline, cooling zone threadline, and spindle rotational velocities are equal.
5. The twist in the texturing zone has two uniform levels, one for the cold zone, the second for the hot and cooling zones.
6. Tension and torque in the texturing threadline are uniform from the entry roll to the spindle.
7. Inertial effects on threadline mechanics are considered negligible.
8. Filaments in the twisted threadline follow ideal

right circular helices.

9. Threadline torque at the entrance to the hot zone is primarily due to fiber tension.
10. In order to calculate twist contraction in the cold zone two different models are used, one based on an averaging over the entire cross section, the other based on an averaging over the yarn radius. The former model (averaged over the entire yarn section) is used to calculate twist contraction in all other zones.

In the next section computations based on these steady state analyses are compared with measured experimental results obtained in draw texturing of partially oriented polyester yarn (POY-PET). In a subsequent section we will furnish similar comparisons for texturing experiments with partially oriented nylon.

2.4 EXPERIMENTAL STUDY OF STEADY STATE DRAW TEXTURING

2.4.1 Materials and Texturing Apparatus

Polyester partially oriented yarn (POY PET) produced by the DuPont Company has been used for the experimental study. The dimensions and properties of the feed yarn are as follows:

Undrawn Filament Denier 245/30	8.17
Undrawn Filament Radius	5.7×10^{-4} in
Undrawn Filament Tensile Modulus	4.8×10^{5} psi
Undrawn Filament Bending Rigidity	3.97×10^{-8} lb-in^2

Undrawn Filament Torsional Rigidity 1.30×10^{-8} lb-in^2

Filament dimensions and tensile modulus were measured in the Fibers and Polymers Laboratories at M.I.T. The bending modulus was calculated from the tensile modulus based on the assumption of equal axial tensile and compressive moduli. The torsional rigidity (GI_p) measured on drawn PET by Mr. J. Donovan of F.R.L. was considered applicable to the current partially drawn specimen in accordance with Ward's [11] observation that GI_p does not vary significantly with axial draw ratio.

A laboratory pin-spindle false twist texturing machine developed at MIT (MITEX False Twister) has been used for our draw texturing studies. A picture of the MITEX False Twister is presented in Appendix 4. In this apparatus the surface speed of the feed rollers is 0.29 inches per second. The take up roller speed is varied in accordance with the required draw ratio. The pin-spindle is driven by a motor-belt combination and the spindle speed is controlled by a Variac Speed Controller and monitored periodically by a General Radio Strobotac. The spindle speed is varied in accordance with the desired machine twist. The heater temperature controller unit is a standard Rosemount device which is used in commerical texturing operations. Its accuracy is within ±3°C. The threadline

torque and threadline tension are measured by the MITEX torque -tension Meter. Its method of operation is described in Appendix 4.

2.4.2 Results and Discussion

Given the machine settings, i.e. machine draw ratio, basic or machine twist, and heater temperature, and material properties,one can use the computer subroutine "YARN" listed in Appendix 5 to determine the cold threadline,hot and cooling threadline twist levels and threadline torque and tension. Comparisons of the experimental and predicted results are given in Table 2.2 and Figures 2.10, 2.11 and 2.12. Model 1 includes the method of radial averaging for cold twist contraction given in section 2.3.2 and Model 2 incorporates Hearle's method of determining cold twist contraction given in Section 2.3.2.

The results show that there is good agreement over a wide range of machine twists between the experimental data and the predicted threadline behavior for both cold twist contraction models. At machine twists above 70 TPI the agreement is reduced. For example at 80 TPI machine twist, the percentage differences between the experimental and predicted cold twist, hot twist, threadline torque, and threadline tension are 24.6%, 29.6%, 2.4%, and 11.9% respectively for Model 1, and 38.8%, 29.6%, 22.8% and 11.3% respectively for Model 2. Observation of texturing threadline segments presented in Figure 2.13 in-

Table 2.2

COMPARISON OF MEASURED AND PREDICTED VALUES OF THREADLINE PARAMETERS

Machine Twist	Draw Ratio	Heater Temp.	Tension, grams			Torque(10^{-4}) in lbs			Cold Twist, TPI			Cooling Twist, TPI		
			Measured	Predicted Model 1	Model 2	Measured	Predicted Model 1	Model 2	Measured	Predicted Model 1	Model 2	Measured	Predicted Model 1	Model 2
45	1.60	210°C	30.9	26.2	28.7	1.25	1.25	1.35	20.6	23.4	24.2	57.1	54.3	54.3
50	1.60	210°C	24.8	25.0	27.9	1.47	1.43	1.57	25.2	26.9	28.0	63.7	63.4	63.4
55	1.60	210°C	23.8	23.6	26.9	1.64	1.61	1.80	28.7	30.7	32.2	71.7	74.0	74.0
60	1.60	210°C	20.3	22.1	25.8	1.67	1.80	2.04	38.0	34.8	36.8	80.2	86.3	86.3
65	1.60	210°C	18.4	20.4	24.4	2.34	1.99	2.29	39.9	39.2	41.9	99.7	101.2	101.2
70	1.60	210°C	17.7	18.6	22.8	2.34	2.18	2.54	40.6	44.0	47.6	102.6	119.7	119.7
80	1.60	210°C	16.8	14.8	18.7	2.50	2.56	3.07	44.3	55.2	61.5	134.9	174.8	174.8
50	1.60	190°C	24.4	25.1	27.6	1.54	1.40	1.52	22.3	26.4	27.4	61.0	63.4	63.4
60	1.60	190°C	20.5	22.2	25.4	2.40	1.75	1.96	36.1	34.0	35.8	81.8	86.3	86.3
65	1.60	190°C	18.7	20.6	24.0	2.39	1.93	2.20	39.0	38.2	40.7	90.4	101.2	101.2
70	1.60	190°C	17.7	18.8	22.4	2.31	2.12	2.40	39.2	42.8	46.1	100.5	119.7	119.7
65	1.60	230°C	17.5	20.1	23.6	2.24	1.93	2.20	38.1	38.4	41.0	99.6	101.2	101.2

(note: each data point represents at least five independent measurements)

Figure 2.10

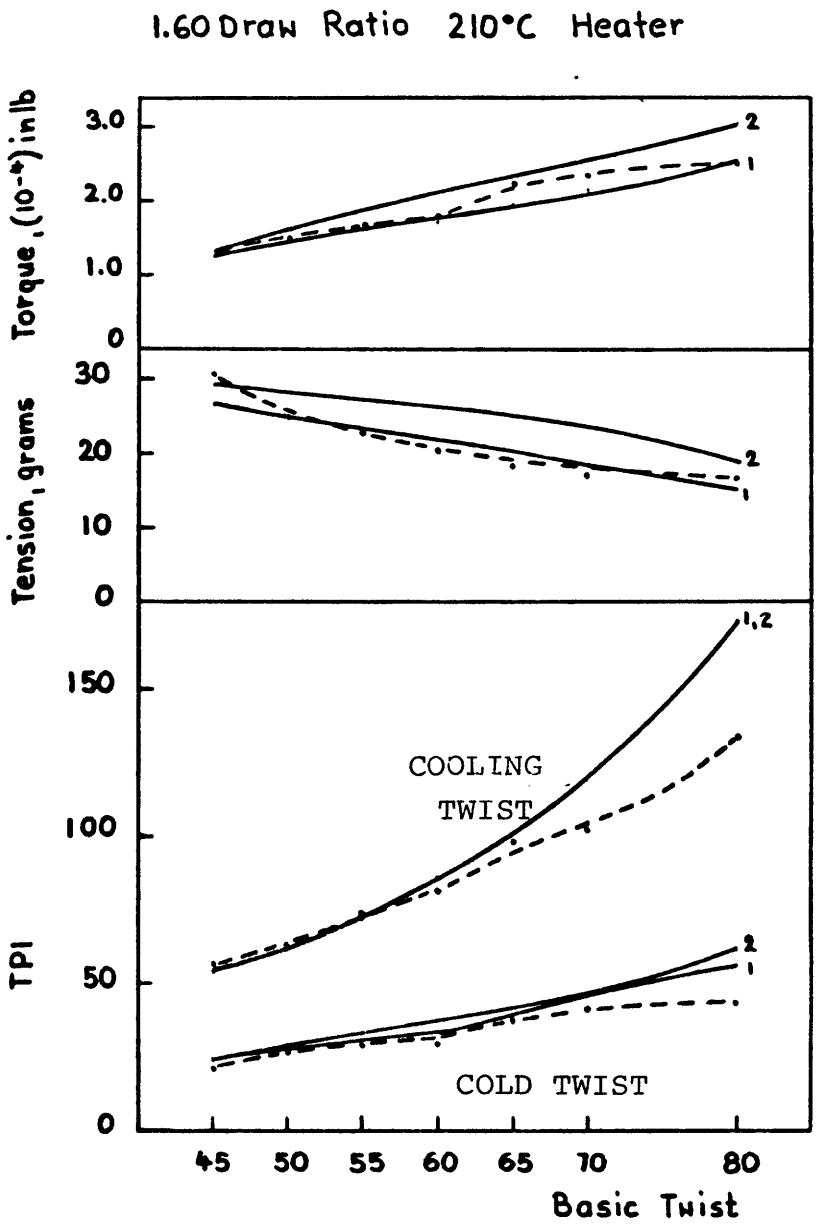
1.60 Draw Ratio 210°C Heater
Torque, (10⁻⁴) in lb
3.0
2.0
1.0
0
Tension, grams
30
20
10
0
TPI
150
100
50
0
COOLING TWIST
COLD TWIST
45
50
55
60
65
70
80
Basic Twist
experimental
predicted

Figure 2.11

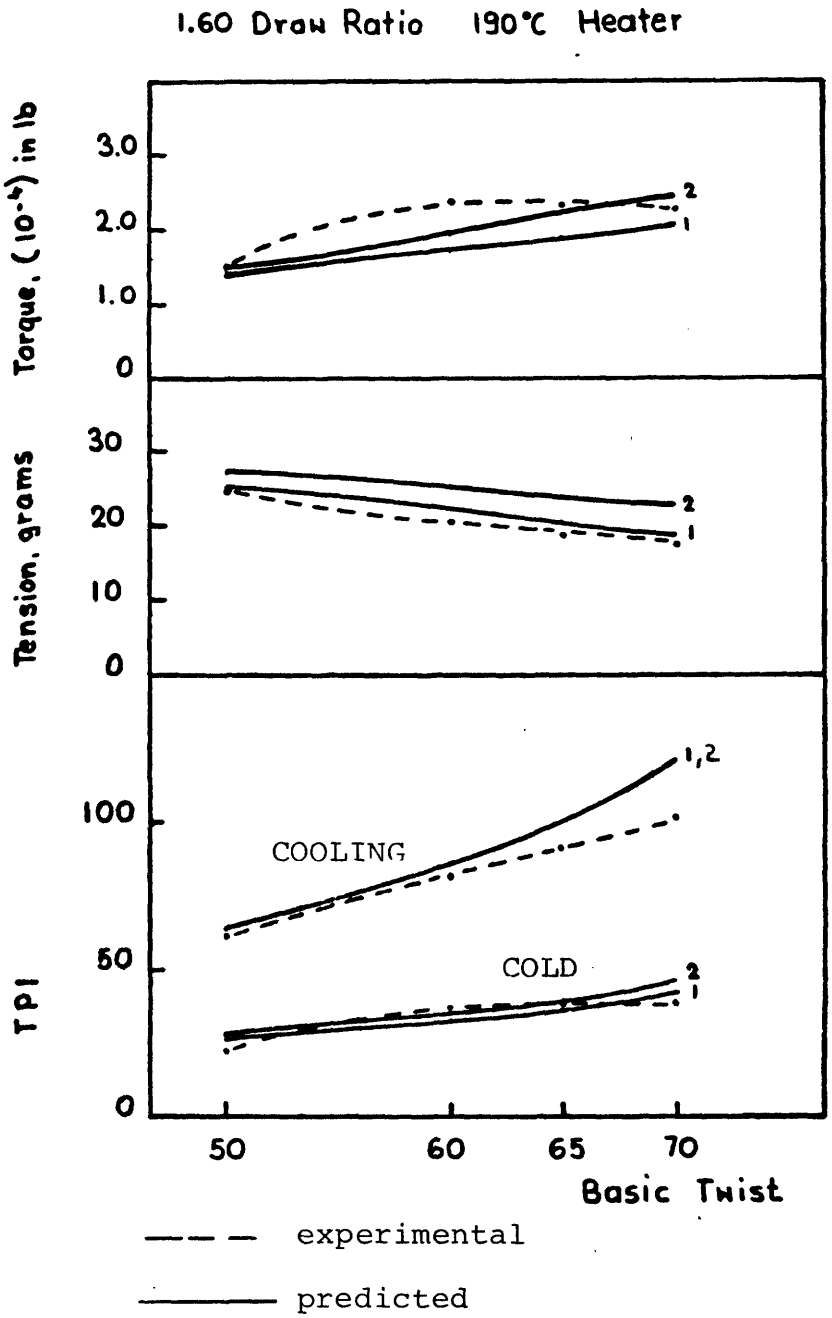
1.60 Draw Ratio 190°C Heater
Torque, (10^{-4}) in lb
3.0
2.0
1.0
0
Tension, grams
30
20
10
0
TPI
100
50
0
COOLING
COLD
1,2
2
1
50
60
65
70
Basic Twist
experimental
predicted

Figure 2.12

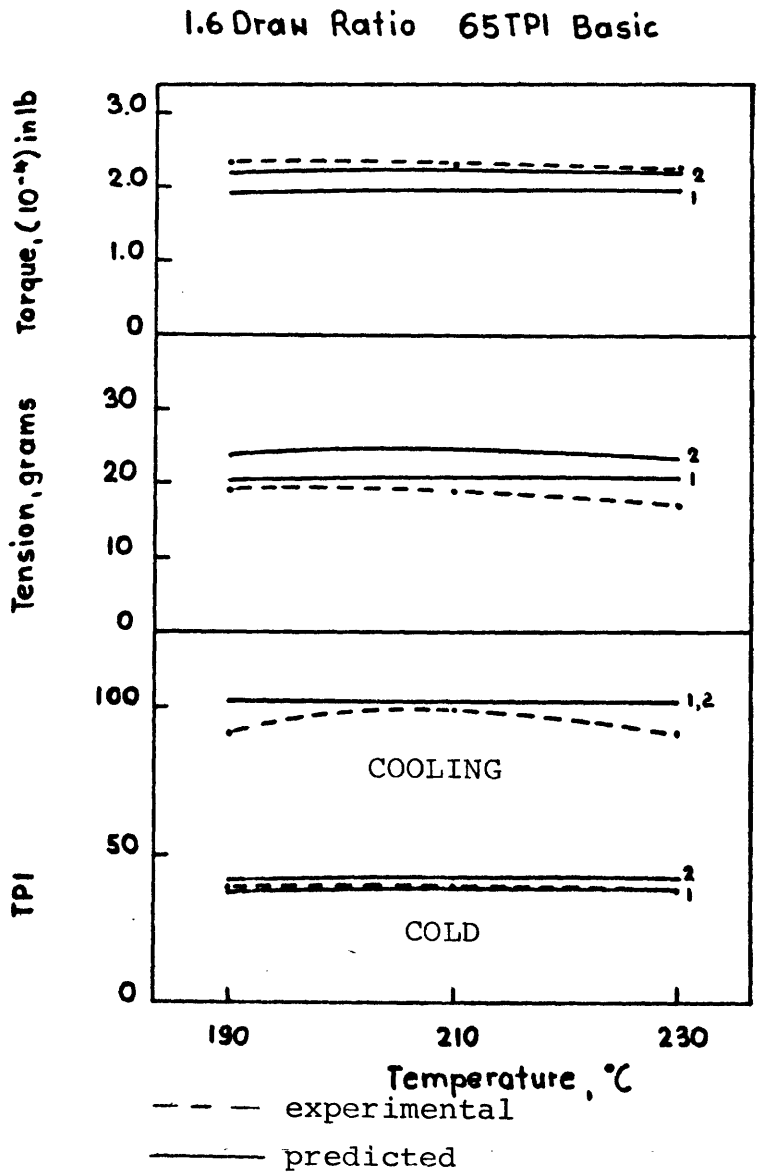
1.6 Draw Ratio 65TPI Basic
Torque, (10⁻⁴) in lb
3.0
2.0
1.0
0
Tension, grams
30
20
10
0
TPI
100
50
0
2
1
1,2
COOLING
COLD
190
210
230
Temperature, °C
experimental
predicted

DRAW TEXTURING THREADLINES

245·34 POY PET 1.60 DRAW RATIO 210°C. HEATER

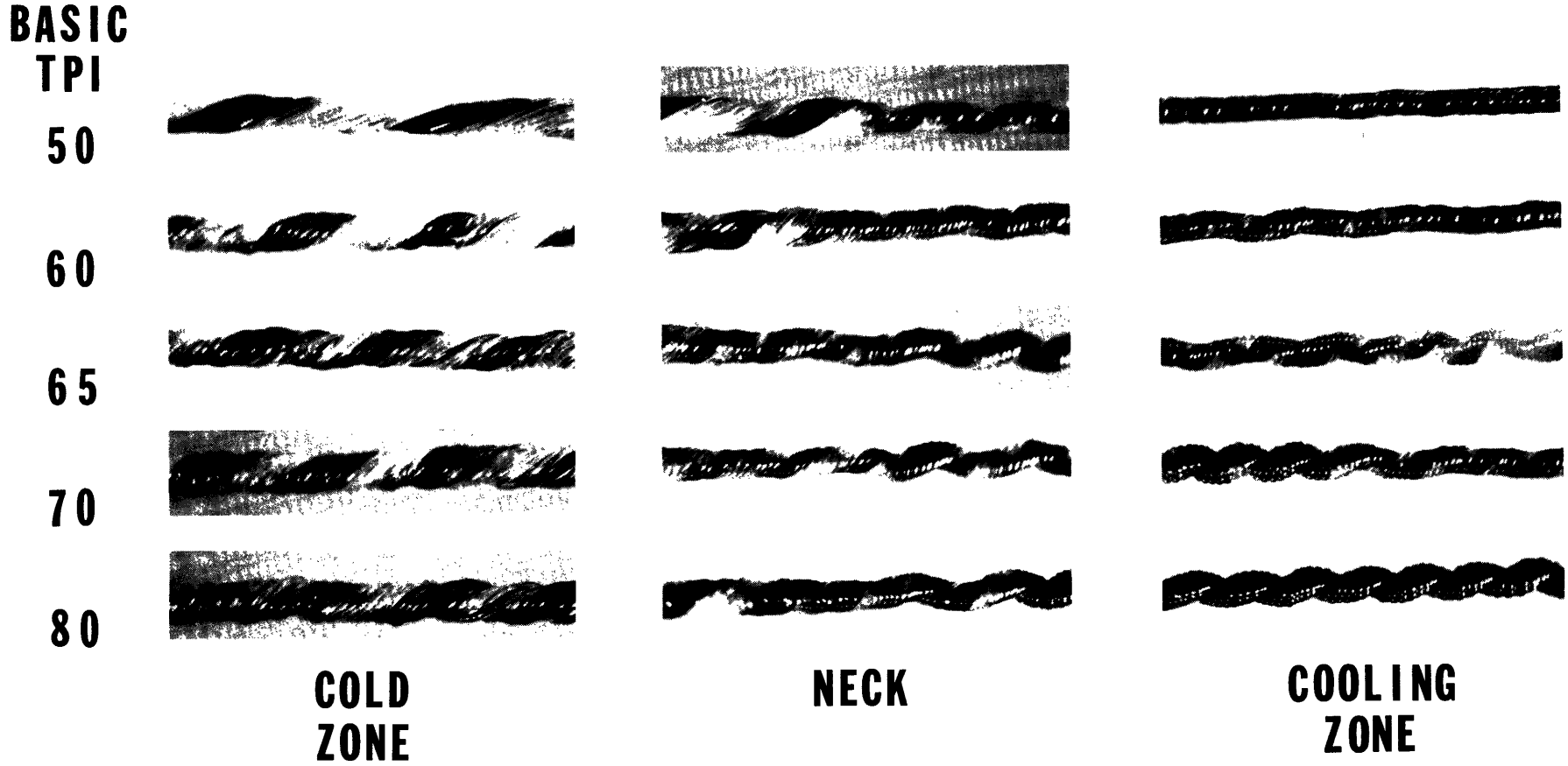

dicated when machine twist is increased to and beyond 65 TPI, twisted filaments lose their circular helical geometry. At 80 TPI the cooling zone segments are continuously torsionally buckled. Such buckling invalidates the geometric components of our assumptions so that the disagreement at 80 TPI is not unexpected.

We have calculated the root mean square of the percentage error for threadline cold twist and hot twist, threadline torque and threadline tension for each of these models under a variety of processing conditions and these values are given below:

Table 2.3

	Model 1	Model 2
Tension	9.3%	23.4%
Torque	12.2%	12.0%
Hot Twist	12.3%	12.3%
Cold Twist	10.9%	16.7%

It is clear that Model 1 provides better agreement between theory and experiment and so it will be employed in the analysis of unsteady operation of the draw texturing process.

Figures 2.10 and 2.11 (which represent somewhat different operating conditions) show that as machine twist is increased while heater temperature and machine draw ratio are kept constant, threadline tension decreases and the threadline torque increases. This seemingly contrary behavior can be

attributed to the increase in local filament helix angles in the outer layers of the yarn, which reduces the yarn axial component of filament tension and increases its circumferential component.

As the machine twist increases, the variation of draw ratios in different filament layers in the drawing neck increases. Table 2.4 presents the draw ratios computed for each layer of filaments as well as the draw ratio RMS value for all filaments in a given yarn cross section at a given machine draw ratio.

Table 2.4

Machine Draw Ratio 1.60 Heater Temperature 210°C

Machine Twist	Core	1st Layer	2nd Layer	3rd Layer	RMS
45 TPI	1.374	1.428	1.565	1.735	13.9%
50 TPI	1.323	1.394	1.564	1.760	16.0%
55 TPI	1.266	1.358	1.565	1.784	18.0%
60 TPI	1.204	1.322	1.569	1.809	20.1%
65 TPI	1.134	1.286	1.577	1.833	22.3%
70 TPI	1.057	1.251	1.589	1.857	24.8%

It should be noted that even though there is a radial distribution of filament draw ratios. The weighted average of the filament draw ratios must equal the machine draw ratio during steady state operations.

Figure 2.12 shows that temperature of the heater over the range tested does not greatly affect the threadline proper-

ties. This follows from the fact that the common range of texturing temperatures has minimal effect on hot filament drawing forces.

2.5 EFFECT OF MATERIAL PORPERTIES ON STEADY STATE THREADLINE BEHAVIOR

If the fiber producer were to alter two material properties of the texturing, i.e. cold shear modulus and cold extensional modulus, such modification would affect the threadline behavior during texturing. The predicted influence of changes in either modulus, while the other is kept constant is shown in Figures 2.14 and 2.15 These graphs indicate that if the shear modulus or extensional modulus is increased, both threadline torque and tension increase, while cold zone twist level decreases. Since the hot zone twist was previously indicated to be a function solely of yarn throughput speed and spindle speed, the hot zone twist remains unchanged for this case in which the cold feed yarn properties are modified.

The effect of doubling either modulus on a given threadline response, i.e. threadline torque, threadline tension, or cold twist level is presented in Table 2-5. It can be concluded that the relative changes in threadline response are minimal considering the magnitude of either modulus change.

Figure 2.14

Threadline Parameters vs. Young's Modulus

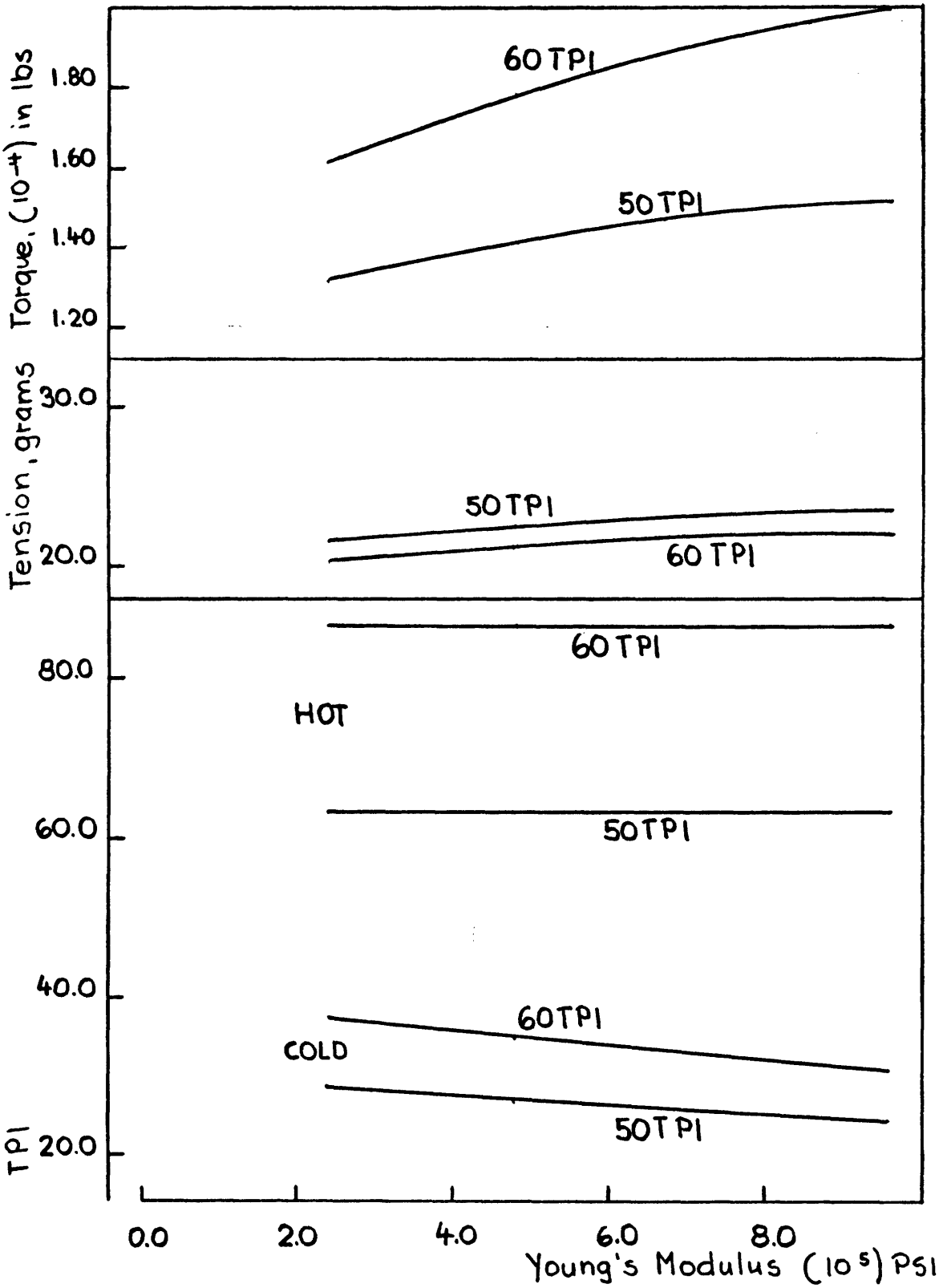

Figure 2.15

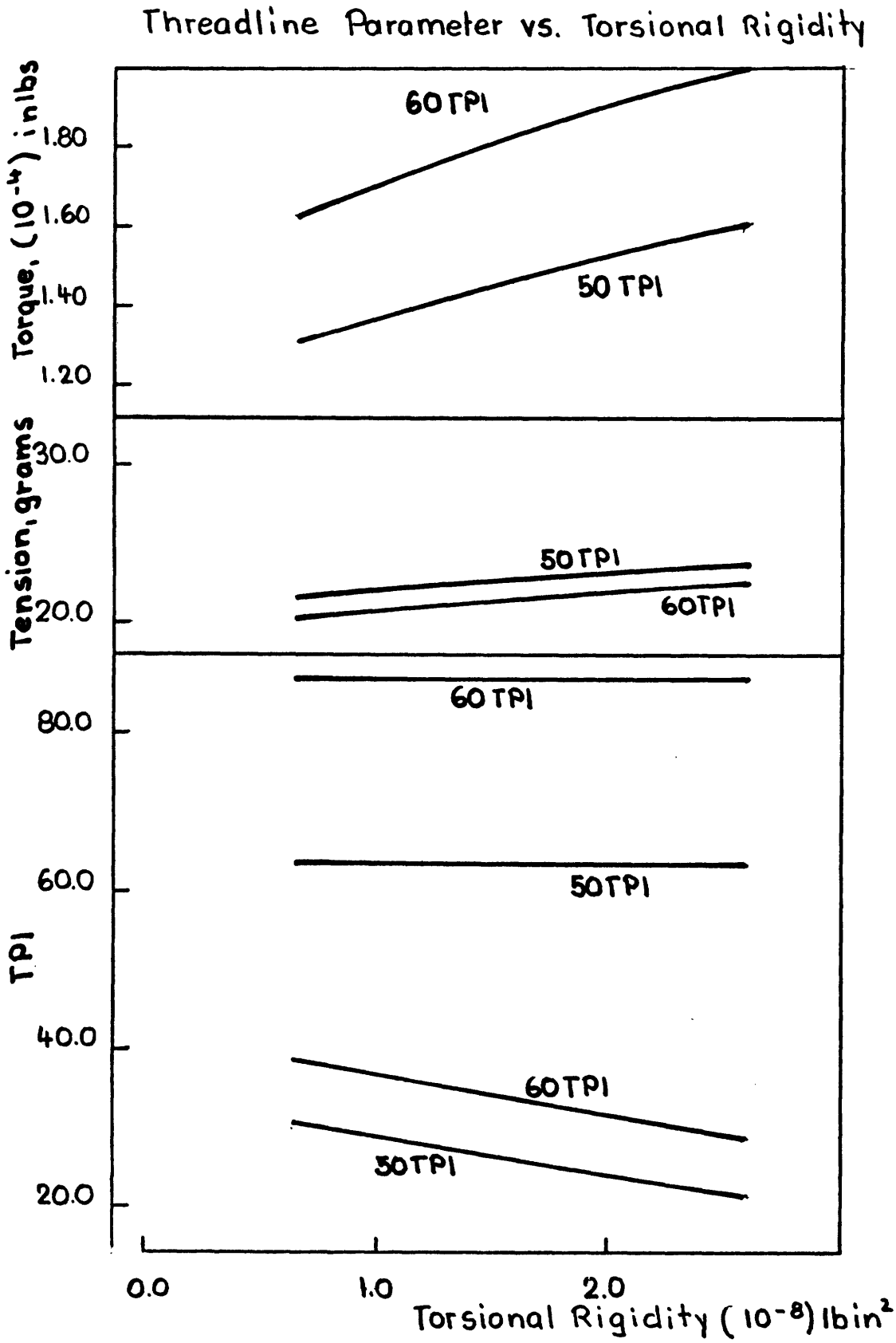
Threadline Parameter vs. Torsional Rigidity
Torque, (10^{-4}) in lbs
1.80
1.60
1.40
1.20
60 TPI
50 TPI
Tension, grams
30.0
20.0
50 TPI
60 TPI
80.0
60.0
60 TPI
50 TPI
TPI
40.0
20.0
60 TPI
50 TPI
0.0
1.0
2.0
Torsional Rigidity (10^{-8}) lbin^2

Table 2.5

Machine TPI	Per Cent Torque Increase 50	60	Per Cent Tension Increase 50	60	Per Cent Cold Twist Increase 50	60
Shear Modulus, + 100%	15%	15%	5%	5%	-23%	-23%
Extensional Modulus + 100%	6 %	7%	2%	2%	-10%	-10%

As has been often pointed out in the literature, the cold tensile modulus is dependent on the draw ratio of the feed yarn, but the cold shear modulus according to Ward [11] is not. Therefore changes in cold tensile modulus are easily accomplished via the fiber producers process control but shear modulus changes require more fundamental alterations in polymer composition or fine structure. (We will discuss the effect of material changes in a later section dealing with experiments on partially drawn nylon).

Obviously, the simplest modification which can be brought about in feed yarn properties is accomplished by changing filament denier for a given yarn denier. One would expect that lower filament deniers in such a case, would increase the tensile contribution to yarn torque in the cold zone. This direction of change is being developed in the fiber industry. Further changes for a given fiber and yarn denier are easily brought about by altering the filament cross sectional profile, and this method is also under industrial development.

CHAPTER 3

TRANSIENT OPERATION

3.1 INTRODUCTION

It was observed in earlier studies that when texturing spindle speeds were suddenly altered, the first signs of twist change in the threadline occurred at the entry to the heater.[12] It was at this location, during steady state texturing of PET pre-drawn yarns, that the yarn softened and the twist rose rapidly from a relatively low cold zone value to a relatively high hot zone value. Transient twist changes introduced at the heater entrance during non-steady spindle rotation appeared to lock in, remaining essentially unchanged as they moved with the threadline down towards the spindle. And a short time after the distrubance one observed that the transient twist distribution beyond the heater was tilted downward in the downstream direction for a spindle speed increase and tilted up in the downstream direction for a spindle speed decrease. Seemingly, the threadline achieved unusually high torsional rigidity after it passed the heater and locally at the heater entry, it appeared to be torsionally soft.

An experimental study was undertaken to confirm the presence of a torsionally "soft" segment in the threadline at the heater entrance and of a highly rigid segment at the

heater exit and reaching beyond to the spindle. The results of these experiments clearly confirm the presence of a soft segment and a rigid segment in the threadline beyond the heater. Further they indicate the presence of an additional soft segment located at the entry to the cold zone and a rigid segment consisting of the remainder of the cold zone.

A complementary study was undertaken to determine to what extent this mode of threadline behavior occurs in the draw texturing system. Experimental results indicate that in the draw texturing threadline there are also regions of torsionally soft material at the cold zone and heater entrance and rigid segments in the remainder of the cold zone and cooling zone.

This twist formation behavior during non-steady operation is significant since the twist level at the spindle at a given moment is not necessarily the same as the twist level at the heater entry. Rather, the twist level at the spindle at a given moment is equal to that which formed at the heater entrance at an earlier time.

This chapter is divided into three parts. First, we present the experimental observations which are subsequently used to model transient operation of the draw texturing system. In the second part we develop two theoretical models of the transient operation of the draw texturing system along with experimental verification of their validity.

Finally the models used to predict threadline response to unsteady machine operation resulting from such causes as unsteady material delivery or material take up, oscillating spindle speed, etc.

3.2 OBSERVATIONS OF TORSIONAL BEHAVIOR OF THE TEXTURING THREADLINE

3.2.1 Experiments Using Pre-Drawn PET Yarns

The interactions between processing parameters and threadline tension of the textured yarn were measured on the MITEX False Twist Texturing Device, which permitted monitoring of threadline tension through strain gage detection of the in-line forces acting on the feed roll assembly[6]. For these particular tests the machine conditions were, set as follows, unless otherwise specified:

Feed Speed	1.1 in/sec	Cold Zone Length	5 in
Overfeed	1.8%	Cooling Zone Length	5 in
Temperature	210°C	Twist Direction	S
Heater Length	1.5 in	Pretension	0 g.f.

The machine parameter varied was machine (or basic) twist, defined as the RPM of the spindle divided by surface velocity of the take-up roller. Four levels of twist were used: 30,45,56, and 60 TPI (basic). The texturing machine was stopped after operating in steady state at each of the above conditions and yarn segments from the cold zone and

from the cooling zone were affixed to a temporary cardboard-clamp system to prevent retraction and/or untwisting. The yarn segment was then transferred to a torsion wire instrument, clamped at its top end to the base of the vertical calibrated wire, and attached to a T-bar clamp at its bottom end. This mounting procedure was completed without releasing the twist and without causing further extension of the yarn segment being tested. Suitable weights were then added to the T-bar so as to apply to the yarn that level of tension which had been recorded during texturing, but without permitting the T-bar to rotate. Thus, the yarn segment in the instrument was kept under a tension equal to that of the texturing zone. At this moment, the angular rotation of the torsion wire was observed and the yarn torque was calculated. In all, it was a matter of 30 minutes between the stopping of the texturing machine and the measurement of yarn segment torque.

There was no simple way to determine the extent of torque relaxation which may have taken place during this interval. But it was observed that, except in one case, the threadline torque measurements on cold zone segments were within 20% of the measurements of segments taken from the cooling zone, with the cold zone values being the lower. This was not unexpected since it was likely that the yarn which had been uptwisted over the heater and cooled at constant torque for a

period of about 30 seconds, would have encountered sufficient torsional creep as to minimize subsequent torsional relaxation. On the other hand, the yarn in the cold zone which had shorter exposure to the given torque during texturing and which was not subjected to hot creep should manifest greater subsequent torque relaxation.

The yarn segment was then uptwisted slightly at the same tension to permit measurement of incremental torques. Similar experiments were run with incremental downtwisting. In this manner, it was possible to calculate the torsional rigidity of the yarn for four different twist levels and for two different zones of the threadline.

In addition to experiments involving yarn uptwisting at constant tension, experiments were also run at constant twist with tension increments added or removed. And the resulting torque increments were measured. Finally, fresh threadline yarn samples were untwisted completely and a full torque twist curve was plotted. This last test procedure also allowed for measurement of yarn extensions which accompanied untwisting and these data were employed to calculate twist contraction factors.

The structural data for the threadline observed in these tests are listed in Table 3.1 and the torsional data in Table 3.2. The data show an increase in cold zone twist as well as in cooling zone twist with machine twist (basic),

Table 3.1

STRUCTURE OF THREADLINE

Machine* Twist (TPI)	Twist/in of Threadline Zones		Retraction		Tangent Q**	
	Cold	Cooling	Cold	Cooling	Cold	Cooling
40	13.0	34.4	2%	8%	.22	.55
45	30.8	57.1	8%	20%	.53	.97
56	48.8	75.4	18%	36%	.89	1.24
60	56.2	91.5	26%	53%	1.05	1.75

*Basic twist, turns/in of untwisted yarn

**Surface helix angle calculated on the basis of a packing factor or 0.85.

Table 3.2

TORSIONAL PROPERTIES OF THREADLINE ZONES

Machine Twist (TPI)	Tangent Q**		Steady State Tension gf	Steady State Torque in-lbs x 10^{-4}		Torsional Stiffness lb-in^2 x 10^{-4}	
	Cold	Cooling		Cold	Cooling	Cold	Cooling
30	.22	.55	16.1	.33	.39	.017	.12
45	.53	.97	16.7	.79	.91	.044	.24
56	.89	1.24	15.0	1.48	1.91	.17	.32
60	1.06	1.75	14.1	1.65	1.91	.27	.36

*Basic Twist

** Surface helix angle, calculated

although the ratio of twist in the two zones goes from 0.38 to 0.61. In other words, a higher proportion of twist takes place in the cold zone at the higher spindle speeds.

Table 3.2 shows the steady state torque values for yarn segments taken from the cold zone and from the cooling zone. The latter values are somewhat higher for each condition of texturing. As was stated above, torsional relaxation of the cooling zone specimens is more likely to have occurred during processing, hence it is logical to select the cooling zone values as more representative of actual threadline torques.

It is noted that over the machine twist range of 30 to 60 TPI, the torque values increase by about a factor of five, that is, from 0.4 to 1.9 times 10^{-4} in/lbs. The cooling zone twist increases by a factor of 2.7, but the cold zone twist increases by a factor of 4.3. Threadline tensions are seen to rise slightly from 30 to 45 TPI machine twist, then decrease steadily (about 16%) as machine twist increases from 45 to 60 TPI. This is consistent with the behavior noted by Backer and Yang [4]. The level of cold zone twist manifests a linear reflection of increases in threadline torque as determined from measurements on yarn segments from the cooling zone. This holds up to 56 TPI machine twist (basic).

If threadline tension is relatively constant at machine twists of 60 TPI the threadline torque remains the same as at 56 TPI, though the cold twist does increase somewhat.

The reason for this flattening of the torque-twist curve becomes evident when one views photographs of threadline configurations[4] showing the onset of torsional buckling at 60 TPI basic twist for texturing overfeed conditions of 0%. For the corresponding current tests at 1.8% overfeed, the torsional buckling at machine twists of 60 TPI basic is even greater than for 0% O/F.

Figure 3.1, 3.2, 3.3, 3.4, show results of uptwisting tests on a single yarn segment taken from the cold and cooling zones for the four test conditions listed in Tables 3.1 and 3.2. The torque plotted in each case for a twist increment of zero, corresponds to the offline measurement of threadline torque reading for both cold zone and cooling zone actual twist values as reported in Tables 3.1 and 3.2. Again, it is noted that torques for the cold zone yarn segments are consistently below those measured for the cooling zone segments. The uptwist-torque values for the most part vary linearly with the uptwist increments (plotted in radians-per-inch, rather than in TPI). Upon removal of twist increments, the relationship is still quite linear, with a slight hysteresis for the cooling zone segments, but with considerably greater hysteresis for cold zone segments, again reflecting the history of more earlier relaxation in the cooling zone segments in actual processing.

In view of the conclusion that the cooling zone yarn tor-

Figure 3.1

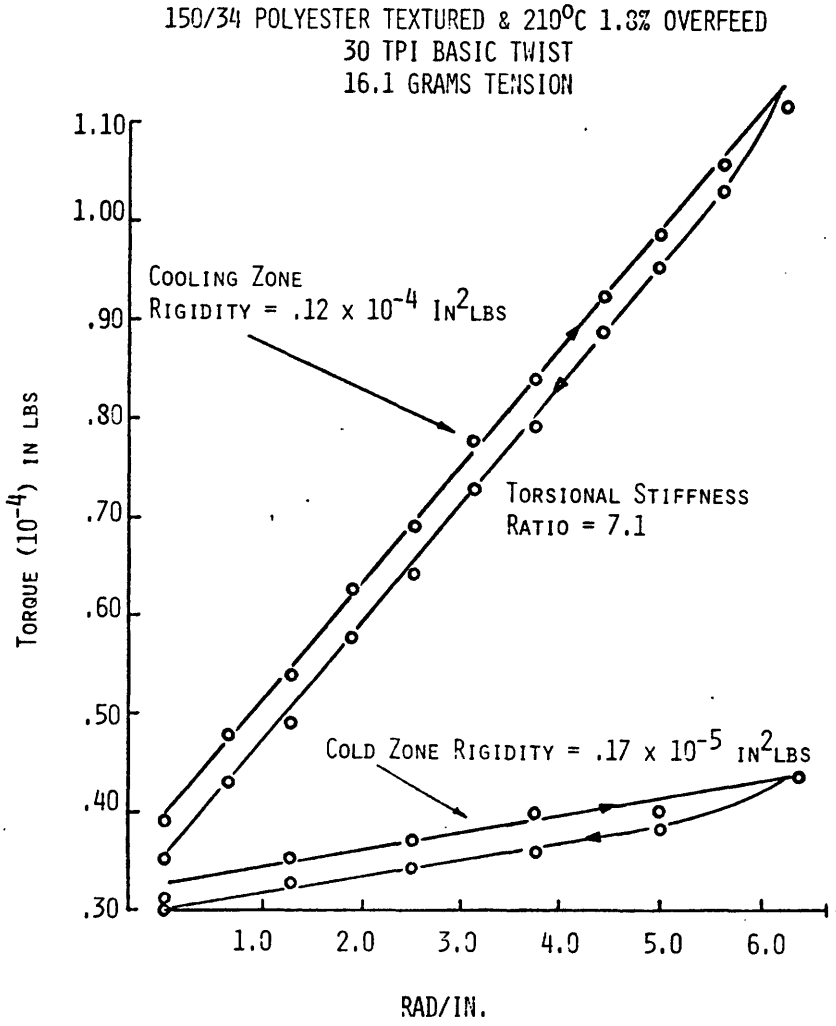
150/34 POLYESTER TEXTURED & 210°C 1.8% OVERFEED
30 TPI BASIC TWIST
16.1 GRAMS TENSION
COOLING ZONE
RIGIDITY = .12 x 10⁻⁴ IN²LBS
TORSIONAL STIFFNESS
RATIO = 7.1
COLD ZONE RIGIDITY = .17 x 10⁻⁵ IN²LBS
TORQUE (10⁻⁴) IN LBS
1.10
1.00
.90
.80
.70
.60
.50
.40
.30
1.0
2.0
3.0
4.0
5.0
6.0
RAD/IN.

Figure 3.2

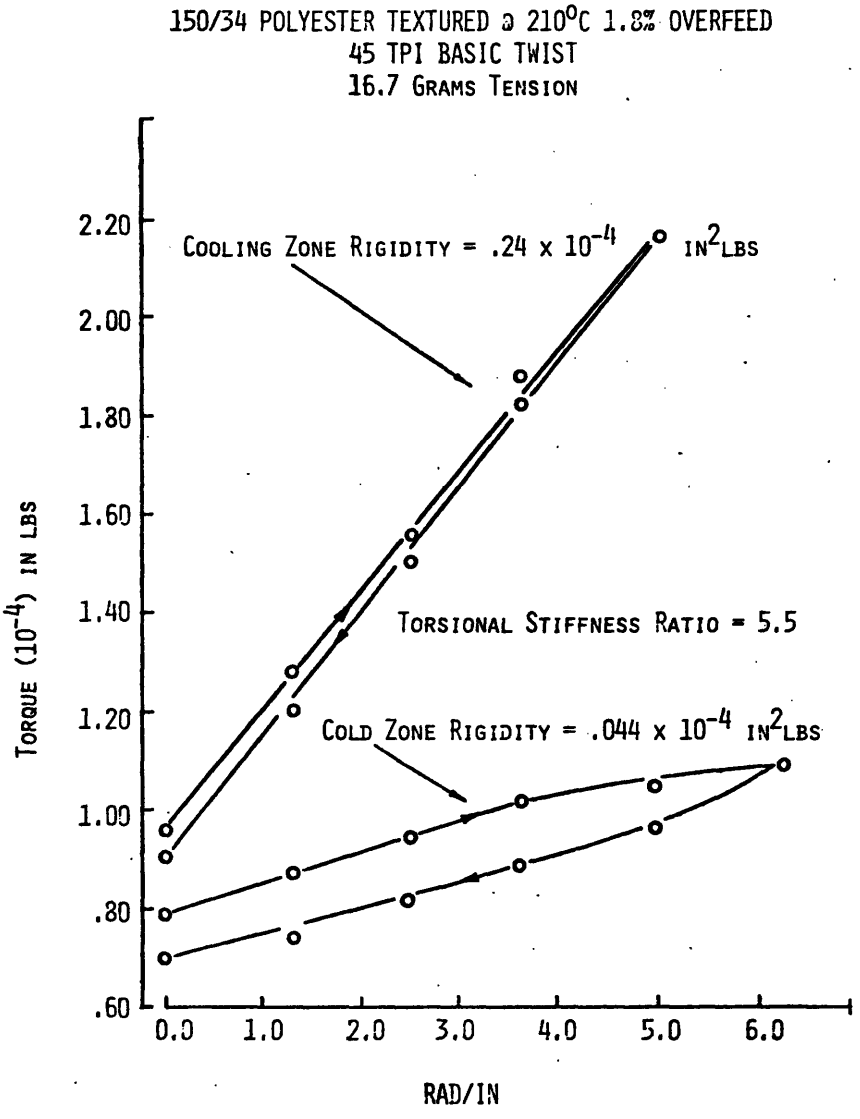
150/34 POLYESTER TEXTURED @ 210°C 1.8% OVERFEED
45 TPI BASIC TWIST
16.7 GRAMS TENSION
COOLING ZONE RIGIDITY = .24 x 10⁻⁴ IN²LBS
TORSIONAL STIFFNESS RATIO = 5.5
COLD ZONE RIGIDITY = .044 x 10⁻⁴ IN²LBS
TORQUE (10⁻⁴) IN LBS
2.20
2.00
1.80
1.60
1.40
1.20
1.00
.80
.60
0.0
1.0
2.0
3.0
4.0
5.0
6.0
RAD/IN

Figure 3.3

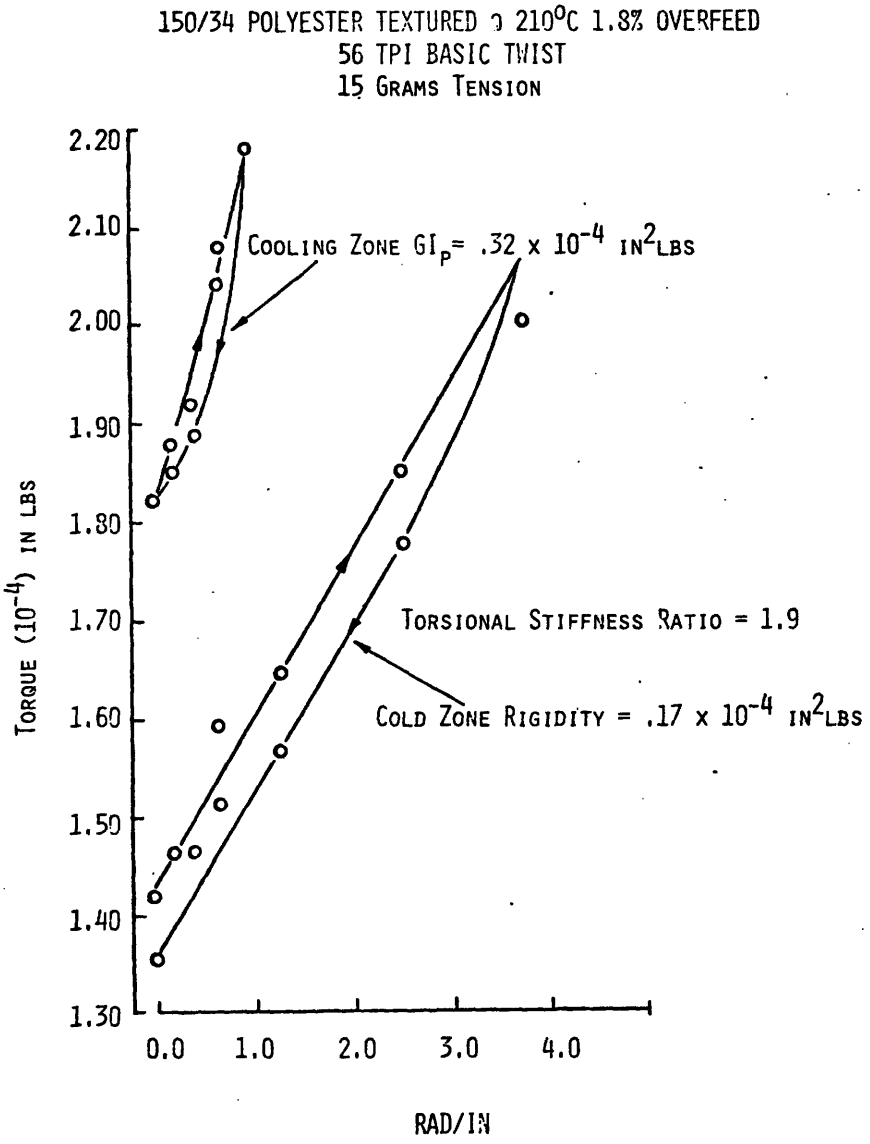
150/34 POLYESTER TEXTURED @ 210°C 1.8% OVERFEED
56 TPI BASIC TWIST
15 GRAMS TENSION
COOLING ZONE GI_p= .32 x 10^{-4} IN^2LBS
TORSIONAL STIFFNESS RATIO = 1.9
COLD ZONE RIGIDITY = .17 x 10^{-4} IN^2LBS
TORQUE (10^{-4}) IN LBS
2.20
2.10
2.00
1.90
1.80
1.70
1.60
1.50
1.40
1.30
0.0
1.0
2.0
3.0
4.0
RAD/IN

Figure 3.4

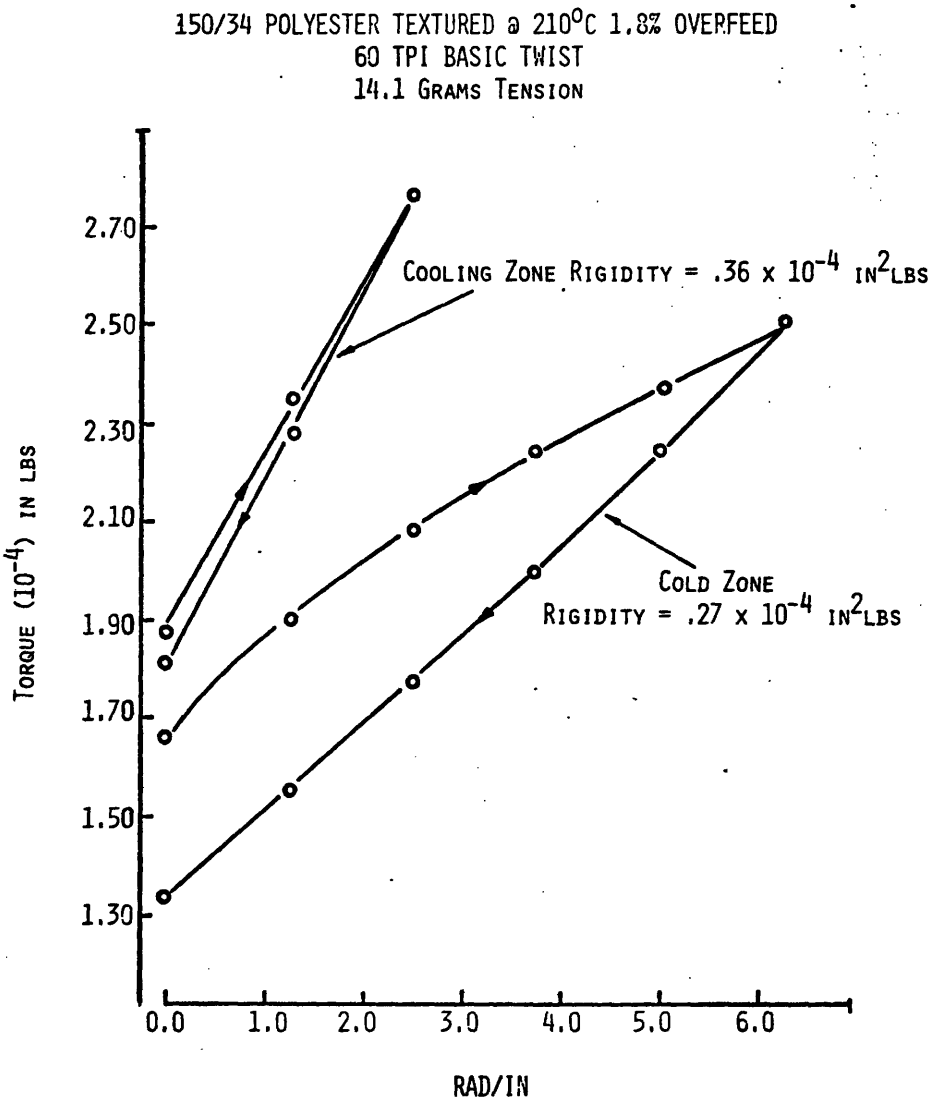
150/34 POLYESTER TEXTURED @ 210°C 1.8% OVERFEED
60 TPI BASIC TWIST
14.1 GRAMS TENSION
COOLING ZONE RIGIDITY = .36 x 10⁻⁴ IN²LBS
COLD ZONE
RIGIDITY = .27 x 10⁻⁴ IN²LBS
TORQUE (10⁻⁴) IN LBS
2.70
2.50
2.30
2.10
1.90
1.70
1.50
1.30
0.0
1.0
2.0
3.0
4.0
5.0
6.0
RAD/IN

ques were the more accurate values, additional incremental uptwist tests were run on a number of cooling zone segments. The results of these tests for 30, 45, and 60 TPI machine twists are furnished in Fig. 3.5 and indicate the spread of the experimental values observed, as well as the typical curve selected for Figs. 3.1, 3.2, 3.3, and 3.4. The slope of the incremental torque-twist curve is obviously greater for the 60 TPI machine twist segment than for the 45 or 30 TPI cases, and this is reflected in Table 3.2 as a three-fold increase in torsional stiffness over the test range.

The torsional data are summarized in Fig. 3.5, which highlights the tremendous difference between the slope of the forming torque-twist curve (shown as the solid bars), and the incremental torque-twist curves (shown as the open bars). It is also seen that the incremental rigidities vary over the test range by about 15 times for the cold zone, and only 3 times for the cooling zone materials. Thus, the data fully confirm the hypothesis that was put forth on the basis of observations of tilting in transient twist distributions after changing of spindle speeds, i.e. that threadline twist increases imparted at the entry to hot zone are in effect locked in by the development of high torsional rigidities to incremental uptwist over the heater and beyond. But the data also reveal that a similar high torsional rigidity to incremental twist develops right after initial formation of

Figure 3.5

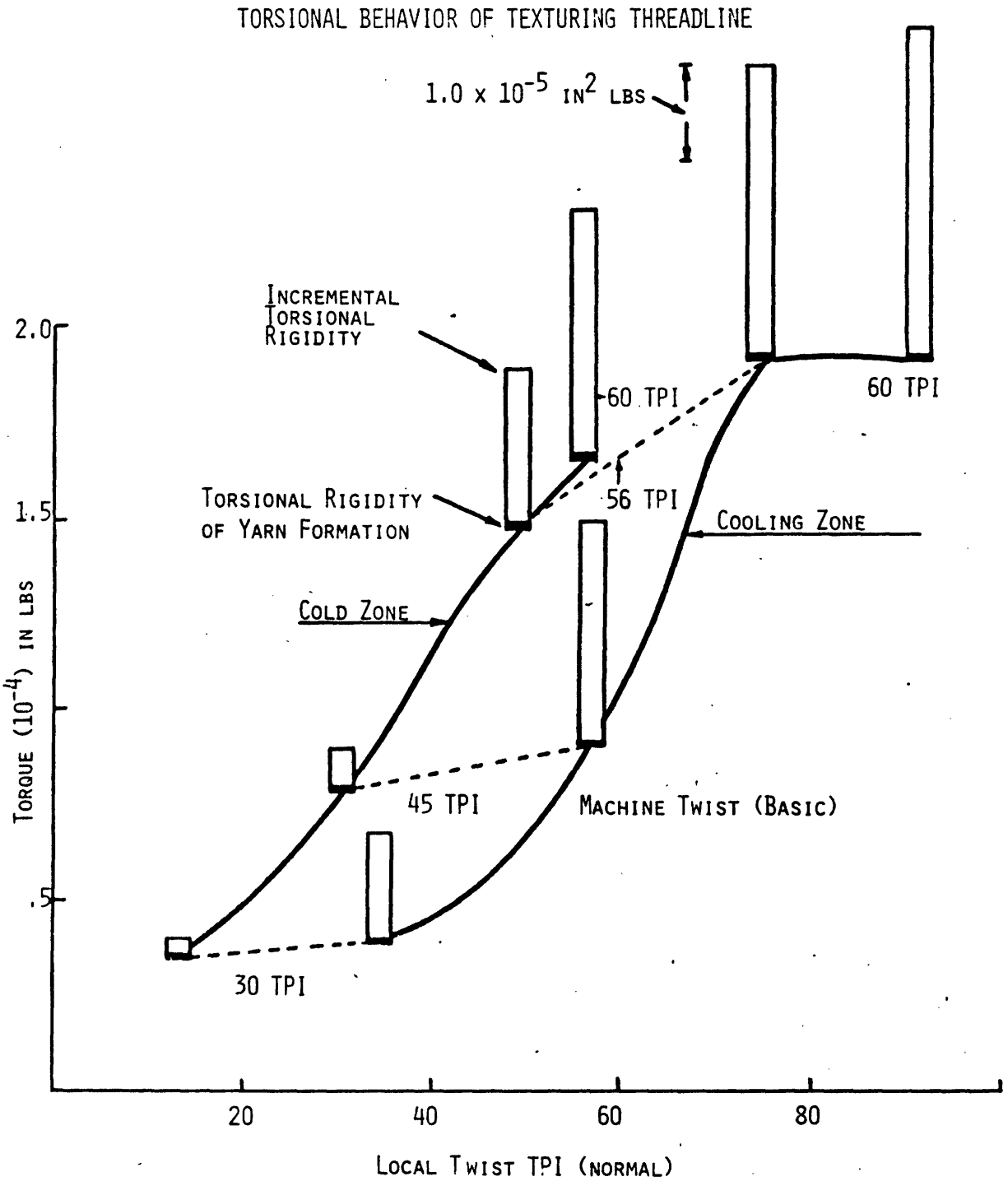
TORSIONAL BEHAVIOR OF TEXTURING THREADLINE
1.0 x 10^-5 IN^2 LBS
INCREMENTAL TORSIONAL RIGIDITY
60 TPI
60 TPI
56 TPI
TORSIONAL RIGIDITY OF YARN FORMATION
COOLING ZONE
COLD ZONE
45 TPI
MACHINE TWIST (BASIC)
30 TPI
2.0
1.5
.5
TORQUE (10^-4) IN LBS
20
40
60
80
LOCAL TWIST TPI (NORMAL)

Figure 3.6

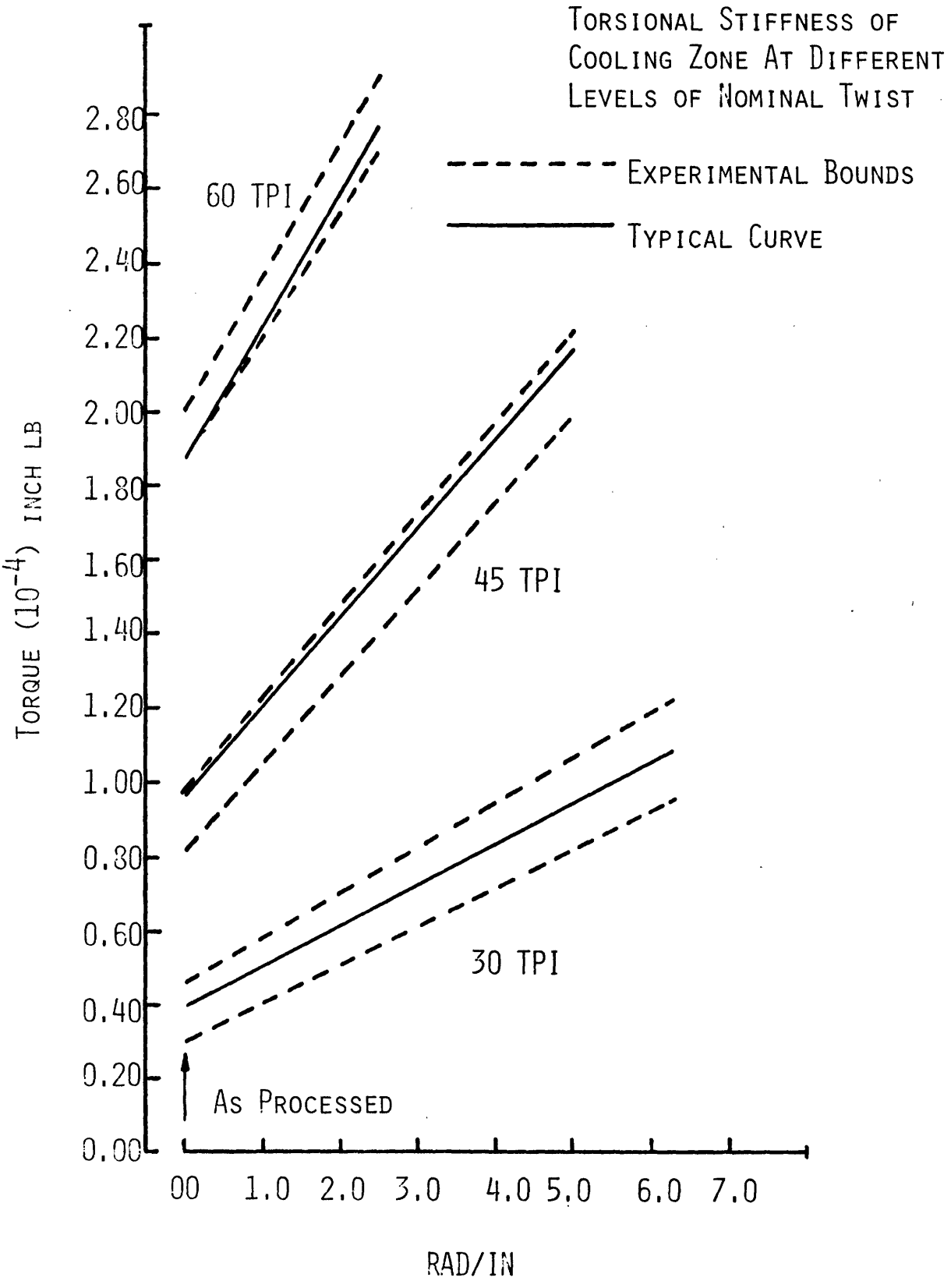
TORSIONAL STIFFNESS OF COOLING ZONE AT DIFFERENT LEVELS OF NOMINAL TWIST
EXPERIMENTAL BOUNDS
TYPICAL CURVE
60 TPI
45 TPI
30 TPI
AS PROCESSED
TORQUE (10^{-4}) INCH LB
2.80
2.60
2.40
2.20
2.00
1.80
1.60
1.40
1.20
1.00
0.80
0.60
0.40
0.20
0.00
00
1.0
2.0
3.0
4.0
5.0
6.0
7.0
RAD/IN

the yarn in the cold zone. Although cold zone rigidities are somewhat less than the cooling zone rigidities, they are nonetheless orders of magnitude greater than the cold forming "rigidity". Likewise, the cooling zone incremental rigidity is orders of magnitude greater than the hot uptwisting "rigidity". Stated another way, the entries to the cold zone and to the heater zone are, in effect, dynamic torsional soft zones in the threadline and any sudden changes which may occur in threadline torque, for whatever reason, will be reflected in large local twist changes at these entry zones and negligible changes elsewhere. And it is to be expected that twist changes introduced at these points, will be propagated along the threadline with translational movement of the yarn.

The second series of tests were run on the yarn segments removed from the threadline. In these experiments, as was indicated, the twist of the threadline segment was kept constant while the tension was varied incrementally around the value recorded as the operating threadline tension. Incremental changes in yarn torque resulting from these tension changes were recorded as are reported in Figs. 3.7, 3.8, 3.9, and 3.10. The slopes of the curves plotted in these figures indicate the influence of tension on torque in the cold zone and cooling zone yarn segments. There is some increase in the tension-torque effect as the machine twist is increased

Figure 3.7

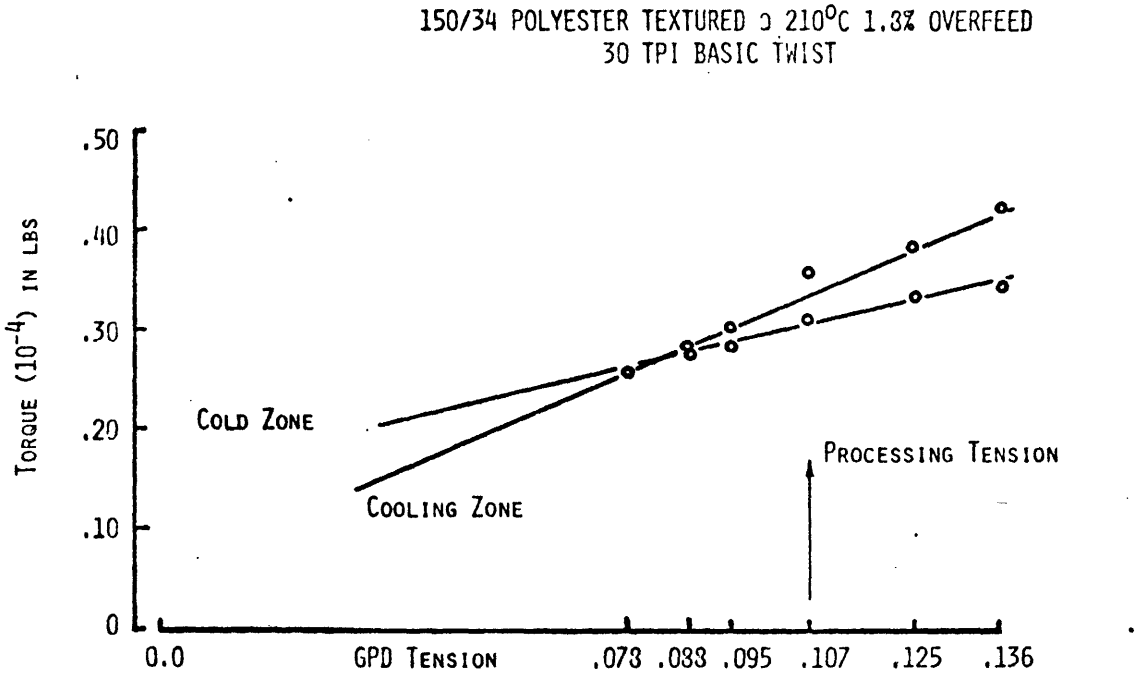
150/34 POLYESTER TEXTURED @ 210°C 1.8% OVERFEED
30 TPI BASIC TWIST
TORQUE (10^{-4}) IN LBS
.50
.40
.30
.20
.10
0
COLD ZONE
COOLING ZONE
PROCESSING TENSION
0.0
GPD TENSION
.073
.083
.095
.107
.125
.136

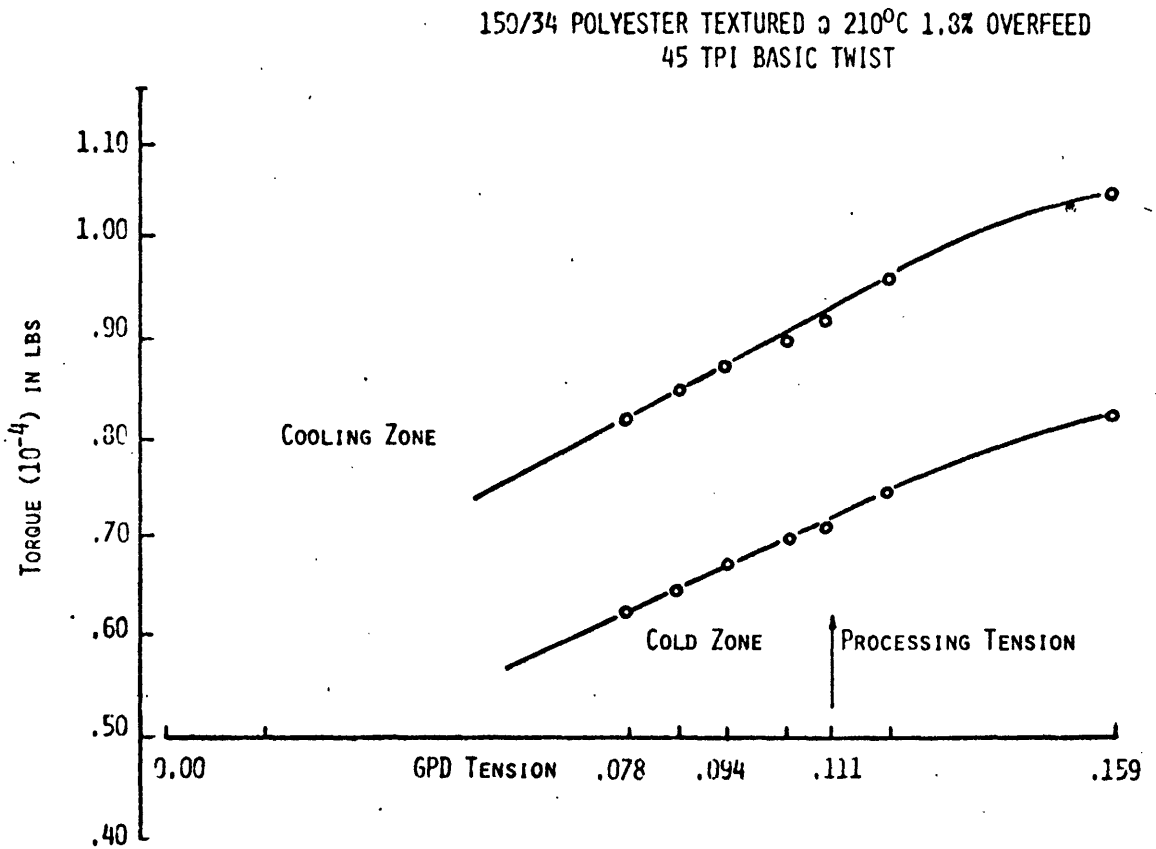
150/34 POLYESTER TEXTURED @ 210°C 1.8% OVERFEED
45 TPI BASIC TWIST
TORQUE (10^{-4}) IN LBS
1.10
1.00
.90
.80
.70
.60
.50
.40
COOLING ZONE
COLD ZONE
PROCESSING TENSION
0.00
GPD TENSION
.078
.094
.111
.159

Figure 3.8

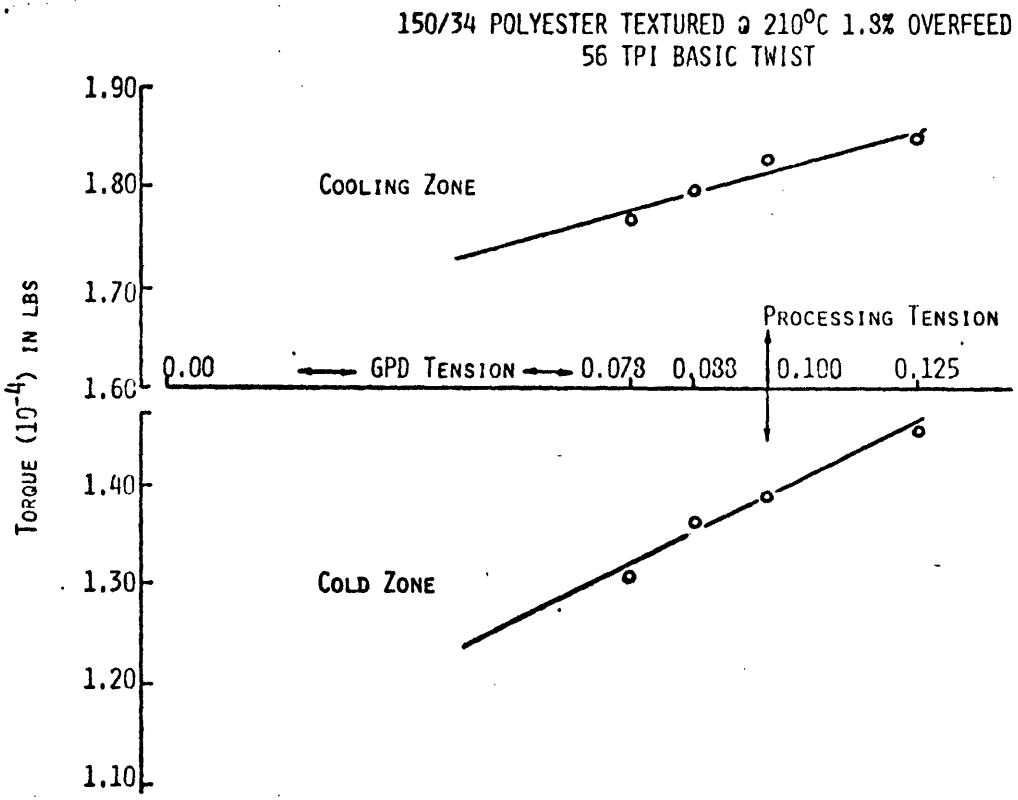
150/34 POLYESTER TEXTURED @ 210°C 1.8% OVERFEED
56 TPI BASIC TWIST
1.90
1.80
1.70
1.60
1.40
1.30
1.20
1.10
TORQUE (10^{-4}) IN LBS
COOLING ZONE
COLD ZONE
PROCESSING TENSION
0.00
GPD TENSION
0.078
0.088
0.100
0.125

Figure 3.9

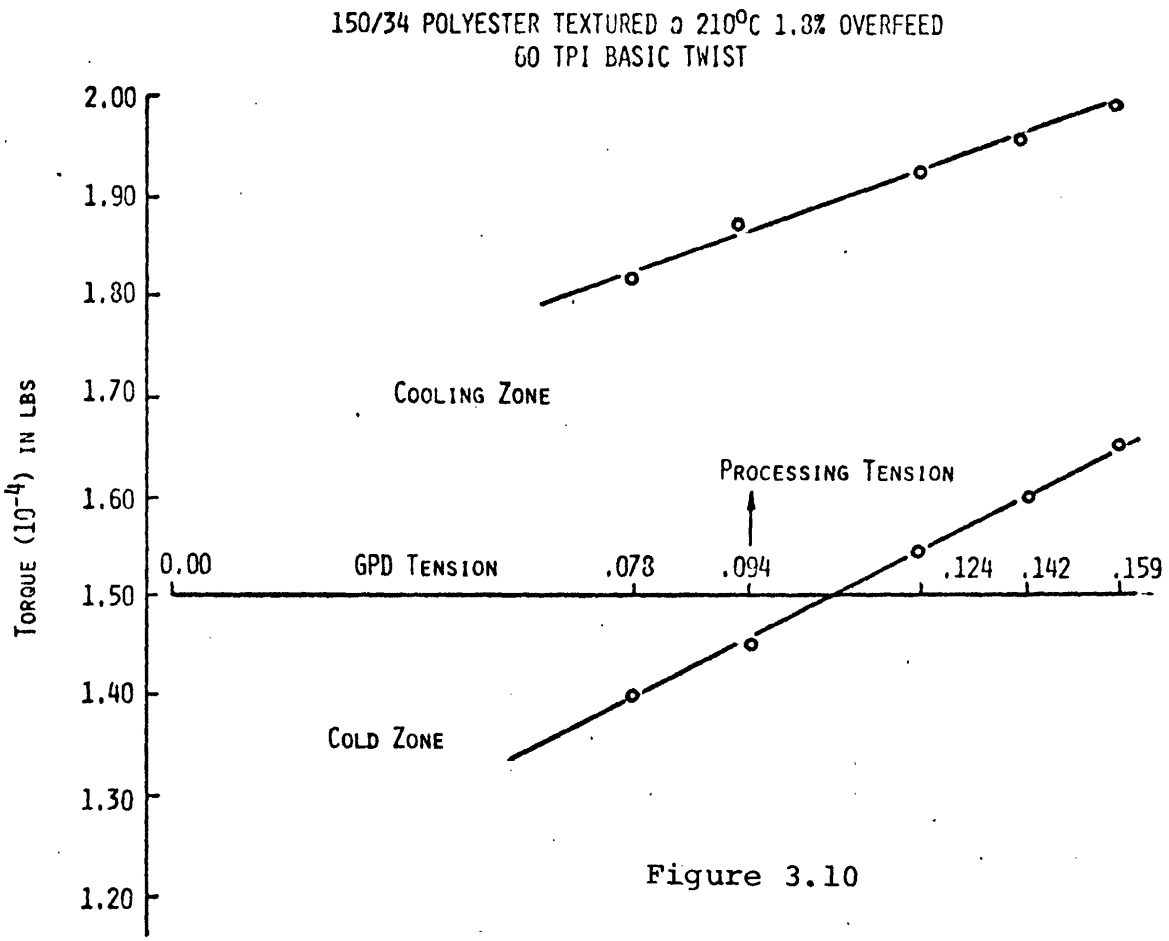
150/34 POLYESTER TEXTURED @ 210°C 1.8% OVERFEED
60 TPI BASIC TWIST
2.00
1.90
1.80
1.70
1.60
1.50
1.40
1.30
1.20
TORQUE (10^{-4}) IN LBS
COOLING ZONE
PROCESSING TENSION
0.00
GPD TENSION
.078
.094
.124
.142
.159
COLD ZONE

Figure 3.10

which, in turn, increases both cold zone twist and cooling zone twist as reported in Table 3.1. But, above machine twists of 45 TPI (basic), the changes in the tension-torque effect are not consistent. However, it can be noted that the tension-torque effect for 30 TPI basic machine twist is greater for the cooling zone segment than for the cold zone segment. And this condition reverses as the machine twist is increased to 56 and 60 TPI (basic).

One expects the tension-torque effect, or the slope of the torque-tension curve (at constant twist) to depend in the actual twist in the local yarn segment. Thus, the larger slope observed at 30 TPI basic machine twist in the more highly twisted cooling segment vs. the less twisted cold segment is according to expectation. The reversal which occurs at higher machine twists in the comparative levels of cooling and of cold zone tension-torque effects suggests the possibility of interfilament interactions in the cooling zones which serve to suppress the torsional response to changes in yarn tension.

The torque-tension slopes differ significantly from the cold zone to the cooling zone in a given threadline. This fact combined with the confirmed existence of torsional soft zones at the cold entry and the heater entry suggests that sudden (and large) changes in threadline tension for whatever reason will result in immediate (slight) redistribution

of twists between threadline zones to suppress the torque differences followed by considerable twist changes at the soft zones in response to the new uniform (along the threadline) level of torque. Thus, tensile transients in the threadline can be expected to cause torque transients as well, and these will introduce significant changes in soft zone twisting levels, which will then propagate along the threadline.

Finally, the torque-twist relationship of the cooling zone segments was determined for the range of untwisting down to zero torque. Typical data from such experiments are plotted in Figure 3.11 where it is seen for the 60 TPI machine basic twist case (with 91.5 TPI local twist) that the torque-untwist curve (note, for a 5-inch specimen) is fairly linear from a torque value of about 1.75×10^{-4} in/lbs down to about 0.25×10^{-4} in/lbs, at which point only one TPI out of ninety has been untwisted. The curve then flattens significantly as the small residual torque is reduced with further twisting The significance of this behavior will be discussed in Chapter 4 as it relates to product uniformity.

Figure 3.11

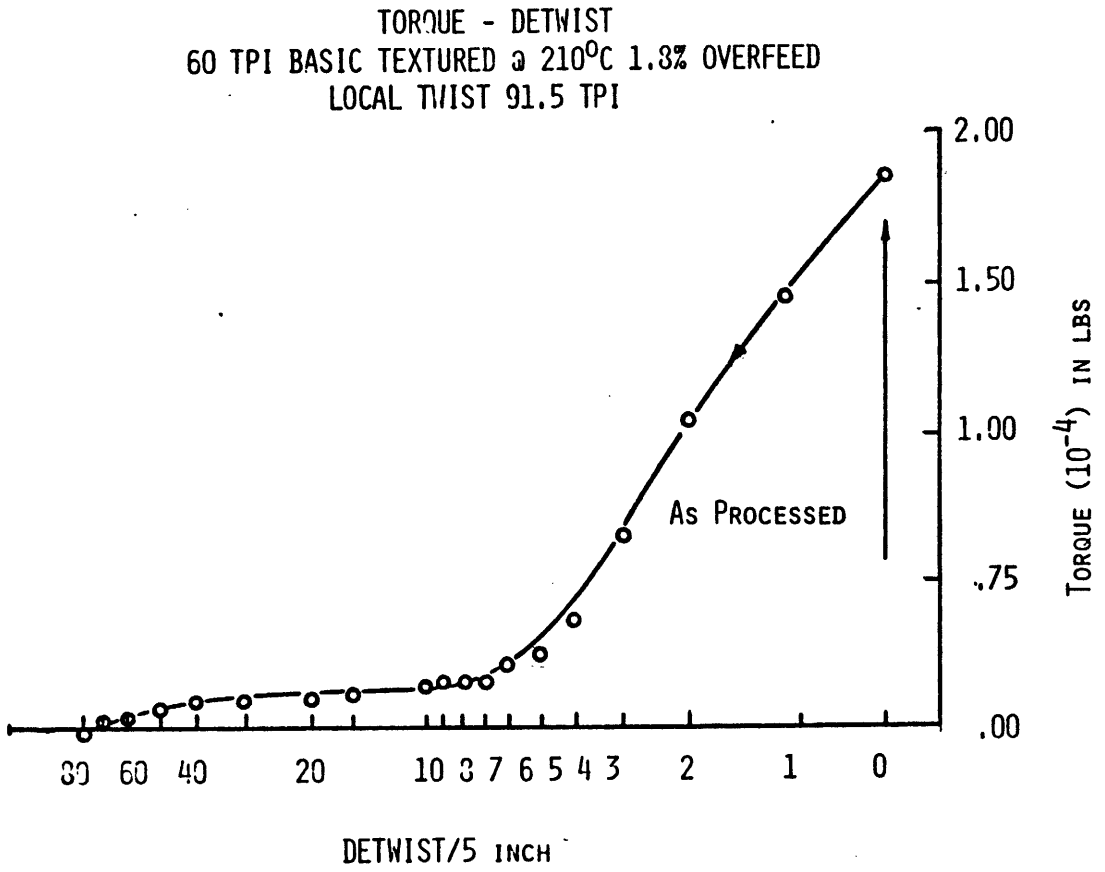
TORQUE - DETWIST
60 TPI BASIC TEXTURED @ 210°C 1.8% OVERFEED
LOCAL TWIST 91.5 TPI
2.00
1.50
1.00
.75
.00
TORQUE (10^{-4}) IN LBS
AS PROCESSED
80 60 40 20 10 8 7 6 5 4 3 2 1 0
DETWIST/5 INCH

3.2.2 Experiments Concerning Transient Twist, Using Predrawn PET Yarns

In their photographic study of twist levels during transient operation of the false twist process Backer and Yang did not include twist measurements at the entrance to the cold twist formation zone[4]. In the current study a photographic analysis was accordingly undertaken to determine how twist changed at the cold formation zone, cold zone, hot formation zone, hot zone, cooling zone, and post spindle zone during transient operation of the conventional false twist texturing process. In this case a Bolex 16 mm motion picture camera equipped with a telephoto lens was used. The feed yarns used for photographic twist measurement consisted of black and white filaments supplied by the DuPont Company. The yarn (predrawn polyester) was 140 denier with 68 filaments.

To measure local twist at the cold formation zone, a glass slide was pressed against a relatively friction free roller to trap threadline twist and prevent it from propagating behind the defined formation point at the slide -- roller 'nip'. This twist trap assembly was placed slightly downstream of the feed rollers. A schematic diagram of the experimental set up is shown in Figure 3.12.

The machine twist was set either at 30 TPI or 40 TPI and the system was allowed to reach steady state operating condi-

Figure 3.12

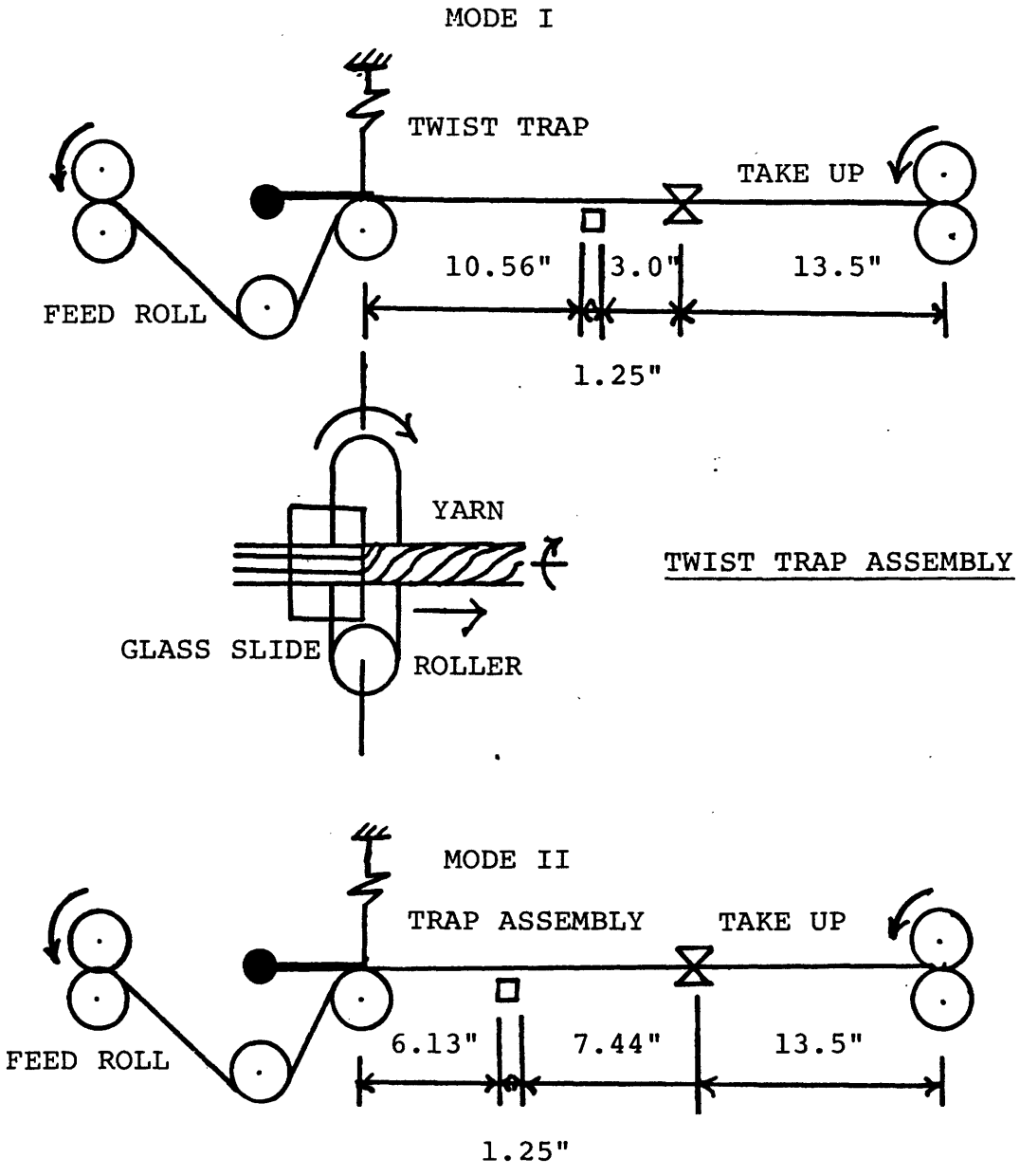
MODE I
TWIST TRAP
TAKE UP
10.56"
3.0"
13.5"
FEED ROLL
1.25"
YARN
GLASS SLIDE
ROLLER
TWIST TRAP ASSEMBLY
MODE II
TRAP ASSEMBLY
TAKE UP
6.13"
7.44"
13.5"
FEED ROLL
1.25"

tions. The machine twist was then step changed by 10 TPI to either 40 TPI or 30 TPI depending on the previous twist level. Motion pictures of the threadline were taken at different positions so that twist levels could be determined as functions of time (after disturbance) and position. These pictures were taken at the following positions:

IN COLD ZONE:	Cold Zone Entrance
	3.50 Inches Past Cold Zone
	6.88 Inches Past Cold Zone
IN HOT ZONE:	Heater Entrance
	Midway Through Heater
	Heater Exit
IN COOLING ZONE:	Immediately After Heater
	.50 Inches Past Heater Exit
	3.00 Inches Past Heater Exit
	7.37 Inches Past Heater Exit
IN POST SPINDLE ZONE:	7.00 Inches Past Spindle

Graphs of twist versus time at different positions of the threadline after a step change in spindle speed are given in Figures 3.13, 3.14, 3.15, 3.16, 3.17, 3.18, and 3.19.

Figures 3.13 and 3.14 show that there is an apparent time lag in the cold twist redistribution during transient operation. Twist levels at the entrance to the cold zone manifest immediate change after the spindle speed is changed. Twist

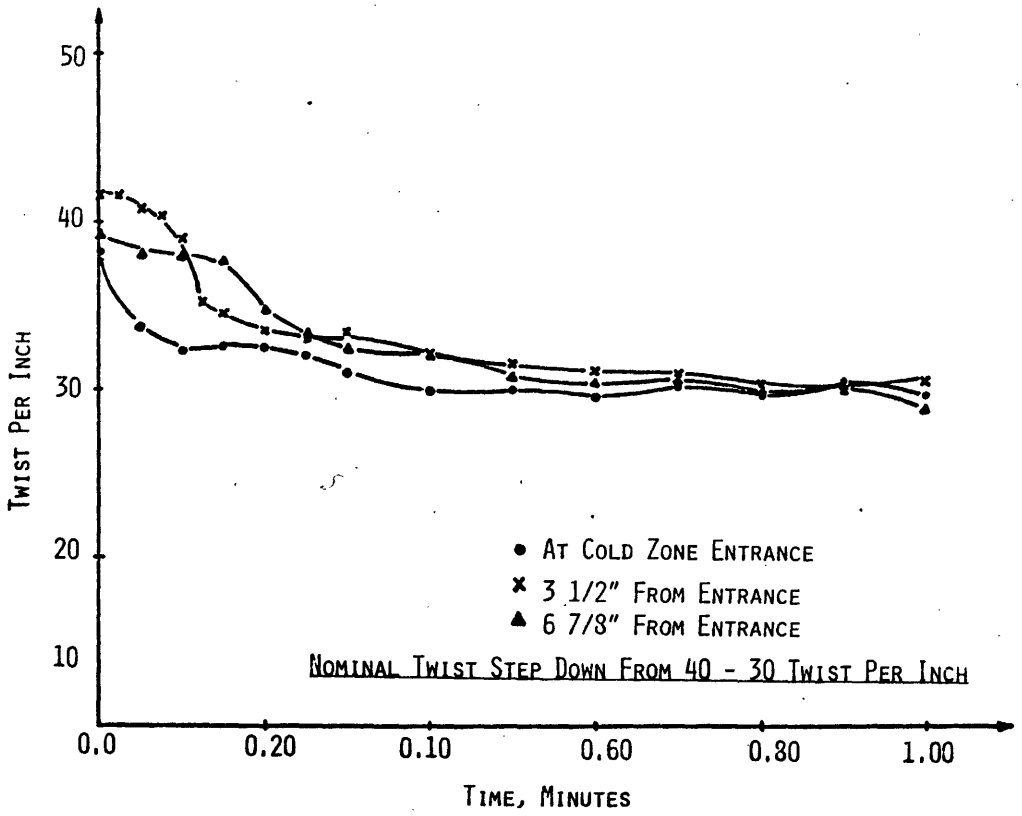
50
40
30
20
10
TWIST PER INCH
0.0
0.20
0.10
0.60
0.80
1.00
TIME, MINUTES
• AT COLD ZONE ENTRANCE
× 3 1/2" FROM ENTRANCE
▲ 6 7/8" FROM ENTRANCE
NOMINAL TWIST STEP DOWN FROM 40 - 30 TWIST PER INCH

Figure 3.13

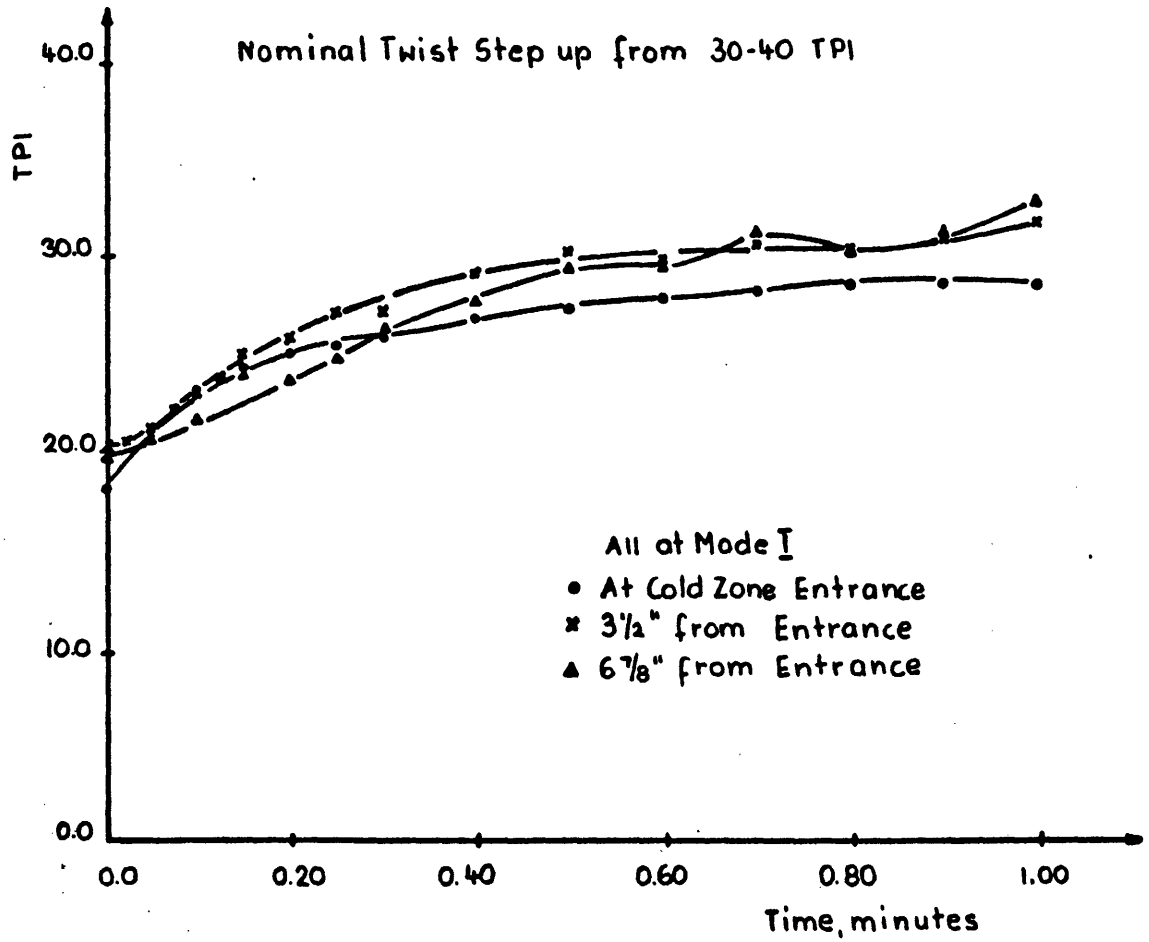
Nominal Twist Step up from 30-40 TPI
TPI
40.0
30.0
20.0
10.0
0.0
0.0
0.20
0.40
0.60
0.80
1.00
Time, minutes
All at Mode I
At Cold Zone Entrance
3½" from Entrance
6⅞" from Entrance

Figure 3.14

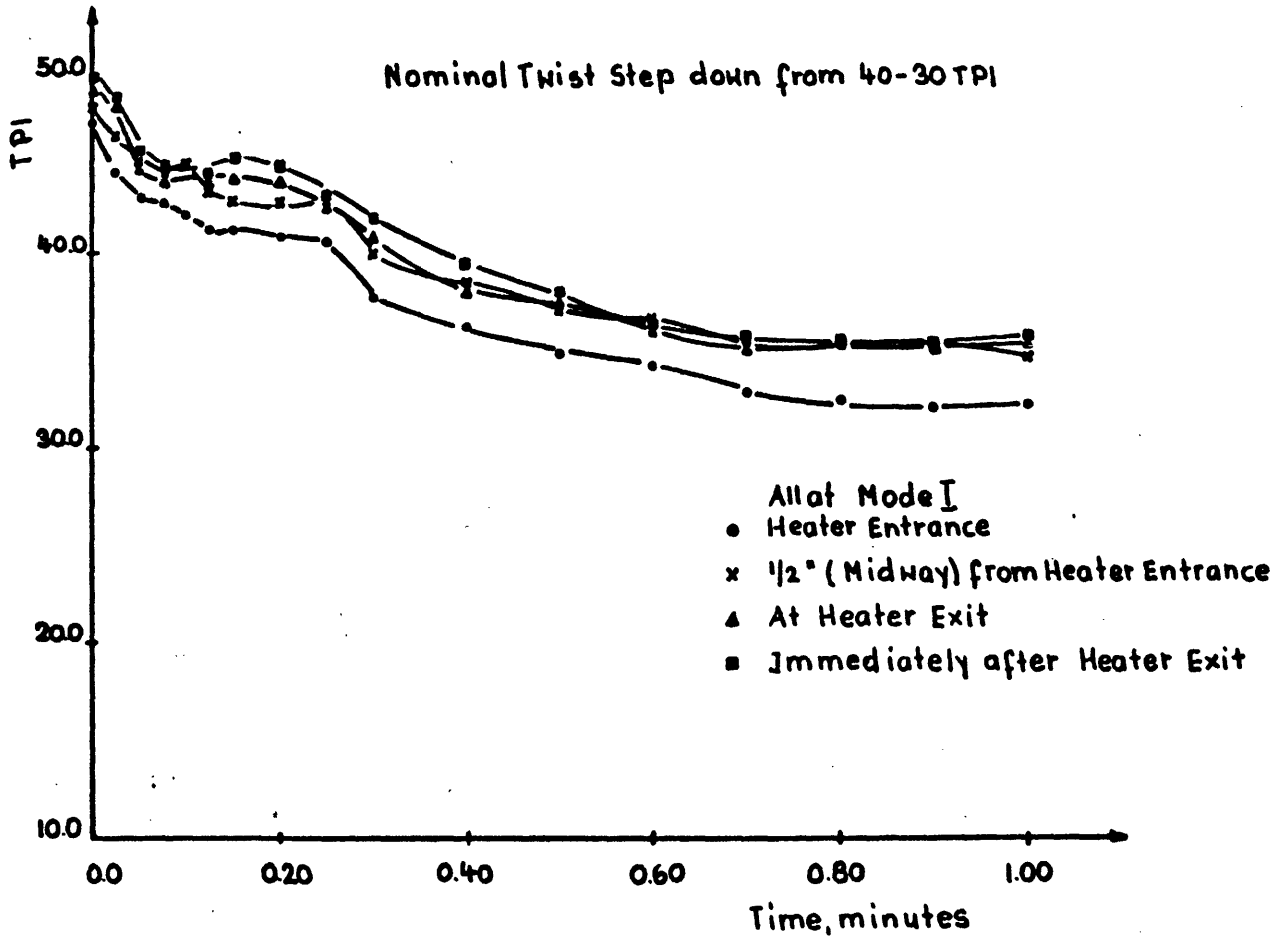
Nominal Twist Step down from 40-30 TPI
TPI
50.0
40.0
30.0
20.0
10.0
0.0
0.20
0.40
0.60
0.80
1.00
Time, minutes
All at Mode I
Heater Entrance
½" (Midway) from Heater Entrance
At Heater Exit
Immediately after Heater Exit

Figure 3.15

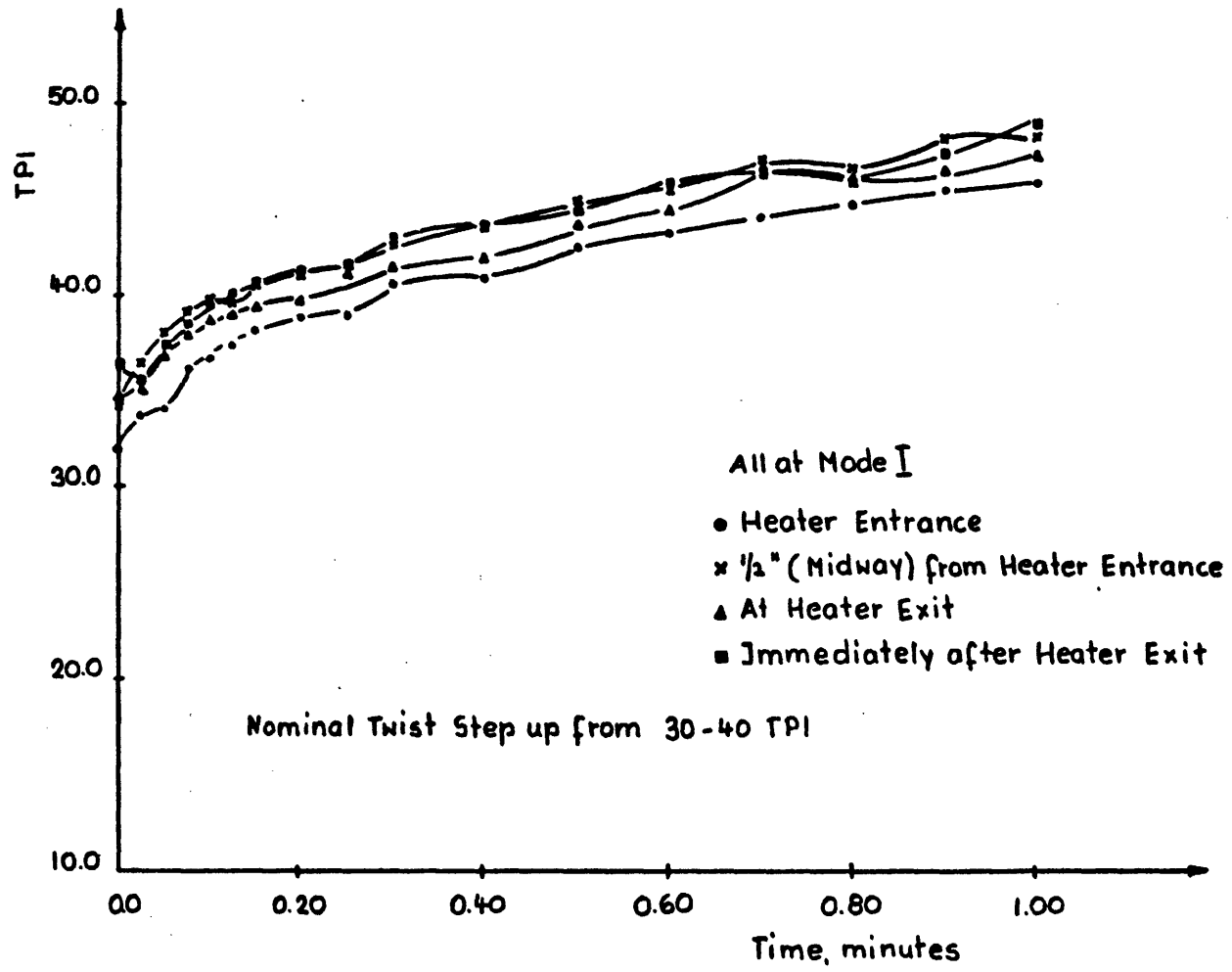
TPI
50.0
40.0
30.0
20.0
10.0
0.0
0.20
0.40
0.60
0.80
1.00
Time, minutes
All at Mode I
• Heater Entrance
× ½" (Midway) from Heater Entrance
▲ At Heater Exit
■ Immediately after Heater Exit
Nominal Twist Step up from 30-40 TPI

Figure 3.16

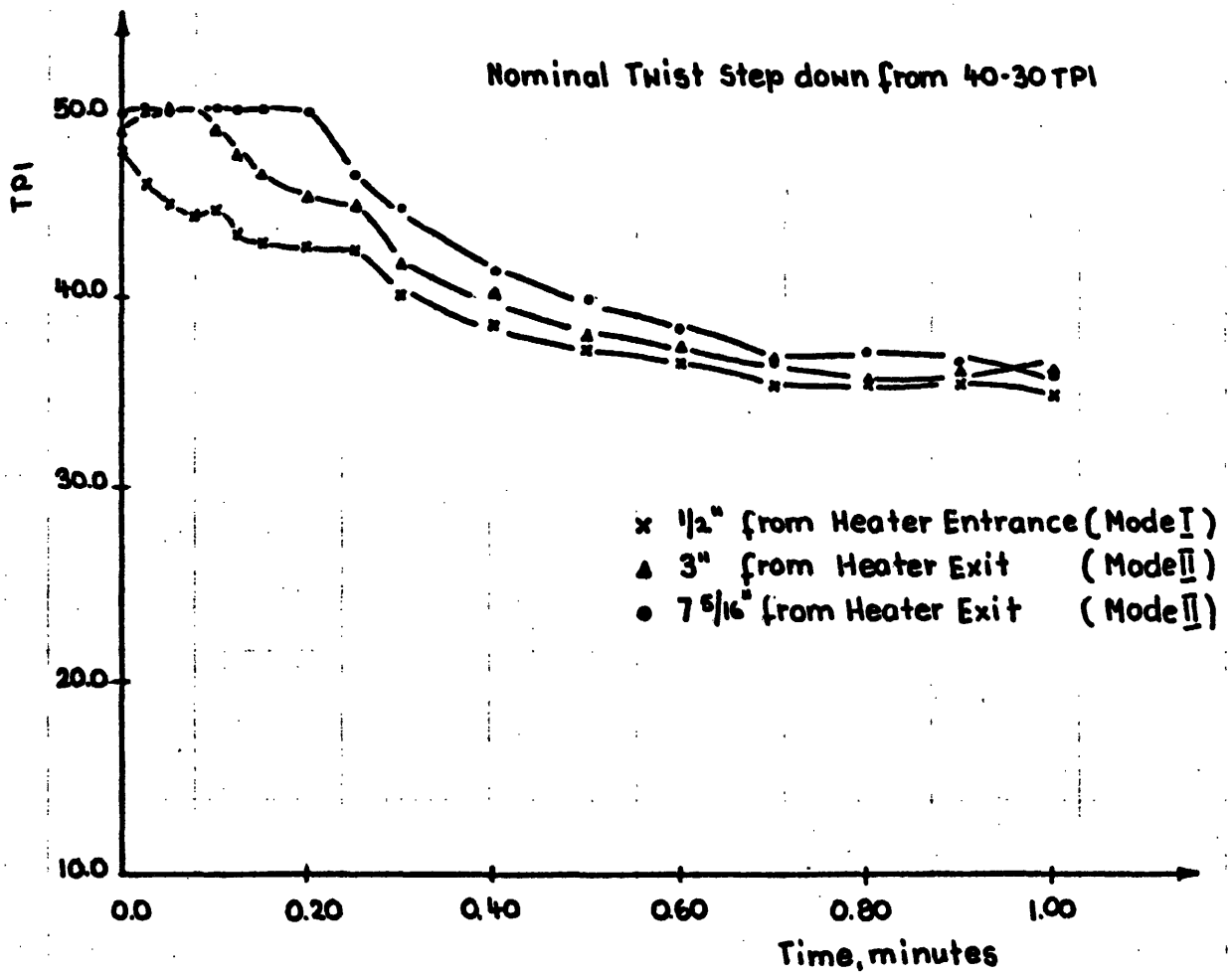
Nominal Twist Step down from 40-30 TPI
TPI
50.0
40.0
30.0
20.0
10.0
0.0
0.20
0.40
0.60
0.80
1.00
Time, minutes
× 1/2" from Heater Entrance (Mode I)
▲ 3" from Heater Exit (Mode II)
● 7 5/16" from Heater Exit (Mode II)

Figure 3.17

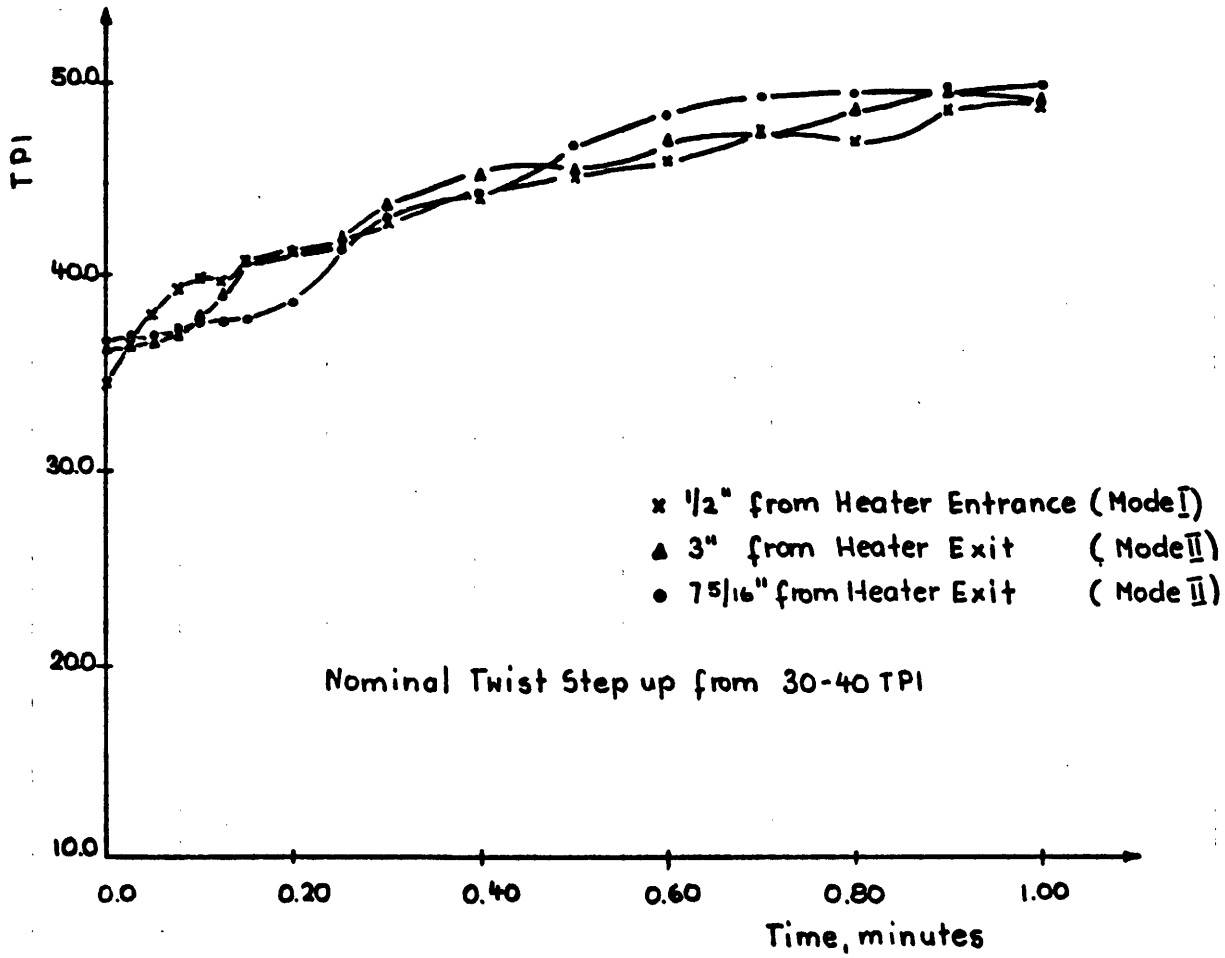
TPI
50.0
40.0
30.0
20.0
10.0
0.0
0.20
0.40
0.60
0.80
1.00
Time, minutes
x 1/2" from Heater Entrance (Mode I)
▲ 3" from Heater Exit (Mode II)
● 7 5/16" from Heater Exit (Mode II)
Nominal Twist Step up from 30-40 TPI

Figure 3.18

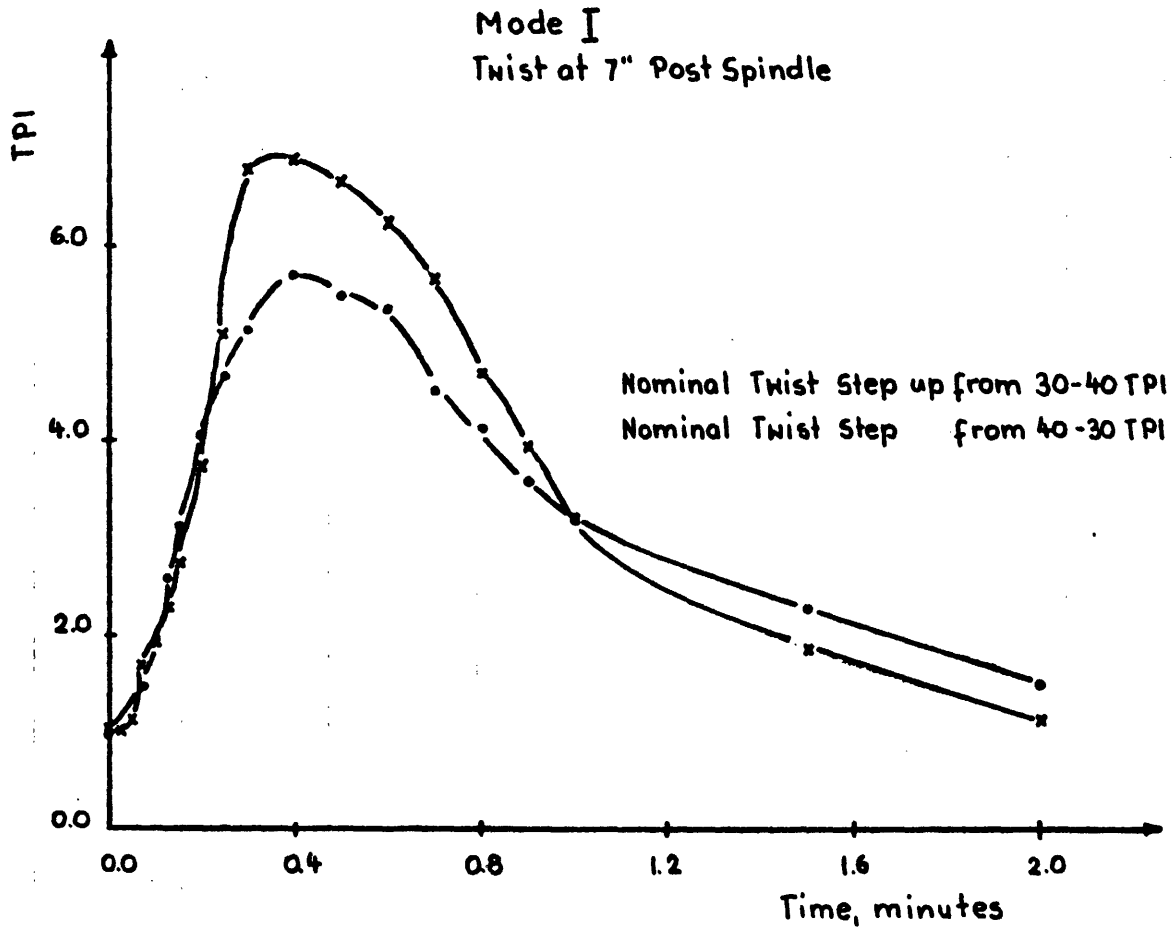
Mode I
Twist at 7" Post Spindle
TPI
6.0
4.0
2.0
0.0
0.0
0.4
0.8
1.2
1.6
2.0
Time, minutes
Nominal Twist Step up from 30-40 TPI
Nominal Twist Step from 40-30 TPI

Figure 3.19

levels downstream of the entrance to the cold zone appear relatively unchanged at first. About 6 seconds later the twist level 3.5 inches downstream of the entrance changes; the twist level 6.88 inches downstream of the entrance changes soon thereafter. The time for a sudden twist change at a given threadline position in the cold zone is plotted against the downstream distance of that position in Figure 3.20. The slope of the line connecting the experimental points approximates the value of the nominal yarn throughput speed. Figures 3.17 and 3.18 show this same type of twist behavior downstream of the heater.

Earlier observations of tilting threadline twist distributions following upon sudden changes in spindle speed provided the basis for the hypothesis that torsional rigidity of the conventional texturing threadline is significantly lower at the at the heater than beyond in the cooling zone. The existence of the "soft" torsional zone at the entry to the heater has been confirmed but it has been also shown that the entry to the cold zone in conventional texturing is likewise a torsional soft zone. Torsional disturbances in the threadline are evidenced primarily as twist changes at the soft zones and these changes then propagate downstream with yarn movement.

The formation rigidities of the texturing threadline essentially reflect the rigidity of the soft forming zones under

Figure 3.20

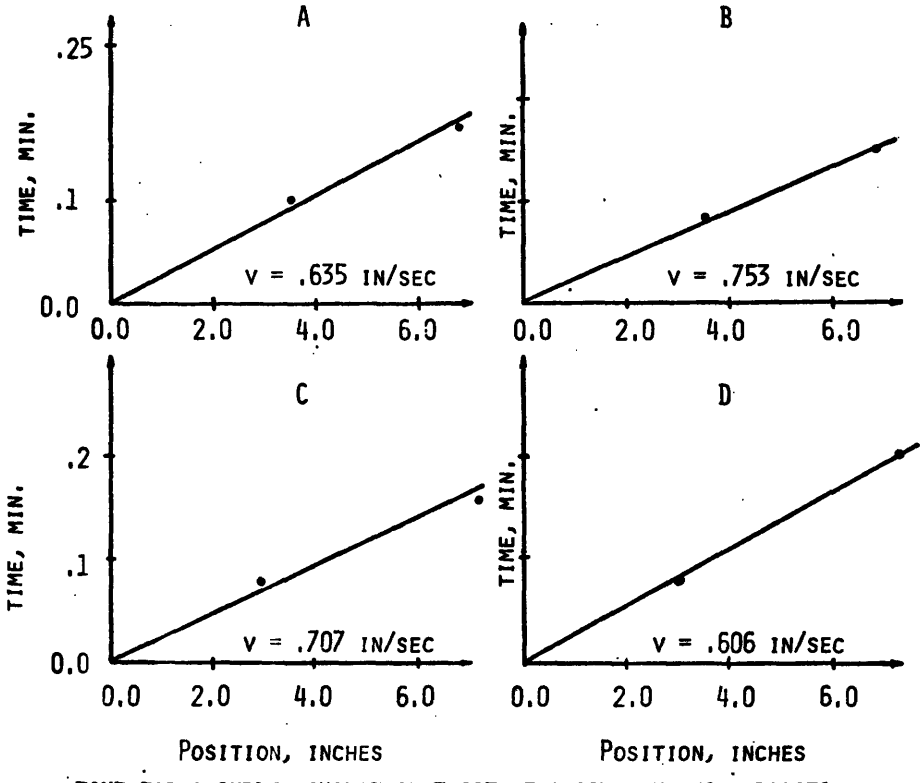

TIME FOR A SUDDEN CHANGE IN TWIST AT A GIVEN MACHINE POSITION AFTER A STEP INPUT

A. STEP CHANGE FROM 40-30 NOMINAL TPI OBSERVED IN COLD ZONE
B. STEP CHANGE FROM 30-40 NOMINAL TPI OBSERVED IN COLD ZONE
C. STEP CHANGE FROM 30-40 NOMINAL TPI OBSERVED IN COOLING ZONE
D. STEP CHANGE FROM 40-30 NOMINAL TPI OBSERVED IN COOLING ZONE

NOTE: NOMINAL THROUGHPUT SPEED IS .734 IN/SEC

the conditions of local twist insertion. The twist response of cold zone and cooling zone segments to incremental changes in spindle speed reflects the very high incremental torsional rigidity of these threadline segments.

The obvious question to be asked concerns the reasons for the sudden stiffening of the threadline a short distance beyond the two entry zones. One can attribute these rigidity differences to the variation in twisting deformation modes at each of the soft zones and in segments which lie downstream of these soft zones.

Observations of dynamic twist formation in larger models indicate that many filaments approaching the twist triangle apex are already twisted around their axes and sometimes around neighboring pairs.[13] They are then wound onto the newly formed end of the yarn, with little additional twisting observed thereafter. After the twist is inserted at the cold zone entrance, interfilament friction and transverse stresses cause the yarn to behave like a helically anisotropic solid rod with subsequent high torsional rigidity. This yarn segment can now accomadate relatively large threadline torque variations with very small changes in threadline twist level.[14]

The situation at the uptwist zone at the heater involves sudden stress relaxation or softening of the tensioned filaments as might be expected from thermomechanical studies. The requirement of constant threadline torque in presence of this stress relaxation results in a cranking up of the twist at the heater.

As the new hot twist level is being reached, the lateral forces due to filament tensions and local curvatures will also reach a new high level. And this increased interfilament pressure accompanied by thermal softening will result in lateral compressive creep and in growth of contact areas between filaments. Higher friction and interfilament shear stresses will then result in higher incremental torsional rigidities.

Experience thus far suggests that it will require extensive additional experimentation to verify these hypotheses. An alternative approach is to model the yarn on the basis of these various hypotheses, then to predict threadline behavior on the basis of these models.

Thwaites[14] has taken this approach in his theoretical analysis of the torsional behavior of the false twist threadline.

3.2.3 Experiments Using POY PET Yarn

After experimental characterization of the torsional behavior of the conventional false twist threadline it is necessary to do the same for the draw texturing threadline. Accordingly, partially oriented yarns (POY PET) supplied by the Du Pont Company were used for the study. The POY PET consists of 30 filaments and is 245 denier with a prescribed draw ratio of 1.60.

The results of the torsional rigidity study are given in Table 3.3 and in Figures 3.21, 3.22, and 3.23. Figure 3.21 shows that for a fixed machine draw ratio and heater temperature

Table 3.3

TORSIONAL RIGIDITY OF DRAW TEXTURING THREADLINE, (10^{-5}) in^2 lbs

HEATER 210°C 1.60 DR

MACHINE TWIST	50 TPI	60 TPI	65 TPI	70 TPI	80 TPI
COLD YARN SEGMENT RIGIDITY (LOCAL TPI)	0.84 (25.2)	1.75 (38.0)	1.90 (39.9)	1.93 (40.6)	2.22 (44.3)
COOLING YARN SEGMENT RIGIDITY (LOCAL TPI)	2.68 (63.7)	3.55 (80.2)	3.37 (99.7)	3.24 (102.6)	2.95 (134.9

HEATER 210°C 65 TPI MACHINE TWIST

DRAW RATIO	1.57 DR	1.60 DR	1.64 DR
COLD YARN SEGMENT RIGIDITY (LOCAL TPI)	1.62 (39.0)	1.90 (39.9)	1.56 (38.5)
COOLING YARN SEGMENT RIGIDITY (LOCAL TPI)	3.08 (100.8)	3.37 (99.7)	3.45 (92.9)

1.60 DRAW RATIO 65 TPI MACHINE TWIST

HEATER TEMPERATURE	190°C	210°C	230°C.
COLD YARN SEGMENT RIGIDITY (LOCAL TPI)	1.52 (39.0)	1.90 (39.9)	1.55 (38.1)
COOLING YARN SEGMENT RIGIDITY (LOCAL TPI)	2.83 (90.4)	3.37 (99.7)	2.93 (99.6)

Figure 3.21

INCREMENTAL TORSIONAL RIGIDITY

DRAW TEXTURED YARNS

TEXTURING CONDITIONS: 245 DENIER YARN

1.60 DRAW RATIO

210° C.

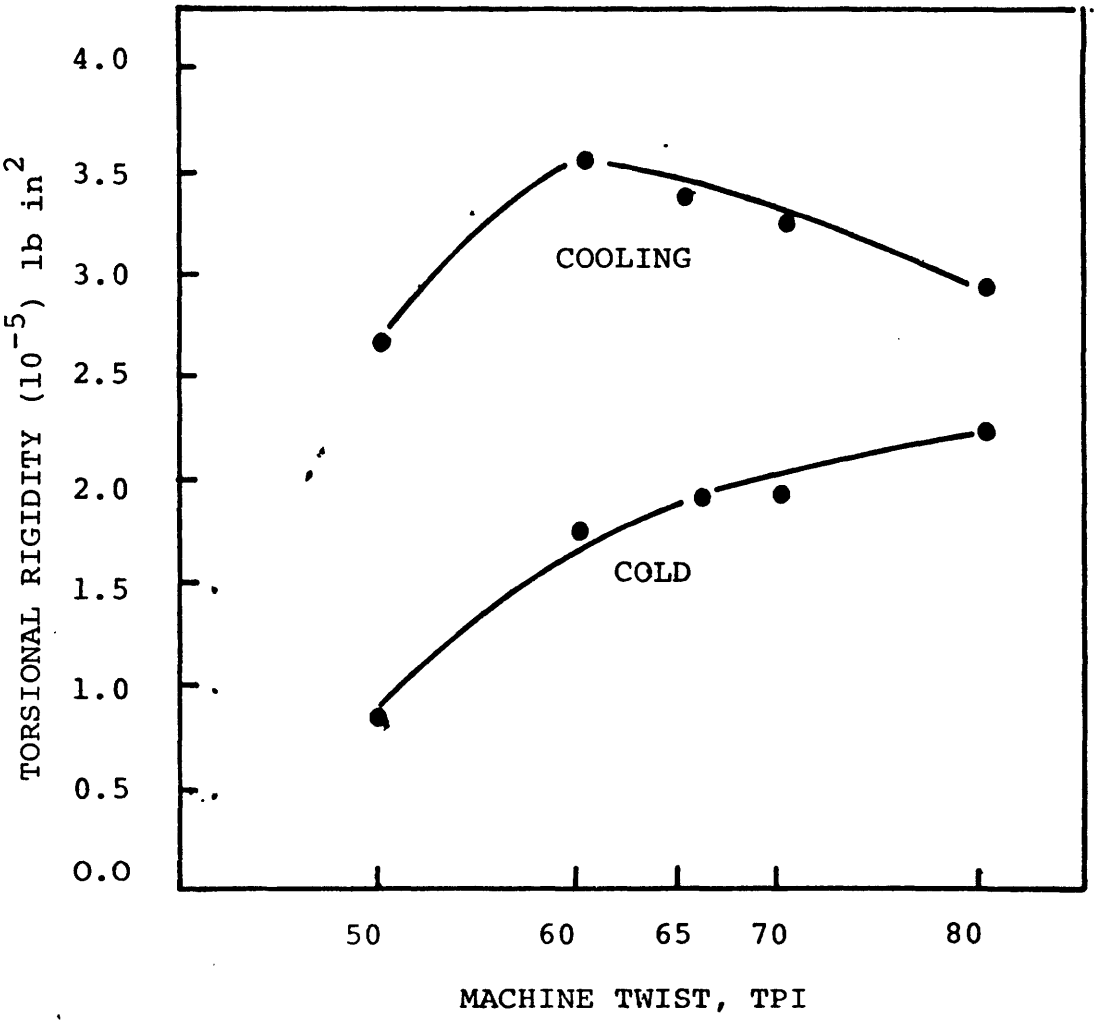

Figure 3.22

INCREMENTAL TORSIONAL RIGIDITY

DRAW TEXTURED YARNS

TEXTURING CONDITIONS: 245 DENIER
65 TPI BASIC TWIST
1.6 DRAW RATIO

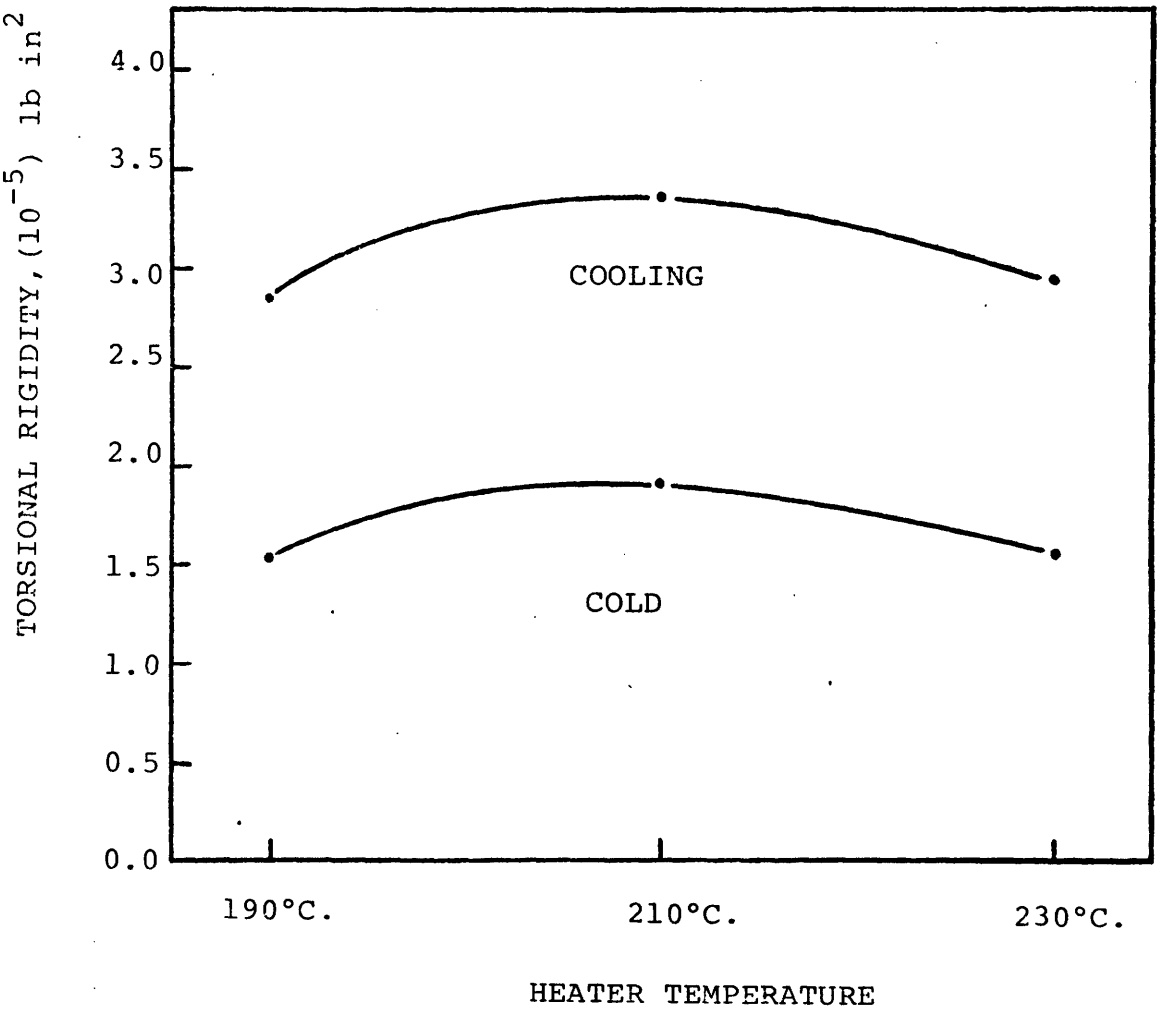

Figure 3.23

INCREMENTAL TORSIONAL RIGIDITY

DRAW TEXTURED YARNS

TEXTURING CONDITIONS: 245 DENIER

65 TPI BASIC TWIST

210°C HEATER

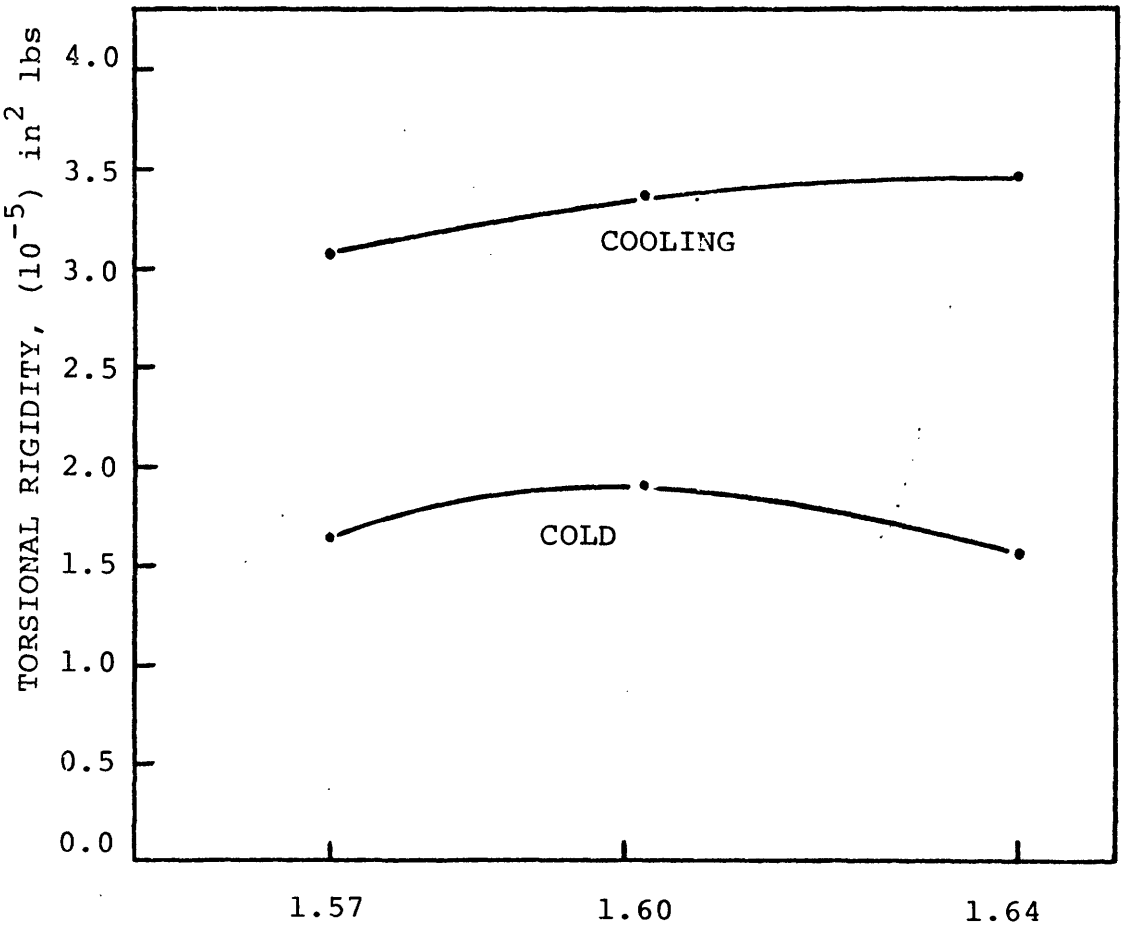

increases in machine twist cause the incremental rigidity of the cold zone yarn segments to increase. However, the incremental torsional rigidity of segments taken from the cooling zone peaks at 60 TPI machine twist and then drops as machine twist is increased. The behavior of the cooling zone segments is attributed to the observed torsional buckling of the cooling zone segments at high machine twist levels (Figure 2.13) Figure 3.22 shows that as the heater temperature is changed there appears to be a maximum torsional rigidity at 210°C. This corresponds to the maximum cooling zone twist observed when the POY PET is textured at 210°C, as shown in Table 3.3.

Lastly, as the machine draw ratio increases, the torsional rigidity of the cooling zone segments increase as seen in Figure 3.23. For the cold zone segments, the torsional rigidity reaches a peak at 1.60 machine draw ratio. This corresponds to the peak in twist level for this machine draw ratio.

3.2.4 Experiments Concerning Transient Twist, Using POY PET Yarns

The cold zone twist distribution was photographed as before for the conventional false twist texturing threadline. The machine parameters were set as follows:

Cold Zone Length	6.00 in	Post Spindle Length	9.00 in
Cooling Zone Length	7.00 in	Heater Temperature	210° C
Hot Zone Length	1.25 in	Machine Draw Ratio	1.60

Pictures of the threadline twist levels were taken at a position one inch downstream of the cold zone entrance and five inches downstream.

Twist observations are recorded in Figure 3.24 and 3.25. The twist level one inch into the cold zone appears to undergo a rapid change, a short time after the step increase in spindle speed.(Fig. 3.24) At five inches into the cold zone there is a definite time lag after the step increase in spindle speed before the twist level begins to change significantly.

Difficulties were encountered in repeating the above experiments for the hot zone and the cooling zone. For with the texturing machine operating in the same twist level as that used in measuring cold twist, the hot and cooling twist levels were too high in the "semi-welded" yarn to permit measurement of twist. To overcome this difficulty, a lower steady state machine twist level was employed and the spindle speed was suddenly reduced. The hot and cooling zone transient twist distribution was then observed. The machine parameters in the latter experiment were:

Cold Zone Length	6.0 inches
Cooling Zone Length	15.0 inches

Figure 3.24

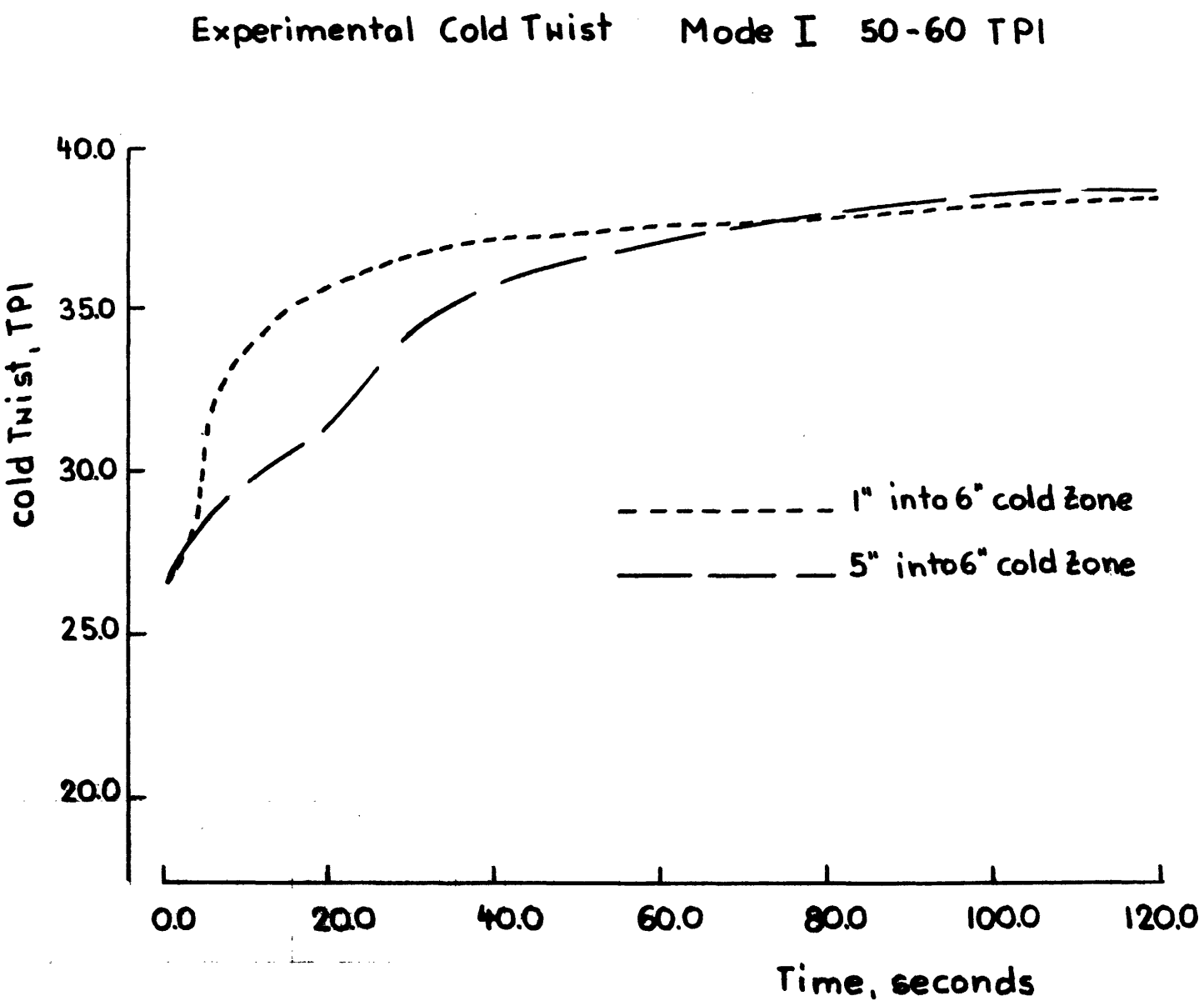
Experimental Cold Twist Mode I 50-60 TPI
40.0
35.0
30.0
25.0
20.0
Cold Twist, TPI
1" into 6" cold zone
5" into 6" cold zone
0.0
20.0
40.0
60.0
80.0
100.0
120.0
Time, seconds

Figure 3.25

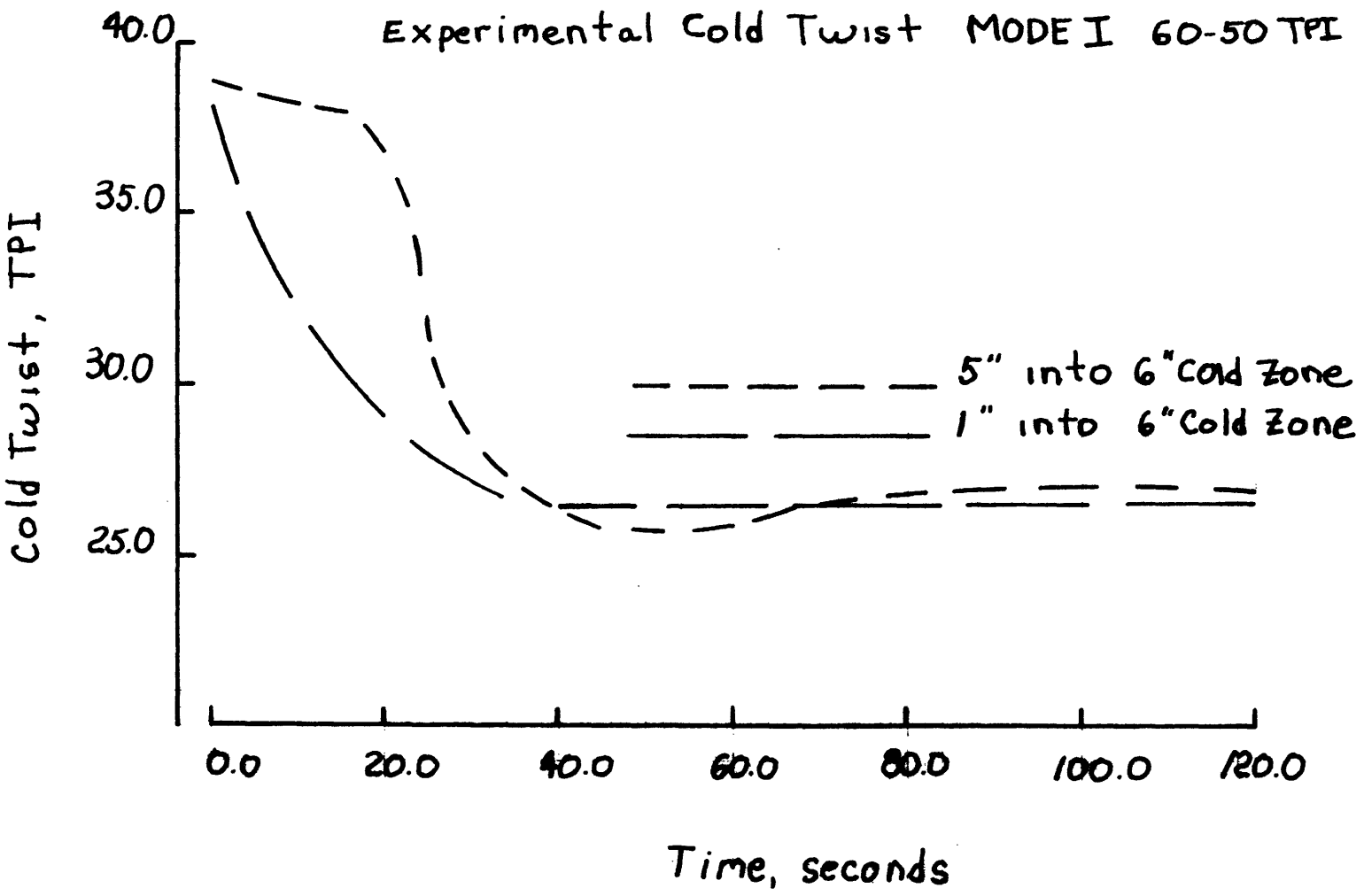
Experimental Cold Twist MODE I 60-50 TPI
40.0
35.0
30.0
25.0
Cold Twist, TPI
5" into 6" Cold Zone
1" into 6" Cold Zone
0.0
20.0
40.0
60.0
80.0
100.0
120.0
Time, seconds

Hot Zone Length	1.25 inches
Post Spindle Zone	9.00 inches
Heater Temperature	210° C
Machine Draw Ratio	1.60

Motion pictures of the threadline twist levels were taken at the beginning of the heater, at the end of the heater, immediately after the heater, and nine inches from the heater in the cooling zone. Figures 3.26 and 3.27 show the results from the twist measurements. Just as occurred in the cold zone the twist level at the heater entrance drops off immmediately after the spindle speed is reduced while there is a definite time lag for the twist to drop off nine inches into the cooling zone. It should be noted that local twist at the downstream end of the heater and at the entrance to the cooling zone, also respond to the step drop in spindle speed, with no clear evidence of a time lag. Finally Figure 3.27 shows that the twist level across the heater and through the cooling zone is not actually uniform at steady state. This slight amount of uptwisting is probably due to further relaxation of filament tensile forces. Also at the heater-cooling zone interface there is a slight steplike uptwist of about one turn per inch. Backer and Yang[4] have identified this behavior for conventional texturing threadlines. Thwaites [14] analytically describes this uptwist as that which causes a cooling zone incremental torque equal to the threadline torque.

Figure 3.26

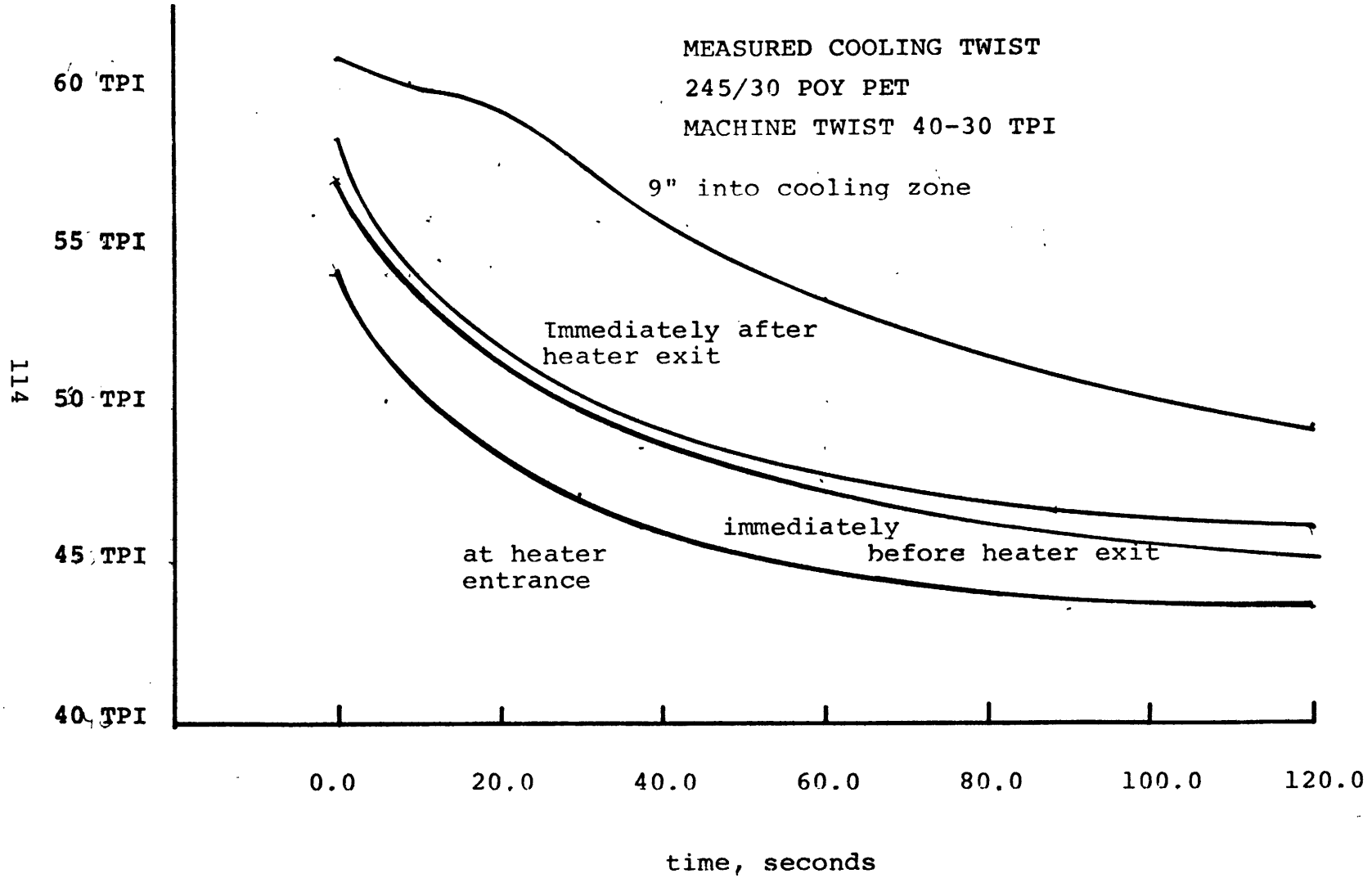
MEASURED COOLING TWIST
245/30 POY PET
MACHINE TWIST 40-30 TPI
9" into cooling zone
Immediately after heater exit
immediately before heater exit
at heater entrance
60 TPI
55 TPI
50 TPI
45 TPI
40 TPI
0.0
20.0
40.0
60.0
80.0
100.0
120.0
time, seconds

Figure 3.27

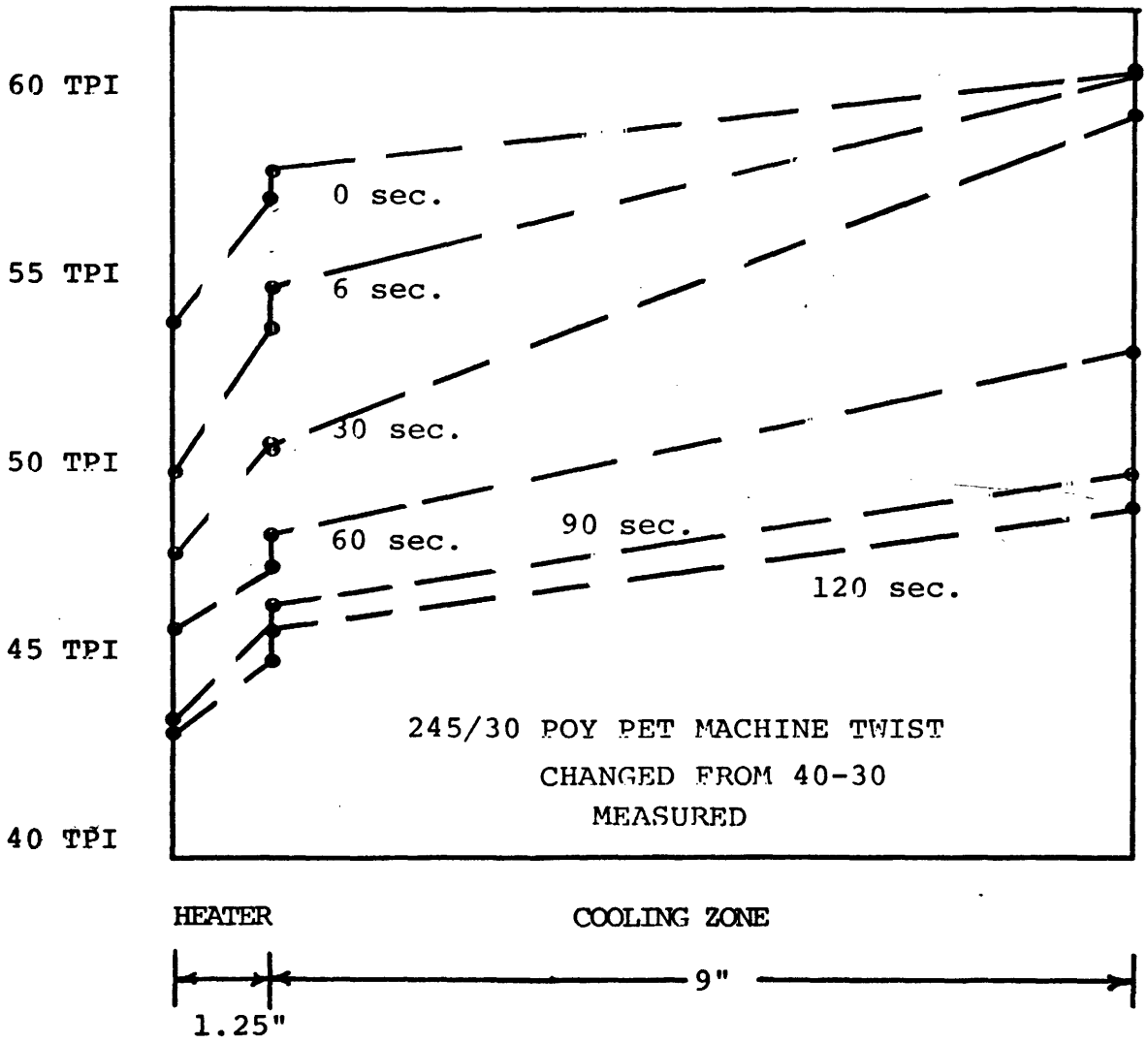
60 TPI
55 TPI
50 TPI
45 TPI
40 TPI
0 sec.
6 sec.
30 sec.
60 sec.
90 sec.
120 sec.
245/30 POY PET MACHINE TWIST
CHANGED FROM 40-30
MEASURED
HEATER
COOLING ZONE
1.25"
9"

3.3 ANALYSIS OF TRANSIENT OPERATION

3.3.1 Introduction

The analysis of steady state operation as developed in Chapter 2 was based on the fact that the threadline tension and threadline torque are essentially uniform along the texturing zone and that during transient operation there are no transient material or twist buildups in any zone of the process. During steady state operation it was shown that there are essentially three levels of twist between the feed rollers and the take up rollers: the cold twist level, the hot or cooling twist level, and the post spindle level.

Transient operation generates material buildups and twist buildups with respect to time in different zones of the texturing system. However, the threadline tension and threadline torque at any given instant are considered uniform along the texturing zone during transient operation, as well as in steady state operation.

This section presents two models which are used to calculate threadline response to transient machine operation. Each model is used to predict cold, hot, cooling, and post spindle twist levels as well as threadline tension and threadline torque. The first model is based on the physical simplification that uniform twist levels persist during transient operation in the cold, hot, cooling, and post spindle zones. The second model provides for non-uniform twist distribution in the cold zone

and in the cooling zone and it formulates these distributions according to experimental observations discussed in the previous section.

The numerical results derived from these two models will be compared to experimental data to determine the effectiveness of the models. After comparison is made, a parametric study is reported showing how unsteady machine behavior affects the transient operation of the draw texturing process.

3.3.2 Method of Solution

During steady state operation of the draw texturing process threadline tension and threadline torque are considered uniform in the zone between the feed rollers and the spindle. Since inertial effects are indicated to be negligible, threadline tension and threadline torque can also be considered uniform along the texturing zone during transient operation. We can now determine the material-system constitutive relations, yarn geometry, and system compatibility at any yarn cross-section, and use these relations to predict threadline torque and threadline tension.

During steady state operation neither the number of turns nor the amount of material in any threadline zone changes with respect to time. Therefore in each zone, i.e., the cold zone, hot zone, cooling zone, and post spindle zone, the input turn flow rate is equal to the output turn flow rate and the input

material flow rate equals the output material flow rate. During transient operation these flow equalities no longer obtain and the number of turns and amount of material in any zone generally varies with time.

Transient analysis of the draw texturing process must include material balances and turn balances for each defined zone of the texturing threadline(i.e. cold, hot, cooling, and post spindle). To complete the analysis,these balances are coupled with the requirements of threadline tension and threadline torque uniformity in the zone between the feed rollers and spindle. In this section,the relations which describe the transient threadline mechanics will be expressed in functional form. We will then show how these functional relations are used to predict threadline tension, threadline torque, and local twist levels during transient operation. In subsequent sections detailed expressions will be formulated.

A block diagram which shows how the variables in the draw texturing analysis are related to each other is presented in Figure 3.28. For each block there is an equation developed in the text which relates the variables according to threadline mechanics.

Figure 3.28

RELATIONSHIP OF VARIABLES IN DRAW TEXTURING PROCESS

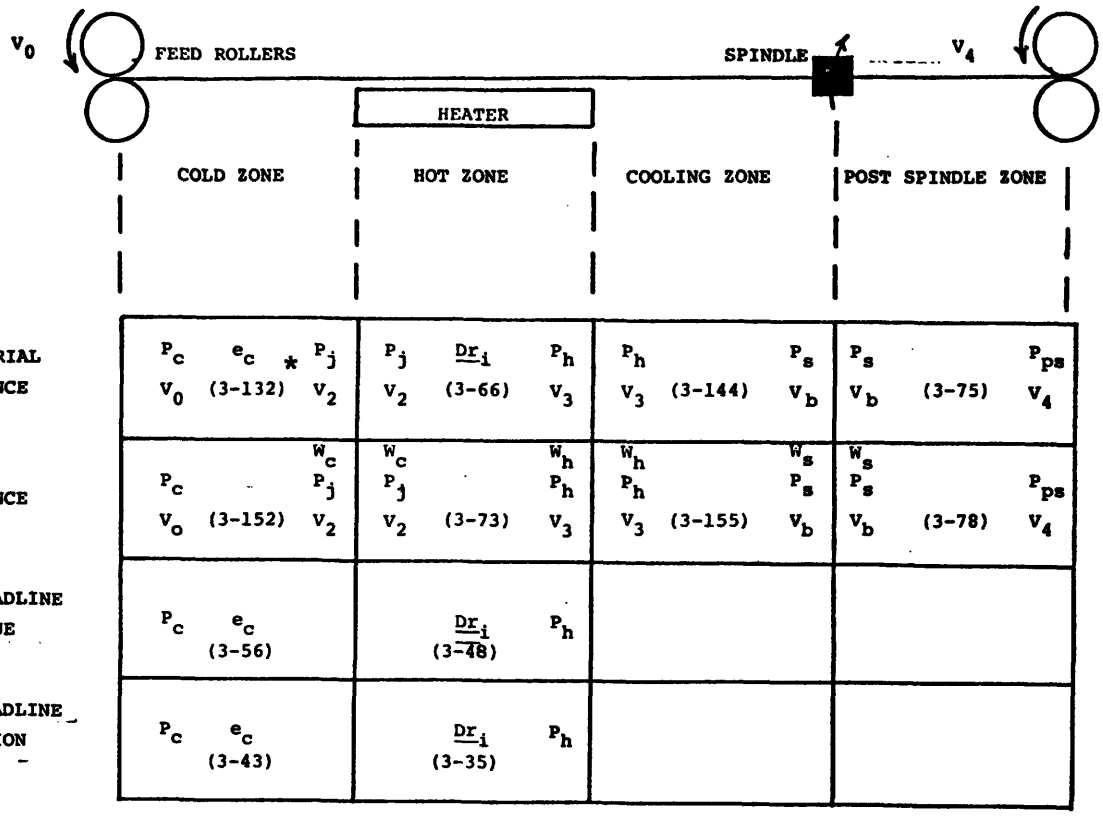

P_c = TWIST/UNIT LENGTH AT UPSTREAM END OF COLD ZONE
P_j = TWIST/UNIT LENGTH AT DOWNSTREAM END OF COLD ZONE
P_h = TWIST/UNIT LENGTH OVER HEATER AND UPSTREAM END OF COOLING ZONE
P_s = TWIST/UNIT LENGTH AT DOWNSTREAM END OF COOLING ZONE
P_{ps} = TWIST/UNIT LENGTH IN POST SPINDLE ZONE
V_0 = FEED ROLLER SURFACE VELOCITY
V_2 = LINEAR VELOCITY OF YARN AT COLD ZONE EXIT
V_3 = LINEAR VELOCITY OF YARN AT HOT ZONE EXIT
V_b = LINEAR VELOCITY OF TWISTED YARN AS IT ENTERS SPINDLE
e_c = STRAIN OF FILAMENTS IN COLD ZONE
Dr_i = DRAW RATIO OF FILAMENTS ON i^{th} RADIAL YARN LAYER IN HOT ZONE
W_c = ANGULAR VELOCITY OF YARN IN COLD ZONE
W_h = ANGULAR VELOCITY OF YARN IN HOT ZONE
W_s = ANGULAR VELOCITY OF SPINDLE

*The numbers in parenthesis refer to equations in text

LIST OF SYMBOLS

$A,B,$ = Hot Moduli of Drawing Coefficients

A_{i1}, A_{i2}, A_{i3} = Defined Coefficients

AN_i = No. of Filaments in Hot Zone i^{th} Radial Layer

BN_i = No. of Filaments in Cold Zone i^{th} Radial Layer

$\underline{Cr}_c$ = Cold Contraction Factor (Alternative Model)

$\underline{Cr}_h$ = Hot Contraction Factor (Hearle's Model)

$\underline{Cr}_j$ = Contraction Factor at Twist Level P_j (Hearle's Model)

$\underline{Cr}_{ps}$ = Contraction Factor at Twist Level P_{ps}(Hearle's Model)

$\underline{Cr}_{set}$ = Contraction Factor in Set Zone (Hearle's Model)

$\underline{Dr}_i$ = Draw Ratio of Filament in i^{th} Radial Layer

E_c = Cold Young's Modulus Cross Sectional Area of Filament

e_c = Average Tensile Strain of Filaments in Cold Zone.

EI_{fiber} = Cold Bending Modulus of Fiber

$F_0,F_1,F_2,F_3,F_4,F_5,F_6,F_7$ = Defined Coefficients

GI_{fiber} = Cold Torsion Modulus of Fiber

$G_1, G_2, G_3, G_4, G_5, G_6, G_7$ = Defined Coefficients

L_c = Cold Zone Length

L_h = Hot Zone Length

L_{ps} = Post Spindle Zone Length

L_s = Length of Set Zone

P_c = Twist in Cold Zone, (Radians/Inch)

P_h = Twist in Hot Zone, (Radians/Inch)

P_j = Twist at Downstream End of Cold Zone (Radians/Inch)

P_{ps} = Twist in Post Spindle Zone (Radians/Inch)

P_s = Twist at Downstream End of Set Zone (Radians/Inch)

Q_1, Q_2, Q_3 = Defined Coefficients

R_{ic} = Radius of i^{th} Radial Layer in Cold Zone

R_{ih} = Radius of i^{th} Radial Layer in Hot Zone

$\text{Sec}\theta_{3i}$ = Secant of Hot Zone Helix Angle at i^{th} Radial Layer

$\text{Sec}\theta_{2i}$ = Secant of Cold Zone Helix Angle at i^{th} Radial Layer

t = Time, Seconds

V_b = Velocity of Hot Twisted Yarn at Spindle Entrance

V_0 = Feed Roller Linear Velocity

V_2 = Linear Velocity of Cold Twisted Yarn

V_3 = Linear Velocity of Hot Twisted Yarn

V_4 = Take Up Roller Linear Velocity

W_c = Angular Velocity of Cold Zone Segments

W_h = Angular Velocity of Hot Zone Segments

W_s = Spindle Speed and Angular Velocity of Cooling Zone Segments

$X_1, X_2, X_3, X_4, X_5, X_6, X_7, X_8$ = Defined Coefficients

Y_1, Y_2, Y_3, Y_4 = Defined Coefficients

Z, Z_1, Z_2 = Defined Coefficients

In Chapter 2 it was shown that the yarn tension at the cold zone entrance can be expressed as

$$T_c = F_1^*(e_c, P_c) \tag{2-1}$$

Differentiating (2-1) with respect to time we obtain

$$\frac{d\,T_c}{dt} = G_1^*\left(\frac{d\,e_c}{dt}, \frac{d\,P_c}{dt}\right) \tag{3-1}$$

Yarn torque at the cold zone entrance was expressed in Chapter 2 as

$$M_{tc} = F_4(e_c, P_c) \tag{2-4}$$

Differentiating (2-4) with respect to time we obtain

$$\frac{d\,M_{tc}}{dt} = G_4\left(\frac{d\,e_c}{dt}, \frac{d\,P_c}{dt}\right) \tag{3-2}$$

At the entrance to the hot drawing zone it was shown in Chapter 2 that

$$T_h = F_5(V_2, V_3, P_c, P_h) \tag{2-5}$$

Taking the variation of filament draw ratio in the yarn cross section into account, we can express (2-5) more simply as

$$T_h = F_5'(\underline{Dr}_i, P_h) \tag{3-3}$$

---

* The symbols F,G,X,Y,Z indicate various functional expressions which are developed later.

And likewise yarn torque at the hot zone entrance is expressed as:

$$M_{th} = F_6'(\underline{Dr}_i, P_h) \tag{3-4}$$

Both (3-3) and (3-4) are differentiated with respect to time to obtain:

$$\frac{d\ T_h}{dt} = G_5\left(\frac{d\ \underline{Dr}_i}{dt}\ ,\ \frac{d\ P_h}{dt}\right) \tag{3-5}$$

$$\frac{d\ M_t}{dt} = G_6\left(\frac{d\ \underline{Dr}_i}{dt}\ ,\ \frac{d\ P_h}{dt}\right) \tag{3-6}$$

Satisfying the requirements of threadline torque and threadline tension uniformity, we can equate (3-1) and (3-5) as well as (3-2) and (3-6) to obtain:

$$0 = G_1\left(\frac{d\ e_c}{dt},\ \frac{d\ P_c}{dt}\right) - G_5\left(\frac{d\ \underline{Dr}_i}{dt},\ \frac{d\ P_h}{dt}\right) \tag{3-7}$$

$$0 = G_2\left(\frac{d\ e_c}{dt},\ \frac{d\ P_c}{dt}\right) - G_6\left(\frac{d\ \underline{Dr}_i}{dt},\ \frac{d\ P_h}{dt}\right) \tag{3-8}$$

Equations (3-7) and (3-8) represent generalized threadline coupled force differential equations They are developed in Section 3.3.3.1. They are 2 equations with 4 unknowns. The analytical relationships required to complete the analysis are developed from the material balance relation and turn balance relation for each zone in the texturing threadline.

In Section 3.2.4 it was reported that the twist distributions observed in both the cold and cooling zones of the threadline operation were not uniform with respect to position. One of our models for transient operation is based on these observations of non-uniform twist distributions. Another model is based on the simplification that the twist levels are uniform throughout zones during transient operation. Common to both models is threadline behavior both in the hot (i.e. over the heater) and the post spindle zones. For it has been observed that twist distribution during transient operation is the same as for steady state operation across the heater and post spindle zones.

The material balance for the hot zone will be fully developed in Section 3.3.3.2 but it can be functionally expressed as

$$V_2 = X_1(P_h, P_c, \underline{Dr}_i, \frac{dP_h}{dt}, V_3, \frac{d\,\underline{Dr}_i}{dt}) \qquad (3\text{-}9)$$

Likewise, the turn balance for the hot zone which is to be developed in Section 3.3.3.2 can be functionally expressed as

$$\frac{dP_h}{dt} = X_2\ (W_h, W_c, P_c, V_2, P_h, V_c) \qquad (3\text{-}10)$$

The post spindle analysis given in Section 3.3.3.2 demonstrates that

$$\frac{dP_{ps}}{dt} = X_3(P_{ps}, P_s, W_{ps}, V_b) \qquad (3\text{-}11)$$

and

$$V_b = X_4(P_{ps}, W_h, P_s, \frac{dp_{ps}}{dt}) \qquad (3\text{-}12)$$

where V_b = linear velocity of twisted yarn as it enters spindle. Since we assume that the cooling and hot zone segments rotate at the same angular speed as the pin spindle ($W_h = W_c = W_s$) equations (3-7), (3-8), (3-9), (3-10), (3-11), and (3-12) can be combined to yield 5 differential equations with 10 unknowns; $P_c, P_h, \underline{Dr_i}, e_c, V_b$, V_3, V_2, P_{ps}, P_s, and W_c. The analysis can be completed considering the material balances and turn balances in the cold and cooling zones. To deal with the turn balances, we resort to the two models for twist distribution as mentioned above.

3.3.2.1 MODEL 1: Flat Twist Distribution

Model 1 is based on the simplifying assumption that the twist distribution is uniform flat in the cold zone and in the hot and cooling zones during transient operation. The latter twists are equal at all times. The material balance for the cold zone developed in Section 3.3.3.3 shows that

$$V_z = X_5 \left(e_c, P_c, \frac{dP_c}{dt}, \frac{d\,e_c}{dt}\right) \qquad (3\text{-}13)$$

The turn balance for the cold zone developed in Section 3.3.3.3 shows that

$$\frac{dP_c}{dt} = X_6 \ (W_c, P_c, V_2) \tag{3-14}$$

The material balance for the cooling zone developed in Section 3.3.3.3 shows that

$$\frac{dP_s}{dt} = X_7(P_s, V_3, V_b, P_h) \tag{3-15}$$

where P_s = turns/twisted length in cooling zone.

The turn balance for the cooling zone is expressed as

$$\frac{d P_s}{dt} = X_8(P_h, V_3, V_b, P_s) \tag{3-16}$$

Lastly, by definition

$$P_s = P_h \tag{3-17}$$

In summary, equations (3-7), (3-8), (3-9), (3-10), (3-11), (3-12), (3-13), (3-14), (3-15), (3-16) and (3-17) represent 11 expressions of which 10 are differential equations with 10 unknowns; P_c, P_h, P_s, P_{ps}, W_c, V_2, V_3, V_b, e_c, $\underline{Dr}_i$.

After considerable manipulation these equations can be reduced to the following:

$$\frac{d P_c}{dt} = Z_1 \ [P_c, P_h, e_c, \underline{Dr}_i, P_{ps}] \tag{3-18}$$

$$\frac{d P_h}{dt} = Z_2[P_c, P_h, e_c, \underline{Dr}_i, P_{ps}] \tag{3-19}$$

$$\frac{d e_c}{dt} = Z_3[P_c, P_h, e_c, \underline{Dr}_i, P_{ps}] \tag{3-20}$$

$$\frac{d \underline{Dr}_i}{dt} = Z_4[P_c, P_h, e_c, \underline{Dr}_i, P_{ps}] \tag{3-21}$$

$$\frac{d P_{ps}}{dt} = Z_5[P_c, P_h, e_c, \underline{Dr}_i, P_{ps}] \tag{3-22}$$

This system of non-linear ordinary differential equations is solved numerically by a digital computer. The solution technique is described in Section 3.3.4.

After obtaining P_c, P_h, e_c, and $\underline{Dr}_i$ as functions of time, we substituted these values into (2- 1),(2-4), (3-3) and (3-4) to determine threadline tension and threadline torque at any instant during transient operation.

3.3.2.2 Model 2: Tilted Twist Distribution

Model 2 is based on the assumption that the twist is not uniform, along the cold zone nor along the cooling zone. An approximat kinematic relation (twist transport equation) is formulated which relates the twist level at the downstream end of either zone to the corresponding twist level at the upstream portion of that zone. The

upstream twist levels are determined by the appropriate force, material and turn balances.

The twist transport equations for the cold zone and cooling zone are developed in Section 3.3.3.4 and are expressed functionally as

$$\frac{d P_j}{dt} = X_9[P_c, P_j, V_2] \tag{3-23}$$

and

$$\frac{d P'_s}{dt} = X_{10}[P_s', P_h, V_b] \tag{3-24}$$

where P_j = twist/unit length at downstream end of cold zone

P'_s = twist/unit length at downstream end of cooling zone

The material balance for the cold zone developed in Section 3.3.3.4 shows that

$$V_2 = X_{11}\left[e_c, P_j, P_c, \frac{d P_j}{dt}, \frac{d P_c}{dt}, \frac{d e_c}{dt}\right] \tag{3-25}$$

Likewise, the turn balance for the cold zone developed in Section 3.3.3.4 shows that

$$\frac{d P_c}{dt} = X_{12}\left[W_c, P_c, P_j, V_2, \frac{d P_j}{dt}\right] \tag{3-26}$$

The material balance for the cooling zone shows that

$$\frac{d P'_s}{dt} = X_{13}\left(\frac{dP_h}{dt}, P_h, P'_s, V_3, V_b\right) \tag{3-27}$$

Finally, the turn balance for the cooling zone can be expressed as

$$\frac{d P_s}{dt} = X_{14} \left[\frac{d P_h}{dt}, P_s, P_h, V_3, V_b \right] \tag{3-28}$$

In summary equations (3-7), (3-8), (3-9), (3-10), (3-11), (3-12), (3-23), (3-24), (3-25), (3-26), (3-27) and (3-28) represent a system of 12 differential equations with 11 unknowns; P_c, P_j, P_h, P_s', P_{ps}, W_c, V_2, V_3, V_b, e_c, and $\underline{Dr}_i$. After considerable manipulation these can be reduced to the following:

$$\frac{d P_c}{dt} = Y_1 [P_c, P_j, P_h, P_s', P_{ps}, e_c, \underline{Dr}_i] \tag{3-29}$$

$$\frac{d P_h}{dt} = Y_2 [P_c, P_j, P_h, P_s', P_{ps}, e_c, \underline{Dr}_i] \tag{3-30}$$

$$\frac{d e_c}{dt} = Y_3 [P_c, P_j, P_h, P_s', P_{ps}, e_c, \underline{Dr}_i] \tag{3-31}$$

$$\frac{d \underline{Dr}_i}{dt} = Y_4 [P_c, P_j, P_h, P_s', P_{ps}, e_c, \underline{Dr}_i] \tag{3-32}$$

$$\frac{d P_j}{dt} = Y_5 [P_c, P_j, P_h, P_s', P_{ps}, e_c, \underline{Dr}_i] \tag{3-33}$$

$$\frac{d P_s'}{dt} = Y_6 [P_c, P_j, P_h, P_s', P_{ps}, e_c, \underline{Dr}_i] \tag{3-34}$$

$$\frac{d P_{ps}}{dt} = Y_7[P_c, P_j, P_h, P'_s, P_{ps}, e_c, \underline{Dr}_i] \qquad (3\text{-}34a)$$

This system of non-linear ordinary differential equations is solved numerically by digital computer. The solution technique is described in Section 3.3.4. After obtaining P_c, P_h, e_c, and $\underline{Dr}_i$ as functions of time we substitute these values into (2-1), (2-4), (3-3) and (3-4) to determine threadline torque and threadline tensions at any instant during transient operation.

3.3.3 Transient Threadline Mechanics

3.3.3.1 General Tension & Torque Relationships

In Chapter 2 the yarn tension at the hot zone entrance was derived as*

$$T_h = AN_0 \cdot (A \cdot \underline{Dr}_0^2 + B \cdot Dr_0^3) + AN_1 \cdot (A \cdot \underline{Dr}_0^2 + B \cdot \underline{Dr}_1^3) \cdot \frac{1}{\sqrt{1+P_h^2 R_{1h}^2}} + AN_2 \cdot (A \cdot \underline{Dr}_2^2 + B \cdot \underline{Dr}_2^3) \cdot \frac{1}{\sqrt{1+P_h^2 R_{2h}^2}} + AN_3 \cdot (A \cdot \underline{Dr}_3^2 + B \cdot \underline{Dr}_3^3) \cdot \frac{1}{\sqrt{1+P_h^2 R_{3h}^2}} \quad (3\text{-}35)$$

Equation (3-35) is now differentiated with respect to time to obtain.

---

*Note: Since most yarns which are draw textured are 3 layer multifilament yarns and the yarns used for experimental study are such, the analysis will be formulated to accommodate this type of yarn. Simple arithmetical changes could be made if this were not the case.

$$\frac{dT_h}{dt} = AN_0 \cdot (2 \cdot A \cdot \underline{Dr}_0 + 3 \cdot B \cdot \underline{Dr}_0^2) \frac{d\underline{Dr}_0}{dt}$$

$$+ AN_1 \cdot \frac{(2 \cdot A \cdot \underline{Dr}_1 + 3 \cdot B \cdot \underline{Dr}_1^2}{(1+P_h^2 R_{1h}^2)^{1/2}} \frac{d\underline{Dr}_1}{dt}$$

$$+ AN_2 \cdot \frac{(2 \cdot A \cdot \underline{Dr}_2 + 3 \cdot B \cdot \underline{Dr}_2^2)}{(1+P_h^2 R_{2h}^2)^{1/2}} \frac{d\underline{Dr}_2}{dt}$$

$$+ AN_3 \cdot \frac{(2 \cdot A \cdot \underline{Dr}_3 + 3 \cdot B \cdot \underline{Dr}_3^2}{(1+P_h^2 R_{3h}^2)^{1/2}} \frac{d\underline{Dr}_3}{dt}$$

$$-P_h \left[AN_1 (A \cdot \underline{Dr}_1^2 + B \cdot \underline{Dr}_1^3) \frac{R_{1h}^2}{(1+P_h^2 R_{1h}^2)^{3/2}} \right.$$

$$+ AN_2 (A \cdot \underline{Dr}_2^2 + B \cdot \underline{Dr}_2^3) \frac{R_{2h}^2}{(1+P_h^2 R_{2h}^2)^{3/2}}$$

$$\left. + AN_3 (A \cdot \underline{Dr}_3^2 + B \cdot \underline{Dr}_3^3) \frac{R_{3h}^2}{(1+P_h^2 R_{3h}^2)^{3/2}} \right] \frac{dP_h}{dt} \quad (3\text{-}36)$$

To simplify equation (3-36) we define the following

$$F_0 \equiv AN_0 (2A\underline{Dr}_0 + 3B\underline{Dr}_0^2) \quad (3\text{-}37)$$

$$F_1 \equiv AN_1 (2A\underline{Dr}_1 + 3B\underline{Dr}_1^2) \quad (3\text{-}38)$$

$$F_2 \equiv AN_2 (2A\underline{Dr}_2 + 3B\underline{Dr}_2^2) \quad (3\text{-}39)$$

$$F_3 \equiv AN_3 (2A\underline{Dr}_3 + 3B\underline{Dr}_3^2) \quad (3\text{-}40)$$

$$F_5 \equiv -P_h \left[AN_1 (A \cdot \underline{Dr}_1^2 + B \cdot Dr_1^3) \frac{R_{1h}^2}{(1+P_h^2 R_1^2)^{3/2}} \right.$$

$$+AN_2 (A \cdot \underline{Dr}_2^2 + B \cdot \underline{Dr}_2^3) \frac{R_{2h}^2}{(1+P_h^2 R_2^2)^{3/2}}$$

$$\left. +AN_3 (A \cdot Dr_3^2 + B \cdot \underline{Dr}_3^3) \frac{R_{3h}^2}{(1+P_h^2 R_3^2)^{3/2}} \right] \qquad (3\text{-}41)$$

Substitution of (3-37), (3-38), (3-39), (3-40) and (3-41) into (3-36) gives

$$\frac{dT_h}{dt} = F_0 \frac{d\underline{Dr}_0}{dt} + F_1 \frac{d\underline{Dr}_1}{dt} + F_2 \frac{d\underline{Dr}_2}{dt} + F_3 \frac{d\underline{Dr}_3}{dt}$$

$$+ F_5 \frac{dP_h}{dt} \qquad (3\text{-}42)$$

In Chapter 2 yarn tension in the <u>cold zone entrance</u> was derived as

$$T_c = E_c e_c \left[\frac{BN_1}{(1+P_c^2 R_{1c}^2)^{1/2}} + \frac{BN_2}{(1+P_c^2 R_{2c}^2)^{1/2}} \right.$$

$$\left. + \frac{BN_3}{(1+P_c^2 R_{3c}^2)^{1/2}} \right] \qquad (3\text{-}43)$$

where E_c = Cold tensile modulus x Area of filament

Equation (3-43) applies during both transient and steady state operation. Therefore if we know the cold filament

strain and the cold twist at any time, the threadline tension can be determined therefrom. Equation (3-43) is differentiated with respect to time to obtain

$$\frac{d(T_c)}{dt} = E_c \left[\frac{BN_1}{(1+P_c^2 R_{1c}^2)^{1/2}} + \frac{BN_2}{(1+P_c^2 R_{2c}^2)^{1/2}} + \frac{BN_3}{(1+P_c^2 R_{3c}^2)^{1/2}} \right] \frac{de_c}{dt}$$

$$- \frac{dP_c}{dt} E_c e_c \left[\frac{BN_1 \cdot P_c \cdot R_{1c}^2}{(1+P_c^2 R_{1c}^2)^{3/2}} + \frac{BN_2 \cdot P_c \cdot R_{2c}^2}{(1+P_c^2 R_{2c}^2)^{3/2}} + \frac{BN_3 \cdot P_c \cdot R_{3c}^2}{(1+P_c^2 R_{3c}^2)} \right] \qquad (3\text{-}44)$$

To simplify equation (3-44) we define the following

$$F_6 \equiv E_c \frac{BN_1}{(1+P_c^2 R_{1c}^2)^{1/2}} + \frac{BN_2}{(1+P_c^2 R_{2c}^2)^{1/2}} + \frac{BN_3}{(1+P_c^2 R_{3c}^2)^{1/2}} \qquad (3\text{-}45)$$

$$F_7 \equiv E_c e_c P_c \left[\frac{BN_1 \cdot R_{1c}^2}{(1+P_c^2 R_{1c}^2)^{3/2}} + \frac{BN_2 \cdot R_{2c}^2}{(1+P_c^2 R_{2c}^2)^{3/2}} + \frac{BN_3 \cdot R_{3c}^2}{(1+P_c^2 R_{3c}^2)^{3/2}} \right] \qquad (3\text{-}46)$$

where BN_i = Number of filament in i^{th} radial layer in the cold zo

To obtain:

$$\frac{dT_c}{dt} = F_6\frac{de_c}{dt} + F_7\frac{dP_c}{dt} \qquad (3\text{-}47)$$

In Chapter 2,yarn torque at the hot zone entrance was derived as

$$M_{th} = AN_1(A\cdot\underline{Dr}_1^2 + B\cdot\underline{Dr}_1^3)\cdot\frac{P_hR_{1h}^2}{(1+P_h^2R_{1h}^2)^{1/2}}$$

$$+ AN_2(A\cdot\underline{Dr}_2^2 + B\cdot\underline{Dr}_2^3)\cdot\frac{P_hR_{2h}^2}{(1+P_h^2R_{2h}^2)^{1/2}}$$

$$+ AN_3(A\cdot\underline{Dr}_3^2 + B\cdot\underline{Dr}_3^3)\cdot\frac{P_hR_{3h}^2}{(1+P_h^2R_{3h}^2)^{1/2}} \qquad (3\text{-}48)$$

Equation (3-48) applies during transient and during steady state operation. Therefore,given the individual draw ratios of the filaments and the hot twist at any time, we can determine the corresponding threadline torque. Equation (3-48) is now differentiated with respect to time to obtain.

$$\frac{d(M_{th})}{dt} = \left[AN_1\cdot(2\cdot A\cdot\underline{Dr}_1 + 3\cdot B\cdot\underline{Dr}_1^2)\frac{P_hR_{1h}^2}{(1+P_h^2R_{1h}^2)^{1/2}}\right]\frac{d\underline{Dr}_1}{dt}$$

$$+ AN_1 \cdot \left[(A\underline{Dr}_1^2 + DB\underline{r}_1^3) R^2_{1h} \right] \cdot \left[\frac{1}{(1+P_h^2 R_{1h}^2)^{1/2}} - \frac{P_h^2 R_{1h}^2}{(1+P_h^2 R_{1h}^2)^{3/2}} \right] \frac{dP_h}{dt}$$

$$+ \left[AN_2 (2 \cdot A \cdot \underline{Dr}_2 + 3 \cdot B \cdot \underline{Dr}_2^2) \frac{P_h R_{2h}^2}{(1+P_h^2 R_{2h}^2)^{1/2}} \right] \frac{d\underline{Dr}_2}{dt}$$

$$+ AN_2 \left[(A \cdot \underline{Dr}_2^2 + B \cdot \underline{Dr}_3^3) R_{2h}^2 \right] \left[\frac{1}{(1+P_h^2 R_{2h}^2)^{1/2}} \right]$$

$$- \frac{P_h^2 R_{2h}^2}{(1+P_h^2 R_{2h}^2)^{3/2}}\Bigg] \frac{dP_h}{dt} + AN_3\Bigg[(2\cdot A\cdot \underline{Dr}_3 + 3\cdot B\cdot \underline{Dr}_3^2)$$

$$\frac{P_h R_{3h}^2}{(1+P_h^2 R_{3h}^2)^{1/2}}\Bigg] \frac{d\underline{Dr}_3}{dt} + AN_3\Bigg[(A\cdot \underline{Dr}_3^2 + B\cdot \underline{Dr}_3^3)$$

$$R_{3h}^2\Bigg]\Bigg[\frac{1}{(1+P_h^2 R_{3h}^2)^{1/2}} - \frac{P_h^2 R_{3h}^2}{(1+P_h^2 R_{3h}^2)^{3/2}}\Bigg] \frac{dP_h}{dt} \qquad (3\text{-}49)$$

To simply Equation (3-49) we define the following

$$G_1 = AN_1(2\cdot A\cdot \underline{Dr}_1 + 3\cdot B\cdot \underline{Dr}_1^2) \frac{P_h R_{1h}^2}{(1+P_h^2 R_{1h}^2)^{1/2}} \qquad (3\text{-}50)$$

$$G_2 = AN_2(2\cdot A\cdot \underline{Dr}_2 + 3\cdot B\cdot \underline{Dr}_2^2) \frac{P_h R_{2h}^2}{(1+P_h^2 R_{2h}^2)^{1/2}} \qquad (3\text{-}51)$$

$$G_3 = AN_3(2\cdot A\cdot \underline{Dr}_3 + 3\cdot B\cdot \underline{Dr}_3^2) \frac{P_h R_{3h}^2}{(1+P_h^2 R_{3h}^2)^{1/2}} \qquad (3\text{-}52)$$

$$G_5 = AN_1(A\cdot \underline{Dr}_1^2 + B\cdot \underline{Dr}_1^3) R_{1h}^2\Bigg[\frac{1}{(1+P_h^2 R_{1h})^{1/2}}$$

$$- \frac{P_h^2 R_{1h}^2}{(1+P_h^2 R_{1h}^2)^{3/2}}\Bigg] + AN_2\Bigg[(A\cdot \underline{Dr}_2^2 + B\cdot \underline{Dr}_2^3)$$

$$R_{2h}^2\Bigg]\Bigg[\frac{1}{(1+P_h^2 R_{2h}^2)^{1/2}} - \frac{P_h^2 R_{2h}^2}{(1+P_h^2 R_{2h}^2)^{3/2}}\Bigg]$$

$$+ AN_3\left[(A\cdot \underline{Dr}_3^2 + B\cdot \underline{Dr}_3^3)\right]R_{3h}^2 \left[\frac{1}{(1+P_h^2R_{3h}^2)^{1/2}} - \frac{P_h^2R_{3h}^2}{(1+P_h^2R_{3h}^2)^{3/2}}\right] \quad (3\text{-}53)$$

Therefore

$$\frac{dM_{th}}{dt} = G_1\frac{d\underline{Dr}_1}{dt} + \frac{G_2 d\underline{Dr}_2}{dt} + \frac{G_3 d\underline{Dr}_3}{dt} + G_5\frac{dP_h}{dt} \quad (3\text{-}54)$$

In Chapter 2 yarn torque at the <u>cold zone entrance</u> was derived as

$$M_{tc} = \text{Torque}_{\text{fiber tension}} + \text{Torque}_{\text{fiber bending}} + \text{Torque}_{\text{fiber torsion}} \quad (3\text{-}55)$$

$$M_{tc} = P_cE_ce_c\left\{\frac{BN_1\cdot R_{1c}^2}{(1+P_c^2R_{1c}^2)^{1/2}} + \frac{BN_2\cdot R_{2c}^2}{(1+P_c^2R_{2c}^2)^{1/2}} + \frac{BN_3\cdot R_{3c}^2}{(1+P_c^2R_{3c}^2)^{1/2}}\right\}$$

$$+(EI)_{\text{fiber}}\left\{\frac{BN_1\cdot P_c^3R_{1c}^2}{(1+P_c^2R_{1c}^2)^{3/2}} + \frac{BN_2\cdot P_c^3R_{2c}^2}{(1+P_c^2R_{2c}^2)^{3/2}} + \frac{BN_3\cdot P_c^3R_{3c}^2}{(1+P_c^2R_{3c}^2)^{3/2}}\right\}$$

$$(GI_p)_{fiber} \left\{ BN_0 \cdot P_c \cdot + \frac{BN_1 P_c}{(1+P_c^2 R_{1c}^2)^{3/2}} \right.$$

$$\left. + \frac{BN_2 P_c}{(1+P_c^2 R_{2c}^2)^{3/2}} + \frac{BN_3 P_c}{(1+P_c^2 R_{3c}^2)^{3/2}} \right\} \qquad (3\text{-}56)$$

Equation (3-56) is differentiated with respect to time to obtain

$$\frac{dM_{tc}}{dt} = \frac{de_c}{dt} \cdot P_c \cdot E_c \left\{ \frac{BN_1 \cdot R_{1c}^2}{(1+P_c^2 R_{1c}^2)^{1/2}} \right.$$

$$\left. + \frac{BN_2 \cdot R_{2c}^2}{(1+P_c^2 R_{2c}^2)^{1/2}} + \frac{BN_3 \cdot R_{3c}^2}{(1+P_c^2 R_{3c}^2)^{1/2}} \right\}$$

$$+ e_c \cdot E_c \cdot \left[\left\{ BN_1 \left[\frac{R_{1c}^2}{(1+P_c^2 R_{1c}^2)^{1/2}} - \frac{P_c^2 R_{1c}^4}{(1+P_c^2 R_{1c}^2)^{3/2}} \right] \right\} \right.$$

$$+ \left\{ BN_2 \cdot \left[\frac{R_{2c}^2}{(1+P_c^2 R_{2c}^2)^{1/2}} - \frac{P_c^2 R_{2c}^4}{(1+P_c^2 R_{2c}^2)^{3/2}} \right] \right\}$$

$$\left. + \left\{ BN_3 \cdot \frac{R_{3c}^2}{(1+P_c^2 R_{3c}^2)^{1/2}} - \frac{P_c^2 R_{3c}^4}{(1+P_c^2 R_{3c}^2)^{3/2}} \right\} \right] \frac{dP_c}{dt}$$

$$+ 3 \cdot (EI)_{fiber} \cdot \left[BN_1 \cdot \left\{ \frac{P_c^2 R_{1c}^2}{(1+P_c^2 R_{1c}^2)^{3/2}} - \frac{P_c^4 R_{1c}^4}{(1+P_c^2 R_{1c}^2)^{5/2}} \right\} \right.$$

$$+BN_2\left\{\frac{P_c^2R_{2c}^2}{(1+P_c^2R_{2c}^2)^{3/2}} - \frac{P_c^4R_{2c}^4}{(1+P_c^2R_{2c}^2)^{5/2}}\right\}$$

$$+BN_3\left\{\frac{P_c^2R_{3c}^2}{(1+P_c^2R_{3c}^2)^{3/2}} - \frac{P_c^4R_{3c}^4}{(1+P_c^2R_{3c}^2)^{5/2}}\right\}\Bigg]\frac{dP_c}{dt}$$

$$+(GI_p)_{fiber}\cdot\Bigg[BN_0 + BN_1\left\{\frac{1}{(1+P_c^2R_{1c}^2)^{3/2}}\right.$$

$$\left. - \frac{3P_c^2R_{1c}^2}{(1+P_c^2R_{1c}^2)^{5/2}}\right\}$$

$$+BN_2\left\{\frac{1}{(1+P_c^2R_{2c}^2)^{3/2}} - \frac{3P_c^2R_{2c}^2}{(1+P_c^2R_{2c}^2)^{5/2}}\right\}$$

$$+BN_3\left\{\frac{1}{(1+P_c^2R_{3c}^2)^{3/2}} - \frac{3P_c^2R_{3c}^2}{(1+P_c^2R_{3c}^2)^{5/2}}\right\}\Bigg]\frac{dP_c}{dt} \qquad (3\text{-}57)$$

In order to simplify equation (3-57) we define the first term of (3-57) which is multiplied by $\frac{de_c}{dt}$ as G_6 and the remainder of the terms which are multiplied by $\frac{dP_c}{dt}$ as G_7 so that

$$\frac{dM_{tc}}{dt} = G_6\frac{de_c}{dt} + G_7\frac{dP_c}{dt} \qquad (3\text{-}58)$$

Since tension at the cold zone entrance is equal to tension at the hot zone entrance

$$\text{Tension}_{cold} = \text{Tension}_{hot}$$

and torque at the cold zone entrance is equal to torque at the hot zone entrance

$$\text{Torque}_{cold} = \text{Torque}_{hot}$$

the time derivatives of these relations must also be equal

$$\frac{d\text{Tension}_{cold}}{dt} = \frac{d\text{Tension}_{hot}}{dt} \qquad (3\text{-}59)$$

$$\frac{d\text{Torque}_{cold}}{dt} = \frac{d\text{Torque}_{hot}}{dt} \qquad (3\text{-}60)$$

Now substituting (3-42), (3-47), (3-54), and (3-58) into (3-59) and (3-60) we obtain

$$0 = F_0 \frac{d\underline{Dr}_0}{dt} + F_1 \frac{d\underline{Dr}_1}{dt} + F_2 \frac{d\underline{Dr}_2}{dt} + F_3 \frac{d\underline{DR}_3}{dt} + F_5 \frac{dP_h}{dt} - F_6 \frac{de_c}{dt} - F_7 \frac{dP_c}{dt} \qquad (3\text{-}61)$$

$$0 = G_1 \frac{d\underline{Dr}_1}{dt} + G_2 \frac{d\underline{Dr}_2}{dt} + G_3 \frac{d\underline{Dr}_3}{dt} + G_5 \frac{dP_h}{dt} - G_6 \frac{de_c}{dt} - G_7 \frac{dP_c}{dt} \qquad (3\text{-}62)$$

Equations (3-61) and (3-62) are rearranged to obtain

$$\frac{de_c}{dt} = \frac{F_0}{F_6}\frac{d\underline{Dr}_0}{dt} + \frac{F_1}{F_6}\frac{d\underline{Dr}_1}{dt} + \frac{F_2}{F_6}\frac{d\underline{Dr}_2}{dt} + \frac{F_3}{F_6}\frac{d\underline{Dr}_3}{dt}$$

$$+ \frac{F_5}{F_6}\frac{dP_h}{dt} - \frac{F_7}{F_6}\frac{dP_c}{dt} \qquad (3\text{-}63)$$

$$\frac{de_c}{dt} = \frac{G_1}{G_6}\frac{d\underline{Dr}_1}{dt} + \frac{G_2}{G_6}\frac{d\underline{Dr}_2}{dt} + \frac{G_3}{G_6}\frac{d\underline{Dr}_3}{dt} + \frac{G_5}{G_6}\frac{dP_h}{dt}$$

$$- \frac{G_7}{G_6}\frac{dP_c}{dt} \qquad (3\text{-}64)$$

Equations (3-63) and (3-64) represent generalized threadline force coupled differential equations. Seven dependent variables (unknowns) are present in these two coupled equations. To determine threadline torque and threadline tension during transient operation it is necessary to consider in addition, appropriate material balance and turn balance relations for each zone in the texturing threadline. As stated in the introduction to this section two models will be used for determining local material balances and turn balances. Both models will be applied to equations (3-63) and (3-64).

3.3.3.2 General Material and Turn Balances for the Hot Zone and the Post Spindle Zone

Common to both analytical models of transient behavior are the material balances and turn balances for the hot zone and post spindle zone. Along these zones the twist level is observed to be essentially uniform for both steady state and transient operation of the texturing system.

Material Balance for Hot Zone

In Chapter 2 it was pointed out that each radial layer of filaments in the hot drawing zone has a unique draw ratio, therefore it is necessary to formulate a separate material balance for each layer, i.e.:

$$\Delta(\text{Material})_{hot} = \text{Material}_{in} - \text{Material}_{out}$$

The material balance for each radial layer can be quantitatively formulated as

$$\frac{\Delta}{\Delta t}\left(L_h \frac{\sec\theta_{3i}}{Dr_i}\right) = V_2 \sec\theta_{2i} - \frac{V_3 \sec\theta_{3i}}{Dr_i} \qquad (3\text{-}65)$$

where L_h = Hot zone length

and as $\Delta t \rightarrow 0$

$$\left\{\frac{P_h R_{ih}^2}{(1+P_h^2 R_{ih}^2)^{1/2}} \quad \frac{1}{\underline{Dr}_i}\right\} \frac{dP_h}{dt} - \left\{\frac{(1+P_h^2 R_{ih}^2)^{1/2}}{\underline{Dr}_i^2}\right\} \frac{d\underline{Dr}_i}{dt}$$

$$= V_2 \frac{(1+P_c^2 R_{ic}^2)^{1/2}}{L_h} - V_3 \frac{(1+P_h^2 R_{ih}^2)^{1/2}}{L_h \underline{Dr}_i} \qquad (3\text{-}66)$$

Equation (3-66) can be rearranged:

$$V_2 = \left\{\frac{L_h \cdot P_h \cdot R_{ih}^2}{(1+P_h^2 R_{ih}^2)^{1/2} (1+P_c^2 R_{ic}^2)^{1/2}}\right\} \frac{1}{\underline{Dr}_i} \frac{dP_h}{dt}$$

$$+ \frac{V_3 (1+P_h^2 R_{ih}^2)^{1/2}}{\underline{Dr}_i (1+P_c^2 R_{ic}^2)^{1/2}} - \left\{\frac{L_h \cdot (1+P_h^2 R_{ih}^2)^{1/2}}{\underline{Dr}_i^2 (1+P_c^2 R_{ic}^2)^{1/2}}\right\} \frac{d\underline{Dr}_i}{dt} \qquad (3\text{-}67)$$

Equation (3-67) represents independent equations depending on how many radial layers of filaments exist in the hot zone. This equation can be simplified by defining

$$A_{i1} \equiv \frac{L_h \cdot P_h \cdot R_{ih}^2}{(1+P_h^2 R_{ih}^2)^{1/2} (1+P_c^2 R_{ic}^2)^{1/2}} \cdot \frac{1}{\underline{Dr}_i} \qquad (3\text{-}68)$$

$$A_{i2} \equiv \frac{V_3 (1+P_h^2 R_{ih}^2)^{1/2}}{\underline{Dr}_i (1+P_c^2 R_{ic}^2)^{1/2}} \qquad (3\text{-}69)$$

$$A_{i3} \equiv \frac{L_h (1+P_h^2 R_{ih}^2)^{1/2}}{\underline{Dr}_i^2 (1+P_c^2 R_{ic}^2)^{1/2}} \qquad (3\text{-}70)$$

Then,

$$V_2 = A_{i1} \frac{dP_h}{dt} + A_{i2} - A_{i3} \frac{d\underline{Dr}_i}{dt} \qquad (3\text{-}71)$$

Turn Balance for Hot Zone

The quantitative basis for the turn balance is simply that the rate of change of the number of turns of twist in a given yarn zone equals the difference in the angular velocities at the ends of the zone, plus the net rate of transport of twist to and from the zone. Following this a turn balance for the hot zone can be expressed as

$$\frac{\Delta}{\Delta t} (L_h P_h) = W_h - W_c + P_c V_2 - P_h V_3 \qquad (3\text{-}72)$$

and as $\Delta t \to 0$

$$\frac{dP_h}{dt} = \frac{W_h - W_c + P_c V_2 - P_h V_3}{L_h} \qquad (3\text{-}73)$$

Material Balance in the Post Spindle Zone

During steady state operation, twist generally is not present in the post spindle region if the feed yarn is initially twist free. However, during transient operation twist does occur in the post spindle region and this twist may affect the linear speed of the yarn as it moves downstream through the spindle. The material balance in the zone can be formulated as

$$\frac{\Delta}{\Delta t}\ (L_{ps}\underline{Cr}_{ps}) = V_b\underline{Cr}_s - V_4\underline{Cr}_{ps} \qquad (3\text{-}74)$$

where $\underline{Cr}_{ps}$ = Twist contraction factor in post spindle

L_{ps} = Post spindle zone length.

as $\Delta t \to 0$ (3-74) becomes

$$\frac{L_{ps}}{2}\ \frac{P_{ps}R_{3h}^2}{(1+P_{ps}^2R_{3h}^2)^{1/2}}\ \frac{dP_{ps}}{dt} = \frac{V_b}{2}\ (1+(1+P_s^2R_{3h}^2)^{1/2})$$

$$-\frac{V_4}{2}\ (1+(1+P_{ps}^2R_{3h}^2)^{1/2}) \qquad (3\text{-}75)$$

Turn Balance in the Post Spindle

The post spindle turn balance is formulated as

$$\frac{\Delta}{\Delta t}\ (L_{ps}P_{ps}) = (V_bP_s - V_4P_{ps} - W_s) \qquad (3\text{-}76)$$

and as $\Delta t \to 0$

$$L_{ps}\ \frac{dP_{ps}}{dt} = V_bP_s - V_4P_{ps} - W_s \qquad (3\text{-}77)$$

Combine (3-75) and (3-77) to obtain

$$\frac{dP_{ps}}{dt} = \frac{\left\{\frac{V_4P_{ps} + W_s}{P_s}\ (1+(1+P_s^2R_{3h}^2)^{1/2}) - V_4(1+(1+P_{ps}^2R_{3h}^2)^{1/2})\right\}}{L_{ps}\left\{\frac{P_{ps}R_{3h}^2}{(1+P_{ps}^2R_{3h}^2)^{1/2}} - \frac{(1+(1+P_s^2R_{3h}^2)^{1/2})}{P_s}\right\}} \qquad (3\text{-}78)$$

Equation (3-78) can be substituted into (3-77) to obtain

$$V_b = \frac{V_4 P_{ps} + W_s}{P_s} + \frac{L_{ps}}{P_s} \frac{dP_{ps}}{dt} \qquad (3\text{-}79)$$

where V_b = The linear velocity of twisted yarn as it enters the spindle.

3.3.3.3 Material and Turn Balances for the Cold and Cooling Zones: Model 1 - Flat Twist Distribution

Material Balance in Cold zone

In Chapter 2 it was assumed that all of the filaments in the twisted yarn of the cold zone are under equal tension and therefore equal axial strain. With this consideration it is only necessary to have one material balance equation that represents all cold filaments. The material balance in the cold zone is quantitatively expressed as

$$\frac{\Delta}{\Delta t}\left(\frac{L_c \underline{Cr}_c}{1+e_c}\right) = V_0 - \frac{V_2 \underline{Cr}_c}{1+e_c} \qquad (3\text{-}80)$$

as $\Delta t \to 0$

$$\frac{1}{1+e_c}\frac{d\underline{Cr}_c}{dt} - \frac{\underline{Cr}_c}{(1+e_c)^2}\frac{de_c}{dt} = \frac{V_0}{L_c} - \frac{V_2}{L_c}\frac{\underline{Cr}_c}{(1+e_c)} \qquad (3\text{-}81)$$

where

$$\underline{Cr}_c^* = 1/2 \quad (1+P_c^2 R_{3c}^2)^{1/2} + \frac{\ln\left(P_c R_{3c} + (1+P_c^2 R_{3c}^2)^{1/2}\right)}{P_c R_{3c}} \qquad (3\text{-}82)$$

* Note: Cold twist contraction factor obtained by radial averaging method.

$$Z \equiv \frac{P_c R_{3c}^2}{2(1+P_c^2 R_{3c}^2)^{1/2}} + \frac{1}{2(P_c(P_c R_{3c} + (1+P_c^2 R_{3c}^2)^{1/2})}$$

$$+ \frac{R_{3c}}{2\ (1+P_c^2 R_{3c}^2)^{1/2}\ (P_c R_{3c} + (1+P_c^2 R_{3c}^2)^{1/2}} \qquad (3\text{-}83)$$

$$- \frac{\ln(P_c R_{3c} + (1+P_c^2 R_{3c}^2)^{1/2}}{2P_c^2 R_{3c}}$$

and

$$\frac{dCr_c}{dt} = Z \frac{dP_c}{dt} \qquad (3\text{-}84)$$

Substitution of (3-84) into (3-81) gives

$$V_2 = \frac{1+e_c}{Cr_c} V_0 - \frac{ZL_c}{Cr_c} \frac{dP_c}{dt} + \frac{L_c}{1+e_c} \frac{de_c}{dt} \qquad (3\text{-}85)$$

Equation (3-85) can be simplified by defining

$$Q_1 \equiv \frac{L_c}{(1+e_c)} \qquad (3\text{-}86)$$

$$Q_2 \equiv \frac{1+e_c}{Cr_c} \cdot V_0 \qquad (3\text{-}87)$$

$$Q_3 \equiv \frac{ZL_c}{Cr_c} \qquad (3\text{-}88)$$

Then

$$V_2 = Q_1 \frac{de_c}{dt} + Q_2 - Q_3 \frac{dP_c}{dt} \qquad (3\text{-}89)$$

Equations (3-71) and (3-89) can be coupled to obtain

$$\frac{dDr_i}{dt} = \frac{A_{i1}}{A_{i3}} \frac{dP_h}{dt} + \frac{A_{i2}}{A_{i3}} - \frac{Q_1}{A_{i3}} \frac{de_c}{dt}$$

$$- \frac{Q_2}{A_{i3}} + \frac{Q_3}{A_{i3}} \frac{dP_c}{dt} \qquad (3\text{-}90)$$

Equation (3-90) represents as many equations as there are radial layers of filaments plus the central layer at the hot zone entrance. As stated earlier, most yarns which are presently being draw textured consist of one core filament and three radial layers. Accordingly, from this point on it will be assumed that the yarns have but one core and three layers. If larger yarns are encountered appropriate arithemetical changes can be made, still, the threadline physics would remain unchanged. Equation (3-90) is substituted into (3-63) to obtain

$$\frac{de_c}{dt} = \frac{F_0}{F_6} \cdot \frac{A_{01}}{A_{03}} \cdot \frac{dP_h}{dt} + \frac{A_{02} - Q_2}{A_{03}} - \frac{Q_1}{A_{03}} \cdot \frac{de_c}{dt}$$

$$+ \frac{Q_3}{A_{03}} \cdot \frac{dP_c}{dt}$$

$$+ \frac{F_1}{F_6} \cdot \frac{A_{11}}{A_{13}} \cdot \frac{dP_h}{dt} + \frac{A_{12} - Q_2}{A_{13}} - \frac{Q_1}{A_{13}} \cdot \frac{de_c}{dt} + \frac{Q_3}{A_{13}} \cdot \frac{dP_c}{dt}$$

$$+\frac{F_2}{F_6}\cdot\frac{A_{21}}{A_{23}}\cdot\frac{dP_h}{dt} + \frac{A_{22}-Q_2}{A_{23}} - \frac{Q_1}{A_{23}}\cdot\frac{de_c}{dt} + \frac{Q_3}{A_{23}}\cdot\frac{dP_c}{dt}$$

$$+\frac{F_3}{F_6}\cdot\frac{A_{31}}{A_{33}}\cdot\frac{dP_h}{dt} + \frac{A_{32}-Q_2}{A_{33}} - \frac{Q_1}{A_{33}}\cdot\frac{de_c}{dt} + \frac{Q_3}{A_{33}}\cdot\frac{dP_c}{dt}$$

$$+\frac{F_5}{F_6}\cdot\frac{dP_h}{dt} - \frac{F_7}{F_6}\cdot\frac{dP_c}{dt} \qquad (3\text{-}91)$$

Equation (3-91) can be simplified by introducing abbreviated symbols

$$X_1 \equiv \frac{F_0}{F_6}\cdot\frac{A_{01}}{A_{03}} + \frac{F_1}{F_6}\cdot\frac{A_{11}}{A_{13}} + \frac{F_2}{F_6}\cdot\frac{A_{21}}{A_{23}} + \frac{F_3}{F_6}\cdot\frac{A_{31}}{A_{33}}\cdot\frac{F_5}{F_6} \qquad (3\text{-}92)$$

$$X_2 \equiv \frac{F_0}{F_6}\cdot\frac{Q_1}{A_{03}} + \frac{F_1}{F_6}\cdot\frac{Q_1}{A_{13}} + \frac{F_2}{F_6}\cdot\frac{Q_1}{A_{23}} + \frac{F_3}{F_6}\cdot\frac{Q_1}{A_{33}} \qquad (3\text{-}93)$$

$$X_3 \equiv \frac{F_0Q_3}{F_6A_{03}} + \frac{F_1Q_3}{F_6A_{13}} + \frac{F_2Q_3}{F_6A_{23}} + \frac{F_3}{F_6}\cdot\frac{Q_3}{A_{33}} - \frac{F_7}{F_6} \qquad (3\text{-}94)$$

$$X_4 \equiv \frac{F_0}{F_6}\frac{(A_{02}-Q_2)}{A_{03}} + \frac{F_1}{F_6A_{13}}(A_{12}-Q_2) + \frac{F_2(A_{22}-Q_2)}{F_6A_{23}}$$

$$+\frac{F_3(A_{32}-Q_2)}{F_6A_{33}} \qquad (3\text{-}95)$$

Equations (3-92), (3-93), (3-94), (3-95) are substituted into (3-91) to obtain

$$\frac{de_c}{dt} = \frac{X_1}{1-X_2}\frac{dP_h}{dt} + \frac{X_3}{1-X_2}\frac{dP_c}{dt} + \frac{X_4}{1-X_2} \qquad (3\text{-}96)$$

Likewise the following symbols can be defined

$$Y_1 \equiv \frac{G_1}{G_6}\cdot\frac{A_{11}}{A_{13}} + \frac{G_2A_{21}}{G_6A_{23}} + \frac{G_3}{G_6}\cdot\frac{A_{31}}{A_{33}} + \frac{G_5}{G_6} \qquad (3\text{-}97)$$

$$Y_2 \equiv \frac{G_1}{G_6}\cdot\frac{Q_1}{A_{13}} + \frac{G_2Q_1}{G_6A_{23}} + \frac{G_3Q_1}{G_6A_{33}} \qquad (3\text{-}98)$$

$$Y_3 \equiv \frac{G_1}{G_6}\cdot\frac{Q_3}{A_{13}} + \frac{G_2}{G_6}\cdot\frac{Q_3}{A_{23}} + \frac{G_3Q_3}{G_6A_{33}} - \frac{G_7}{G_5} \qquad (3\text{-}99)$$

$$Y_4 \equiv \frac{G_1}{G_6A_{13}}\cdot(A_{12} - Q_2) + \frac{G_2}{G_6A_{23}}\cdot(A_{22} - Q_2) + \frac{G_3}{G_6A_{33}}\cdot(A_{32} - Q_2) \qquad (3\text{-}100)$$

Finally we substitute (3-97), (3-98), (3-99), (3-100) into (3-62) to obtain

$$\frac{de_c}{dt} = \frac{Y_1}{1-Y_2}\frac{dP_h}{dt} + \frac{Y_3}{1-Y_2}\frac{dP_c}{dt} + \frac{Y_4}{1-Y_2} \qquad (3\text{-}101)$$

Equation (3-101) and Equation (3-100) represent two simultaneous first order differential equations with three unknown time derivatives and seven unknown variables.

Turn Balance in the Cold Zone

In Chapter 2 it was shown that during steady state operation of the draw texturing process the cold zone twist level is a fraction of the hot zone twist level. Since we assume that the hot zone rotates at the same angular velocity of the pin spindle, the angular velocity of the cold zone must be somewhat less.

The turn balance for the cold zone can be quantified as

$$\frac{\Delta}{\Delta t}\,(L_c P_c) = W_c - P_c V_2 \qquad (3\text{-}102)$$

and as $\Delta t \to 0$

$$\frac{dP_c}{dt} = \frac{W_c - P_c V_2}{L_c} \qquad (3\text{-}103)$$

where W_c = The unknown rotational velocity of the cold zone

The cold zone turn balance (3-104) can be added to the hot zone turn balance (3-73) to obtain

$$L_h \frac{dP_h}{dt} = W_h - L_c \frac{dP_c}{dt} - P_h V_3 \qquad (3\text{-}104)$$

To simplify equations (3-104) the following symbols are defined as

$$X_5 \equiv \frac{W_h - P_h V_3}{L_h} \qquad (3\text{-}105)$$

$$X_6 \equiv \frac{L_c}{L_h}\,\frac{dP_c}{dt} \qquad (3\text{-}106)$$

so that (3-104) becomes

$$\frac{dP_h}{dt} = X_5 - X_6 \frac{dP_h}{dt} \qquad (3\text{-}107)$$

Material Balance in the Cooling Zone

During steady state operation, the linear speed of the twisted yarn as it leaves the hot zone is assumed equal to the linear speed of the yarn as it approaches the rotating pin spindle, i.e., there is no material buildup in the cooling zone. During transient operation this is not the case and a material balance over the zone is necessary.

$$\frac{\Delta}{\Delta t} (L_s \underline{\underline{Cr}}_{set}) = V_3 \underline{\underline{Cr}}_{hot} - V_b \underline{\underline{Cr}}_{set} \qquad (3\text{-}108)$$

where $\underline{\underline{Cr}}_{set}$ = Twist contraction factor all along the cooling zone

and as $\Delta t \to 0$

$$\frac{L_s}{2} \frac{P_s R_{3h}^2}{(1+P_s^2 R_{3h}^2)^{1/2}} \frac{dP_s}{dt} = \frac{V_3}{2} (1+(1+P_h^2 R_{3h}^2)^{1/2})$$

$$- \frac{V_b}{2} (1+(1+P_s^2 R_{3h}^2)^{1/2}) \qquad (3\text{-}109)$$

For Model 1 the assumption is made that the twist in the set zone is equal to the twist in the hot zone at all times. Therefore

$$P_s = P_h \qquad (3\text{-}110)$$

Then (3-109) becomes

$$V_3 = \left\{ \frac{L_s P_h R_{3h}^2}{(1+P_h^2 R_{3h}^2)^{1/2} + 1+P_h^2 R_{3h}^2} \right\} \frac{dP_h}{dt} + V_b \qquad (3\text{-}111)$$

Equation (3-111) is now substituted into (3-69) so that

$$A_{i2} = \left\{ \frac{L_s P_h R_{3h}^2}{(1+P_h^2 R_{3h}^2)^{1/2} + 1+P_h^2 R_{3h}^2} \right\} \frac{dP_h}{dt} + V_b$$

$$\left\{ \frac{(1+P_h^2 R_{ih}^2)^{1/2}}{\underline{Dr}_i (1+P_c^2 R_{ic}^2)^{1/2}} \right\} \qquad (3\text{-}112)$$

A_{i2} is now substituted into (3-90). A_{i1} and A_{i2} are re-defined as

$$A_{i1} = \frac{L_h P_h R_{ih}^2}{(1+P_h^2 R_{ih}^2)^{1/2} (1+P_c^2 R_{ic}^2)^{1/2} \underline{Dr}_i}$$

$$+ \left\{ \frac{L_s P_h R_{3h}^2}{(1+P_h^2 R_{3h}^2)^{1/2} + 1 + P_h^2 R_{3h}^2} \right\} \cdot \left\{ \frac{(1+P_h^2 R_{ih}^2)^{1/2}}{\underline{Dr}_i (1+P_c^2 R_{ic}^2)^{1/2}} \right\}$$

(3-113)

$$A_{i2} = \frac{V_b (1+P_h^2 R_{1h}^2)^{1/2}}{\underline{Dr}_i (1+P_c^2 R_{ic}^2)^{1/2}} \qquad (3\text{-}114)$$

Turn Balance in the Cooling Zone

A turn balance is formulated for the cooling zone.

$$\frac{\Delta}{\Delta t} (L_s P_s) = V_3 P_h - V_b P_s \qquad (3\text{-}115)$$

where L_s = Length of cooling zone

and with $P_h = P_s$ (assumed for model 1)

We also assume that there is no difference in the net rates of rotation at the ends of the zone.

$$L_s \frac{dP_h}{dt} = V_3 P_h - V_b P_h \qquad (3\text{-}116)$$

Adding (3-116) to (3-107) the following turn balance is derived for the full texturing zone.

$$(L_h + L_s) \frac{dP_h}{dt} = W_h - L_c \frac{dP_c}{dt} - P_h V_b \qquad (3\text{-}117)$$

Defining

$$X_5 \equiv \frac{W_h - P_h V_b}{(L_h + L_s)} \qquad (3\text{-}118)$$

$$X_6 \equiv \frac{L_c}{L_h + L_s} \qquad (3\text{-}119)$$

To get

$$\frac{dP_h}{dt} = X_5 - X_6 \frac{dP_c}{dt} \qquad (3\text{-}120)$$

Equation (3-120) is now substituted into Equations (3-96), and (3-101) to obtain

$$\frac{de_c}{dt} = \frac{Y_1 X_5 + Y_4}{1 - Y_2} + \frac{Y_3 - Y_1 X_6}{1 - Y_2} \frac{dP_c}{dt} \qquad (3\text{-}121)$$

$$\frac{de_c}{dt} = \frac{X_1 X_5 + X_4}{1 - X_2} + \frac{X_3 - X_1 X_6}{1 - X_2} \frac{dP_c}{dt} \qquad (3\text{-}122)$$

Equations (3-121) and (3-122)are coupled to obtain

$$\frac{dP_c}{dt} = \left\{ \frac{\frac{Y_1X_5+Y_4}{1-Y_2} - \frac{X_1X_5+X_4}{1-X_2}}{\frac{X_3-X_1X_6}{1-X_2} - \frac{Y_3-Y_1X_6}{1-Y_2}} \right\} \qquad (3\text{-}123)$$

Equation (3-123) can be functionally expressed as

$$\frac{dP_c}{dt} = Z_1(P_c, P_h, e_c, \underline{Dr}_i, P_{ps}) \qquad (3\text{-}124)$$

Equation (3-123) is substituted into (3-120) to obtain

$$\frac{dP_h}{dt} = Z_2(P_c, P_h, e_c, \underline{Dr}_i, P_{ps}) \qquad (3\text{-}125)$$

Equation (3-125) is then substituted into (3-121) to obtain

$$\frac{de_c}{dt} = Z_3(P_c, P_h, e_c, \underline{Dr}_i, P_{ps}) \qquad (3\text{-}126)$$

Equations (3-124), (3-125) and (3-126) are now substituted into (3-90) to obtain

$$\frac{d\underline{Dr}_i}{dt} = Z_4(P_c, P_h, e_c, \underline{Dr}_i, P_{ps}) \qquad (3\text{-}127)$$

Finally

$$\frac{dP_{ps}}{dt} = Z_5(P_c, P_h, e_c, \underline{Dr}_i, P_{ps}) \qquad (3\text{-}128)$$

Threadline tension is obtained by solving the preceeding set of five differential equations and substituting values of e_c,

P_c into (3-43). Finally, these values of e_c, and P_c are also substituted into (3-56) to obtain threadline torque.

3.3.3.4 Twist Transport, Material Balances and Turn Balances in the Cold and Cooling Zones: Model 2 - Tilted Twist Distribution

Twist Transport Formula of the Tilted Twist Model 2

The previous model (MODEL 1) for transient operation was based on the physical simplification that **uniform** twist levels during transient operation persist in each of the four zones of the threadline (cold, hot, cooling, and post spindle). Actual photographic measurements of twist as a function of time and position after a step change in spindle speed, indicate that the twist level in both the cold and cooling zones is not uniform with position during transient operation. Experimental evidence presented earlier, in Section 3.2.3, indicates that twist changes incurred at the entrance to the cold or cooling zones propagate downstream with the movement of the threadline. As a first approximation the twist level in either the cold zone or the cooling zone can be considered to vary linearly with position along that zone. This distribution is illustrated on the following page.

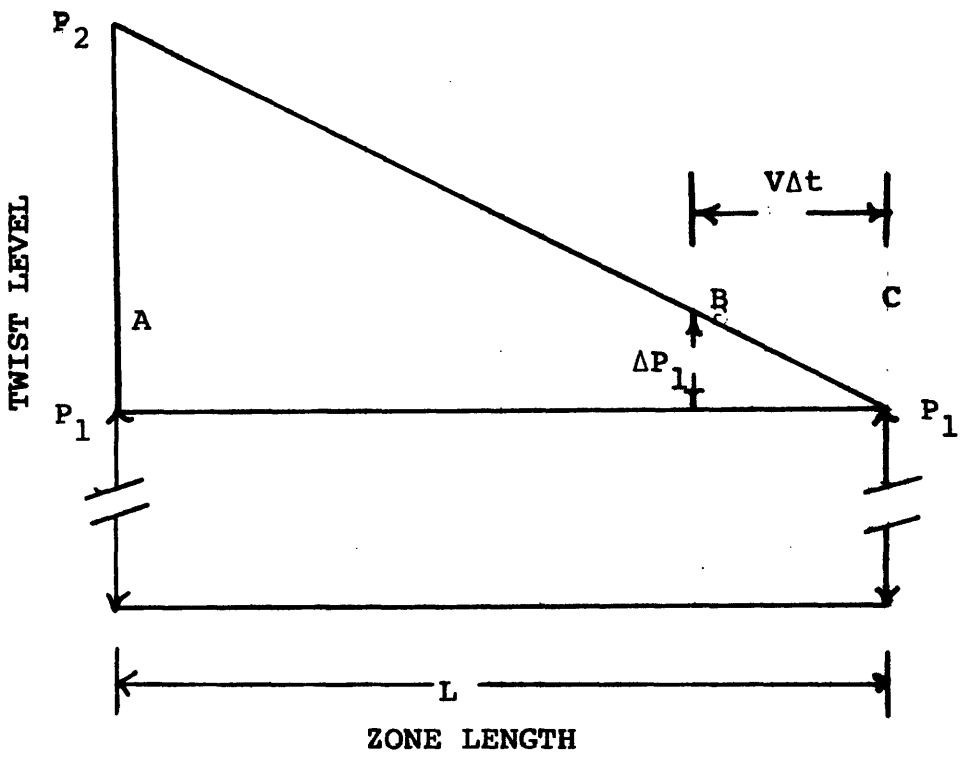

This model of the twist distribution operates as follows. At position C, (which is the downstream limit of the zone in question) the twist level at anytime,t, is P_1. At the same time,t, the twist level at position A,(the upstream end of the zone), is P_2. P_2 is dictated by threadline mechanics. At position B, located a distance $V\Delta t$ upstream of C, the twist for time, t, is $P_1 + \Delta P_1$. During the time interval Δt the twist at position B migrates downstream to position C establishing the new twist level there as $P_1 + \Delta P_1$. It follows that:

$$\frac{P_2-P_1}{L} = \frac{\Delta P_1}{V\Delta t} \qquad (3\text{-}129)$$

where V is the linear yarn velocity at C. Now, letting $\Delta t \to 0$

$$\frac{dP_1}{dt} = \frac{(P_2 - P_1)}{L} \quad V \qquad (3\text{-}130)$$

This twist transport relation is now inserted in subsequent treatments of material and turn balances for the cold and cooling zones.

Material Balance in the Cold Zone for the Tilted Twist Model 2

We have assumed that the twist distribution in the cold zone varies linearly along the threadline during transient operation. Therefore the length of material in the cold zone is

$$\left[\frac{\underline{Cr}_c + \underline{Cr}_j}{1+e_c}\right]\frac{L_c}{2}$$

Further, we assume that the constant filament strain which obtains at the entrance to the cold zone at a given time,t, is uniform along the cold zone. Since filament strains at the cold zone entrance are of the order of 1% or less, the error introduced by this assumption in the following expressions is seen to be negligible. The material balance in the cold zone is

$$\frac{\Delta L_c}{\Delta t}\left[\frac{\underline{Cr}_c + \underline{Cr}_j}{2(1+e_c)}\right] = V_0 - \frac{V_2\underline{Cr}_j}{(1+e_c)} \qquad (3\text{-}131)$$

where $\underline{Cr}_j$ = Cold twist contraction factor at downstream end of the cold zone

as $\Delta t \to 0$

$$V_2 = \frac{(1+e_c)V_0}{\underline{Cr}_j} - \frac{L_c}{2\underline{Cr}_j} \cdot \frac{d\underline{Cr}_c}{dt} - \frac{L_c}{2\underline{Cr}_j} \cdot \frac{d\underline{Cr}_j}{dt}$$

$$+ \frac{L_c}{2} \frac{\underline{Cr}_c + \underline{Cr}_j}{\underline{Cr}_j(1+e)} \cdot \frac{de}{dt} \qquad (3\text{-}132)$$

let $$\frac{d\underline{Cr}_c}{dt} = Z_1 \cdot \frac{dP_c}{dt} \qquad (3\text{-}133)$$

where $$Z_1 = \frac{P_c R_{3c}^2}{(1+P_c^2 R_{3c}^2)^{1/2}} + \frac{1}{(P_c(P_c R_{3c} + (1+P_c^2 R_{3c}^2)^{1/2})} \qquad (3\text{-}134)$$

and $$\frac{d\underline{Cr}_i}{dt} = Z_2 \cdot \frac{dP_j}{dt} \qquad (3\text{-}135)$$

where $$Z_2 = \frac{P_j R_{3c}^2}{(1+P_j^2 R_{3c}^2)^{1/2}} + \frac{1}{(P_j(P_j R_{3c} + (1+P_j^2 R_{3c}^2)^{1/2})} \qquad (3\text{-}136)$$

where P_j = Cold twist per twisted length at cold zone exit.

Then equation (3-132) can be expressed as

$$V_2 = \frac{(1+e_c)}{\underline{Cr}_j} \cdot V_0 - \frac{L_c}{2\underline{Cr}_j} \cdot Z_1 \cdot \frac{dP_c}{dt} - \frac{L_c}{2\underline{Cr}_j} \cdot Z_2 \frac{dP_j}{dt}$$

$$+ \frac{L_c}{2} \cdot \frac{\underline{Cr}_c + \underline{Cr}_j}{\underline{Cr}_j(1+e_c)} \frac{de}{dt} \qquad (3\text{-}137)$$

The twist transport relation for the cold zone is

$$\frac{dP_j}{dt} = \frac{P_c - P_j}{L_c} \cdot V_2 \qquad (3\text{-}138)$$

Equation (3-138) is now substituted into (3-137) to obtain

$$V_2 \cdot \left\{1+\frac{(P_c - P_j)Z_2}{2\underline{Cr}_j}\right\} = \frac{1+e_c}{\underline{Cr}_j} \cdot V_0 - \frac{L_c}{2\underline{Cr}_j} \cdot Z_1 \cdot \frac{dP_c}{dt}$$

$$+ \frac{L_c}{2} \cdot \frac{\underline{Cr}_c + \underline{Cr}_j}{\underline{Cr}_j(1+e_c)} \frac{de}{dt} \qquad (3\text{-}139)$$

Equation (3-139) can be simplified by defining

$$Q_1 \equiv \frac{\frac{L_c}{2}\left\{\frac{\underline{Cr}_c + \underline{Cr}_j}{\underline{Cr}_j(1+e_c)}\right\}}{1 + \frac{(P_c - P_j)Z_2}{2\underline{Cr}_j}} \qquad (3\text{-}140)$$

$$Q_2 \equiv \frac{\left\{\frac{(1+e_c)}{\underline{Cr}_j}\right\}V_0}{1 + \frac{(P_c-P_j)Z_2}{2\underline{Cr}_j}} \qquad (3\text{-}141)$$

$$Q_3 \equiv \frac{L_c Z_1}{\left\{1+\frac{(P_c-P_j)Z_2}{2\underline{Cr}_j}\right\}(2\underline{Cr}_j)} \qquad (3\text{-}142)$$

Equations (3-140), (3-141), and (3-142) are now substituted into (3-89) in place of (3-86), (3-87), and (3-88), so that V_2 is still expressed as

$$V_2 = Q_1 \frac{de}{dt} + Q_2 - Q_3 \frac{dP_c}{dt} \qquad (3\text{-}89)$$

Material Balance in the Cooling Zone for the Tilted Twist Model 2.

If we assume that the twist distribution in the cooling zone is linear as seen in the twist sketch the length of the cooling zone segment in its untwisted state is

$$\frac{L_s}{2}\ (\underline{Cr}_h + \underline{Cr}_s)$$

The mass balance in the cooling zone is then

$$\frac{\Delta}{\Delta t}\ L_s\ \frac{(\underline{Cr}_h + \underline{Cr}_s)}{2} = V_3\ \underline{Cr}_h - V_b \underline{Cr}_s \qquad (3\text{-}143)$$

where $\underline{Cr}_h$ = Twist contraction factor at upstream end of set zone

$\underline{Cr}_s$ = Twist contraction factor at downstream end of set zone.

Using Hearle's expression for twist contraction we convert (3-143) to

$$\frac{L_s}{2} \cdot \frac{P_h R_{3h}^2}{2(1+P_h^2 R_{3h}^2)^{1/2}} \cdot \frac{dP_h}{dt} + \frac{P_s R_{3h}^2}{2(1+P_s^2 R_{3h}^2)^{1/2}} \cdot \frac{dP_s}{dt}$$

$$= \frac{V_3}{2}\ (1+(1+P_h^2 R_{3h}^2)^{1/2}) - \frac{V_b}{2}\ (1+(1+P_s^2 R_{3h}^2)^{1/2}) \qquad (3\text{-}144)$$

The twist transport equation for the cooling zone

$$\frac{dP_s}{dt} = \frac{(P_h - P_s)}{L_s} \quad V_b \qquad (3\text{-}145)$$

is substituted in (3-144) to obtain

$$V_3 = \frac{L_s}{2} \quad \frac{P_h R_{3h}^2}{(1+P_h^2 R_{3h}^2)^{1/2} \ (1+(1+P_h^2 R_{3h}^2)^{1/2})} \quad \frac{dP_h}{dt}$$

$$+ \quad \frac{P_s R_{3h}^2 (P_h - P_s) V_b}{2(1+P_s^2 R_{3h}^2)^{1/2} \ (1+(1+P_h^2 R_{3h}^2)^{1/2})}$$

$$+ \ V_b \ \frac{(1+(1+P_s^2 R_{3h}^2)^{1/2})}{(1+(1+P_h^2 R_{3h}^2)^{1/2})} \qquad (3\text{-}146)$$

Equation (3-146) is now substituted into (3-69) with A_{i1}, A_{i2}, A_{i3}, defined as

$$A_{i1} = \frac{L_h P_h R_{ih}^2}{(1+P_j^2 R_{ic}^2)^{1/2} \ (1+P_h^2 R_{ih}^2) \ \underline{Dr}_i}$$

$$+ \quad \frac{1/2 \ L_s P_h R_{3h}^2 (1+P_h^2 R_{ih}^2)^{1/2}}{(1+P_h^2 R_{3h}^2)^{1/2} \ (1+(1+P_h^2 R_{3h}^2)^{1/2}) \ (1+P_j^2 R_{ic}^2)^{1/2} \ \underline{Dr}_i} \qquad (3\text{-}147)$$

$$A_{i2} = \frac{(1+(1+P_s^2R_{3h}^2)^{1/2})(1+P_h^2R_{ih}^2)^{1/2}}{(1+(1+P_h^2R_{3h}^2)^{1/2})\ \underline{Dr}_i\ (1+P_j^2R_{ic}^2)^{1/2}}$$

$$+ \frac{P_sR_{3h}^2\ (P_h-P_s)(1+P_h^2R_{ih}^2)^{1/2}}{2\ (1+P_s^2R_{3h}^2)^{1/2}\ (1+(1+P_h^2R_{3h}^2)^{1/2})\ \underline{Dr}_i\ (1+P_j^2R_{ic}^2)^{1/2}} \qquad (3\text{-}148)$$

$$A_{i3} = \frac{L_h(1+P_h^2R_{ih}^2)^{1/2}}{\underline{Dr}_i^2\ (1+P_j^2R_{ic}^2)^{1/2}} \qquad (3\text{-}149)$$

which leads to :

$$V_2 = A_{i1}\frac{dP_h}{dt} + A_{i2} - A_{i3}\frac{d\underline{Dr}_i}{dt} \qquad (3\text{-}150)$$

Equation (3-150) can be added to (3-89) and an expression is obtained for the time derivative of the draw ratio for each filament layer in the yarn. This expression is identical to equation (3-90) for the time derivative of draw ratio for the flat twist distribution Model #1. However, the expressions for A_{i1}, A_{i2}, A_{i3}, Q_1, Q_2, and Q_3 are now defined differently, i.e., as shown in (3-147), (3-148), (3-149), (3-140), (3-141) and (3-142) for the case of the tilted twist Model #2.

Turn Balances

A turn balance exists for each of the four zones (cold, hot,

cooling, and post spindle). Each turn balance requires that in a given zone, the rate of change of the number of turns in a given zone is equal to the difference in the rates of rotation of the yarns at the ends of the zone plus the net gain by transport to and from the adjacent zones. As in Model 1 we assume here that the twist levels are uniform along the hot and post spindle zones.

Turn Balance in the Cold Zone for the Tilted Twist Model 2

We assume that if the twist varies linearly in the cold zone from P_c to P_j, then the amount of turns in the cold zone is

$$\frac{L_c\ (P_c+P_j)}{2}$$

Therefore the cold zone twist balance is

$$\frac{\Delta}{\Delta t}\left[\frac{L_c(P_j+P_c)}{2}\right] = W_c - P_jV_2 \qquad (3\text{-}151)$$

where P_j = Cold twist per twisted length at downstream end of the cold zone

and as $\Delta t \to 0$

$$\frac{L_c}{2}\cdot\frac{dP_j}{dt} + \frac{L_c}{2}\cdot\frac{dP_c}{dt} = W_c - P_jV_2 \qquad (3\text{-}152)$$

Turn Balance in the Hot Zone

The hot zone turn balance for Model 2 is the same as for Model 1, i.e.:

$$L_h \frac{dP_h}{dt} = W_h - W_c + P_j V_2 - P_h V_3 \qquad (3\text{-}153)$$

Turn Balance in the Cooling Zone for the Tilted Twist Model 2

If we assume that the twist distribution is linear in the cooling zone, the number of turns in that zone is

$$L_s\left(\frac{P_h+P_s}{2}\right)$$

The cooling zone twist balance in then:

$$\frac{\Delta}{\Delta t} \quad L_s \frac{(P_h+P_s)}{2} = P_h V_3 - P_s V_b + W_s - W_h \qquad (3\text{-}154)$$

and as $\Delta t \to 0$

$$\frac{L_s}{2} \frac{dP_h}{dt} + \frac{L_s}{2} \frac{dP_s}{dt} = P_h V_3 - P_s V_b + W_s - W_h \qquad (3\text{-}155)$$

Observation indicates that for practical purposes $W_h = W_s$.

where W_h = Angular speed of hot zone segments

W_s = Angular speed of cooling zone segments

A composite turn balance for all zones upstream of the spindle is formulated by adding the cold, hot, and cooling zone turn balances to obtain

$$\frac{L_c}{2} \frac{dP_c}{dt} + \frac{L_c}{2} \frac{dP_i}{dt} + L_h \frac{dP_h}{dt} + \frac{L_s}{2} \frac{dP_h}{dt} + \frac{L_s}{2} \frac{dP_s}{dt}$$

$$= W_s - P_s V_b \qquad (3\text{-}156)$$

The twist transport equation for $\frac{dP_j}{dt}$ and $\frac{dP_s}{dt}$ can be substituted in (3-156) to obtain.

$$1/2\left\{L_c \frac{dP_c}{dt}\right\}+ 1/2\left\{(P_c-P_j)\right\}V_2 +\left\{L_h \frac{dP_h}{dt}\right\}$$

$$+ 1/2\left\{L_s \frac{dP_h}{dt}\right\}+ 1/2\left\{(P_h- P_s)\right\}V_b = W_h - P_sV_b \qquad (3\text{-}157)$$

V_b is determined by the post spindle analysis. V_2 is obtained from the cold material balance.

$$V_2 = Q_1 \frac{de}{dt} + Q_2 - Q_3 \frac{dP_c}{dt} \qquad (3\text{-}158)$$

Substituting V_2 into the composite turn balance we obtain

$$\frac{dP_h}{dt} = \frac{w_h-P_sV_b}{L_h+1/2\ L_s} + 1/2\left\{\frac{(P_c-P_j)Q_3}{L_h+1/2\ L_s} - \frac{L_c}{L_h+1/2\ L_s}\right\}\frac{dP_c}{dt}$$

$$- 1/2\ \frac{(P_h-P_s)V_b}{L_h + L_s} - \left\{\frac{Q_1(P_c-P_j)}{2L_h + L_s}\right\}\frac{de}{dt} - Q_2\frac{(P_c-P_j)}{2L_h+L_s} \qquad (3\text{-}159)$$

We now define

$$X_5 \equiv \frac{W_h-P_sV_b}{L_h+1/2\ L_s} \qquad (3\text{-}160)$$

$$X_6 \equiv \frac{L_c}{2L_h + L_s} \qquad (3\text{-}161)$$

$$X_7 \equiv \frac{P_c - P_j}{2L_h + L_s} \qquad (3\text{-}162)$$

$$X_8 \equiv \frac{(P_h - P_s)V_b}{2L_h + L_s} \qquad (3\text{-}163)$$

so that

$$\frac{dP_h}{dt} = X_5 + (Q_3X_7 - X_6)\frac{dP_c}{dt} - Q_1X_7\frac{de}{dt} - Q_2X_7 - X_8 \qquad (3\text{-}164)$$

Using the values of $A_{i1}, A_{i2}, A_{i3}, Q_1, Q_2$, and Q_3 for Model 2 a new set of $X_1, X_2, X_3, X_4, Y_1, Y_2, Y_3$, and Y_4 can be obtained from equations (3-92), (3-93), (3-94), (3-95), (3-97), (3-98), (3-99) and (3-100). The general threadline force equations are then expressed as:

$$(1-X_2)\frac{de}{dt} = X_1\frac{dP_h}{dt} + X_3\frac{dP_c}{dt} + X_4 \qquad (3\text{-}165)$$

and

$$(1-Y_2)\frac{de}{dt} = Y_1\frac{dP_h}{dt} + Y_3\frac{dP_c}{dt} + Y_4 \qquad (3\text{-}166)$$

substituting the composite turn balance (3-164) into (3-165) and (3-166) we obtain

$$(1-X_2)\frac{de}{dt} = X_1\left\{X_5 + (Q_3X_7 - X_6)\frac{dP_c}{dt} - Q_1X_7\frac{de}{dt} - Q_2X_7 - X_8\right\} + X_3\frac{dP_c}{dt} + X_4 \qquad (3\text{-}167)$$

and $$(1-Y_2)\ \frac{de}{dt} = Y_1\left\{X_5+(Q_3X_7 - X_6)\ \frac{dP_c}{dt} - Q_1X_7\ \frac{de}{dt} - Q_2X_7 - X_8\right\} + Y_3\ \frac{dP_c}{dt} + Y_4 \qquad (3\text{-}168)$$

Equations (3-167) and (3-168) are combined to obtain

$$\frac{dP_c}{dt} = \left[\frac{\dfrac{Y_1X_5-Y_1Q_2X_7-X_1X_8+Y_4}{1-Y_2+Y_1Q_1X_7} - \dfrac{X_1X_5-X_1Q_2X_7-X_1X_8+X_4}{1-X_2+X_1Q_1X_7}}{\dfrac{X_1Q_3X_7- X_1X_6+X_3}{1-X_2 + X_1Q_1X_7} - \dfrac{Y_1Q_3X_7- Y_1X_6 + Y_3}{1-Y_2 + Y_1Q_1X_7}}\right] \qquad (3\text{-}169)$$

Equation (3-169) can be functionally expressed as

$$\frac{dP_c}{dt} = Y_1(P_c,P_j,P_h,P_s,P_{ps},e_c,\underline{Dr}_i) \qquad (3\text{-}170)$$

Equation (3-170) is then substituted into (3-168) to obtain

$$\frac{de}{dt} = Y_3(P_c,P_j,P_h,P_s,P_{ps},e_c,\underline{Dr}_i) \qquad (3\text{-}171)$$

Equations (3-170) and (3-171) are substituted into the composite turn balance to obtain

$$\frac{dP_h}{dt} = Y_2(P_c,P_j,P_h,P_s,P_{ps},e_c,\underline{Dr}_i) \qquad (3\text{-}172)$$

Equations (3-170), (3-171) and (3-172) are substituted into (3-90) to obtain

$$\frac{d\underline{Dr}_i}{dt} = Y_4(P_c, P_h, P_j, P_s, P_{ps}, \underline{Dr}_i, e_c) \qquad (3\text{-}90)$$

Finally

$$\frac{dP_j}{dt} = Y_5(P_c, P_h, P_j, P_s, P_{ps}, \underline{Dr}_i, e_c) \qquad (3\text{-}173)$$

$$\frac{dP_s}{dt} = Y_6(P_c, P_h, P_j, P_s, P_{ps}, \underline{Dr}_i, e_c) \qquad (3\text{-}174)$$

$$\frac{dP_{ps}}{dt} = Y_7(P_c, P_j, P_h, P_s, P_{ps}, \underline{Dr}_i, e_c) \qquad (3\text{-}175)$$

Threadline tension and torque are obtained by solving the preceeding set of differential equations and substituting values of e_c, P_c, into equations (3-43) and (3-56).

3.3.4 Solution Technique for the Transient Analysis

Each of the analytical models of transient threadline mechanics is represented by a system of non-linear ordinary differential equations. The transient solution to these systems of equations is solved by the DYSYS (DYnamic SYstem Simulation) subroutine provided in the MIT Mechanical and Civil Engineering Joint Computer Facility. DYSYS uses a fourth order Runge-Kutta integration to obtain approximate solutions to the system of equations. The form of equations which DYSYS can solve is:

$$\frac{d}{dt} y_1 = f_1(t, y_1, y_2, \ldots\ldots y_n)$$

$$\frac{d}{dt} y_2 = f_2(t, y_1, y_2, \ldots\ldots\ldots y_n)$$

$$\vdots$$

$$\frac{d}{dt} y_n = f_n(t, y_1, y_2, \ldots\ldots\ldots y_n)$$

This may be compactly written as:

$$\frac{d}{dt} Y = F(t, y)$$

where Y is an n-dimensional vector made up of the current values of $y_1 \ldots . y_n$ and F is a vector valued function composed of the current values of $f_1 \ldots . f_n$.

The Computer programs that use DYSYS to give transient solutions are listed in Appendix 6 for Model 1 and 2. The initial values for the transient analysis are obtained from solutions derived from the steady state analysis presented in Chapter 2.

3.4 EXPERIMENTAL STUDY OF TRANSIENT OPERATION OF THE DRAW TEXTURING PROCESS: USING POY POLYESTER

Experiments were done with POY polyester yarns supplied by the Du Pont Company so that we could compare measured threadline behavior, i.e. threadline tension, torque, and twist distribution, with predicted results during transient operation of the draw texturing process. The dimensions and properties of these yarns are given in Section 2.4.1. The yarns are textured on the MITEX False Twister. Threadline torque and tension were measured by the MITEX Torque-Tension Meter placed slightly downstream of the feed rollers. The placement of the latter device at this position causes the actual length of the threadline to be increased by the distance from the feed rollers to the twist trap on the device, but this added length has only a minimal effect on transient threadline response since no twist is included in this extra length. For it is change in twist with respect to time which affects threadline response most. Finally, threadline twist was measured optically by taking pictures of the threadline at different stations along its length and counting twists.

Unsteady machine operation was activated by changing the machine twist stepwise. Three combinations of machine dimensions were used in these experiments.

	COLD ZONE	HOT ZONE	COOLING ZONE	POST SPINDLE ZONE
Mode I	6.00"	1.25"	7.00"	9.00"
Mode II	6.00"	3.00"	5.25"	9.00"
Mode III	13.00"	1.25"	0.0 "	9.00"

The nominal yarn throughput speed was 0.47 inches per second; the machine draw ratio was 1.60; the heater temperature was 210°C.

Two complimentary sets of experiments were carried out for each mode of machine operation. In one set the process was allowed to operate at steady state with the machine twist at 50 TPI before the machine twist was step changed to 60 TPI. For the complimentary set of experiments the machine twist was reduced stepwise from 60 TPI to 50 TPI. Table 3.4 lists the critical threadline responses during transient operation for all experiments using POY polyester.

Twist Increased to 60 TPI from 50 TPI

Figures 3.29 , 3.30, and 3.31 show predicted and measured transient tensions for each machine mode of operation. The predicted tensions using Analytical Model 2(tilted twist distribution) compare favorably with the measured values for Machine Mode I and Machine Mode II. However, for Machine Mode III the predicted results using Analytical Model I (flat twist distribution) compares more favorably to the measured results than the predictions using Model 2. It

Table 3.4

COMPARISON OF PREDICTED AND MEASURED TRANSIENT THREADLINE RESPONSE

MODE OF MACHINE OPERATION	INITIAL TENSION GRAMS		MAXIMA OR MINIMA TENSION GRAMS		TIME TO REACH MAXIMA OR MINIMA SECONDS		FINAL TENSION GRAMS	
	MEAS.	PRED.	MEASURED	PREDICTED	MEASURED	PREDICTED	MEAS.	PRED.
MODE I 50 to 60 TPI	24.8	25.0	33.3	34.5	19	15	20.3	22.1
MODE I 60 to 50 TPI	20.3	22.1	15.5	15.3	15	15	24.8	25.0
MODE II 50 to 60 TPI	24.8	25.0	33.6	33.0	20	20	20.3	22.1
MODE II 60 to 50 TPI	20.3	22.1	13.2	16.1	19	20	24.8	25.0
MODE III 50 to 60 TPI	24.8	25.0	30.9	33.8	13	14	20.3	22.1
MODE III 60 to 50 TPI	20.3	22.1	15.5	16.0	6	14	24.8	25.0
	INITIAL TORQUE (10^{-4}) in lbs		MAXIMA OR MINIMA TORQUE (10^{-4}) in lbs		TIME TO REACH MAXIMA OR MINIMA SECONDS		FINAL TORQUE (10^{-4}) in lbs	
	MEAS.	PRED.	MEASURED	PREDICTED	MEASURED	PREDICTED	MEAS.	PRED.
MODE I 50 to 60 TPI	1.47	1.43	2.26	2.16	20	19	1.67	1.80
MODE I 60 to 50 TPI	1.67	1.80	1.14	1.18	14	18	1.47	1.43
MODE II 50 to 60 TPI	1.47	1.43	2.32	2.16	22	22	1.67	1.80
MODE II 60 to 50 TPI	1.67	1.80	1.07	1.19	19	26	1.47	1.43
MODE III 50 to 60 TPI	1.43	1.47	2.28	2.17	10	20	1.67	1.80
MODE III 60 to 50 TPI	1.67	1.80	1.29	1.15	10	20	1.47	1.43

Figure 3.29

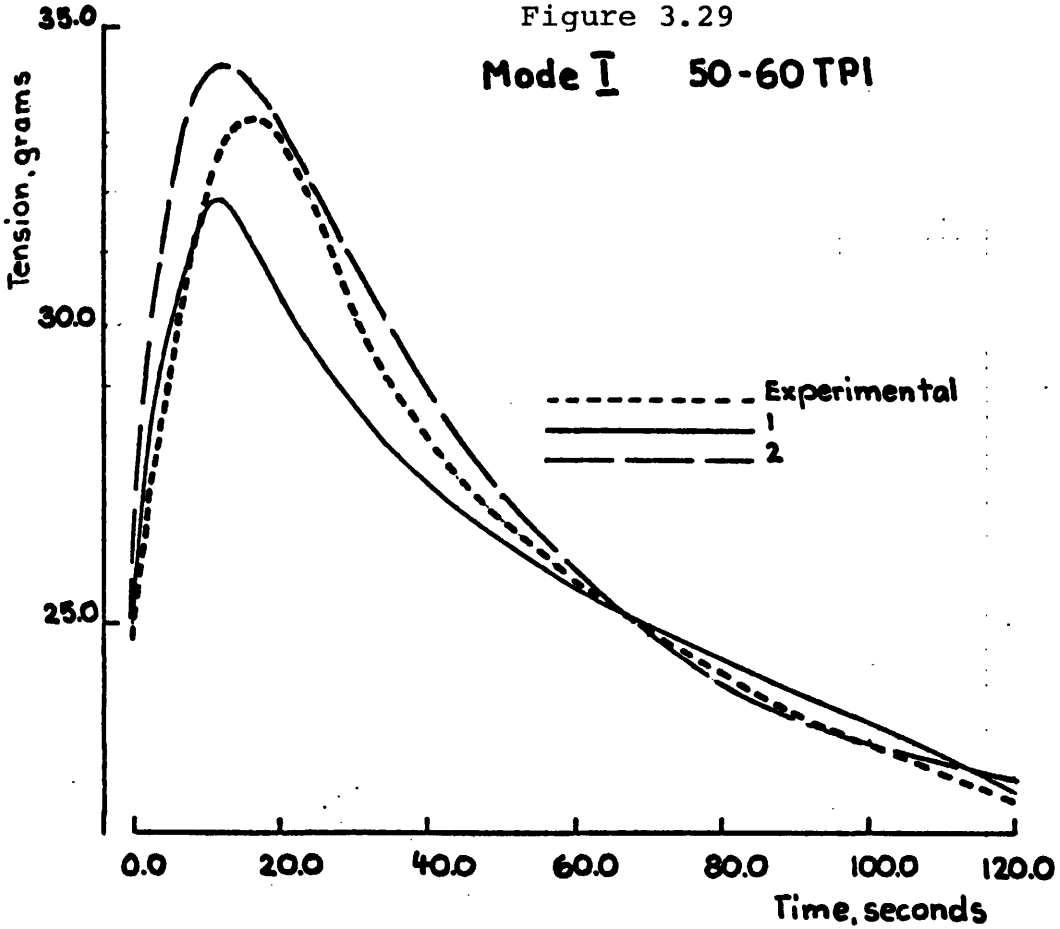
Mode I 50-60 TPI
35.0
30.0
25.0
Tension, grams
Experimental
1
2
0.0
20.0
40.0
60.0
80.0
100.0
120.0
Time, seconds

Figure 3.30

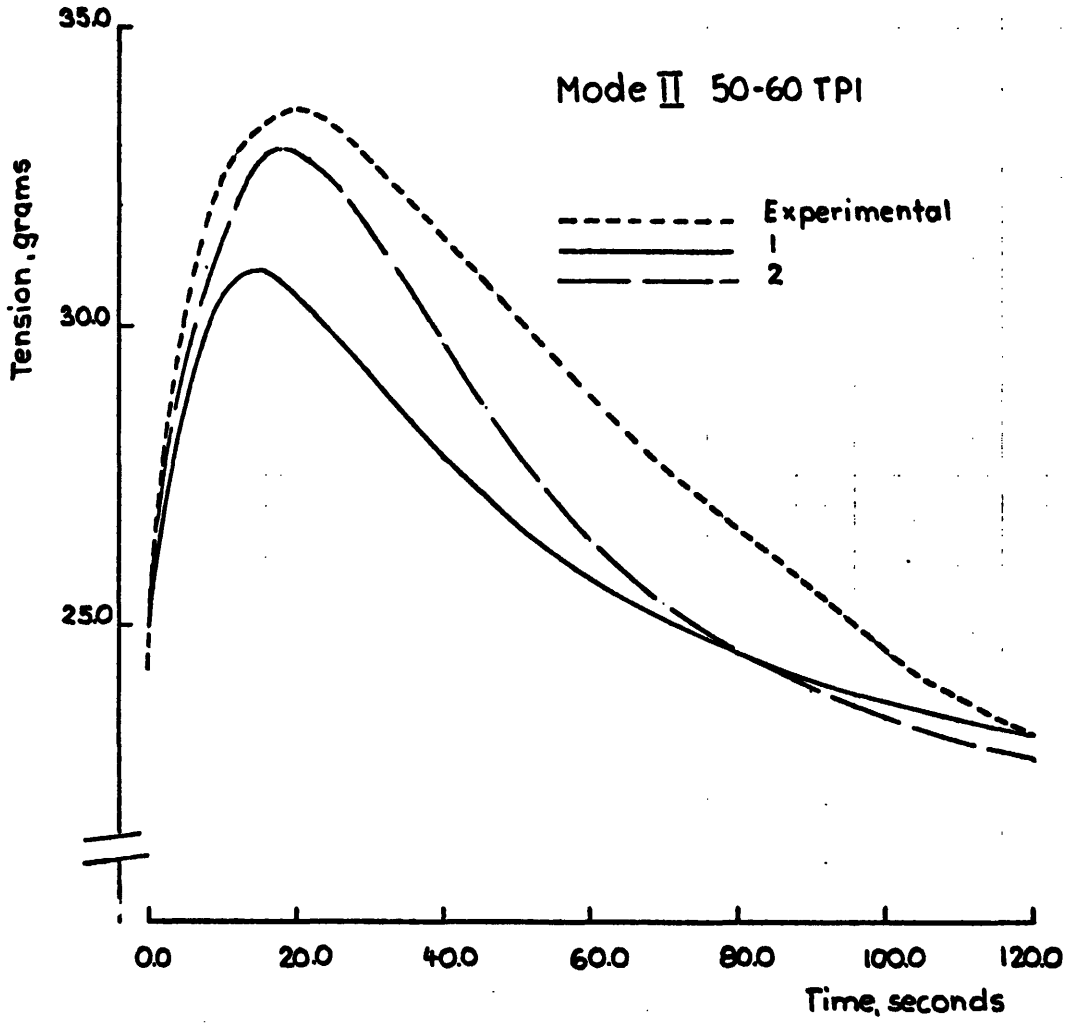
Mode II 50-60 TPI
Experimental
1
2
Tension, grams
35.0
30.0
25.0
0.0
20.0
40.0
60.0
80.0
100.0
120.0
Time, seconds

Figure 3.31

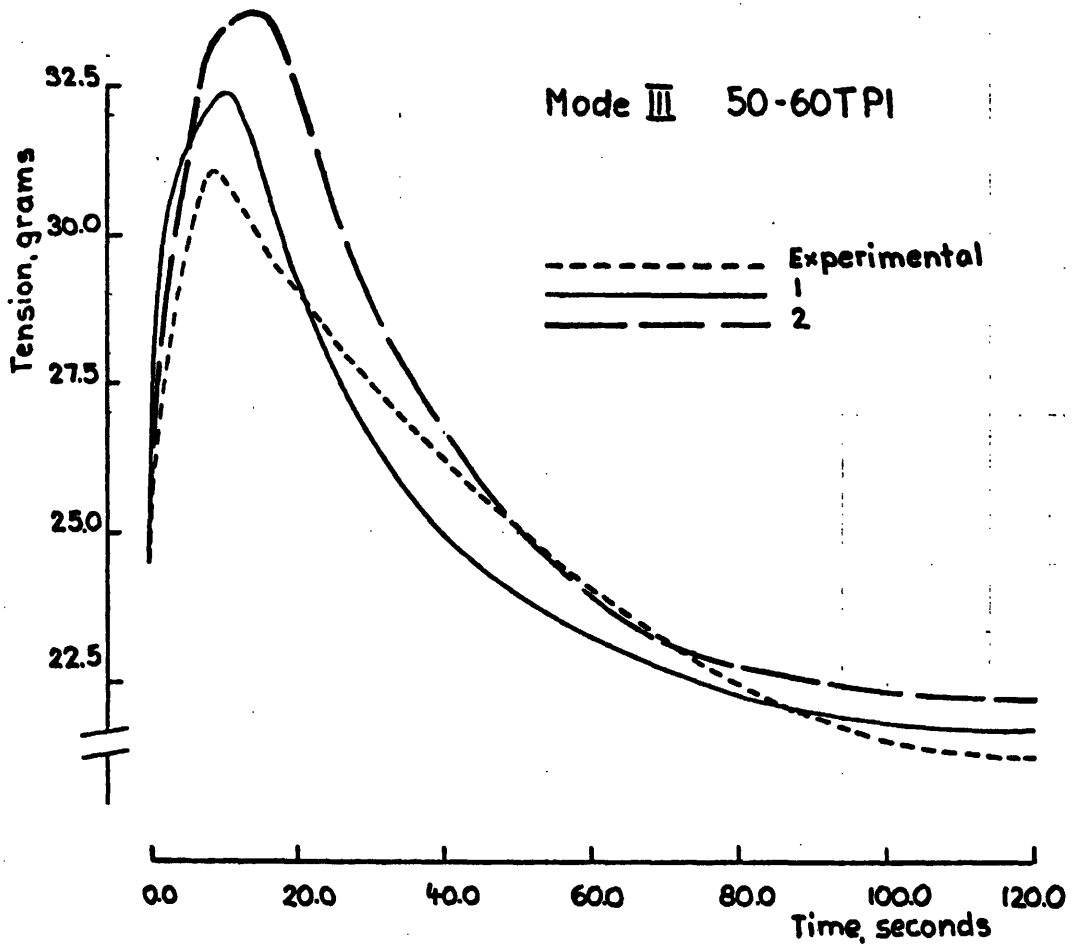
Mode III 50-60TPI
Experimental
1
2
Tension, grams
32.5
30.0
27.5
25.0
22.5
0.0
20.0
40.0
60.0
80.0
100.0
120.0
Time, seconds

should be emphasized that Mode III machine operation does not truly represent common texturing conditions since there is no cooling zone in the threadline before the spindle.

Figures 3.32, 3.33, and 3.34 show predicted and measured threadline torque for each mode of operation. The predicted torques using Analytical Model 2(tilted twist distribution) compare favorably with the measured values for each mode of machine operation. It should be noted that when the cooling zone length is shortened and the heater length increased (Mode II) the peak torque is higher than for Mode I. This is due to the maximum tension in the threadline occuring at a later time for Mode II than for Mode I; at a later time the twist is higher and threadline torque is governed by hot twist and threadline tension.

Twist Decreased to 50 TPI from 60 TPI

Figures 3.35, 3.36, and 3.37 show predicted and measured threadline tension for each mode of machine operation. The predicted values using Analytical Model 2(tilted twist distribution) compare favorably for the most part with the measured values of threadline tension for all modes of machine operation. However, after the tension bottoms out the predicted and measured values for Mode III are not in good agreement.

Figures 3.38, 3.39, and 3.40 show predicted and measured

Figure 3.32

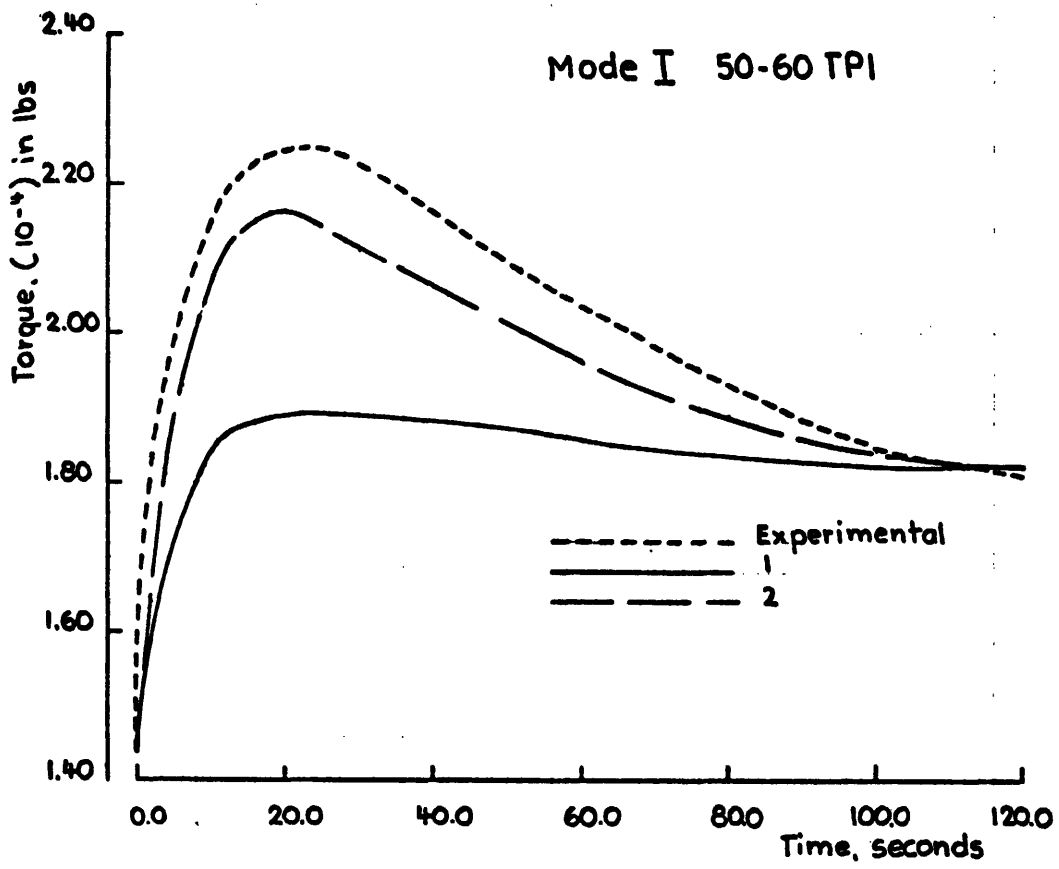
Mode I 50-60 TPI
Torque, (10⁻⁴) in lbs
2.40
2.20
2.00
1.80
1.60
1.40
0.0
20.0
40.0
60.0
80.0
100.0
120.0
Time, seconds
Experimental
1
2

Figure 3.33

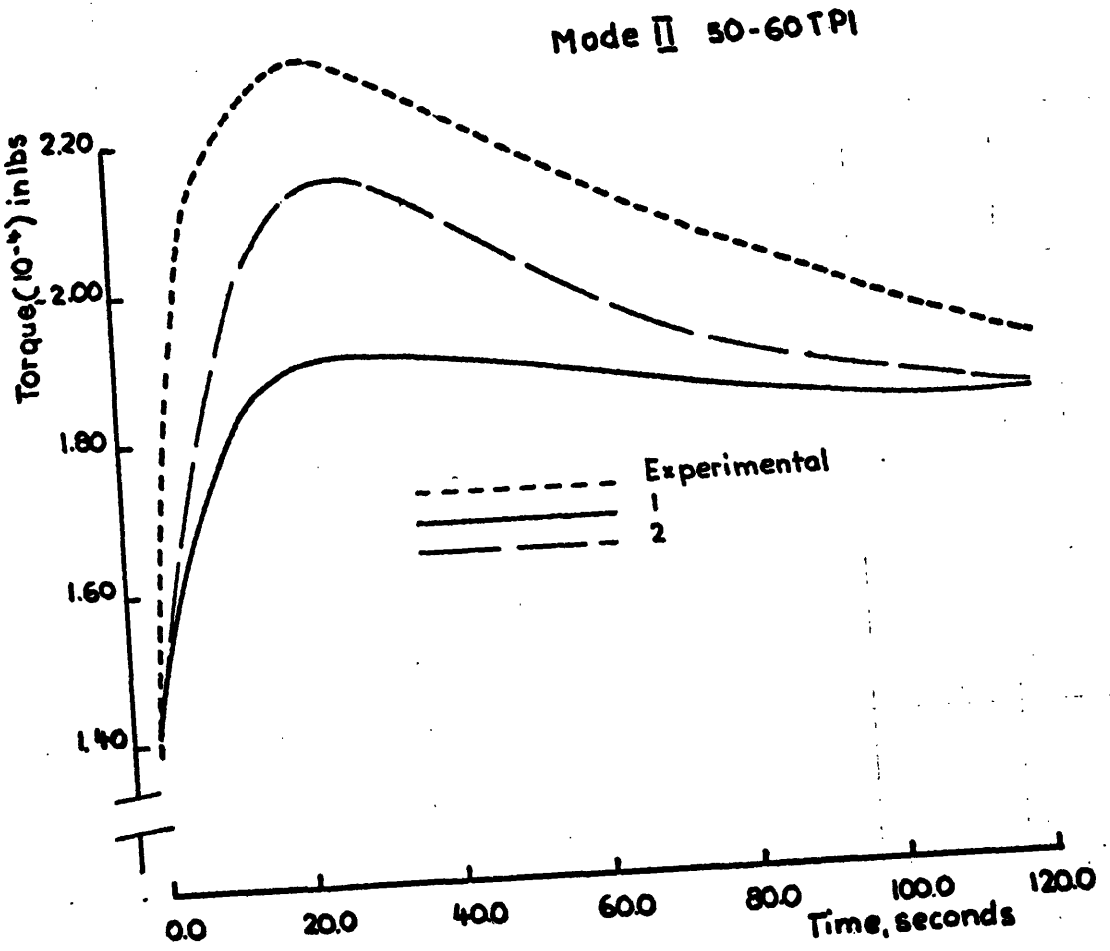
Mode II 50-60 TPI
Torque, (10^{-4}) in lbs
2.20
2.00
1.80
1.60
1.40
Experimental
1
2
0.0
20.0
40.0
60.0
80.0
100.0
120.0
Time, seconds

Figure 3.34

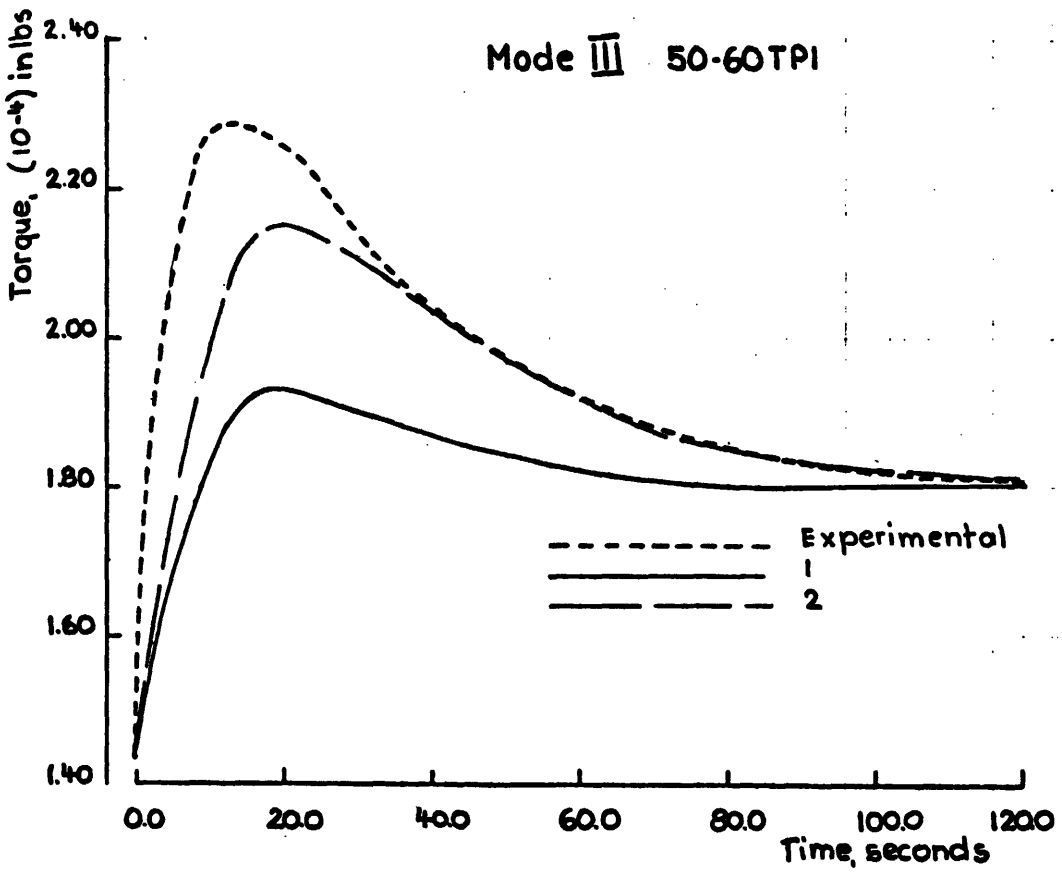
Mode III 50-60TPI
Torque, (10-4) in lbs
2.40
2.20
2.00
1.80
1.60
1.40
0.0
20.0
40.0
60.0
80.0
100.0
120.0
Time, seconds
Experimental
1
2

Figure 3.35

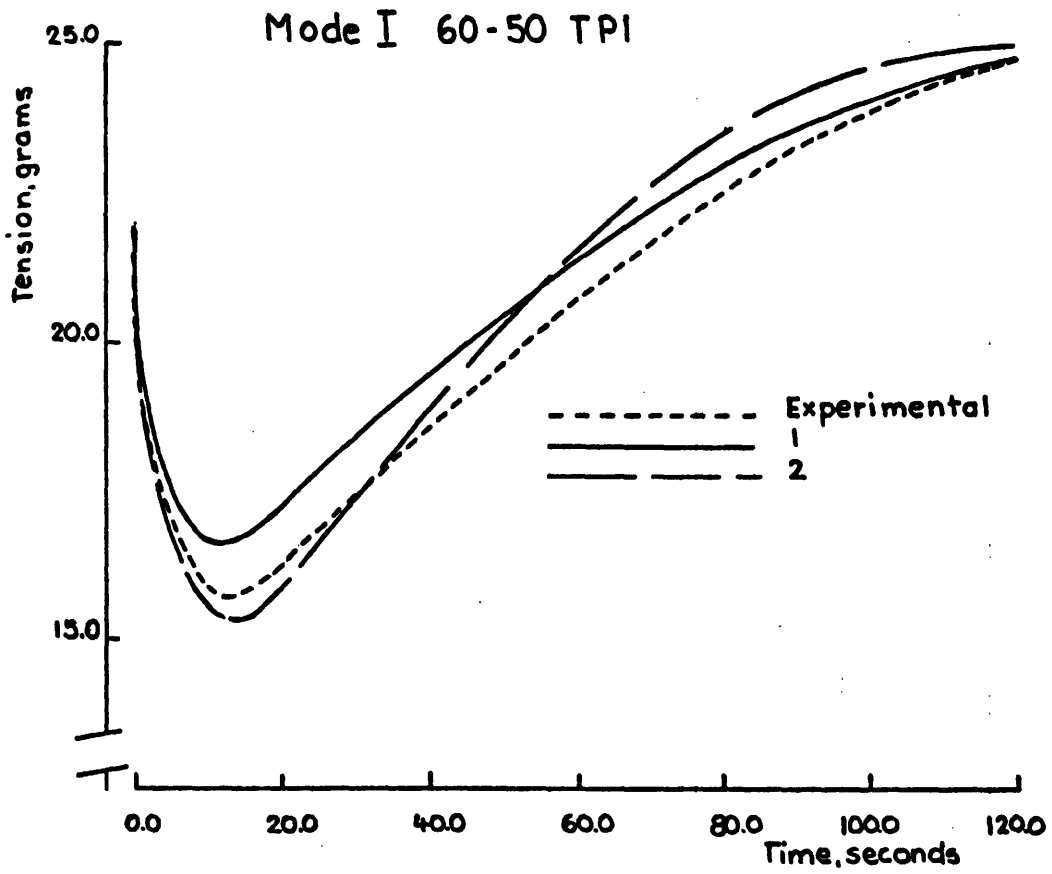
Mode I 60-50 TPI
25.0
20.0
15.0
Tension, grams
Experimental
1
2
0.0
20.0
40.0
60.0
80.0
100.0
120.0
Time, seconds

Figure 3.36

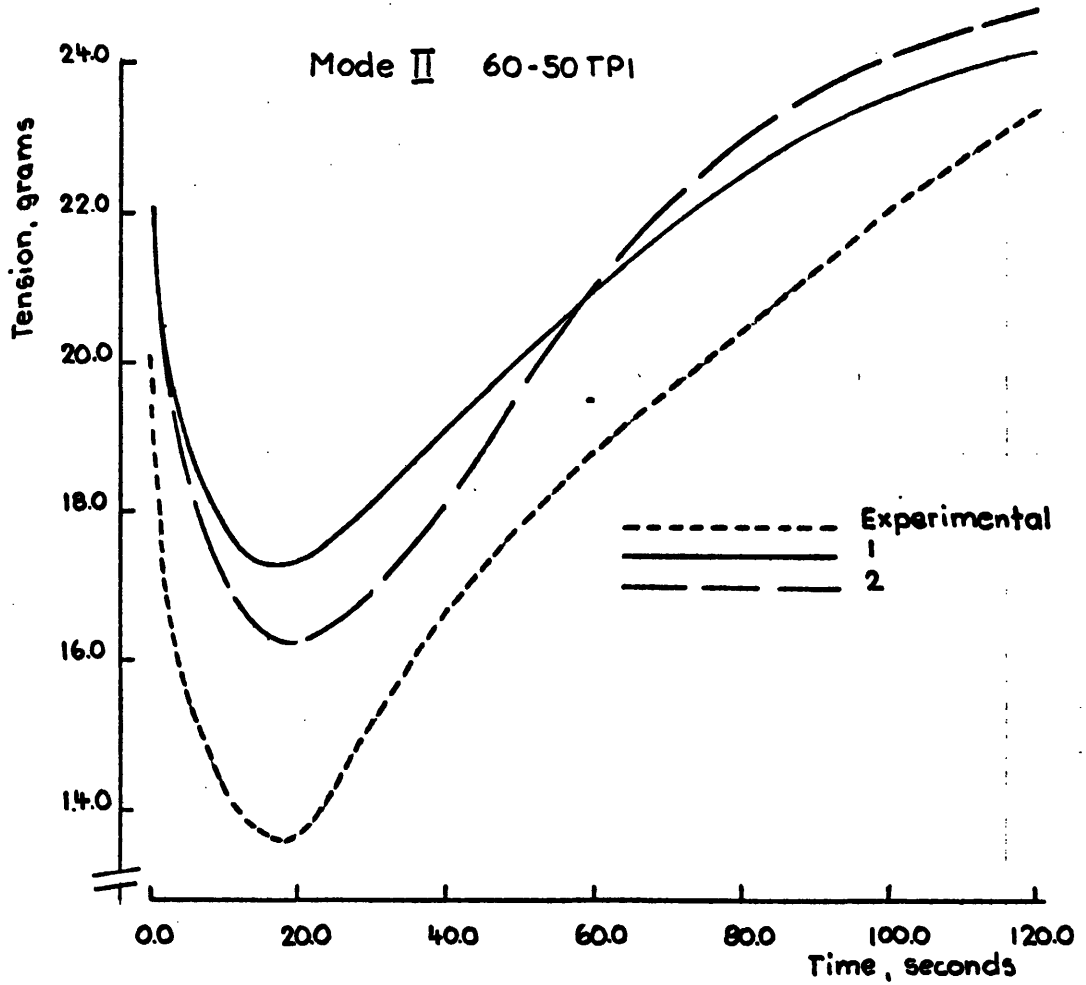
Mode II 60-50 TPI
Tension, grams
24.0
22.0
20.0
18.0
16.0
14.0
0.0
20.0
40.0
60.0
80.0
100.0
120.0
Time, seconds
Experimental
1
2

Figure 3.37

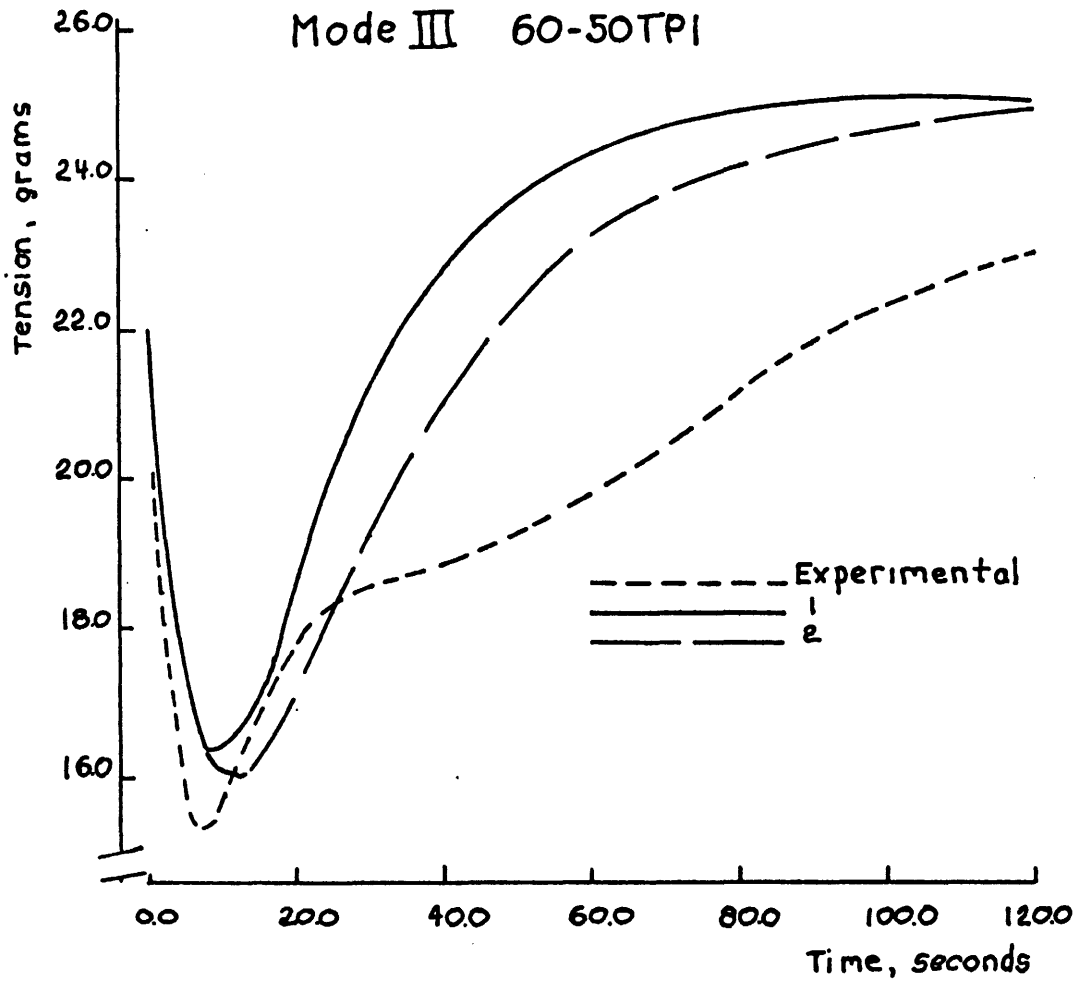
Mode III 60-50TPI
Tension, grams
26.0
24.0
22.0
20.0
18.0
16.0
0.0
20.0
40.0
60.0
80.0
100.0
120.0
Time, seconds
Experimental
1
2

Figure 3.38

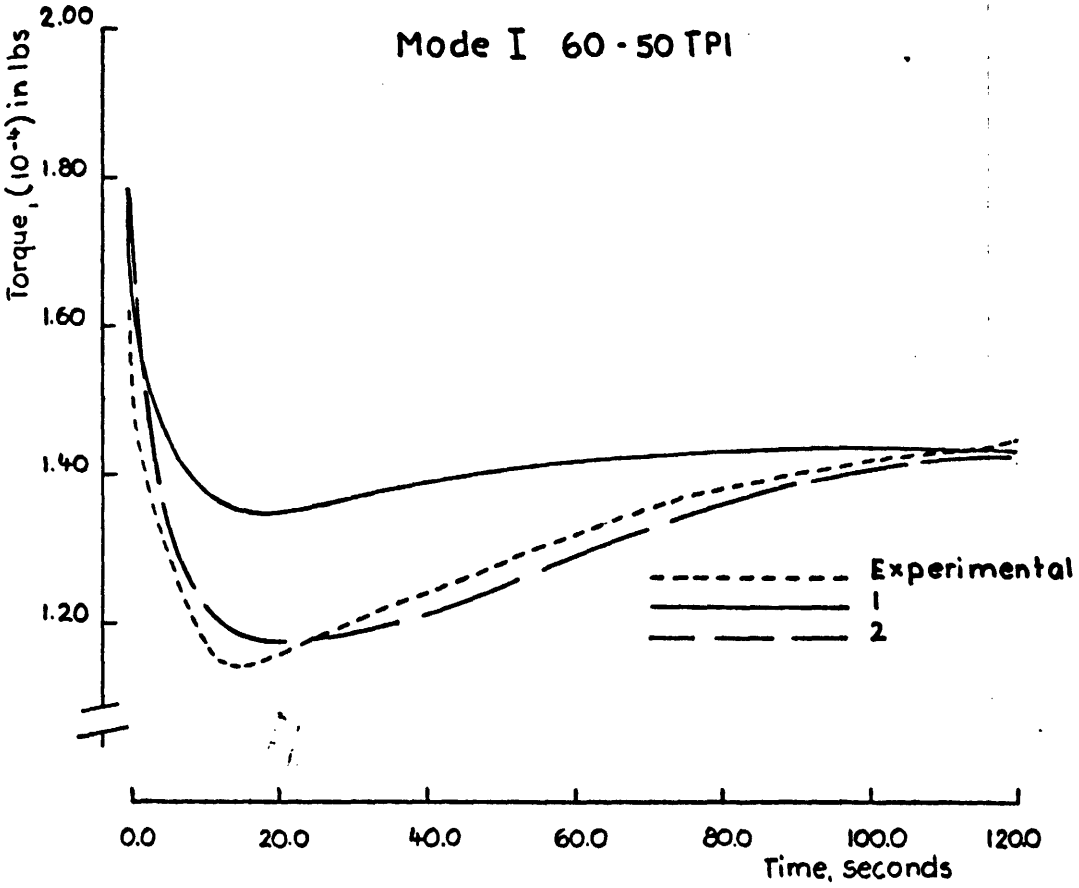
Mode I 60 - 50 TPI
Torque, (10-4) in lbs
2.00
1.80
1.60
1.40
1.20
Experimental
1
2
0.0
20.0
40.0
60.0
80.0
100.0
120.0
Time, seconds

Figure 3.39

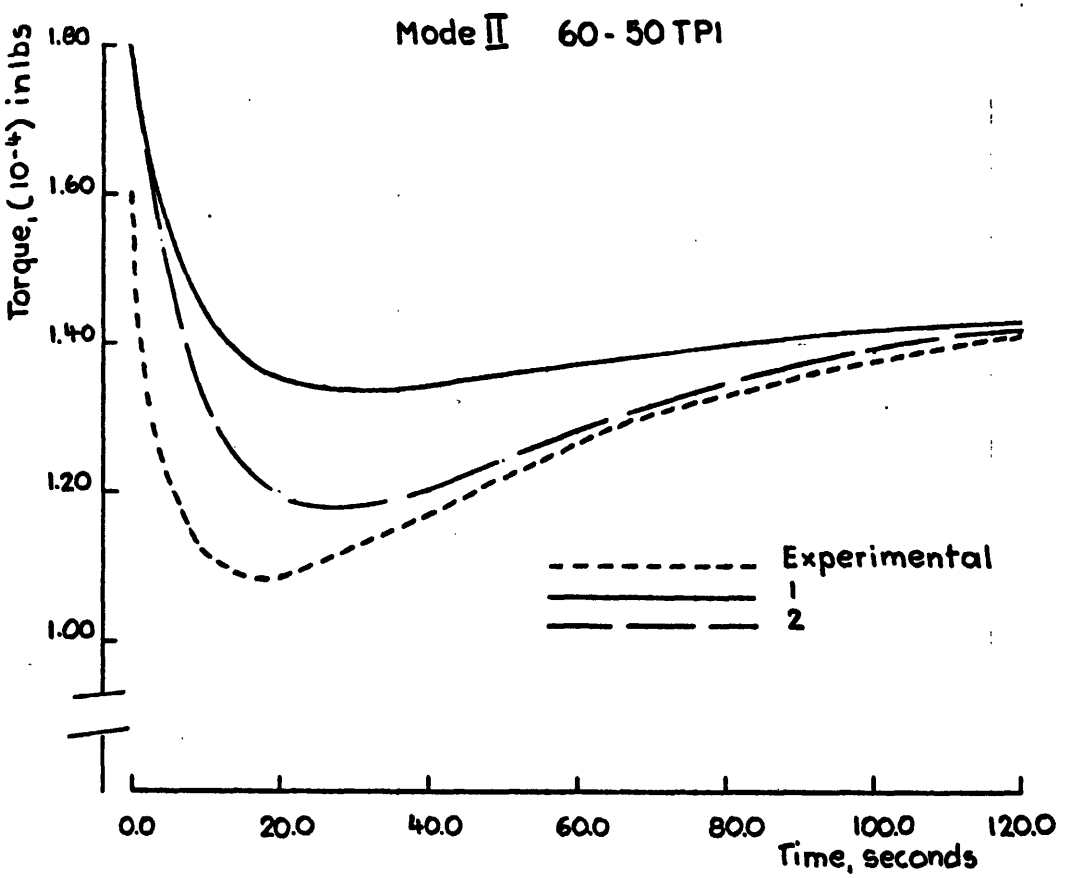
Mode II 60-50 TPI
Torque, (10^{-4}) in lbs
1.80
1.60
1.40
1.20
1.00
Experimental
1
2
0.0
20.0
40.0
60.0
80.0
100.0
120.0
Time, seconds

Figure 3.40

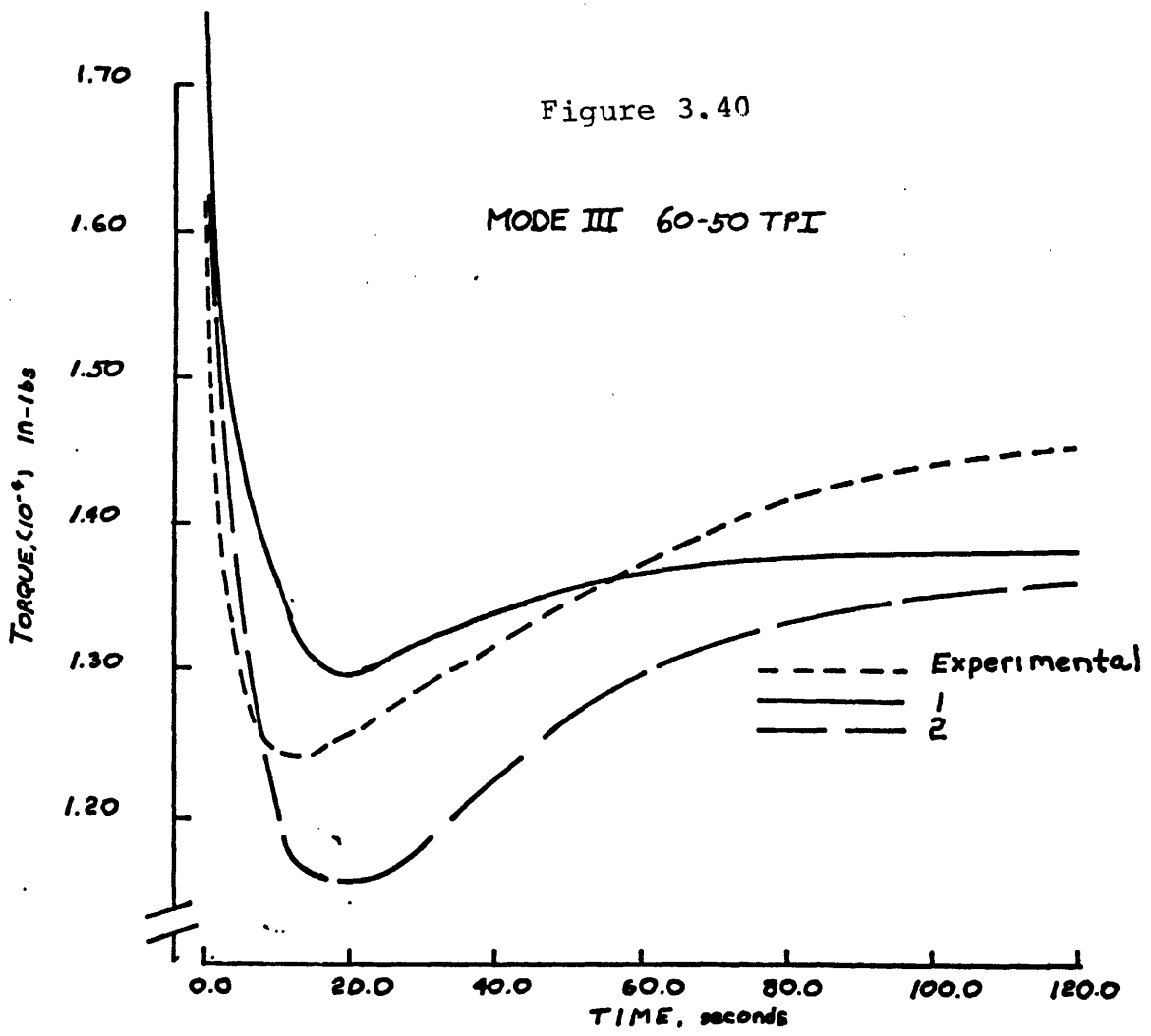
MODE III 60-50 TPI
1.70
1.60
1.50
1.40
1.30
1.20
TORQUE, (10⁻⁴) IN-lbs
0.0
20.0
40.0
60.0
80.0
100.0
120.0
TIME, seconds
Experimental
1
2

threadline torque for each mode of machine operation. The predicted values using Analytical Model 2(tilted twist distribution) compare favorably with the measured values of threadline torque for all modes of machine operation.

Twist Distribution in the Cold Zone

Figures 3.41 and 3.42 show predicted and measured results using Analytical Model 2(tilted twist distribution) for threadline twist as functions of time at two positions in the cold zone for Mode I machine operation. Note the steady state error between predicted and measured twist values at 60 TPI machine twist. However at 50 TPI machine twist the error is negligible. In light of steady state errors, the measured and predicted transient threadline twist levels compare favorably with each other. In Figure 3.43 we connect the measured twist levels at two points in the cold zone by a straight line at different times after a step change in machine twist and compare the slopes of these lines with the predicted slopes using Analytical Model 2. Comparison of the measured and predicted twist distribution slopes at the same time indicates good agreement.

Figure 3.41

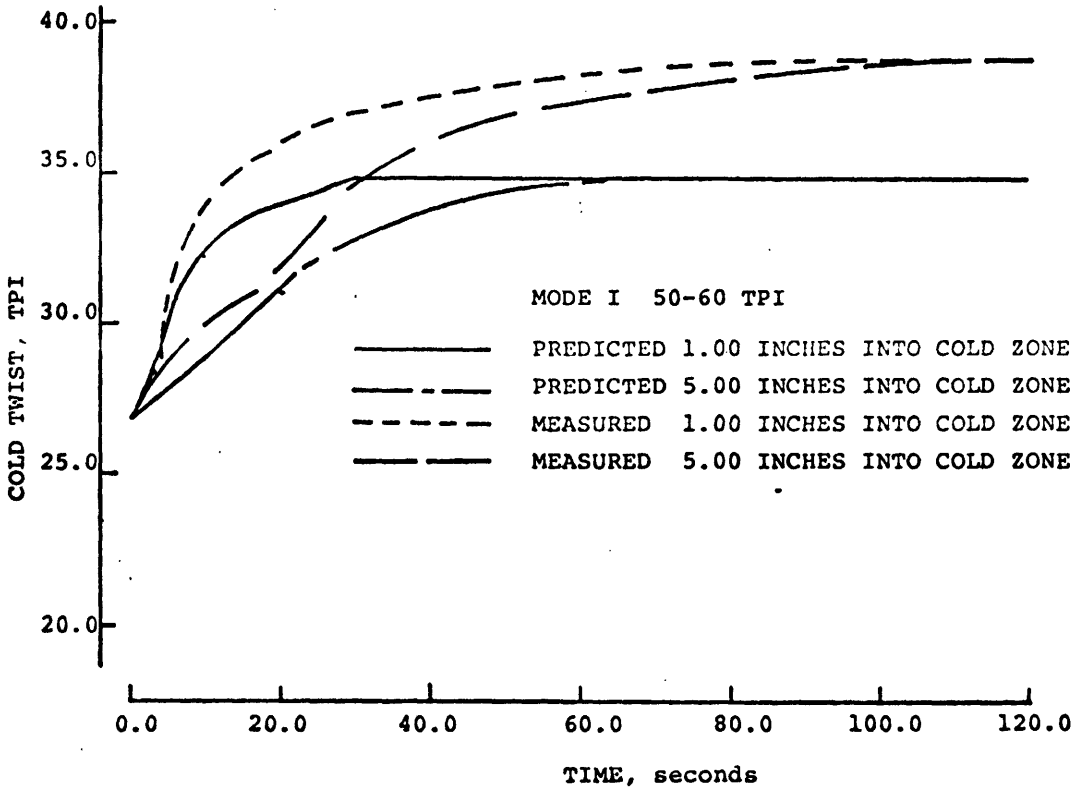
40.0
35.0
30.0
25.0
20.0
COLD TWIST, TPI
MODE I 50-60 TPI
PREDICTED 1.00 INCHES INTO COLD ZONE
PREDICTED 5.00 INCHES INTO COLD ZONE
MEASURED 1.00 INCHES INTO COLD ZONE
MEASURED 5.00 INCHES INTO COLD ZONE
0.0
20.0
40.0
60.0
80.0
100.0
120.0
TIME, seconds

Figure 3.42

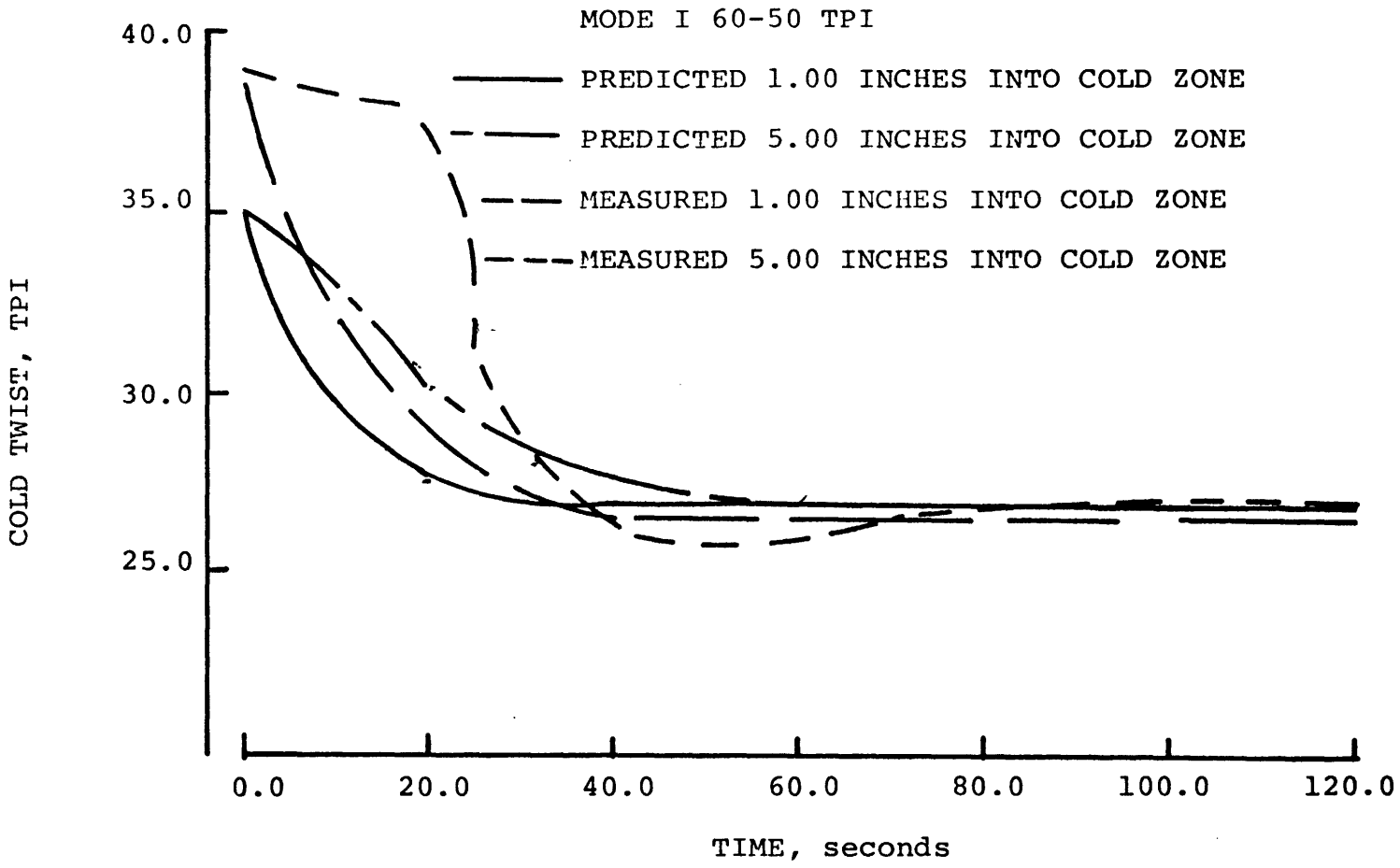
MODE I 60-50 TPI
PREDICTED 1.00 INCHES INTO COLD ZONE
PREDICTED 5.00 INCHES INTO COLD ZONE
MEASURED 1.00 INCHES INTO COLD ZONE
MEASURED 5.00 INCHES INTO COLD ZONE
COLD TWIST, TPI
40.0
35.0
30.0
25.0
0.0
20.0
40.0
60.0
80.0
100.0
120.0
TIME, seconds

Figure 3.43

COMPARISON OF PREDICTED AND MEASURED COLD ZONE TWIST

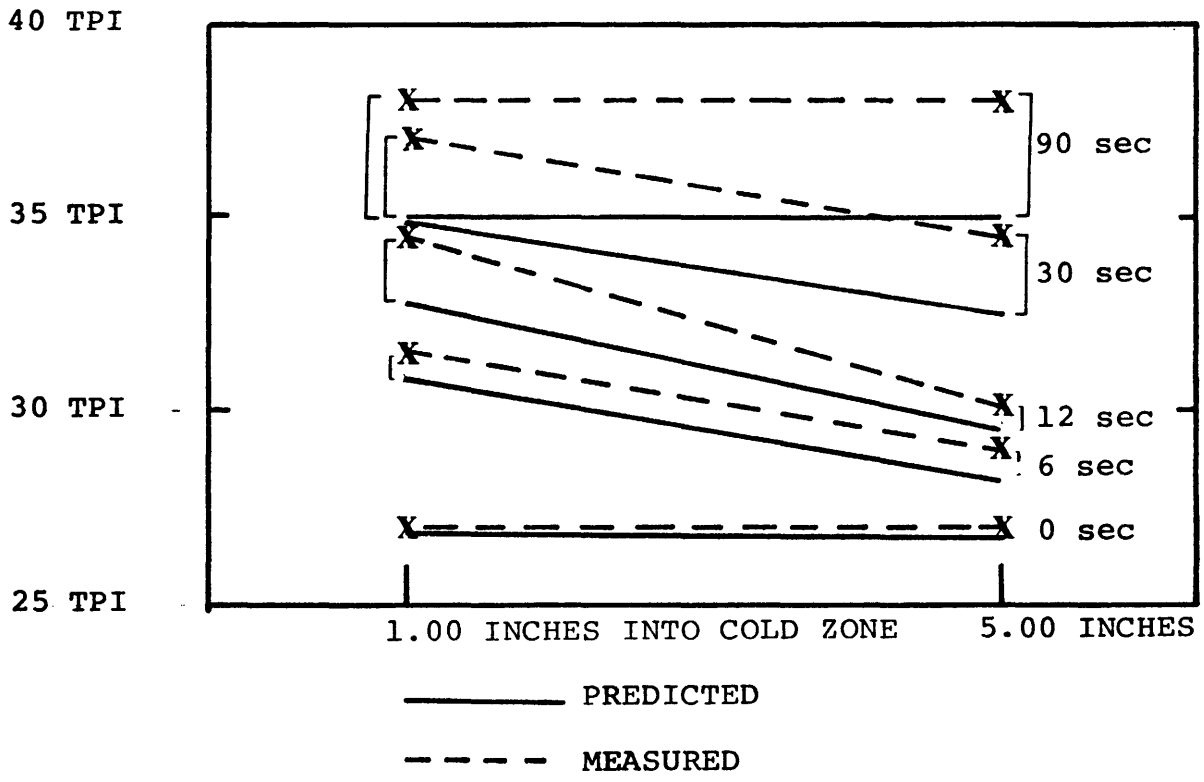

3.5 EXPERIMENTS ON THE DRAW TEXTURING OF POY NYLON

Experiments were conducted on Du Pont POY nylon yarns for the purpose of comparing measured values of threadline parameters , i.e. threadline tension and threadline torque, with predicted results during transient operation of the draw texturing process. The dimensions and properties of the feed yarn used are as follows:

Undrawn Filament Denier:	90/34 - 2.65
Undrawn Filament Radius:	3.57×10^{-4} inches
Undrawn Filament Tensile Modulus :	268,000 psi
Undrawn Filament Bending Rigidity :	3.42×10^{-9} lb in^2
Undrawn Filament Torsional Rigidity :	2.47×10^{-9} lb in^2

Filament dimensions and tensile modulus were measured in the Fibers and Polymers Laboratories at MIT. The bending modulus was calculated from the tensile modulus based on the assumption of equal axial and compressive moduli. The torsional rigidity (GI_p) was obtained from Ward[11].

The yarns were textured on the MITEX False Twister. Threadline tension and torque were measured by the MITEX Torque-Tension Meter. The machine dimensions were set as follows:

Cold Zone	6.00 inches
Hot Zone	1.25 inches
Cooling Zone	7.00 inches

Post Spindle Zone: 9.00 inches

The unsteady machine operation was activated by introducing a step change in the machine twist. The nominal yarn throughput speed was .38 inches per second; the draw ratio was 1.29; the heater temperature was 210°C.

Steady State Threadline Tension and Threadline Torque

For this commercial textured nylon yarn the general level of machine twist is between 60 TPI and 70 TPI, and so threadline tension and threadline torque were measured and predicted for these levels as indicated below:

Machine Twist	Tension, grams		Torque(10^{-4}) in lbs	
	Predicted	Measured	Predicted	Measured
60 TPI	23.3	26.5	.78	.86
70 TPI	20.9	23.0	.89	1.01

It is seen that the predicted values of threadline torque and tension are about 10% less than the measured values. No effort has been made to experimentally characterize in full threadline behavior with this POY nylon. The above data were obtained to reinforce our confidence in the utility of the steady state analysis of texturing threadline behavior, which up to now was directed towards the POY PET yarn -machine system. It should be emphasized that the POY nylon feed yarn differs significantly in dimensions and properties from the

POY PET yarns generally used in this study. In particular the nylon differs considerably in its rigidity ratio, i.e. EI/GI_p (1.38 for nylon versus 3.05 for PET), a quantity which can have considerable influence on the determination of cold zone twist and torque.

Transient Threadline Tension and Torque

Using POY nylon described above, we also undertook limited study of transient behavior during the draw texturing process on the MITEX False Twister. Threadline torque and threadline tension were measured by the MITEX Torque-Tension Meter. Unsteady machine operation was activated by changing the machine twist stepwise. The texturing machine dimensions were the same as those used for the steady state study described above.

Figures 3.44 and 3.45 compare predicted threadline tension and torque using Analytical Model 2(tilted twist distribution) with measured values when the machine twist was changed from 60 TPI to 70 TPI. It is noted that the time response for tensions and torque maxima and minima are consistent for experimental and calculated values. There appears to be considerable difference in transient tension and torque levels but if we correct for the before and after steady state error between the predicted and measured threadline tension and torque, we conclude that the transient changes in thread-

Figure 3.44

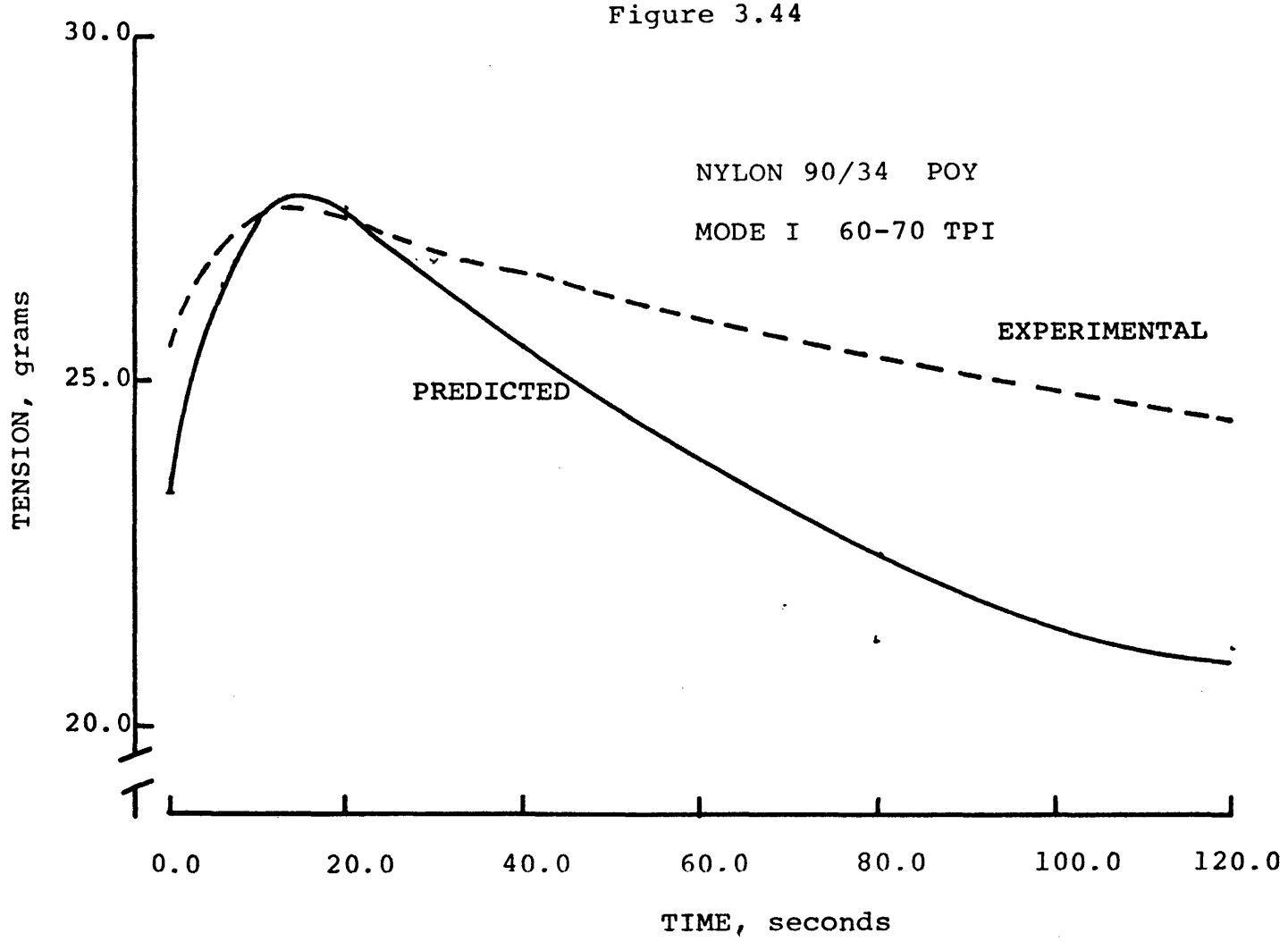
30.0
25.0
20.0
NYLON 90/34 POY
MODE I 60-70 TPI
EXPERIMENTAL
PREDICTED
TENSION, grams
0.0
20.0
40.0
60.0
80.0
100.0
120.0
TIME, seconds

Figure 3.45

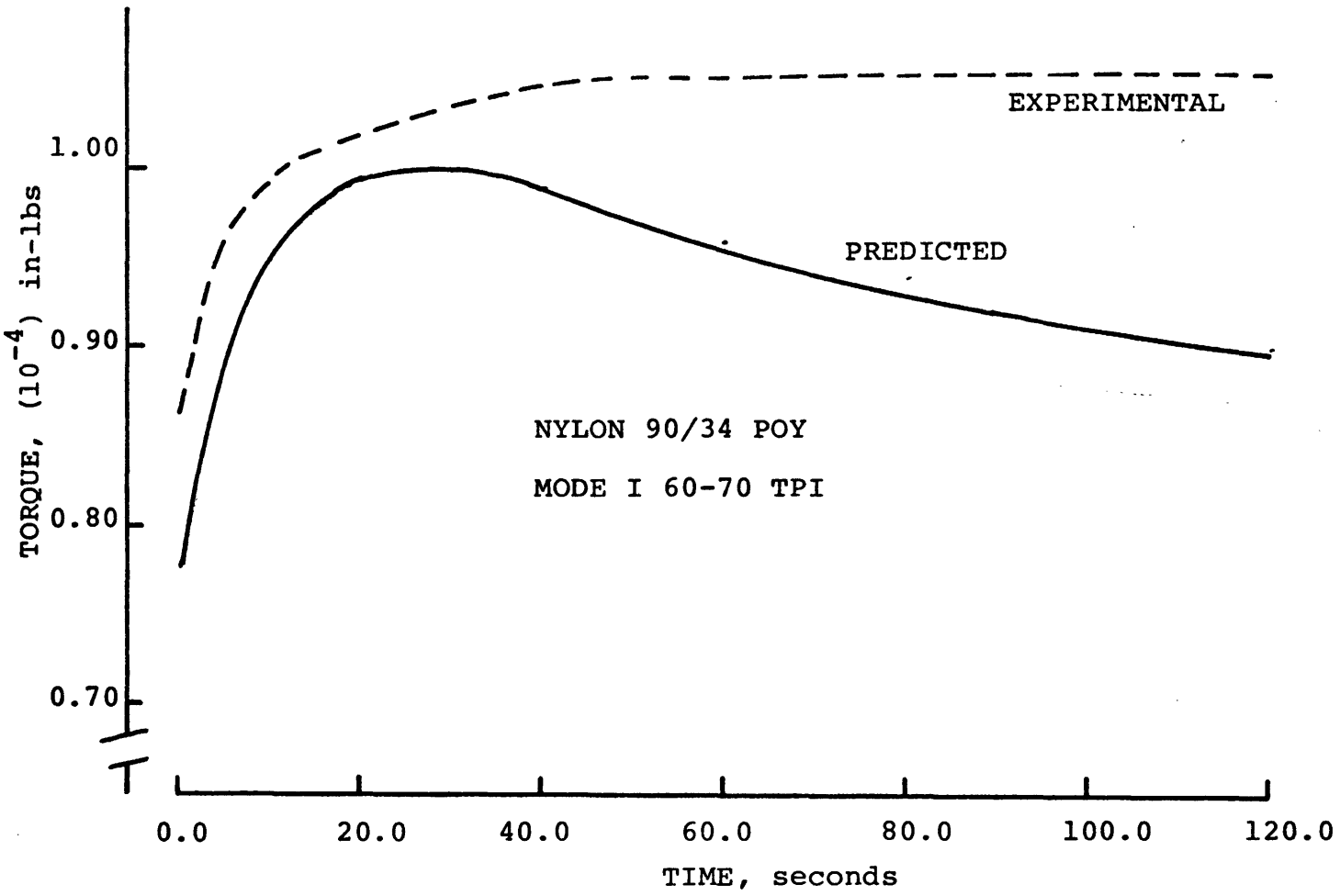
EXPERIMENTAL
PREDICTED
NYLON 90/34 POY
MODE I 60-70 TPI
TORQUE, (10^{-4}) in-lbs
1.00
0.90
0.80
0.70
0.0
20.0
40.0
60.0
80.0
100.0
120.0
TIME, seconds

line tension and torque compares favorably with the measured changes. Likewise, Figures 3.46 and 3.47 compare the predicted threadline tension and torque using Analytical Model 2(tilted twist distribution) with the measured values when the machine twist is dropped from 70 TPI to 60 TPI. Again, with the suggested steady state correction, predicted and measured changes in threadline tension and torque compare favorably, although one cannot claim the extent of agreements observed in the POY PET experimental study.

One point should be noted for the nylon yarn, i.e. that the measured torque levels during transient operation approach their new steady state levels virtually without overshoot. This behavior may play a role in preventing the cycling of tension and torque during unsteady operation as discussed in Chapter 4.

Figure 3.46

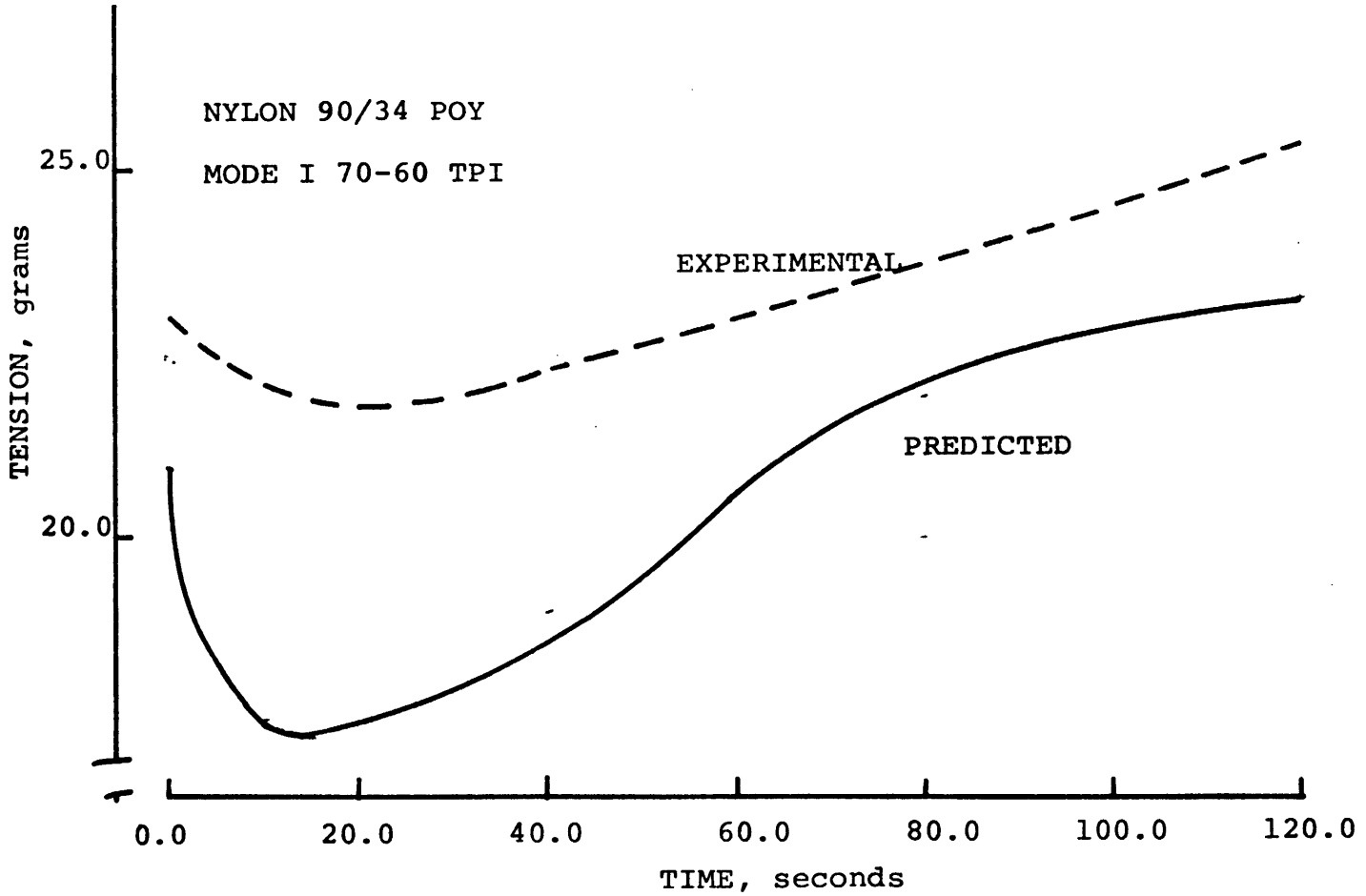
NYLON 90/34 POY
MODE I 70-60 TPI
EXPERIMENTAL
PREDICTED
TENSION, grams
25.0
20.0
0.0
20.0
40.0
60.0
80.0
100.0
120.0
TIME, seconds

Figure 3.47

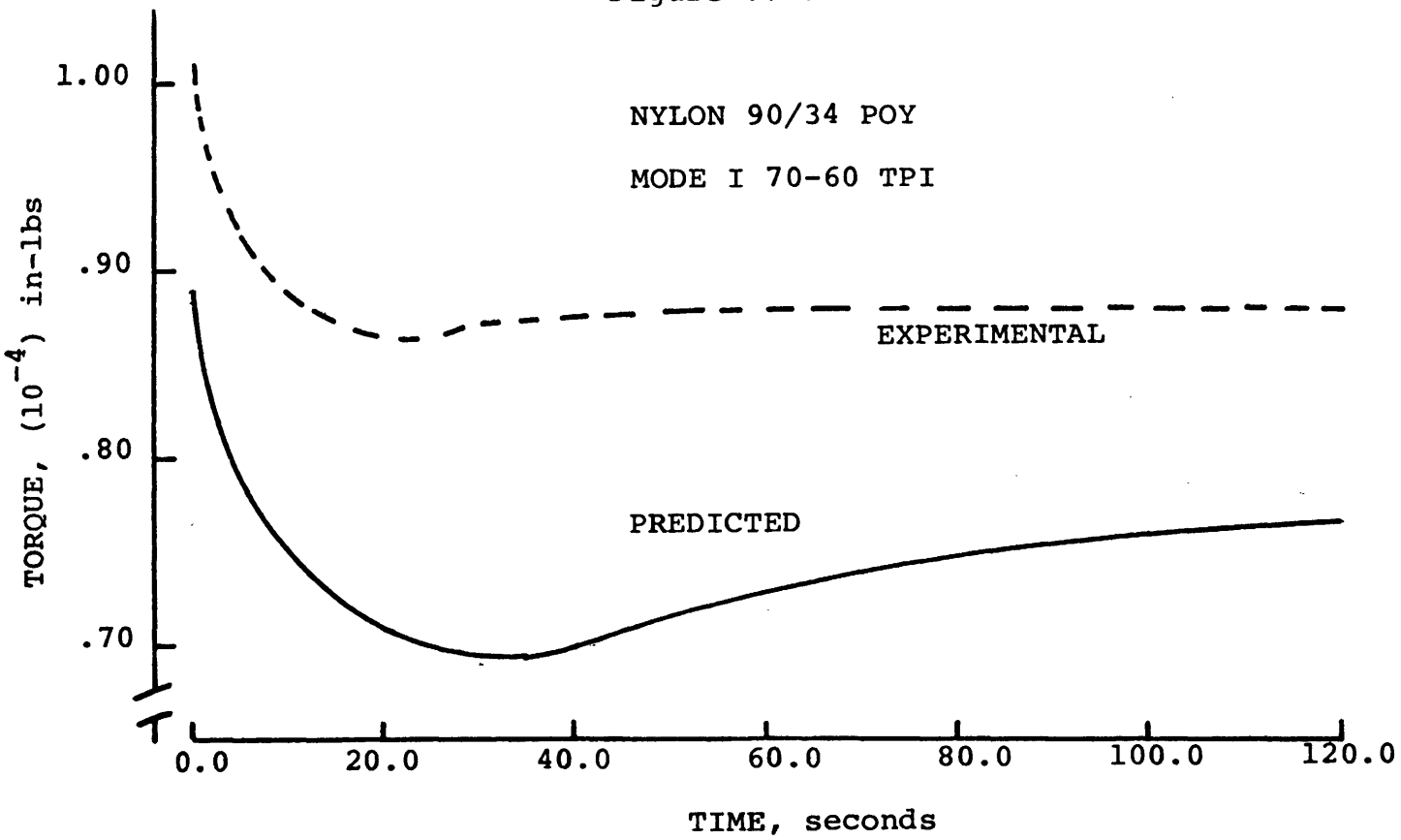
NYLON 90/34 POY
MODE I 70-60 TPI
EXPERIMENTAL
PREDICTED
1.00
.90
.80
.70
TORQUE, (10^{-4}) in-lbs
0.0
20.0
40.0
60.0
80.0
100.0
120.0
TIME, seconds

3.6 PREDICTED EFFECT OF OSCILLATORY OPERATION ON THREADLINE RESPONSE

A commercial texturing machine running twenty four hours a day is subject to all kinds of wear. Critical machine parts subjected to wear, such as feed rollers, take up rollers, and spindle drive, may run unsteadily due to changes in critical dimensions with use. This section considers how machine tolerances affect threadline response. The effect of three such operating defects will be examined including:

1. Oscillating Spindle Speed
2. Oscillating Feed Roller Surface Speed
3. Oscillating Take Up Roller Surface Speed

3.6.1 Oscillating Spindle Speed

Under normal texturing conditions the spindle speed is assumed to be constant although wear in the spindle drive could cause the spindle speed to oscillate slightly above and below the nominal speed. To provide some understanding of how oscillatory changes affect the threadline forces, we execute the transient analysis given in Section 3.3 and program the spindle speed to oscillate sinusoidally 1% above and below the nominal spindle speed of 177.33 radians per second(60 TPI Machine Twist). The machine draw ratio was programmed as 1.60; the throughput speed was programmed as 0.47 inches per second. The frequencies of spindle speed disturbances and corresponding peak to peak variation ratios are :

FREQUENCY OF FORCED DISTURBANCE	PEAK TO PEAK VARIATION RATIO		
	SPINDLE SPEED	THREADLINE TENSION	THREADLINE TORQUE
.177 Radians/sec	.02	.0304	.0285
1.77 Radians/sec	.02	.0032	.0030
177. Radians/sec	.02	.0003	.0004

The predicted peak to peak variation ratios given above show that as the frequency of the spindle speed disturbance increases, the effect on threadline behavior decreases. Accordingly, since the nominal speed is 177. radians per second we can conclude that spindle speed disturbances near that frequency do not cause significant variations in threadline behavior. However if the disturbance frequency is several orders of magnitude smaller than the nominal spindle speed, the effect on threadline behavior is more pronounced.

This finding is significant since one way of driving the spindle is to use a magnetic roller (in contact with the spindle) with a radius several orders larger than that of the spindle radius. If such a magnetic roller were to become eccentric due to wear, the disturbing frequency would be low enough to create substantial threadline force variations.

3.6.2 Oscillating Feed Roller Surface Speed

Wear on the feed roller surface can cause an oscillating rate of material delivery to the texturing zone. As the rate

of material delivery changes, so do threadline forces. To help understand how the frequency of oscillation of the material delivery rate affects threadline forces, we execute the transient analysis given in Section 3.3 and program the feed roller velocity to oscillate sinusoidally 1% above and below the nominal throughput speed of 0.294 inches per second. The frequency of forced disturbances are:

0.0393 Radians per Second (.1 x Feed Roller Speed)

0.393 Radians per Second (1 x Feed Roller Speed)

3.93 Radians per Second (10 x Feed Roller Speed)

The machine dimensions used in the analysis are the ones for Mode I described in Section 3.4. The programmed machine twist is 60 TPI. Below we present the peak to peak variation ratio for Feed Roller Speed and for the corresponding threadline tension and threadline torque;

FREQUENCY OF FORCED DISTURBANCE	PEAK TO PEAK VARIATION RATIO		
	ROLLER SPEED	THREADLINE TENSION	THREADLINE TORQUE
.0393 Radians/sec	.02	.101	.077
0.393 Radians/sec	.02	.052	.041
3.93 Radians/sec	.02	.006	.005

For the analytical model using Mode I machine dimensions, the entire threadline length is 23.25 inches. Commercial machines generally have a threadline length an order of magnitude greater than this length. If the feed roller was

reduced to 1/10 its present radius in our theoretical model (so that the ratio of roller radius to threadline length were about that of a commercial machine) its angular velocity would have to be increased by tenfold to maintain the original material delivery rate. Accordingly, the effect of a worn eccentric feed roller on threadline behavior is represented by the conditions where the frequency of disturbance is 3.93 radians per second. Thus, we can conclude that the effects of small amplitude transients in the material delivery rate are negligible.

3.6.3 Oscillating Take Up Roller Surface Speed

An analysis identical to the previous analysis in Section 3.6.2 can be undertaken for the case of oscillating take up roller surface speed. The results are given below:

FREQUENCY OF FORCED DISTURBANCE	PEAK TO PEAK VARIATION RATIO		
	TAKE UP ROLLER SPEED	THREADLINE TENSION	THREADLINE TORQUE
0.0629	.02	.052	.024
0.629	.02	.019	.013
6.29	.02	.002	.001

Comparing the results above with the results given in Section 3.6.2 we see that the steadiness of take up rate is not as critical a parameter as material delivery rate with regard to variation of threadline forces. This can be attributed to the significantly higher cold fiber tensile modulus than the hot fiber "modulus".

3.7 EFFECT OF INCREASING YARN WRAP ANGLE ON SPINDLE

In Section 2.3.9 we showed that the linear velocity of the twisted yarn, V_3, as it enters the spindle is minimally affected by the range of yarn-spindle contact frictional forces which generally obtain in the texturing process. However if the contact friction is significantly increased, V_3 must accordingly decrease. This decrease of V_3 will reduce the texturing zone tensions and the filaments in the hot zone will be drawn to a lesser degree. Likewise the threadline torque will be reduced if the texturing tension decreases.

A simple way to increase the frictional forces acting against threadline translational movement is to increase the the yarn wrap angle around the spindle pin. Experiments were conducted with the Du Pont POY PET used earlier for the transient study to examine the effect of double wrapping the yarn around the spindle pin on threadline behavior.

Figures 3.48, 3.49, 3.50, and 3.51 show significant differences in threadline behavior depending on whether the yarn is double wrapped or single wrapped around the spindle pin. When the yarn is double wrapped both steady state and transient values of threadline torque and tension are about 15% lower than the corresponding values when the yarn is only single wrapped. Note however that the time response is relatively independent with regard to wrap angle.

Figure 3.48

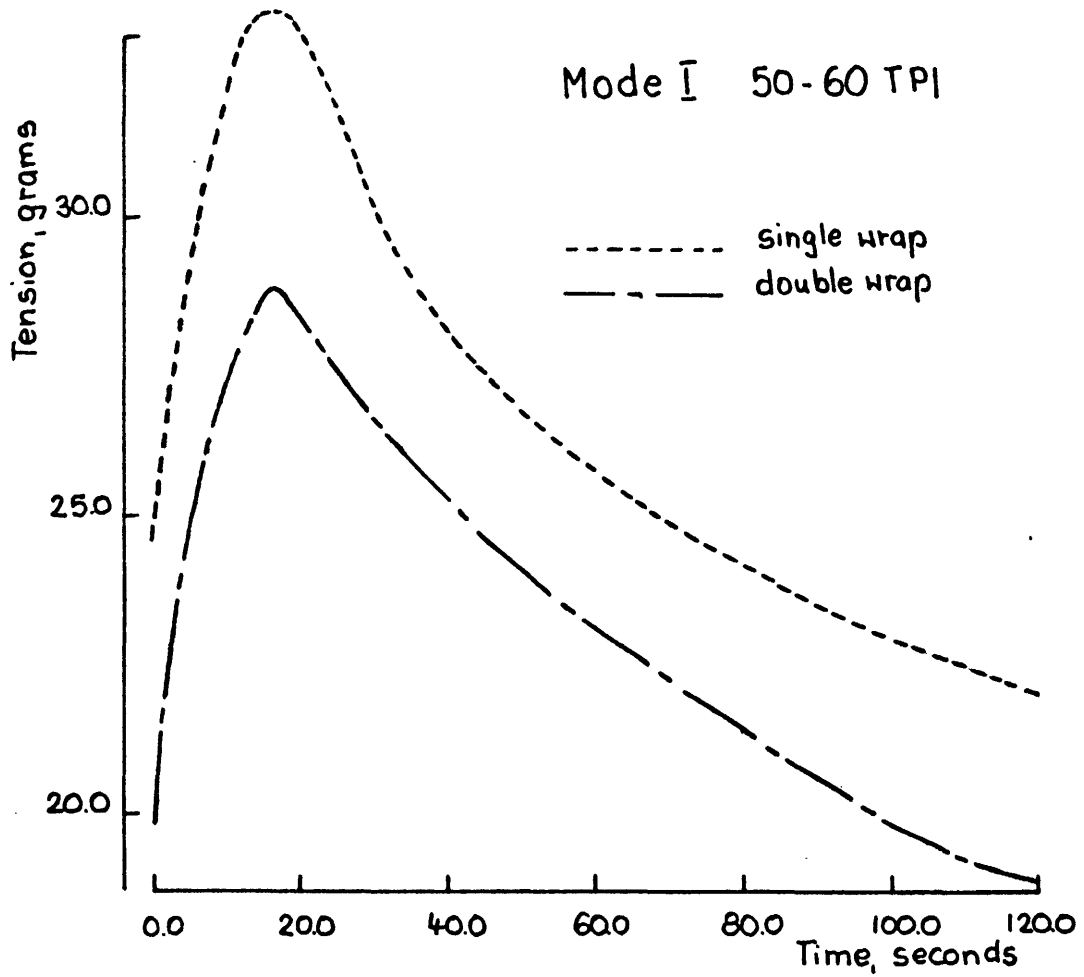
Mode I 50-60 TPI
single wrap
double wrap
Tension, grams
30.0
25.0
20.0
0.0
20.0
40.0
60.0
80.0
100.0
120.0
Time, seconds

Figure 3.49

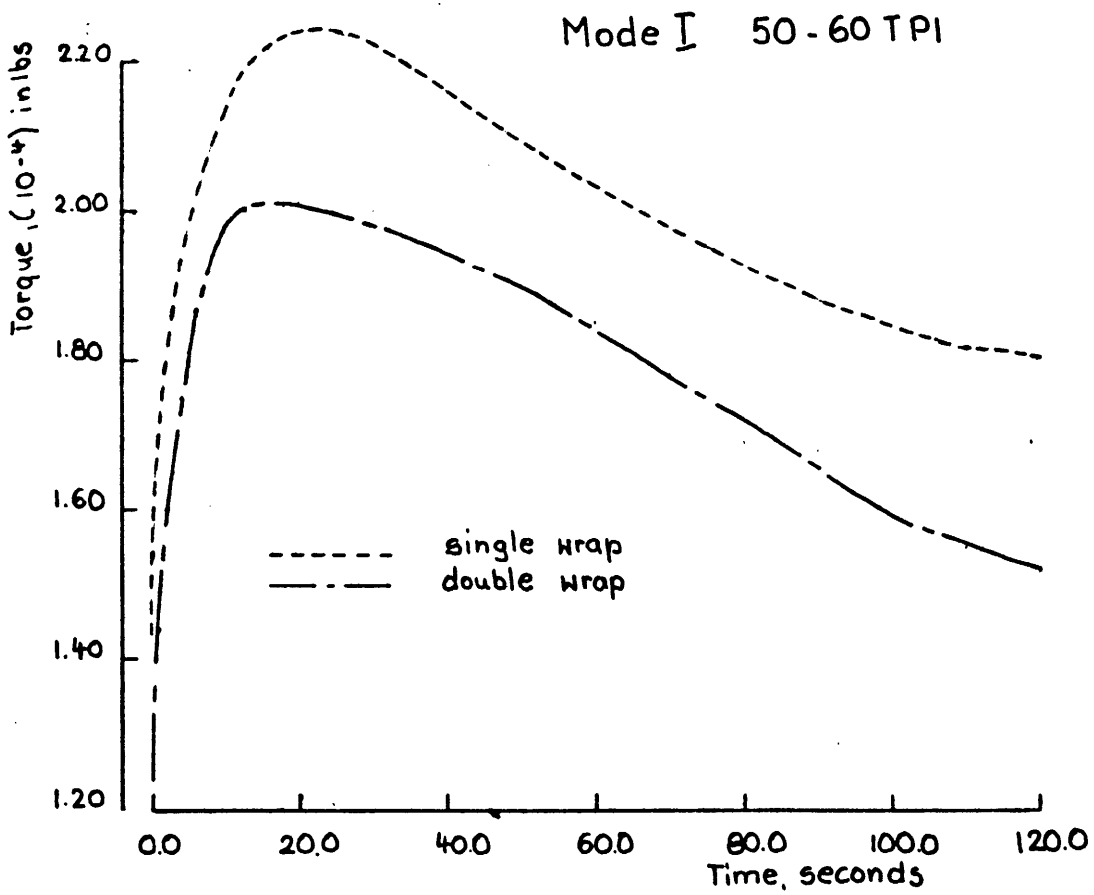
Mode I 50-60 TPI
Torque, (10-4) in lbs
2.20
2.00
1.80
1.60
1.40
1.20
single wrap
double wrap
0.0
20.0
40.0
60.0
80.0
100.0
120.0
Time, seconds

Figure 3.50

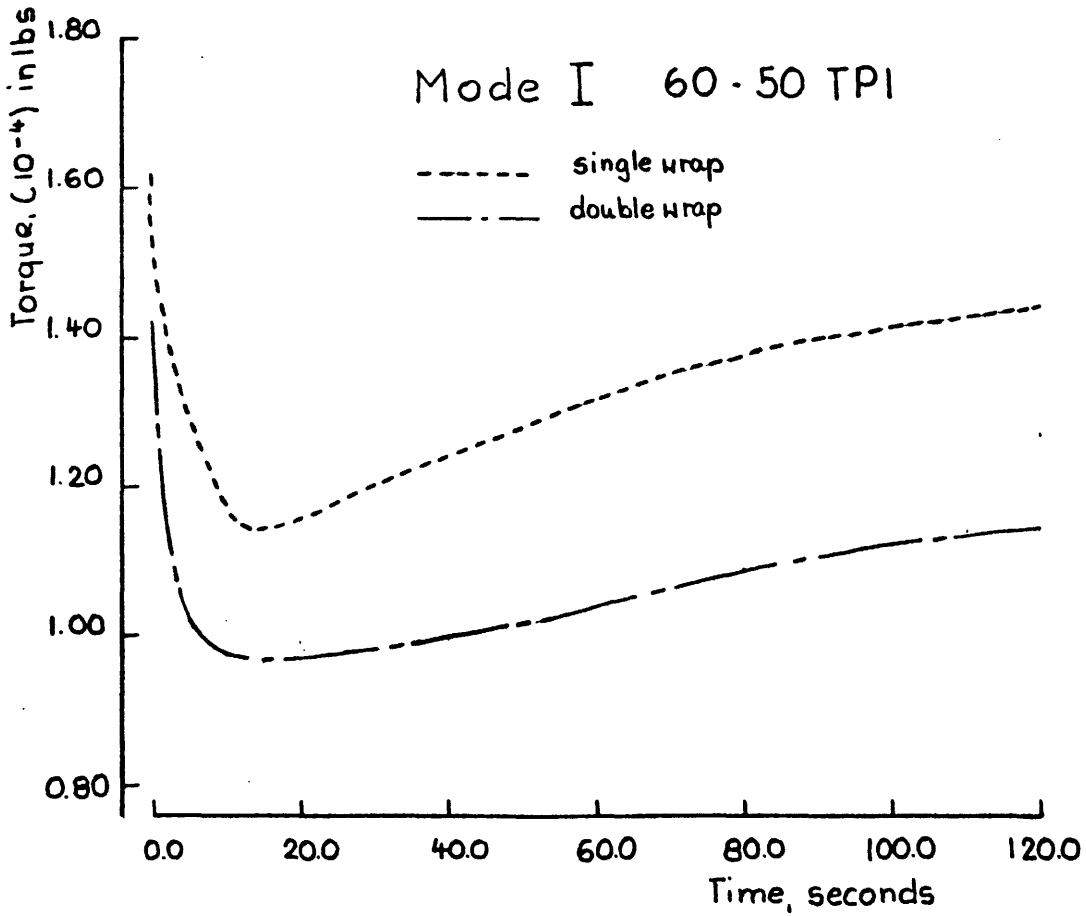
Mode I 60 · 50 TPI
single wrap
double wrap
Torque, (10⁻⁴) in lbs
1.80
1.60
1.40
1.20
1.00
0.80
0.0
20.0
40.0
60.0
80.0
100.0
120.0
Time, seconds

Figure 3.51

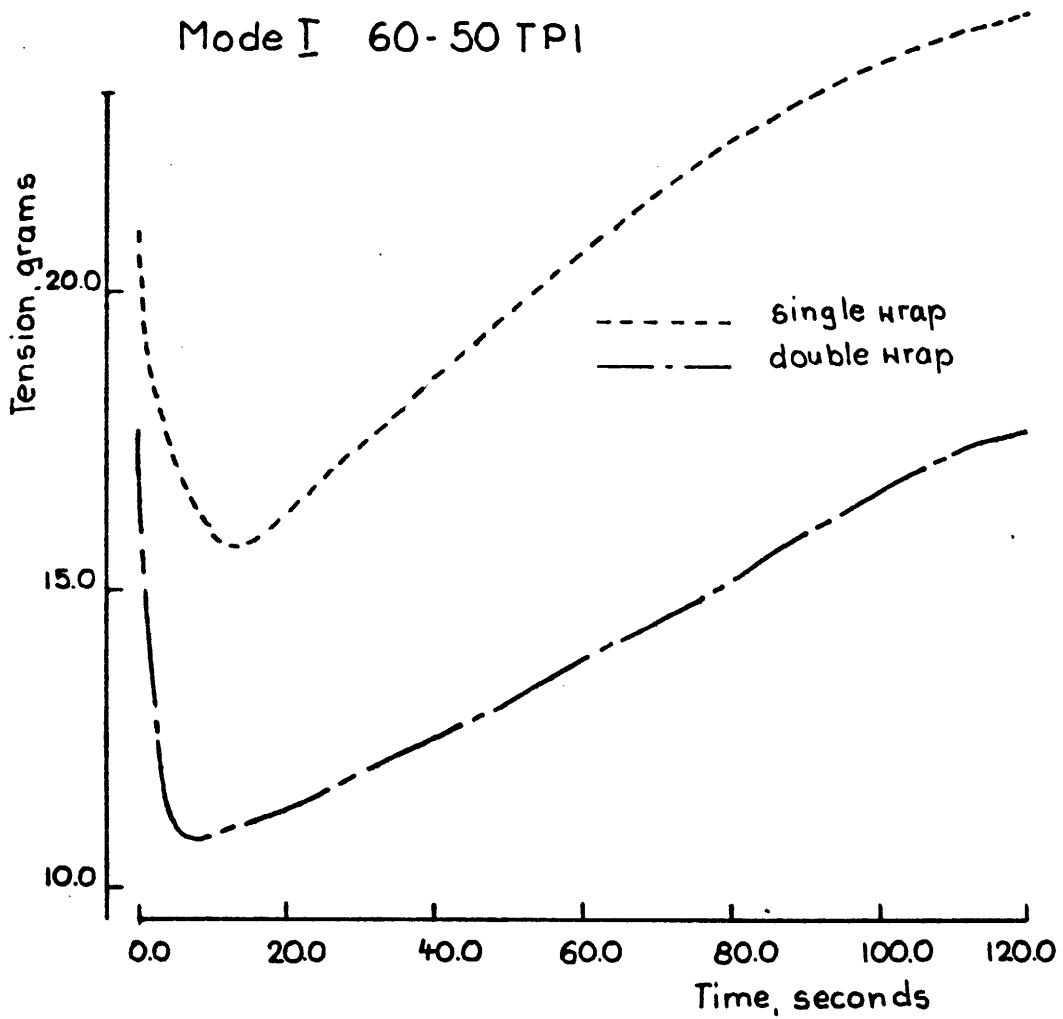
Mode I 60-50 TPI
Tension, grams
20.0
15.0
10.0
single wrap
double wrap
0.0
20.0
40.0
60.0
80.0
100.0
120.0
Time, seconds

Chapter 4

PERIODIC TWIST SLIPPAGE

The translation of spindle rotation into texturing threadline rotation is clearly dependent on friction forces. The generation of these forces is due to the external contact between the yarn and spindle surfaces as well as the internal friction deformation of the yarn as it traverses the spindle[15]. The contact friction forces are dependent on surface conditions (yarn and spindle), threadline tension, and relative velocity between the yarn and spindle[16]; the internal forces are generated by rotation of the yarn in a bent configuration around the pin[15]. Rotation under such flexural conditions will cause cycling of tensile and compressive stresses within the cross section of the yarn which leads to interfiber slippage resulting in energy losses in the yarn due to its viscoelastic behavior and inherent loss modulus. Both of these internal forces act <u>in opposition</u> to the relative motion between the yarn and spindle pin.[15] Thus, internal and external contact activated friction torque join together to balance the combined threadline torque and post spindle torque according to the following relation:

$$M_e + M_i = M_{threadline} + M_{post\ spindle} \qquad (4\text{-}1)$$

where M_e = external contact friction activated torque

M_i = internal friction activated torque

$M_{threadline}$ = texturing zone torque

$M_{post\ spindle}$ = post spindle zone torque

More to the point, the potential internal and external (contact) frictionally activated torque should be equal or exceed the combined threadline torques of equation (4-1).

Yarn-Pin Contact Friction Induced Torque

The standard capstan equation for yarn friction on a capstan is:

$$T_2 = T_1 e^{\mu\theta} \qquad (4\text{-}2)$$

where T_2 = post capstan tension

T_1 = pre capstan tension

μ = coefficient of contact friction between yarn and pin

θ = wrap angle of yarn around pin perimeter

Sasaki and Kuroda[17] show that for textile yarns this simple relation is not entirely accurate and that there is an extra increment of tension resulting from yarn bending. However as a first approximation we will assume that the capstan equation may be used to determine the coefficient of friction between the yarn and spindle.

Experimental work was carried out to determine the values of T_1 and T_2 (pre and post spindle tension) for a range of machine conditions. The yarn tested was the POY PET used for steady state and transient experiments described earlier. The results are listed in Table 4.1.

Table 4.1

THREADLINE TORQUE

MACHINE TWIST TPI	DRAW RATIO	HEATER TEMP.	COEFFICIENT OF FRICTION (YARN-PIN SPINDLE)	EXTERNAL CONTACT SUPPLIED TORQUE (10^{-4}) in lbs	THREADLINE TORQUE (10^{-4}) in lbs
50	1.60	190°C	.069	.90	1.54
60	1.60	190°C	.060	.64	2.40
65	1.60	190°C	.063	.63	2.39
70	1.60	190°C	.062	.58	2.31
80	1.60	190°C	.062	.55	2.23
50	1.60	210°C	.051	.65	1.47
60	1.60	210°C	.071	.78	1.67
65	1.60	210°C	.067	.66	2.34
70	1.60	210°C	.057	.52	2.34
80	1.60	210°C	.037	.30	2.54
50	1.60	230°C	.086	1.17	1.45
60	1.60	230°C	.057	.60	1.58
65	1.60	230°C	.066	.60	2.24
70	1.60	230°C	.055	.48	2.19
80	1.60	230°C	.073	.60	2.19

To determine the yarn-pin friction induced torque, the normal force between the yarn and spindle pin per unit length must be multiplied by the yarn radius and the coefficient of yarn-spindle friction and the product integrated around the full spindle wrap to obtain:

$$M_e = T_{Threadline} R_{yarn}(e^{2\pi\mu}-1) \qquad (4\text{-}3)$$

Applying the measured coefficients of friction given in Table 4.1 to equation (4-3) , we can thus determine yarn-pin frictionally induced torque which acts to rotate the texturing threadline. Table 4.1 lists these externally developed torques and the measured threadline torques.

Comparisons of the values of measured threadline torque and external torque supplied by the spindle shows that the torque thus developed falls short of the threadline torque required for steady state operation. It would appear that the deficit in the required torque is made up by the internal torque developed when the yarn also rotates in the bent state (around its own axis) as it traverses the spindle pin. From the diagram 4.1 (where twist T is plotted against wrap angle θ) it can be seen that there is constant slippage $(T_{machine}-T_\theta)$ over the entire yarn loop on the spindle surface. The difference $(T_{machine}-T_\theta)$ is caused by the untwisting of the yarn as it proceeds on the pin surface. Observations of the twist around the pin indicates that most of the untwisting occurs in the last quadrant of the spindle surface perimeter.[4]

Figure 4.1

TYPICAL TWIST DISTRIBUTIONS ON A PIN-SPINDLE

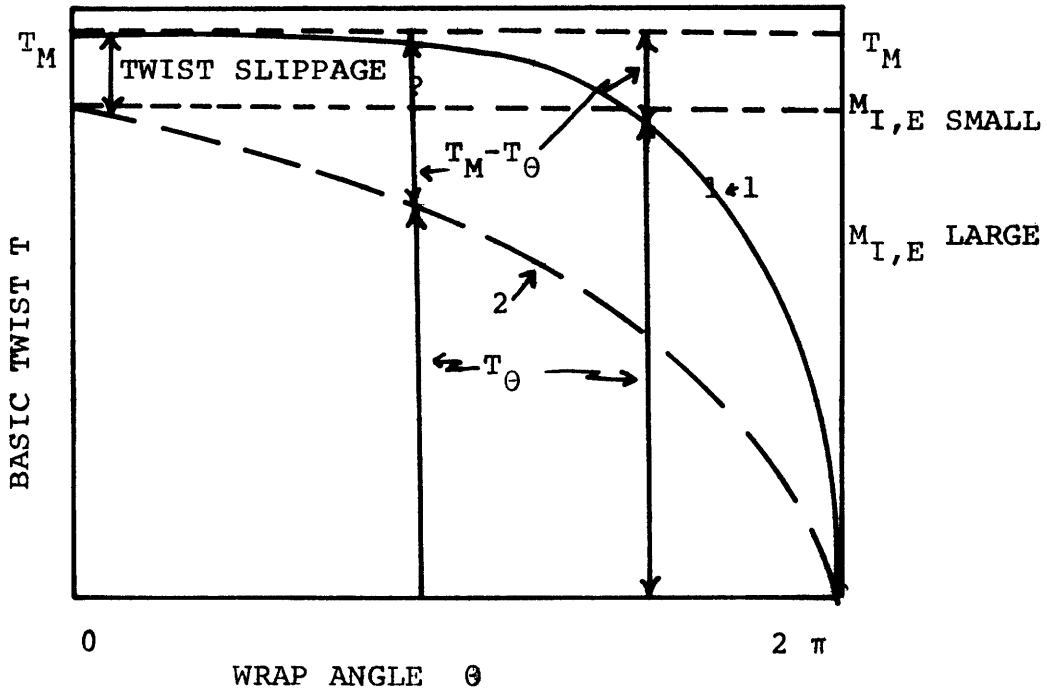

T_M= MACHINE TWIST

T_Θ= TWIST AT WRAP ANGLE Θ

$M_{I,E}$= FRICTION TORQUE (INTERNAL AND EXTERNAL)

1 TWIST DISTRIBUTION

2 TWIST DISTRIBUTION

This condition is shown as Twist Distribution 1. For this case the sum of $M_e + M_i$ would be relatively large. If the sum of $M_e + M_i$ is considerably less than that for Twist Distribution 1 twist can be pictured as Twist Distribution 2 over the spindle surface. The efficiency of this yarn-spindle system is now less than 100%, i.e. the yarn in the cooling zone rotates less than one time for each spindle rotation. During steady state operation with the slippage envisioned for Twist Distribution 2 no real twist will manifest itself in the post spindle region since one pitch length of twisted yarn enters the spindle for each rotation of the cooling yarn segment. This continual rotational slippage need not affect product quality but obviously affects process productivity.

Tight Spots

Rotational slippage at the spindle pin may take place on a steady state basis as has been pointed out. This need not promote product irregularity, only loss in process efficiency. But if rotational slippage takes place periodically or in an irregular manner, an inequality will occur between the time period of twist-pitch translation and the rotation time period of the cooling yarn as it enters the spindle. When this condition occurs, real twist will appear in the post spindle zone.

Real twist can also appear downstream of the spindle without rotational slippage,-- but rather in presence of translational

spurting or acceleration. For this condition also develops an inequality between the period of twist-pitch translation and the period of cooling yarn rotation. Such spurting can cause a tight spot in the existing yarn, i.e. a short yarn segment of high twist amidst long segments of virtually untwisted yarn. The tight(twist) spot prevents local crimp development and causes the appearance of a "pin hole" in the fabric.

A picture of a tight spot is shown in Figure 4.2. This tight spot was formed as a result of the spindle speed being suddenly reduced on the MITEX False Twister after the machine had been operating at steady state. The operating conditions were:

Cold Zone Length	6.00 inches	Machine Draw Ratio 1.60
Heater Length	1.25 inches	Heater Temperature 210°C
Cooling Zone Length	7.00 inches	Yarn 245/30 POY PET
Post Spindle Length	9.00 inches	Machine Twist 60 TPI→50

In the first instant that the spindle speed is reduced, the translational movement of the twist pitch continues as before, and now the rotational period of the pin is greater than the time for the advance of one twist pitch. As a result each turn advanced into the pin is no longer fully untwisted and some real twist starts to build up in the post spindle zone.

TIGHT SPOT

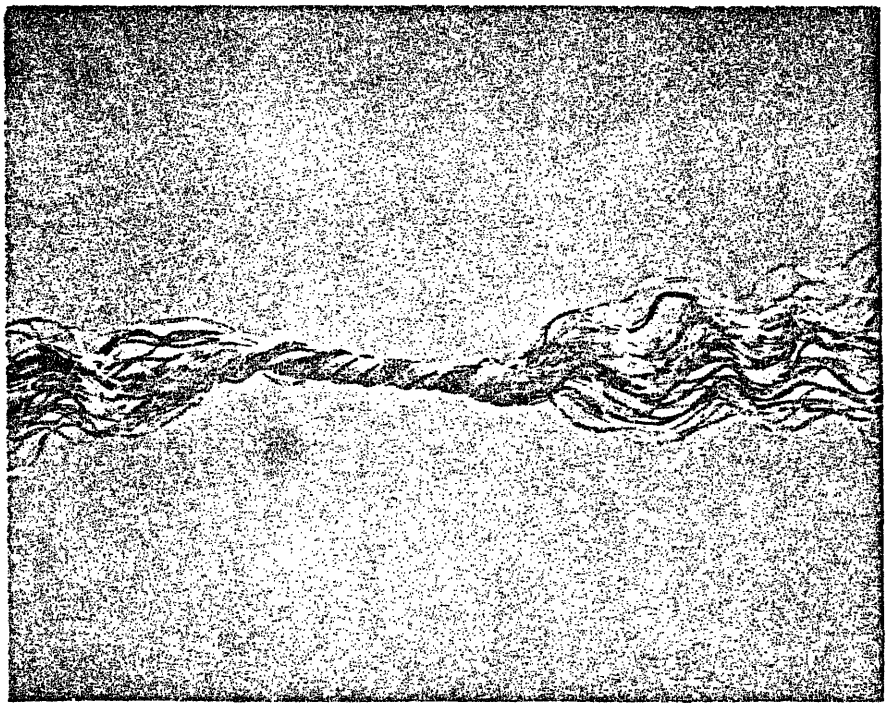

Cold Length	6"
Heater	1.25"
Cooling	7"
Post Spindle	9"
Machine Draw Ratio	1.60"
Heater Temperature	210 ^{o}
Yarn	245/30 POY PET
Spindle Speed	60-50

The reduced rotational speed of the pin results in reduced rotational speed of the cooling zone, and, in turn in a reduced twisting rate at cold and hot entrances. With this step reduction in twisting rate, the threadline tension and torque in the texturing zone drop precipitously. This marked drop in tension upstream of the spindle pin and the slight increase of tension downstream (which is expected because of the real twist occuring in that zone) cause a tension gradient greater than that which can be accommodated by the translational frictional constraint around the pin. Translational spurting will result, carrying segments of high level real twist into the post spindle zone.

This small section of real twist which is of the same sense as the threadline twist does not spread out uniformly in the post spindle zone threadline. Instead it remains concentrated and can easily be observed.

The persistence of this concentration of real twist lies in the nature of the torsional behavior of the texturing threadline. As steady state, the texturing threadline is entirely untwisted as it leaves the spindle and enters the post spindle zone at a small negative torque,(see level C in Figure 4.3). If for any reason, translational spurting takes place in the threadline moving about the spindle pin or sudden rotational slippage takes place,a yarn segment with real twist

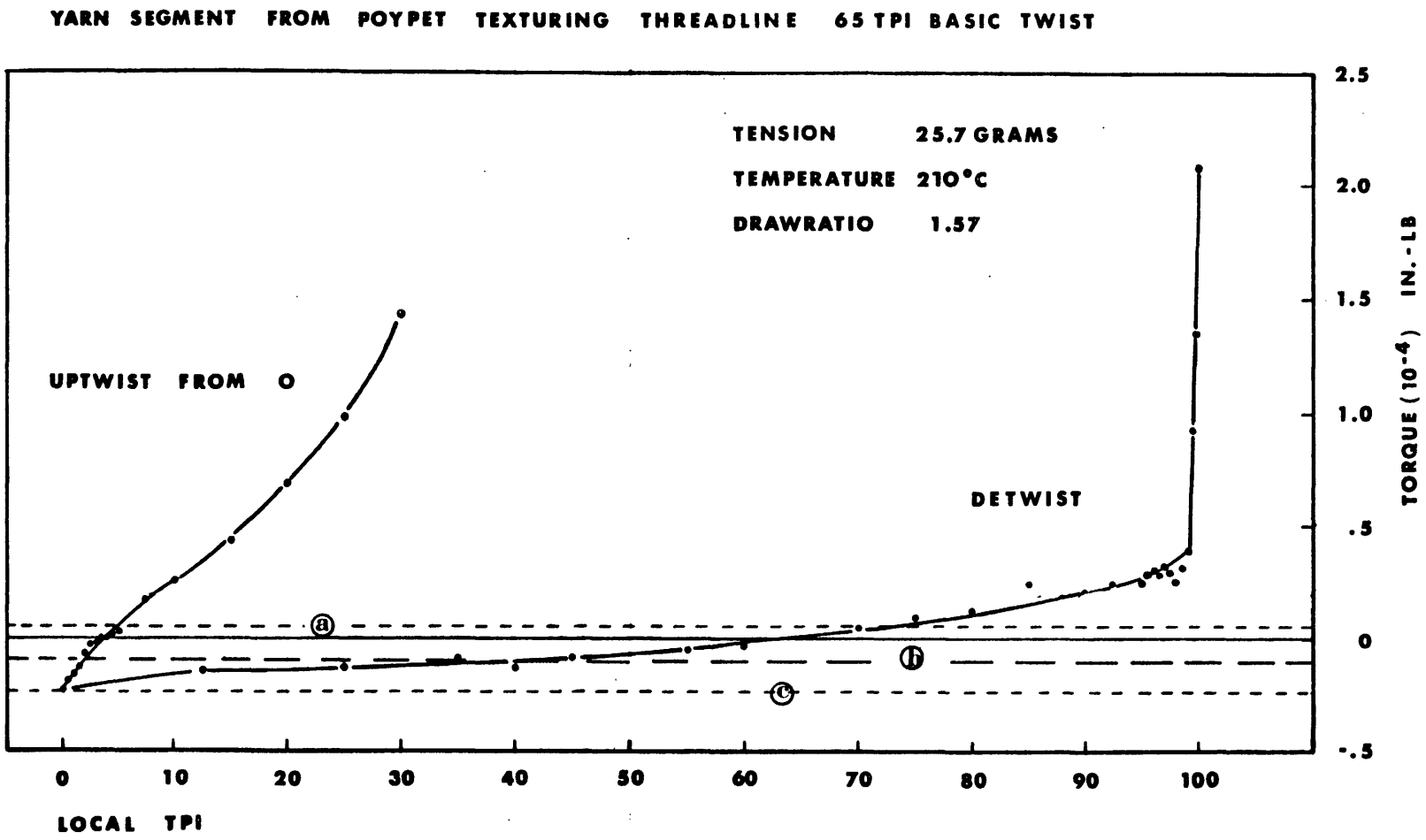
YARN SEGMENT FROM POYPET TEXTURING THREADLINE 65 TPI BASIC TWIST
TENSION 25.7 GRAMS
TEMPERATURE 210°C
DRAWRATIO 1.57
UPTWIST FROM O
DETWIST
TORQUE (10^{-4}) IN.-LB
2.5
2.0
1.5
1.0
.5
0
-.5
0
10
20
30
40
50
60
70
80
90
100
LOCAL TPI

Figure 4.3

at torque level A will enter the post spindle zone. Untwisted yarn further downstream in the post spindle zone at torque level C will then uptwist slightly and the tight spot will downtwist further until the torque in both segments are equal at level B where the twist level in the tight spot is observed to be 50 TPI (about half the threadline twist). The persistence of the tight spot in the post spindle zone is thus attributable to the presence of two different mechancially connected portions of threadline having equal torque but entirely unequal twist geometry.

When the spindle speed is suddenly increased after the process is operating at steady state, real twist of opposite sense to that of the threadline twist appears in the post spindle threadline, spread out uniformly and no tight spots are observed.

Observation of transient texturing zone tension during twist increases reflects marked increase in pre-spindle tension and slight increase in post spindle tension. This condition precludes translational spurting and hence the appearance of segments of concentrated twist.

Continual Occurrence of Tight Spots Along with Threadline Tension and Torque Oscillation

For steady state operation in draw texturing, the torque equality of equation (4.1) obtains. If for some reason the torque generating capacity of the yarn-pin system suddenly fails or if the torque requirement of the texturing threadline suddenly increases, then rotational slippage will occur over the entire contact perimeter of the pin. As a result the rotational speed of the cooling zone will drop precipitously and following this, the threadline tension and torque will rapidly decline as was seen in Section 3.4. Translational surging and the appearance of tight spots may accompany this drop in texturing tension.

When sudden reduction in rotational velocity of the cooling threadline occurs as a result of a stepwise reduction in spindle speed the tensile and torque drop observed will recover after a period of time due to propagation of the new twist level through the machine (and elimination of the effect of transient twist contraction). In the case at hand the tension and torque decline may be checked for other reasons, e.g. because of re-establishment of the torque generating capacity of the yarn-pin system so as to satisfy equation (4.1).

The component of torque generation at the pin which is due to yarn-pin frictional contact can be shown to depend approximately on the level of threadline tension according to

Figure 4.4

PREDICTED THREADLINE TORQUE AND TENSION CYCLING

MACHINE LENGTH 23.25 " THROUGHPUT SPEED .4704 "/sec

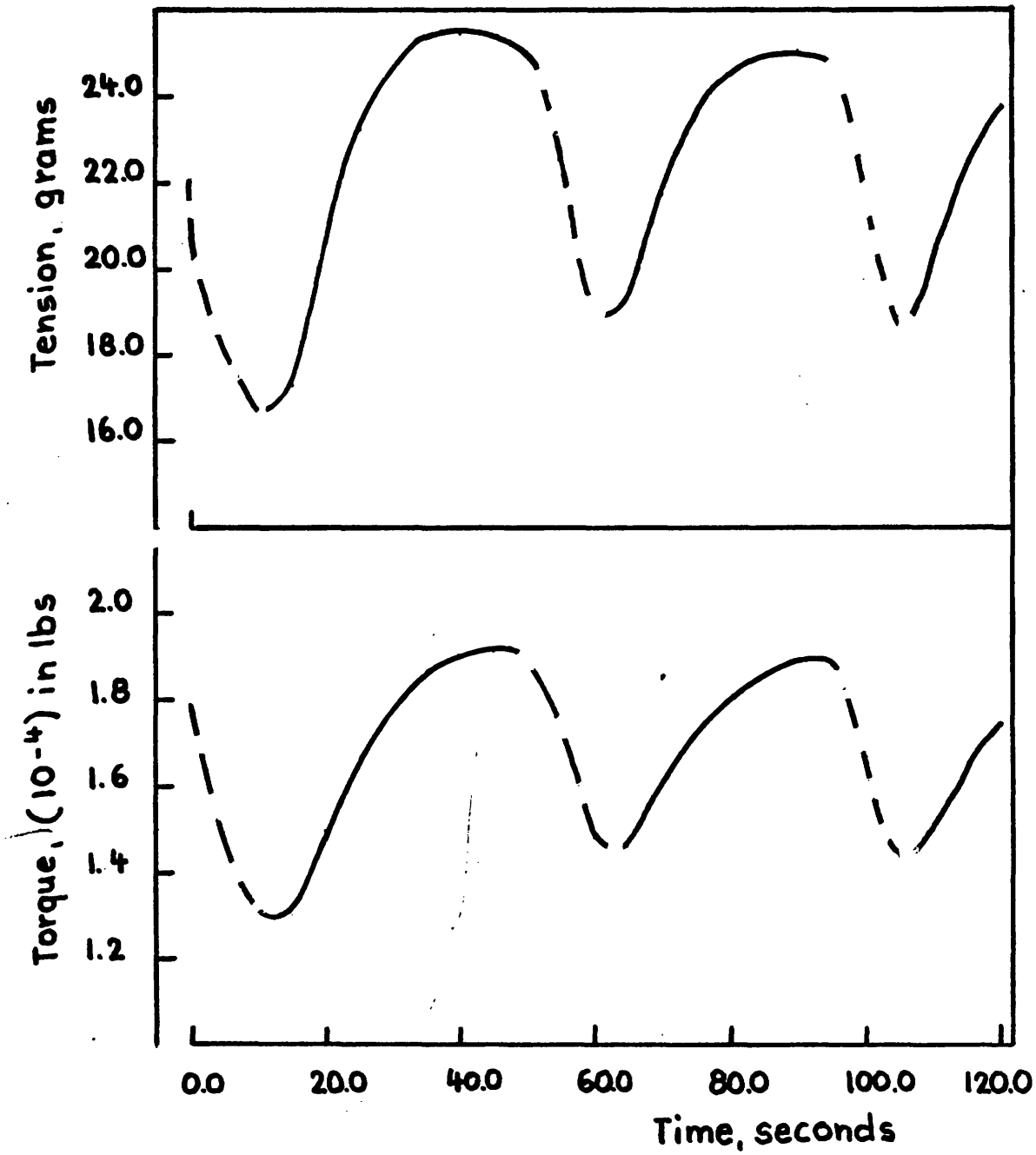

equation (4.3). Likewise one can show that the internally generated torque in a yarn which is rotated in a bent configuration (around the pin) will depend on the level of threadline tension. Thus the sum of components of torque generation at the pin can be related to texturing tension.

For rotational slippage to persist, the total torque generated at the pin must be less than the torque required for non-slip texturing. Or conversely, if the texturing line torque falls below the yarn-pin generated torque, slippage will cease.

Figure 4.4 shows the reduction in line tension and torque which occurs in dotted lines as a result of an initial (unspecified) rotational slippage. The tension value of Figure 4.4 calculated from our transient analysis is used to calculate a generated torque by multiplying by a constant (corresponding to the steady ratio of torque to tension). The indicated torque value in Figure 4.4 is also calculated from our transient analysis. The system is forced to bottom out when the above calculated transient torque falls below the generated torque. At this instant the slippage ceases and the rotational speed of the cooling zone assumes the speed of the spindle. This is now equivalent to a step increase in cooling zone rotational speed and yarn tension and torque will rise accordingly as calculated from the transient analysis and plotted in solid lines in Figure 4.4.

The increasing tension value, will according to the transient analysis, overshoot its steady state value, even while the torque is still rising. Here again we find a situation when the total yarn pin generated torque falls below the instant threadline torque and the onset of rotational slippage at the pin occurs, -- again being designated in Figure 4.4 by the dotted lines. This type of cycling will persist so long as the material and machine parameters are set so as to enhance system sensitivity to cycling. Experience has shown that system sensitivity to cycling is suppressed by proper choice of yarn lubricant and by increasing the ratio of post spindle tension to pre-spindle tension.

Finally it should be pointed out that the internally generated torque in a bent, rotating yarn, will depend on twist level as well as on tension, the lower the twist the greater the internal fiber slippage hence the greater the torque generated. This dependence suggests that twist changes occuring at the heater entrance because of changing threadline rotational speeds will affect internal frictional torque generation once the twist change reaches the spindle pin.

Chapter 5

CONCLUSIONS AND SUMMARY

Steady State Operation of the Draw Texturing Process

During steady state operation of the draw texturing process there are essentially two levels of twist in the threadline between the feed rollers and spindle. In one segment of the threadline (over the heater and beyond) the twist level is determined simply by the spindle speed and the yarn throughput speed. Upstream of this segment lies the threadline cold zone where the twist level is somewhat less. In absence of frictional contact between yarn and heater threadline tension and torque will be constant from position to position between the feedrolls and the spindle. The introduction of twist takes place in essence, at two zones in the system: at the entrance to the cold zone and at the entrance to the hot zone. The equality of tension and torque at these zones suggests that their local twist levels will be inversely proportional to their effective torsional rigidities and this is what we predict analytically and observe experimentally. The torsional resistance at the entry to the cold zone is seen to depend on fiber bending and torsional rigidity as well as on filament tension; at the heater entry, the bending and torsional stresses are thermally relaxed with only the tensile component of yarn torsional rigidity remaining. Thus the twist level in the hot

zone far exceeds that of the cold zone. The threadline tension is developed as an aggregate of the filament tensile components along the yarn axis. The threadline torque is developed as an aggregate of the components of filament bending moments and twisting moments, to the degree that they exist, and of the moments due to filament tension. The prediction of threadline tension and torque therefore requires the determination of the filament-system constitutive relations, the local yarn geometry, and the system compatibility at the entrance to the cold and hot zones. Our analysis predicts that as the operating level of machine twist is increased, with machine draw ratio and heater temperature kept constant, threadline tension decreases, while threadline torque increases. This seemingly contrary behavior can be attributed to the increase in local filament helix angles in outer layers of the yarn, which reduces the yarn axial component of filament tension and increases the circumferential component. As the twist increases, the variation of draw ratios in different filament layers in the yarn drawing neck also increases. It is predicted that the temperature of the heater (over the range of interest) should not affect threadline behavior significantly. This follows from the fact that over the range of common texturing conditions, temperatures have minimal effect on (hot) drawing forces.

Lastly it is predicted that if the cold filament bending

rigidity or torsional rigidity is increased, both threadline torque and tension will increase while cold zone twist level will decrease. Hot zone twist should remain unchanged since this twist level is indicated to be a function solely of yarn throughput speed and spindle speed.

Numerous experiments were conducted on DuPont POY polyester yarns for the purpose of comparing measured values of threadline parameters, i.e. threadline tension, torque and twist levels with predicted results during steady state operation of the draw texturing process. The agreement between predicted and measured values is within 9.3% for tension, 12.2% for torque, 12.3% for hot twist and 10.9% for cold twist.

Transient Operation of the Draw Texturing Process

It has been observed during texturing that when spindle speeds are suddenly altered, the first signs of twist change in the threadline occur at the cold zone entrance and at the heater. These observations provided the basis for the hypothesis that torsional rigidity of the texturing threadline is significantly lower at the cold zone entrance and heater than for the rest of the threadline existing between the feed rollers and spindle. Torsional disturbances in the threadline are evidenced primarily as twist changes at the 'soft' zones and these changes then propagate downstream with yarn movement.

Thus, the formation rigidities of the texturing threadline essentially reflect the rigidity of the soft forming zones under the conditions of local twist insertion. On the other hand, the transient twist response of cold zone and cooling zone segments to incremental changes in spindle speed reflects the very high incremental torsional rigidity of these threadline segments.

To test these hypotheses we have measured the torsional rigidity of cold and cooling zone yarn segments and these were seen to be several orders of magnitude greater than the cold forming 'rigidity' and the hot uptwisting 'rigidity'. One can attribute these rigidity differences to the variation in twisting deformation modes at each of the soft zones and in segments which lie downstream of these zones.

Observations of dynamic twist formation in larger models indicate that many filaments approaching the twist triangle apex are already twisted around their axes and sometimes around neighboring pairs.[13] They are then wound onto the newly formed end of the yarn, with little additional twisting observed thereafter. After the twist is inserted at the cold zone entrance, interfilament friction and transverse stresses cause the yarn to behave like a helically anisotropic solid rod with subsequent high torsional rigidity.

The situation at the uptwist zone at the heater involves sudden stress relaxation or softening of the filaments. The requirement of constant threadline torque in the presence of this stress relaxation results in a cranking up of twist at the heater. As the new hot twist level is reached lateral forces due to filament tensions and local curvatures will also reach a new high level. This increased interfilament pressure accompanied by thermal softening will result in lateral compressive creep and in growth in contact areas between filaments.[9] Higher friction and interfilament shear stresses will then result in higher incremental torsional rigidities.

In our analysis of transient operation of the draw texturing process we have considered the response of the threadline to torsional disturbances, i.e. to changes in spindle speed. We reason that transient operation generates material build-

ups and twist buildups with respect to time in different zones of the texturing system and 'bookkeeping' of these buildups must be based on how the buildups distribute within each zone of the threadline. Further, the material and turn balances for each zone are coupled with the requirement of threadline tension and threadline torque uniformity throughout the texturing zone.

The transient analysis predicts that if the spindle speed is increased stepwise the threadline torque responds by rising sharply with time and then slowly settling to a new value higher than the steady state value before the spindle speed was increased while the threadline tension increases sharply and then settles to a value which was less than the previous value. Correspondingly, if the spindle speed is decreased stepwise the threadline tension and torque should decrease precipitously before the threadline tension settles to a new value, higher than the previous value while the torque settles to a new value, lower than the previous value. Under certain conditions, this type of transient threadline response increases the prospect of threadline tension and torque cycling. For example if rotational slippage of the yarn on the spindle occurs the system reacts as if there were a step change in spindle speed, and recurrence of such slippage will lead to tension, torque and twist cycling in a texturing process nominally operating at steady state.

Numerous experiments were conducted using Du Pont POY polyester yarns for the purpose of comparing measured values of threadline paramenters, i.e. threadline tension, torque, and twist levels with predicted results during transient operation of the draw texturing process. We used Analytical Model 2(tilted twist distribution) and the agreement with respect to time response and absolute levels of threadline parameters was good. Additional experiments were conducted using Du Pont POY nylon yarns to reinforce our confidence in the utility of the analysis of texturing threadline behavior. There was a persistent 10% difference in the predicted and measured values of threadline tension and threadline torque. However the predicted and measured time response of the system was indeed favorable.

Chapter 6

SUGGESTIONS FOR CONTINUING RESEARCH

A number of suggestions for continuing research are presented below. The experimental results and mathematical analyses here presented should provide the direction for continuing research in this rapidly developing segment of industrial technology.

1. Characterization of the Torsional Rigidity of Threadline Segments Over the Heater : The torsional rigidity of yarn segments taken from the cold zone and cooling zone has been determined. Likewise, we have determined the "formation rigidity" of yarn segments at the cold zone entrance and the hot zone entrance. Further, we reasoned that the yarn over the entire heater acts as a soft zone since observation of transient twist over the heater did not indicate any change in its distribution with time. With the use of very short heaters in our experimental machine, the spreading of the "soft zone" over the heater does not disturb the physics of the situation unduly. But further understanding of this important distribution is necessary because of the significantly longer heater lengths which are used in commercial machines and because of the difference in heat transfer characteristics.

2. Effect of Sinusoidally Imposed Machine Disturbances on Threadline Response: Our experiments conducted to study transient operation of draw texturing processes utilized step changes in spindle speeds to disturb the texturing system. More realistic to commercial application would be a sinusoidal machine disturbance such as could be implemented by use of programmable drive motors designed to deliver shaft speeds which vary with time. Results from such experiments could then be compared with the transient results predicted in our analysis.

3. Tension Ratio Over the Spindle During Transient Operation: As a basis for understanding the nature of twist slippage past the spindle it is important that threadline tensions before and after the spindle be measured simultaneously with spurting of the threadline. The pattern of changing tension gradients could then be compared with the lengthwise distribution of tight spots along the threadline.

4. Twist Geometry Around the Spindle Pin: It has been proposed that whenever there is a sudden increase in the in the tension gradient around the spindle pin, a threadline translational surge takes place, accompanied by a tensile jerk upstream of the spindle. This tension increase acting on the yarn in the hot zone causes a proportional increase in line torque. The latter is accompanied by a twist increase

at the cold formation zone in order to keep threadline torque uniform in the texturing zone. Such a sudden twist increase can cause local buckling which may persist in the threadline. Upon traversing the spindle pin surface such a local buckle might cause another translation surge which would result in still another buckling, etc. Photographic study is necessary to confirm this behavior.

BIBLIOGRAPHY

1. Mey, W., Annual Conference of the Textile Institute, Baden-Baden, 1966.
2. Thwaites, J.J., Linear Density Variations in Draw Textured Yarns, J. Textile Institute, 65, 1974, P. 353.
3. Quynn, R.G., Pre-Oriented Polyester as a Feed Yarn for Simultaneous Draw Texturing, Textile Research Journal, 45, 1975, P.88.
4. Backer, S. and Yang, W.L., Mechanics of Texturing Thermoplastic Yarns, Part I: Experimental Observations of Steady State Texturing, Textile Research Journal, (in press).
5. Platt, M.M., Klein, W.G., Hamburger, W.J., Torque Development in Yarn Systems: Singles Yarn, Textile Research Journal, 28, 1958, P.1.
6. Naar, R.Z., Steady State Mechanics of the False Twist Yarn Texturing Process, Sc. D. Thesis, Department of Mechanical Engineering, M.I.T., Cambridge, Massachusetts, 1975.
7. Morton, W.E., The Arrangement of Fibers in Singles Yarns, Textile Research Journal, 26, P. 235.
8. Hearle, J.W.S., Form and Fiber Arrangement in Twisted Yarns, Chapter 3 in Hearle, J.W.S., Grosberg, P., and Backer, S., Structural Mechanics of Fibers, Yarns, and Fabrics, Volume I, Wiley-Interscience, New York, 1969.

9. Brookstein, D.S., On the Mechanics of Draw Texturing, M.S. Thesis, Department of Mechanical Engineering, M.I.T., Cambridge, Massachusetts, 1973.

10. Shealy, O.L., and Kitson, R.E., An Age-Stable Feed Yarn for Draw Texturing, Textile Research Journal, 45, 1975, P. 112.

11. Ward, I.M., Mechanical Properties of Solid Polymers, Wiley-Interscience, New York, 1971, P. 245.

12. Backer, S., and Yang, W.L., Mechanics of Texturing Thermoplastic Yarns, Part II: Experimental Observations of Transient Behavior, Textile Research Journal, (in press)

13. El-Shiekh, A, H., On the Mechanics of Twist Insertion, Sc. D. Thesis, Department of Mechanical Engineering, M.I.T., Cambridge, Massachusetts, 1965.

14. Thwaites, J.J., Mechanics of Texturing Thermoplastic Yarns, Part IV: The Origin and Significance of the Torsional Behavior of the False Twist Threadline, Textile Research Journal, (in press).

15. Ostertag, C., Trummer, A., Theoretical Analysis of the Influence of Internal Yarn Friction on the Twist in False Twisting, Symposium on Man Made Fiber Technology, Part II, 70 th National Meeting, American Institute of Chemical Engineers, 1971.

16. Olsen, J.S., Frictional Behavior of Textile Yarns, Textile Research Journal, 39, 1969, P. 31.

17. Sasaki, T., and Kuroda, K., Additional Tension Caused by Bending of a Yarn on a Slender Cylinder, J. Textile Machinery Society of Japan, 20, No.2 (English Edition) 1974, P.30.

APPENDIX 1

INERTIA EFFECTS ON THREADLINE

TRANSLATIONAL MOMENTUM FORCE

DV^2 where D = Yarn Denier

V = Translational Velocity of Yarn

For the yarns processed (70 to 250 denier) at speeds up to 1 inch per second the translational momentum force is 1.23×10^{-8} GPD compared to .1 GPD tensions.

ROTATIONAL MOMENTUM FORCE

$I\omega^2$ where I= Polar Moment of Inertia

ω= Angular Velocity of Yarn

For the yarns processed (70 to 250 denier) at angular speeds up to 250 radians per second the angular momentum torque is 1.12×10^{-9} in lbs compared to typical threadline torques of 1.0×10^{-4} in lbs.

APPENDIX 2

EXPERIMENTAL VALUES OF THREADLINE TENSION AND TORQUE

(each data point represents the average
of at least 20 points)

EXPERIMENTAL THREADLINE TENSION AND TORQUE

190°C 1.57 DR

Basic Twist	50 TPI	60 TPI	65 TPI	70 TPI	80 TPI
Tension, grams Texturing Zone	20.5	16.6	15.3	13.6	11.4
Tension, grams Post Spindle	48.8	31.7	34.4	30.3	28.8
Torque 10^{-4} in lbs Prespindle	1.09	2.09	2.38	2.25	2.31
Tension Ratio	2.38	1.91	2.25	2.23	2.53

190°C 1.60 DR

Basic Twist	50 TPI	60 TPI	65 TPI	70 TPI	80 TPI
Tension, grams Texturing Zone	24.4	20.5	18.7	17.7	16.9
Tension, grams Post Spindle	37.5	29.9	27.9	26.2	25.0
Torque, 10^{-4} in lbs Prespindle	1.54	2.40	2.39	2.31	2.23
Tension Ratio	1.54	1.46	1.49	1.48	1.48

EXPERIMENTAL THREADLINE TENSION AND TORQUE

230°C 1.57 DR

Basic Twist	50 TPI	60 TPI	65 TPI	70 TPI	80 TPI
Tension, grams Texturing Zone	23.7	17.0	16.1	15.3	13.8
Tension, grams Post Spindle	39.2	28.4	27.6	27.5	28
Torque, 10^{-4} in lbs Prespindle	1.03	2.16	2.19	2.15	2.11
Tension Ratio	1.65	1.67	1.71	1.80	2.03

230°C 1.60 DR

Basic Twist	50 TPI	60 TPI	65 TPI	70 TPI	80 TPI
Tension, grams Texturing Zone	23.8	20.5	17.5	17.2	15.0
Tension, grams Post Spindle	41.0	29.5	26.5	24.3	23.7
Torque, 10^{-4} in lbs Prespindle	1.45	1.58	2.24	2.19	2.19
Tension Ratio	1.72	1.43	1.51	1.41	1.58

EXPERIMENTAL THREADLINE TENSION AND TORQUE

210°C 1.57 DR

Basic Twist	50 TPI	60 TPI	65 TPI	70 TPI	80 TPI
Tension, grams Texturing Zone	19.6	17.7	16.7	14.6	11.7
Tension, grams Post Spindle	42.7	34.3	31.7	32.5	29.6
Torque, 10^{-4} in lbs Prespindle	1.66	2.34	2.36	2.16	2.22
Tension Ratio	2.18	1.94	1.90	2.23	2.53

210°C 1.64 DR

Basic Twist	50 TPI	60 TPI	65 TPI	70 TPI	80 TPI
Tension, grams Texturing Zone	27.0	22.6	20.4	18.9	18.3
Tension, grams Post Spindle	54.9	42.7	36.4	35.6	36.7
Torque, 10^{-4} in lbs Prespindle	1.26	2.38	2.48	2.46	2.46
Tension Ratio	2.03	1.89	1.78	1.88	2.01

APPENDIX 3

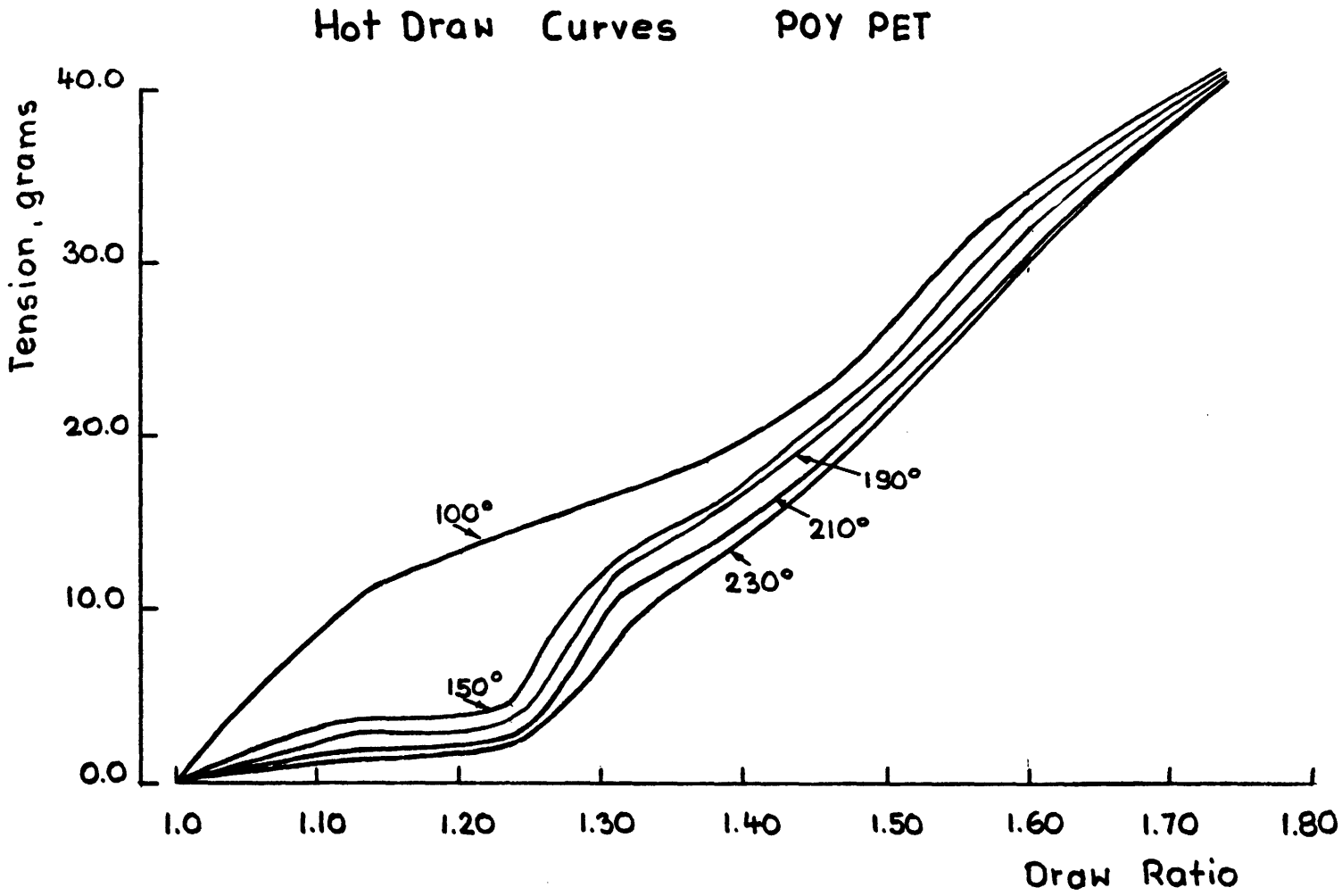
Hot Draw Curves POY PET
Tension, grams
40.0
30.0
20.0
10.0
0.0
100°
150°
190°
210°
230°
1.0
1.10
1.20
1.30
1.40
1.50
1.60
1.70
1.80
Draw Ratio

APPENDIX 4

MITEX TORQUE- TENSION METER

Threadline torque and threadline tension are measured on-line during texturing by the MITEX Torque-Tension Meter(IDR Needham, MA.). The meter sensitivity is on the order of 1 millivolt output per gram of threadline tension and 1 millivolt per 1 x 10^{-6} in lbs of threadline torque.

The principles of operation are as follows. Untwisted feeder yarn which is to be textured enters the device and is wrapped ninety degrees around a near frictionless pulley. The yarn line of action upstream of action is directed through the center of a flexural pivot (pivot A). This pivot twists a calibrated amount when threadline tension imposes a net torque on it. After the yarn travels past the pulley it proceeds through the threadline torque pivot and is then wrapped around a smooth shaft (360°) which traps twist from the texturing threadline and prevents it from bleeding past the defined cold zone entrance. Threadline torque twists the torque pivot(pivot B) a calibrated amount proportional to the threadline torque.

The displacement angle of the torque pivot and the tension pivot is detected by metal flags connected to these pivots which are part of variable push-pull capacitor systems.

MITEX TORQUE TENSION METER

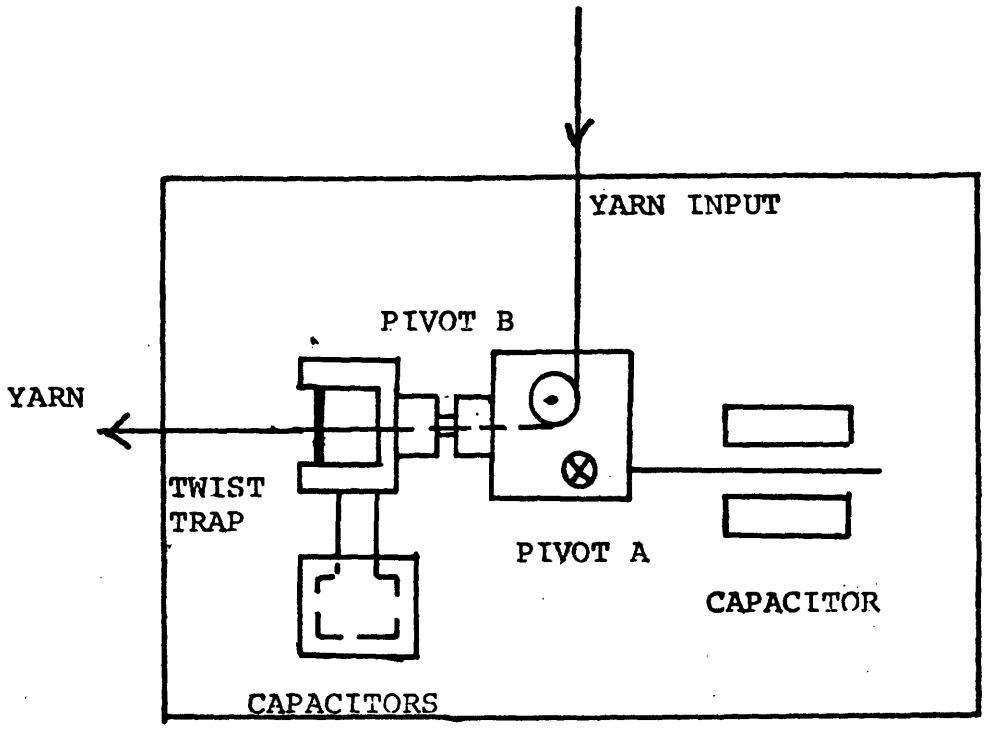

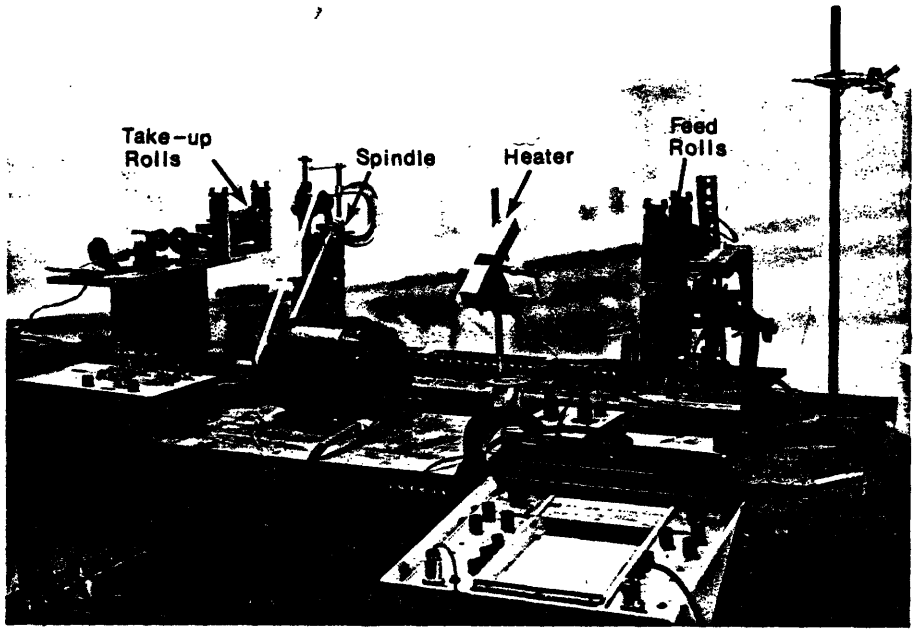

Laboratory False Twist Machine

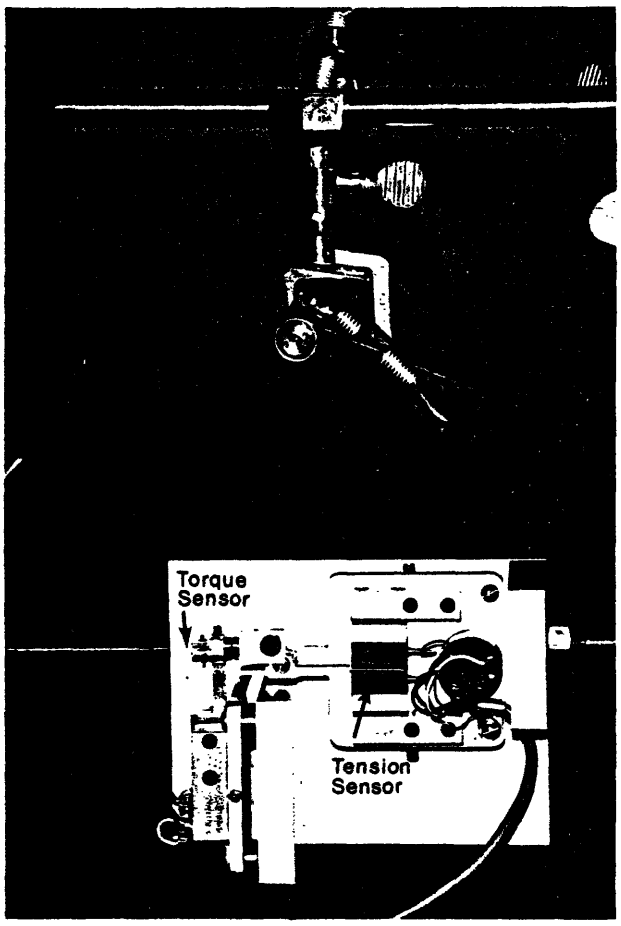

Torque-Tension Meter

APPENDIX 5

COMPUTER PROGRAM FOR STEADY STATE ANALYSIS

```
USER=BROOKS  235  71473     JOINT COMP TER FACILITY, MIT

C      ********** **********************************************
C      **********************************************************
C      THIS MODEL DETERMINES THE STEADY STATE LEVELS OF TWIST,TENSION,
C      AND TORQUE IN THE DRAW TEXTURING THREADLINE
C      **********************************************************
C      **********************************************************
       TEMP=210.
       A=1.E15
       B=1.6E4
       COLTW=5.
       RV=2.16E-3
       V4=1.2E6
       SPIN=40.
       WRITE(5,1212)TEMP,V4,SPIN
       CALL VARN(COLTW,SPIN,V4,A,B,FV)
       SPIN=50.
       WRITE(5,1212)TEMP,V4,SPIN
       CALL VARN(COLTW,SPIN,V4,A,B,FV)
       SPIN=60.
       WRITE(5,1212)TEMP,V4,SPIN
 1212  FORMAT(' HEATER TEMP=',F10.1,'DRAW RATIO=',F10.1,' BASIC TWIST=',F
      $10.1)
       CALL VARN(COLTW,SPIN,V4,A,B,FV)
       SPIN=70.
       WRITE(5,1212)TEMP,V4,SPIN
       CALL VARN(COLTW,SPIN,V4,A,B,FV)
       CALL EXIT
       END
```

```
USER=PROKOP 239 71373     JOINT COMPUTER FACILITY, MIT

      SUBROUTINE YARN(COLTW,SPIN,V4,A,E,RY)
      AN=90.
      C=56.6
      RETL=3.785E-4
      EI=4.466E-9
      ECOLD=2681.0.
      BK=4.74E-9
      AK1=1.0946
      V1=1.0
      AK=AK1
      AK2=AK*AK
      PI=3.14159
      RY2=RY*RY
      R3=RY
      R2=.6667*RY
      R1=.33333*RY
      PH=8.0*PI*SPIN/(4.6-4.0*PI*PI*SPIN*SPIN*RY2)
      ALP3=SQRT(1.0+PH*PH*R3*R3)
      ALP3X=ALP3*ALP3*ALP3
      ALP2=SQRT(1.0+PH*PH*R2*R2)
      ALP1=SQRT(1.0+PH*PH*R1*R1)
      ALP2X=ALP2*ALP2*ALP2
      ALP1X=ALP1*ALP1*ALP1
      V3=V4/(.5*(1.0+ALP3))
      PH2=PH*PH
      TT=0.0
      COTW=COLTW
1     COTW=COTW+.1
      TT=TT+1.
      PC=COTW*PI*2.0
      BET1=SQRT(1.0+AK*AK*PC*PC*R1*R1)
      BET2=SQRT(1.0+AK*AK*PC*PC*R2*R2)
      BET3=SQRT(1.0+AK*AK*PC*PC*R3*R3)
```

```
      BET1X=BET1*BET1*BET1
      BET2X=BET2*BET2*BET2
      BET3X=BET3*BET3*BET3
      PCKR2=PC*PC*AK*AK*RV2
      PCR3=PC*RV*AK
      PCR2=PC*PC
      SP1=SQRT(1.+PC/R2)
      SECAV=.5*(SP1+ALOG(PCR+SP1)/PCR)
      DK1=4.64**PI*FCOLD*RFIL*RFIL*(11./BET3+12./BET2+6./BET1)
      DJ1=DK1*SECAV
      DJ2=DK1
      DK3=(V3*V3)*(ALP3*ALP3/(BET3*BET3))*A
      DK5=(V3*V3)*(ALP2*ALP2/(BET2*BET2))*A
      DK7=(V3*V3)*(ALP1*ALP1/(BET1*BET1))*A
      DK9=A*V3*V3
      DK4=B*V3*V3*V3*(ALP3X/BET3X)
      DK6=B*V3*V3*V3*(ALP2X/BET2X)
      DK8=B*V3*V3*V3*(ALP1X/BET1X)
      DK10=D*V3*V3*V3
      DJ3=14.*DK3/ALP3
      DJ4=14.*DK4/ALP3
      DJ5=9.*DK5/ALP2
      DJ6=9.*DK6/ALP2
      DJ7=6.*DK7/ALP1
      DJ8=6.*DK8/ALP1
      DJ9=DK9
      DJ10=DK10
      DL1=DJ3+DJ5+DJ7+DJ9
      DL2=DJ4+DJ6+DJ8+DJ10
      DAFQ=-DJ2/DJ1
      DCFQ=-DL1/DJ1
      DDFQ=-DL2/DJ1
      FQ=DAFQ*DCFQ=4.0*DDFQ
```

```
USER=BROOKS  (3,  7147)     JOINT COMPUTER FACILITY, MIT

      ECUB=-1.*(DAER*DAEQ*DEEQ+DCEC*DCEQ)
      AKAR1=ECUB*ECUB/4.
      AKAR2=ECUB*ECUB*ECUB/27.0
      AKAR3=-.5*ECUB
      AKAR4=SQRT(AKAR1+AKAR2)
      ACUB=(AKAR3+AKAR4)**.333
      BCUBT=(AKAR4-AKAR3)**.333
      BCUB=-BCUBT
      AKAR5=DAER*DAEQ/4.0
      RQUAD=SQRT(AKAR5+ACUB+BCUB)
      RQUA2=AKAR5+ACUB+BCUB
      AKAR6=3.0*AKAR5
      AKAR7=(8.0*DCEQ+DAEQ*DAEQ*DAEQ)/(4.0*RQUAD)
      DDCUB=SQRT(AKAR6-RQUA2-AKAR7)
  501 V2=-.25*DAEQ+.5*RQUAD+DDCUB*.5
      V223=V3*V3*V2/(V2*V2*V2)
      V222=V3*V3/(V2*V2)
      TTORS=GK*PC*(11./BET3X+12./BET2X+6./BET1X+1.0)
      TTENS=ECOLD*RI*REIL*REIL*PC*(V2*SECAV-1.)*(11.*R3*R3*AK2/BET3+12.*
     *R2*R2*AK2/BET2+6.*R1*R1*AK2/BET1)
      TBEN=RI*PC*PC*(11.*R3*R3*AK2/BET3X+12.*R2*R2*AK2/BET2X+6.*R1*R1*AK
     *2/BET1X)*PC
      TORQ1=TTENS+TTORS+TBEN
      TE3=A*V322*(ALP3*ALP3/(BET3*BET3))+B*V223*(ALP3*ALP3*ALP3/(BET3*BE
     *T3*BET3))
      TE2=A*V322*(ALP2*ALP2/(BET2*BET2))+B*V223*(ALP2*ALP2*ALP2/(BET2*BE
     *T2*BET2))
      TE1=A*V322*(ALP1*ALP1/(BET1*BET1))+B*V223*(ALP1*ALP1*ALP1/(BET1*BE
     *T1*BET1))
      TEM=A*V322+B*V223
      TORQ2=PM*(14.0*TE3*R3*R3/ALP3+9.0*TE2*R2*R2/ALP2+6.0*TE1*R1*R1/AL
     *P1)/45.0
      TOTOR=TORQ2
```

```
USER=BROOKS 235 71972     JOINT COMPUTER FACILITY, MIT

      DIF=(TOTOLD-TORQ1)/TORQ1
      TCOLD=454.*PI*ECOLD*EFIL*RFIL*(V2*SECAV-1.)*(11./BET3+12./BET2+9./
     +BET1)
      TEN2=14.*TF3/ALP3+9.*TF2/ALP2+6.*TF1/ALP1+TF0
      TWIST=COTW
      RMS=EPS/6.6332
      IF (TWIST.EQ.1.) GO TO 2
      BRATE=ADIF/DIF
      IF (DIF.LE.0.) GO TO 1000
    2 ADIF=DIF
      GO TO 1
 1000 WRITE(5,571)
  571 FORMAT(' COLD TWIST',3X,'HOT TWIST',4X,'TORQUE',7X,'TENSION')
      WRITE(5,572)TWIST,EPS,TORQ1,TEN2
  572 FORMAT(4E13.5)
      WRITE(5,714)
      V32=V3/V2
      WRITE(5,713)TF3,TF2,TF1,TF0,TTORS,TTENS,TBEN,V3,V32
      EPS=V2*SECAV-1.
      DRAW0=V3/V2
      DRAW3=V3*ALP3/(V2*BET3)
      DRAW2=V3*ALP2/(V2*BET2)
      DRAW1=V3*ALP1/(V2*BET1)
      CT0=1.0*DRAW0*DRAW0/(V4*V4*30.)
      CT1=6.0*DRAW1*DRAW1/(V4*V4*30.)
      CT2=9.0*DRAW2*DRAW2/(V4*V4*30.)
      CT3=14.0*DRAW3*DRAW3/(V4*V4*30.)
      RMS=SQRT(CT0+CT1+CT2+CT3-1.)
      WRITE(5,8411)EPS
      WRITE(5,1524)SECAV
 1524 FORMAT(' SECAV=',E13.5)
 8411 FORMAT(' THE COLD AVERAGE STRAIN IS',E13.5)
  713 FORMAT(9E13.5)
```

APPENDIX 6

COMPUTER PROGRAM FOR TRANSIENT ANALYSIS

```
USER=BROOKS  235 7197     JOINT COMPUTER FACILITY, MIT

      SUBROUTINE EGSI
      COMMON T,DT,Y(2 ),F(24),STIME,FTIME,NEWDT,IFNRT,N,IPR,ICO,ICU,
     *TNEXT,PNEXT,TRACK
C     ***********************************************************
C
C
C     ********************MIT FIBERS AND POLYMERS LABS************
C
C
C     ***********************************************************
C     TRANSIENT ANALYSIS OF DRAW TEXTURING PROCESS
C
C
C     IN THE FOLLOWING ANALYSIS THREADLINE TORQUE,TENSION,AND TWIST
C     DISTRIBUTION ARE DETERMINED DURING UNSTEADY OPERATION
C     INPUTS-        COLD FORMATION LENGTH
C                    HOT FORMATION LENGTH
C                    SPINDLE SPEED,WH
C                    INPUT ROLLER VELOCITY,V0
C                    OUTPUT ROLLER VELOCITY,V4
C                    HOT MODULI, A AND B
C                    COLD MODULUS
C                    COLD BENDING MODULUS
C                    COLD TORSIONAL MODULUS
C                    YARN RADIAL LAYER STRUCTURE
C     ***********************************************************
C                    INITIAL CONDITIONS
C     COLD TWIST=RAD/INCH
C     HOT TWIST=RAD/INCH
C     COLD AVERAGE FILAMENT STRAIN
C     DRAW RATIOS FOR EACH RADIAL LAYER
C     INITIAL YARN TENSION
```

```
USER=BROOKS  235 7197     JOINT COMPUTER FACILITY, MIT

C       COLD ZONE CL,INCHES
        CL=6.0
C       HOT ZONE HL,INCHES
        HL=1.25
C       SET ZONE SL, INCHES
        SL=7.
C       POST SPINDLE ZONE VL, INCHES
        VL=9.0
C       MACHINE SPEEDS  INPUT ROLLER SPEED V0, OUTPUT ROLLER SPEED V4,
C                       SPINDLE SPEED VH
        V0=.204
        V4=.47 4
C       COLD STRUCTURE  1-6-12-11
        BN0=1.
        BN1=6.
        BN2=12.
        BN3=11.
C       HOT STRUCTURE 1-6-9-14
 75     AN0=1.
        AN1=6.
        AN2=9.
        AN3=14.
C       MATERIAL PROPERTIES
        AK=.490
        B=.911 2
        A=-1.046
        C=222.4
        AP=-2.304E-3
        BP=2.007E-3
        ECOLD=222.4
        EI=3.07E-8
        GK=1.30E-8
C       COMPUTED VARIABLES
```

```
USER=BROOKST 235 7197?     JOINT COMPUTER FACILITY, MIT

C       COLD TWIST PC                          Y(1)
C       HOT TWIST PH                           Y(2)
C       COLD AVERAGE FILAMENT STRAIN           Y(3)
C       CORE FILAMENT DRAW RATIO DR0           Y(4)
C       FIRST LAYER DRAW RATIO  DR1            Y(5)
C       SECOND LAYER DRAW RATIO DR2            Y(6)
C       THIRD LAYER DRAW RATIO DR3             Y(7)
C       YARN TENSION                           Y(8)
C       TWIST AT END OF SET ZONE PS            Y(9)
C       POST SPINDLE TWIST PL                  Y(10)
C       TWIST AT END OF COLD ZONE PV           Y(11)
        PC=Y(1)
        PH=Y(2)
        EPS=Y(3)
        DR0=Y(4)
        DR1=Y(5)
        DR2=Y(6)
        DR3=Y(7)
        PS=Y(9)
        PV=Y(10)
        PL=Y(11)
C       DRAW RATIOS
        DR02=DR0*DR0
        DR03=DR02*DR0
        DR12=DR1*DR1
        DR13=DR1*DR12
        DR22=DR2*DR2
        DR23=DR2*DR22
        DR32=DR3*DR3
        DR33=DR3*DR32
C       YARN RADIAL DIMENSIONS
        R3C=3.28E-4
        R2C=2.85E-4
```

```
      R1C=1.43E-4
      R3H=2.3E-4
      R2H=1.53E-4
      R1H=9.77E-4
C     YAWN GEOMETRY
      R3H2=R3H*R3H
      R2H2=R2H*R2H
      R1H2=R1H*R1H
      R3C2=R3C*R3C
      R2C2=R2C*R2C
      R1C2=R1C*R1C
C     YAWN GEOMETRY RELATIONSHIPS
      ZETA1=SQRT(1.+PJ*PJ*R1C2)
      ZETA2=SQRT(1.+PJ*PJ*R2C2)
      ZETA3=SQRT(1.+PJ*PJ*R3C2)
      B3ET1=SQRT(1.+PC*PC*R3C2)
      B2ET1=SQRT(1.0+PC*PC*R2C2)
      B1ET1=SQRT(1.+PC*PC*R1C2)
      A3LP1=SQRT(1.0+PH*PH*R3H2)
      A2LP1=SQRT(1.0+PH*PH*R2H2)
      A1LP1=SQRT(1.0+PH*PH*R1H2)
      PRC32=Y(1)*Y(1)*R3C2
      PRC22=Y(1)*Y(1)*R2C2
      PRC12=Y(1)*Y(1)*R1C2
      PRC34=PRC32*PRC32
      PRC24=PRC22*PRC22
      PRC14=PRC12*PRC12
      B3ET2=B3ET1*B3ET1
      B3ET3=B3ET1*B3ET2
      B3ET4=B3ET2*B3ET2
      B3ET5=B3ET3*B3ET2
      B2ET2=B2ET1*B2ET1
      B2ET3=B2ET1*B2ET2
```

```
      B2ET4=B2ET2*B2ET2
      B2ET5=B2ET3*B2ET2
      B1ET2=B1ET1*B1ET1
      B1ET3=B1ET2*B1ET1
      B1ET4=B1ET2*B1ET2
      B1ET5=B1ET3*B1ET2
      A3LP2=A3LP1*A3LP1
      A3LP3=A3LP1*A3LP2
      A3LP4=A3LP2*A3LP2
      A3LP5=A3LP3*A3LP2
      A2LP2=A2LP1*A2LP1
      A2LP3=A2LP1*A2LP2
      A2LP4=A2LP2*A2LP2
      A2LP5=A2LP2*A2LP3
      A1LP2=A1LP1*A1LP1
      A1LP3=A1LP2*A1LP1
      A1LP4=A1LP2*A1LP2
      A1LP5=A1LP3*A1LP2
      GAMMA=SQRT(1.0+2S*HS*R3H2)
      PCPR=Y(1)*Y(1)*R3C
      PCPP=Y(1)*R3C
      PCPP2=Y(1)*R3C*R3C
      PHR12=PH*PH*R1H2
      PHR22=PH*PH*R2H2
      PHP32=PH*PH*R3H2
C     COLD CONTRACTION FACTOR
      CONT=.5*(B3ET1+ALOG(PCR+B3ET1)/PCR)
      SKAR=PCR2/B3ET1+1./(Y(1)*(PCR+B3ET1))+R3C/(B3ET1*(B3ET1+PCR))-ALOG
     *(PCR+B3ET1)/PC2P
      SKAR=SKAR/2.
      PJP=Y(11)*R3C
      PJR2=Y(11)*R3C2
      PJ2R=Y(11)*Y(11)*R3C
```

```
USER=BROOKS, 235 7197)     JOINT COMPUTER FACILITY, MIT

      ACONT=.5*(ZETA3+ALOG(PJR+ZETA3)/PJR)
      ASKAR=PJR**2/ZETA3+1./((Y(11)*(PJR+ZETA3))+R3C/(ZETA3*(ZETA3+PJR))-AL
     *OG(PJR+ZETA3)/PJR**2
      ASKAR=ASKAR/2.
C     ***********    MAIN COMPUTATIONAL BODY    ***********
C     ***********************************************************
      FG=ANG*(2.*DR0*A+3.*DR02*B)
      F1=AN1*(2.*DR1*A+3.*DR12*B)/A1LP1
      F2=AN2*(2.*DR2*A+3.*DR22*B)/A2LP1
      F3=AN3*(2.*DR3*A+3.*DR32*B)/A3LP1
      AF5=AN1*(A*DR12+B*DR13)*R1H2/A1LP3
      BF5=AN2*(A*DR22+B*DR23)*R2H2/A2LP3
      CF5=AN3*(A*DR32+B*DR33)*R3H2/A3LP3
      F5=-PH*(AF5+BF5+CF5)
      F6=FCOLD*(BN1/B1ET1+BN2/B2ET1+BN3/B3ET1)
      F7=-PC*FCOLD*EPS*(BN1*R1C2/B1ET1+BN2*R2C2/B2ET1+BN3*R3C2/B3ET1)
      G1=AN1*(2.*AP*DR1+3.*BP*DR12)*PH*P1H2/A1LP1
      G2=AN2*(2.*AP*DR2+3.*BP*DR22)*PH*P2H2/A2LP1
      G3=AN3*(2.*AP*DR3+3.*BP*DR32)*PH*P3H2/A3LP1
      AG5=AN1*(AP*DR12+BP*DR13)*R1H2*(1./A1LP1-PHR12/A1LP3)
      BG5=AN2*(AP*DR22+BP*DR23)*R2H2*(1./A2LP1-PHR22/A2LP3)
      CG5=AN3*(AP*DR32+BP*DR33)*R3H2*(1./A3LP1-PHR32/A3LP3)
      G5=AG5+BG5+CG5
      AG6=BN1*R1C2/B1ET1
      BG6=BN2*R2C2/B2ET1
      CG6=BN3*R3C2/B3ET1
      G6=PC*AK*(AG6+BG6+CG6)
      AG7=BN1*(R1C2/B1ET1-PC*PC*R1C2*R1C2/B1ET3)
      BG7=BN2*(R2C2/B2ET1-PC*PC*R2C2*R2C2/B2ET3)
      CG7=BN3*(R3C2/B3ET1-PC*PC*R3C2*R3C2/B3ET3)
      AAG7=EPS*AK*(AG7+BG7+CG7)
      DG7=(DRC32/B3ET3-DRC34/B3ET5)*BN3
      EG7=(DRC22/B2ET3-DRC24/B2ET5)*BN2
```

```
      FG7=(PRC12/B1ET3-PRC14/B1ET3)*DX1
      FFG7=3.0*EI*(DG7+FG7+FG7)
      WG7=BN3*(1./B3ET3-3.*PRC32/B3ET3)
      XG7=BN2*(1./B2ET3-3.*PRC22/B2ET3)
      YG7=BN1*(1./B1ET3-3.*PRC12/B1ET3)
      ZG7=1.
      WWG7=(WG7+XG7+YG7+ZG7)*GK
      G7=WWG7+FFG7+AAG7
      ATLA=SQRT(1.0+PV*PV*R3H2)
      BOSD=-1.0*(PV*V4+WH)
      BOSA=.5*VL*PV*R3H2/ATLA
      BOSB=.5*(1.0+GAMMA)
      BOSC=-.5*V4*(1.+ATLA)
      GORG=BOSD-PS*BOSC/BOSB
      GORGA=VL-PS*BOSA/BOSB
      F(10)=GORG/GORGA
C     VB IS THE YARN SPEED AT THE DOWNSTREAM END OF THE SET ZONE
      VB=(VI*F(10)-BOSD)/PS
      A01=0.
      A11=HL*PH*R1H2/(B1ET1*DR1*A1LP1)
      A21=HL*PH*R2H2/(B2ET1*DR2*A2LP1)
      A31=HL*PH*R3H2/(B3ET1*DR3*A3LP1)
      B1=.5*PS*R3H2*(PV-PS)/(GAMMA+(1.+A3LP1))+(1.+GAMMA)/(1.+A3LP1)
      ABC=.5*SL*PH*R3H2/((1.+A3LP1)*A3LP1)
      A01=A01+ABC/DR0
      A11=A11+ABC*A1LP1/(B1ET1*DR1)
      A21=A21+ABC*A2LP1/(B2ET1*DR2)
      A31=A31+ABC*A3LP1/(B3ET1*DR3)
      A02=B1*VB/DR0
      A12=B1*VB*A1LP1/(DR1*B1ET1)
      A22=B1*VB*A2LP1/(DR2*B2ET1)
      A32=B1*VB*A3LP1/(DR3*B3ET1)
      A03=HL/DR02
```

```
A12=H1*A1LP1/(D12*B1ET1)
A22=H1*A2LP1/(D22*B2ET1)
A32=H1*A3LP1/(D32*B3ET1)
A11=A11*B1ET1/ZETA1
A21=A21*B2ET1/ZETA2
A31=A31*B3ET1/ZETA3
A12=A12*B1ET1/ZETA1
A22=A22*B2ET1/ZETA2
A32=A32*B3ET1/ZETA3
A13=A13*B1ET1/ZETA1
A23=A23*B2ET1/ZETA2
A33=A33*B3ET1/ZETA3
Q1=(CONT+ACONT)*.5*CL/((1.+EPS)*ACONT)
Q2=V0*(1.+EPS)/ACONT
Q3=CL*SKAR*.5/ACONT
Q4=1.+(PC-PJ)*ASKAR*.5/ACONT
Q1=Q1/Q4
Q2=Q2/Q4
Q3=Q3/Q4
T0=F0/(F6*A03)
T1=F1/(F6*A13)
T2=F2/(F6*A23)
T3=F3/(F6*A33)
X1=T0*A01+T1*A11+T2*A21+T3*A31+F5/F6
X2=-Q1*(T0+T1+T2+T3)
X3=Q3*(T0+T1+T2+T3)-F7/F6
X4=T0*(A02-Q2)+T1*(A12-Q2)+T2*(A22-Q2)+T3*(A32-Q2)
X5=(WH-PS*VB)/(HL+.5*SL)
X6=CL/(2.*HL+SL)
X7=(PC-PJ)/(2.*HL+SL)
X8=(PH-PS)*VB/(2.*HL+SL)
S1=G1/(G6*A13)
S2=G2/(G6*A23)
```

```
      S3=G3/(G6*A33)
      Y1=S1*A11+S2*A21+S3*A31+G5/G6
      Y2=-Q1*(S1+S2+S3)
      Y3=Q3*(S1+S2+S3)-G7/G6
      Y4=S1*(A12-Q2)+S2*(A22-Q2)+S3*(A32-Q2)
      SUF=(Y1*X5-Y1*X7*Q2+Y4-Y1*X8)/(1.-Y2+Y1*X7*Q1)-(X1*X5-X7*X1*Y2+X4
     *X1*X8)/(1.-X2+X1*X7*Q1)
      AKAR=(X3-X1*X6+X1*X7*Q3)/(1.-X2+X1*X7*Q1)-(Y3-Y1*X6+X7*Y1*Q3)/(1.-
     *Y2+Y1*X7*Q1)
C     ******  ********************************************  ********
C     ******  ***********  DIFFERENTIAL EQUATIONS  ********  ********
      F(1)=SUF/AKAR
      F(3)=(Y1*X5-Y1*X7*Q2+Y4-Y1*X8)/(1.+X7*Y1*Q1-Y2)+(Y3-Y1*X6+X7*Y1*Q3
     *)*F(1)/(1.+X7*Q1*Y1-Y2)
      F(2)=X5-Q2*X7-X8+(X7*Q3-X6)*F(1)-Q1*X7*F(3)
      F(4)=(A01*F(2)+A02-Q2-Q1*F(3)+Q3*F(1))/A03
      F(5)=(A11*F(2)+A12-Q2-Q1*F(3)+Q3*F(1))/A13
      F(6)=(A21*F(2)+A22-Q2-Q1*F(3)+Q3*F(1))/A23
      F(7)=(A31*F(2)+A32-Q2-Q1*F(3)+Q3*F(1))/A33
      F(8)=F0*F(4)+F1*F(5)+F2*F(6)+F3*F(7)+F5*F(2)
      F(9)=(PH-PS)*VB/SL
      TTENS=AK*PC*FPS*(11.*R3C2/B3ET1+12.*R2C2/B2ET1+6.*R1C2/B1ET1)
      TTORS=GK*Y(1)*(11./B3ET3+12./B2ET3+6./B1ET3+1.)
      TRFN=FI*Y(1)*Y(1)*Y(1)*(11.*R3C2/B3ET3+12.*R2C2/B2ET3+6.*R1C2/B1ET
     *3)
      Y(12)=TTENS+TTORS+TRFN
      V2=Q1*F(3)+Q2-Q3*F(1)
      F(11)=(PC-PJ)*V2/CL
      Y(13)=Y(1)/6.28
      Y(14)=(.83*Y(1)+.17*Y(11))/6.28
      Y(15)=(.17*Y(1)+.83*Y(11))/6.28
      Y(16)=Y(2)/6.28
      Y(17)=(.86*Y(2)+.14*Y(9))/6.28
```